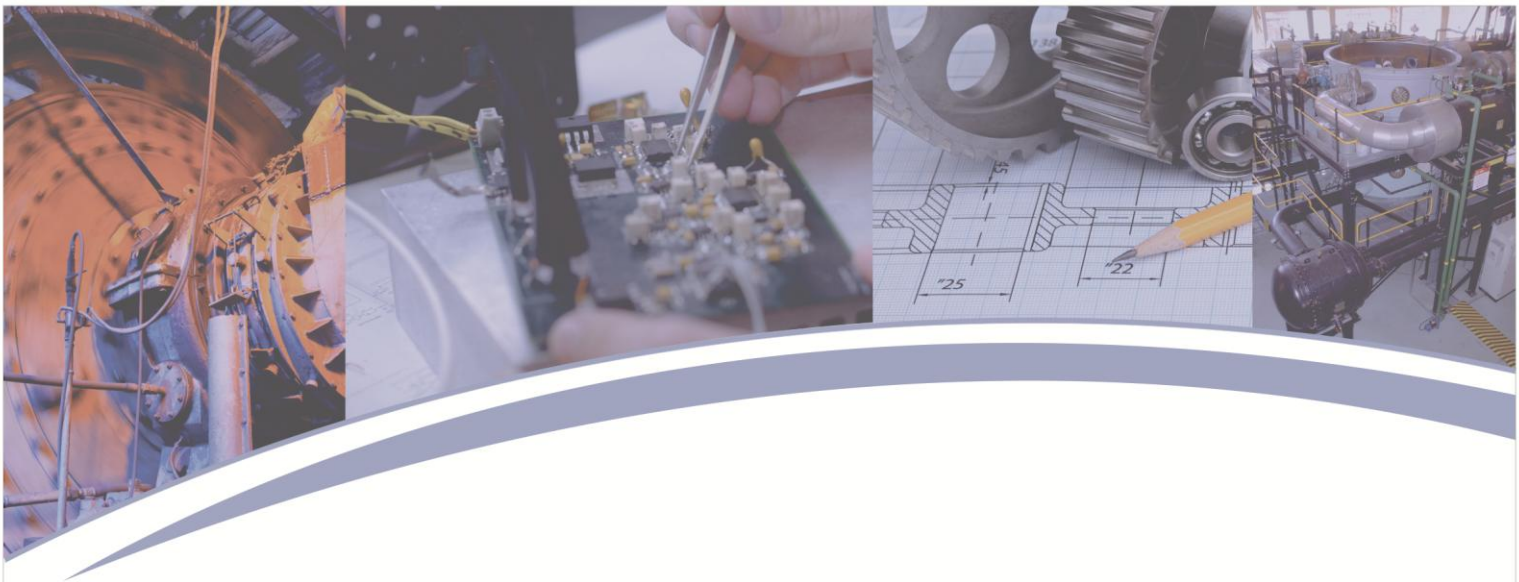

Fermentation coupled with pervaporation: a kinetic study

Maria Magdalena Meintjes (B.Eng, Chemical)

Mini-dissertation submitted in partial fulfilment of the requirements for the degree of Master of Engineering in the School of Chemical and Minerals Engineering of the North-West University, Potchefstroom Campus

Supervisor: Dr. P. van der Gryp

Co-supervisor: Prof. S. Marx

Potchefstroom

November 2011

ABSTRACT

Ethanol production through biomass fermentation is one of the major technologies available to produce liquid fuel from renewable energy sources. A major problem associated with the production of ethanol through fermentation remains the inhibition of the yeast *Saccharomyces cerevisiae* by the produced ethanol. Currently high water dilution rates are used to keep the ethanol concentrations in the fermentation broth at low concentrations, resulting in low yields and increased downstream processing to remove the excess water. Yeast strains that have a high tolerance for ethanol have been isolated but the time and cost associated with doing so poses a challenge.

The fermentation process can be combined with pervaporation, thereby continuously removing ethanol while it is being formed. In this study a mathematical model for ethanol fermentation with yeast, *Saccharomyces cerevisiae*, coupled with pervaporation was developed. The fermentation of glucose was optimised in the first part of the study and experimental data were obtained to find a kinetic model for fermentation. It was found that an optimum ethanol yield can be obtained with an initial glucose concentration of 15wt%, a yeast concentration of 10 $g.L^{-1}$, and a pH between 3.5 and 6. The maximum ethanol yield obtained in this study was 0.441$g.g^{-1}$ (86% of the theoretical maximum) using 15wt% glucose, 10g/L yeast and a pH of 3.5.

Two kinetic models for fermentation were developed based on the Monod model. The substrate-limiting model, predicted fermentation very accurately when the initial glucose concentration was below 20wt%. The second model, the substrate-inhibition model, predicted fermentation very well when high initial glucose concentrations were used but at low glucose concentrations, the substrate-limiting model was more accurate. The parameters for both models were determined by non-linear regression using the simplex optimisation method combined with the Runge-Kutta method.

The PERVAP®4060 membrane was identified as a suitable membrane in this study. The effect of the ethanol content in the feed as well as the influence of the glucose content was investigated. The total pervaporation flux varied with ethanol content of the feed and the highest total flux of 0.853 kg/m^2h was obtained at a feed with 20wt% ethanol. The addition of glucose had almost no effect on the ethanol flux but it lowered the water flux, thereby increasing the enrichment factor of the membrane.

The mass transport through the PERVAP®4060 membrane was modelled using the solution-diffusion model and Greenlaw's model for diffusion coefficients was used. The

limiting diffusion coefficient (D_i^0) and plasticisation coefficients (B_{ij}) were determined by using the Nelder-Mead simplex optimisation method. The theoretical values predicted with the model showed good agreement with the measured experimental values with R^2 values above 0.998.

In the third part of this investigation, the kinetic model developed for fermentation was combined with the transport model developed for pervaporation. The combined kinetic model was compared to experimental data and it was found that it could accurately predict fermentation when coupled with pervaporation. This model can be used to describe and better understand the process when fermentation is coupled with pervaporation.

Keywords: Fermentation, pervaporation, *Saccharomyces cerevisiae*, modelling, ethanol

DECLARATION

I, Maria Magdalena Meintjes, hereby declare that I am the sole author of the mini-dissertation entitled:

Fermentation coupled with pervaporation: a kinetic study

_____

Maria Magdalena Meintjes

Potchefstroom

Nov 2011

ACKNOWLEDGEMENTS

First of all, I would like to thank God for giving me the strength, ability and courage to start and finish this study.

I would also like to thank the following people/organisations for their contributions to this project:

- Dr. Percy van der Gryp for his guidance as my study leader and whose expert opinion was invaluable
- Prof. Sanette Marx for her leadership and advice as my co-supervisor
- My dear husband, Barend, for his support, assistance, and understanding during this study, especially for all of the late nights in the office and in the laboratory
- My parents and my two brothers, for their support and encouragement throughout my studies
- The Centre for Sustainable and Renewable Energy Studies (CRSES) for its financial support of two years
- SANERI for sponsoring the project
- Dr. Tiedt for performing the SEM scans
- Gideon for assistance with the HPLC and general laboratory work
- Adrian Brock for his technical expertise and help with the membrane model design and general maintenance of laboratory equipment
- Eleanor de Koker for her administration assistance
- And lastly, my dear friends Gerhard and Bernhard, who worked with me in the bio-group for all your assistance and friendship during this project and your willingness to always help

TABLE OF CONTENTS

NOMENCLATURE

Symbol	Description	Unit
A	Area	m^2
a_1	Average selectivity of ethanol separation	---
a_2	Total permeate flux	$kg.m^{-2}.h^{-1}$
A_m	Area of the membrane	m^2
B_j	Contois constant	---
c	Concentration	$g.L^{-1}$
D	Diffusion coefficient	$m^2.s^{-1}$
J	Flux	kg/m^2-hr or $kmol/m^2$-hr
k_1	Aiba model constant	$L.g^{-1}$
k_2	Aiba model constant	$L.g^{-1}$
K_{ip}	Inhibition constants ethanol production	$mol.m^{-3}$
K_{ix}	Inhibition constants for cell growth	$mol.m^{-3}$
K_s	Monod constants for cell growth	$g.L^{-1}$
K_s'	Monod constants for ethanol production	$g.L^{-1}$
K_{sp}	Monod constant for product formation	$g.m^{-3}$
K_{sx}	Monod constant for cell growth	$g.m^{-3}$
L	Lactose concentration (Chapter 2)	$kg.m^{-3}$
L	Membrane thickness (Chapter 3)	µm
m	Mass	kg
m_s	Maintenance term	$kg.kg^{-1}.h^{-1}$
M	Swelling ratio (Chapter 3)	---
M	Total mass in reactor (Chapter 4)	kg
n	Reaction order	---
p	Pressure	kPa
P	Product concentration	$g.L^{-1}$
$P_{x,max}$	Product concentration where the fermentation process stops	$g.L^{-1}$
Q	Permeate removal stream	$L.h^{-1}$ or $kg.h^{-1}$
R	Retention time	h
r	Rate of enzymatic reaction	$kg.m^{-3}.h^{-1}$
RPDM	Relative percentage deviation modulus	%
S	Growth controlling substrate	$g.L^{-1}$
t	Time	hr

Symbol	Description	Unit
T	Temperature	°C or K
v_{max}	Maximum specific product production rate	h^{-1}
v_P	Product formation rate	$kg.kg^{-1}.h^{-1}$
v_s	Substrate utilization rate	$kg.kg^{-1}.h^{-1}$
W	Membrane mass	g
x	Mass fraction in feed	$g.g^{-1}$
X	Cell concentration	$g.L^{-1}$
x_E	Mass ratio of ethanol in the feed	---
y	Mass fraction in permeate	$g.g^{-1}$
$Y_{P/S}$	Ratio of ethanol produced per substrate consumed for fermentation.	---
$Y_{X/S}$	Ratio of cells produced per substrate consumed for growth	---

Greek symbol	Description	Unit
α	Selectivity	---
β	Enrichment factor	---
ρ	Density	$kg.m^{-3}$
μ	Specific cell growth rate (Chapter 2)	h^{-1}
μ	Chemical potential (Chapter 3)	$J.mol^{-1}$
μ_{max}	Maximum specific growth rate	h^{-1}
v	Specific product production rate (Chapter 2)	h^{-1}
v	Molar volume (Chapter 3)	$mol.L^{-1}$
γ	Activity coefficients	---

Subscript	Description
0	Initial or at time=0
1, 2, …	Component 1, 2…
∞	Equilibrium
EtOH	Ethanol
i/j	Component for example ethanol

Abbreviation	Description
ACE	Associated chemical enterprise
ADP	Adenosine diphosphate
ATP	Adenosine triphosphate
DMSO	Dimethyl sulphoxide
EM	Embden-Meyerhof
ETBE	Ethyl-tert-butyl-ether
FFV	Flexible fuel vehicles
HPLC	High performance liquid chromatography
Mw	Molecular weight
NAD	Nicotinamide adenine dinucleotide
PAN	Polyacrylonitrile
PB	Polybutadiene
PDMS	Polydimethylsiloxane
PEBA	Polyether-block-polymide
PEI	Polyetherimide
PFK	Phosphofructokinase
PI	Polyimide
POMS	Polyoctylmethylsiloxane
PP	Polypropylene
PTFE	Polytetrafluoro-ethylene
PTMSP	Poly[1-(trimethylsilyl)-1-propyne]
PVA	Polyvinylalcohol
SEM	Scanning electron microscope

LIST OF FIGURES

LIST OF TABLES

CHAPTER 1: GENERAL INTRODUCTION

OVERVIEW

It is the aim of this chapter to present an introduction to the study and to provide a framework in which the investigation was done. In the first section of this chapter, Section 1.1, a general background on the subject and the motivation behind the project is discussed. The main objectives of the investigation are presented in Section 1.2 and the scope of investigation is given in Section 1.3.

1.1 BACKGROUND AND MOTIVATION

A steady, reliable supply of energy is required for all aspects of development, prosperity, and economic growth in modern society. Currently the global energy supply relies predominantly on fossil fuel sources such as oil, natural gas, and coal (Dresselhaus & Thomas, 2001:332). However, fossil fuels are under scrutiny because of serious disadvantages regarding the limited supply of fossil fuel resources and the emission of carbon dioxide (and other pollutants) when these fossil fuels are burned (Dresselhaus & Thomas, 2001:333). An increasing demand for energy worldwide as well as the depletion of fossil fuels and environmental concerns has opened up the search for alternative fuel sources (Dresselhaus & Thomas, 2001:332; Sánchez & Cardona, 2008). Alternative energy resources refer to those energy resources that are renewable and therefore sustainable. Examples of renewable energy are biomass, hydro, geothermal, solar, wind, ocean thermal, wave action, and tidal action energy. According to Demirbas (2008:2107), the potential of energy from biomass is the most promising among the renewable energy sources as it is available worldwide. Biomass has the unique advantage that it offers a solid, liquid, or gaseous fuel that can be stored, transported, and utilised far away from the point of origin. These solid, liquid, or gaseous fuels are referred to as biofuels.

Biofuels, such as bioethanol or biodiesel, have a smaller environmental impact if compared to fossil fuels when considering the low sulphur content and no net release of carbon dioxide (Demirbas, 2008:2107). According to Bomb *et al.* (2007:2256) liquid biofuels are increasingly considered in Europe as an attractive alternative to fossil fuels to enhance energy security, reduce emissions by transportation, and to contribute to regional development by increasing employment opportunities. The Biofuels Industrial Strategy of South Africa propose a 2% biofuel use in the transportation sector of South Africa by 2013, amounting to approximately 400 million litres of biofuel that must be produced per year (SA, 2007:3). This target will create jobs, thereby reducing unemployment and boosting economic growth (SA, 2007:9).

Ethanol production through biomass fermentation is one of the major technologies available to produce liquid fuel from renewable energy sources (Huber and Dumesic, 2006:122). Bioethanol is produced through fermentation using any sugar or starch rich feedstock and more recently, the use of lignocellulosic feedstock for bioethanol production has also come under investigation (Bomb *et al.*, 2007:2257). The wide variety of feedstock that can be used for bioethanol production is part of its appeal as an alternative fuel.

The yeast, *Saccharomyces cerevisiae,* is the microorganism usually used for fermentation (Bai *et al.*, 2008:90). There is, however, a major problem associated with the fermentation process, namely inhibition of *Saccharomyces cerevisiae* by the ethanol it produces. Inhibition affects the overall productivity of the yeast cells and the ethanol yield of the fermentation process.

Currently, yeast inhibition is overcome by diluting the starting sugar solutions and by the addition of water during fermentation to dilute the ethanol concentration in the fermentation broth. The large amount of water carried through the process amounts to higher equipment cost (due to larger equipment required) and higher separation costs later on in the process to remove the water, as the acceptable water content in bioethanol used as transportation fuel is very low. The amount of water required for dilution is also a concern in water scarce countries such as South Africa. If the ethanol is removed as soon as it is formed, it is possible that the effect of inhibition can be overcome, as the ethanol concentration will be constantly kept low with no additional dilution required.

Pervaporation is one method that can be effectively combined with fermentation to remove ethanol from the fermentation broth continuously. Research published in this field is shown in Table 1.1.

Pervaporation is a membrane process in which a phase change takes place over the membrane. The liquid mixture comes into contact with one side of the membrane and the permeated product (known as the permeate) is removed as a low pressure vapour on the other side. The driving force for mass transport over the membrane is the chemical potential gradient created by applying a vacuum pump on the permeate side to lower the partial pressure of the feed liquid and thus lowering the chemical potential of the permeate stream on the downstream side (Feng & Huang, 1998:1048).

Pervaporation is an attractive separation method as it is operated at low feed pressures and temperatures and no additional chemicals are necessary for separation. There is also no significant economy of scale meaning that pervaporation can be used in small and large processing plants (Feng & Huang, 1998:1049). Pervaporation combined with fermentation can keep the ethanol concentration in the fermentation broth low enough so that product inhibition will not take place, thus resulting in higher productivity. The bioethanol obtained through this combined process will contain less water, reducing separation costs to achieve the high grade of bioethanol required for fuel grade ethanol.

Table 1.1 Studies on the coupling of fermentation with pervaporation

Description	Membrane	Focus of study	Reference
Fermentation of glucose using *Saccharomyces cerevisiae* coupled with pervaporation	PDMS	Effect of product removal on fermentation and membrane performance	O'Brien & Craig, 1996
Fermentation of glucose using *Saccharomyces cerevisiae* and *Zymomonas mobilis* coupled with pervaporation	1.PTMSP 2.PDMS	Effect of fermentation on membrane performance	Schmidt *et al*., 1997
Fermentation of glucose using *Saccharomyces cerevisiae* coupled with pervaporation	Hollow fibre micro-porous polypropylene	Effect of pervaporation on ethanol fermentation	Kaseno *et al*., 1998
Fermentation of glucose using *Saccharomyces cerevisiae* coupled with pervaporation	Silicalite coated with silicone rubber	Effect of fermentation on membrane performance	Ikegami *et al*., 2002
Pervaporation of glucose fermentation broth Fermentation of glucose using *Saccharomyces cerevisiae* coupled with pervaporation	Silicalite	Effect of fermentation broth on membrane performance and long term membrane stability	Nomura *et al*., 2002
Pervaporation of cell free fermentation broth	PTMSP	Effect of fermentation broth on membrane performance	Fadeev *et al*., 2003
Fermentation of maize fibre hydrolysate with *Escherichia coli* coupled with pervaporation	PDMS	Effect of pervaporation on fermentation	O'Brien *et al*., 2004
Semi-continuous fermentation and pervaporation of lactose mash	PDMS-PAN-PV	Ethanol productivity and membrane performance	Lewandowska & Kujawski, 2007
Pervaporation of maize fermentation broth	Mixed matrix ZSM-5/PDMS	Effect of fermentation broth on membrane performance	Offerman & Ludvik, 2011
Pervaporation of ethanol- water mixtures and pervaporation of fermented sweet sorghum juice	Cellulose acetate	Effect of process conditions and fermentation on membrane performance	Kaewkannetra *et al*., 2011

Most of the current research in the field of fermentation coupled with pervaporation, as given in Table 1.1, focuses on the different membranes that can be used, the effect that components in fermentation broth has on membranes and the effect that pervaporation has on fermentation. There is, however, a definite lack of research on kinetics of the membrane-reactor system where fermentation and pervaporation are combined. By investigating the kinetics of fermentation and the mass transfer of ethanol over a membrane using pervaporation, a mathematical model describing the process of fermentation combined with pervaporation can be constructed. This model can be used to describe and better understand the process and it is especially important when up scaling the process and to design reactors to achieve optimal product yield. The model can be used to predict performance under different process conditions as well as for process design, process optimisation, and process control, and in doing so reduce research and development time and cost (Dunn *et al.*, 1992:10).

1.2 PROBLEM STATEMENT AND OBJECTIVES

Ethanol is poisonous to *Saccharomyces cerevisiae* and therefore inhibits the fermentation process. Due to this inhibition effect, only low ethanol concentrations can be achieved in a batch process before the yeast cell activity decreases and dilution is often required to maintain a low ethanol concentration in a fermentation broth. The result is low yields and high separation costs to remove excess water from the bioethanol.

By combining fermentation with pervaporation the ethanol concentration in the fermentation vessel will be continuously lowered, which minimises product inhibition and lowers water requirements for dilution. The bioethanol obtained through this combined process will contain less water, thereby reducing separation costs to achieve the high grade of bioethanol required for fuel grade ethanol.

Bioethanol is already produced commercially but to combine this process with pervaporation, membrane-reactor kinetics are required. Therefore, the main objective of this study was to investigate the membrane-reactor kinetics when fermentation was coupled with pervaporation.

The following sub-objectives were necessary to achieve the main objective mentioned above:

- Investigate traditional batch fermentation
    - Evaluate the influence of different conditions, such as sugar concentration, yeast concentration and pH on the fermentation performance

  - Investigate fermentation kinetic models in literature and develop a simple model to describe traditional batch fermentation
- Investigate separation of ethanol and water by pervaporation
  - Screen different membranes for their efficiency in separating ethanol from water and ethanol mixtures
  - Examine the influence of different feed compositions on the separation performance of pervaporation
  - Explore pervaporation separation models in literature and develop a simple model to describe the separation process

1.3 SCOPE OF STUDY

The scope of this study is summarised in Figure 1.1 at the end of this section. In order to achieve the above-mentioned objective this investigation was subdivided into three main parts, namely:

1. Fermentation
2. Pervaporation
3. Fermentation combined with pervaporation

The first part of this study focused on kinetic models for fermentation and cell growth found in literature and the development of a simple model to describe glucose fermentation. The variables that were manipulated were the starting sugar concentration and the starting yeast concentration (also known as cell concentration). The effect that pH would have on fermentation was also investigated. The variables that were measured over time were the ethanol concentration, the sugar concentration, and the cell concentration. This part of the scope will be discussed in Chapter 2, Fermentation. Chapter 2 starts with a background and literature study on the subject of fermentation and fermentation kinetics. This is followed by a discussion of the fermentation experimental work. The results obtained from the fermentation experiments are also discussed in Chapter 2. The experimental data could then be used to model glucose fermentation. The modelling procedure is discussed and a comparison between the modelling results and experimental results is presented.

The second part of the project focused on pervaporation. Membrane screening experiments were completed to find a membrane suitable for ethanol separation. After a suitable membrane had been identified, the effect that the process conditions of a typical fermentation process would have on the separation performance (flux and ethanol selectivity) of pervaporation was determined. The manipulated variables for this part of the

project were the sugar concentration and the ethanol concentration. The mass permeate and fraction ethanol in the permeate were measured in these experiments. This part of the project will be presented and discussed in Chapter 3. A comprehensive theoretical background and literature survey on pervaporation is presented in Chapter 3.1. A detailed description of the apparatus and experimental methods and procedures used for the pervaporation experiments is presented in Section 3.2. This is followed by the results obtained from the pervaporation experiments. With reference to the experimental data, the separation of ethanol and water mixtures by pervaporation could be modelled as reported in the final part of Chapter 3.

The third part of this project was to combine fermentation and pervaporation in a membrane-reactor system. The fermentation kinetics and mass transfer constants calculated in the first two parts of this study could be combined to propose a model to simulate the dynamics of the membrane-reactor system. Fermentation experiments were combined with pervaporation to test the model. The manipulated variable is the fermentation time before pervaporation starts. The variables that were measured were the mass permeate, the ethanol fraction in permeate, the ethanol concentration in the fermentation vessel, the sugar concentration in the fermentation vessel, and the cell concentration in the fermentation vessel. Fermentation coupled with pervaporation is presented in Chapter 4. The literature surrounding this concept is discussed in the first part of Chapter 4, followed by the experimental procedures used. The results of fermentation coupled with pervaporation are discussed in the third section of Chapter 4. Finally, in the last part of Chapter 4 the results from the fermentation model and pervaporation model were combined to obtain a model to represent fermentation coupled with pervaporation. A comparison between model results and experimental data concludes this chapter.

Finally, in Chapter 5 a detailed discussion of the main conclusions drawn from this investigation are given together with some recommendation for future study.

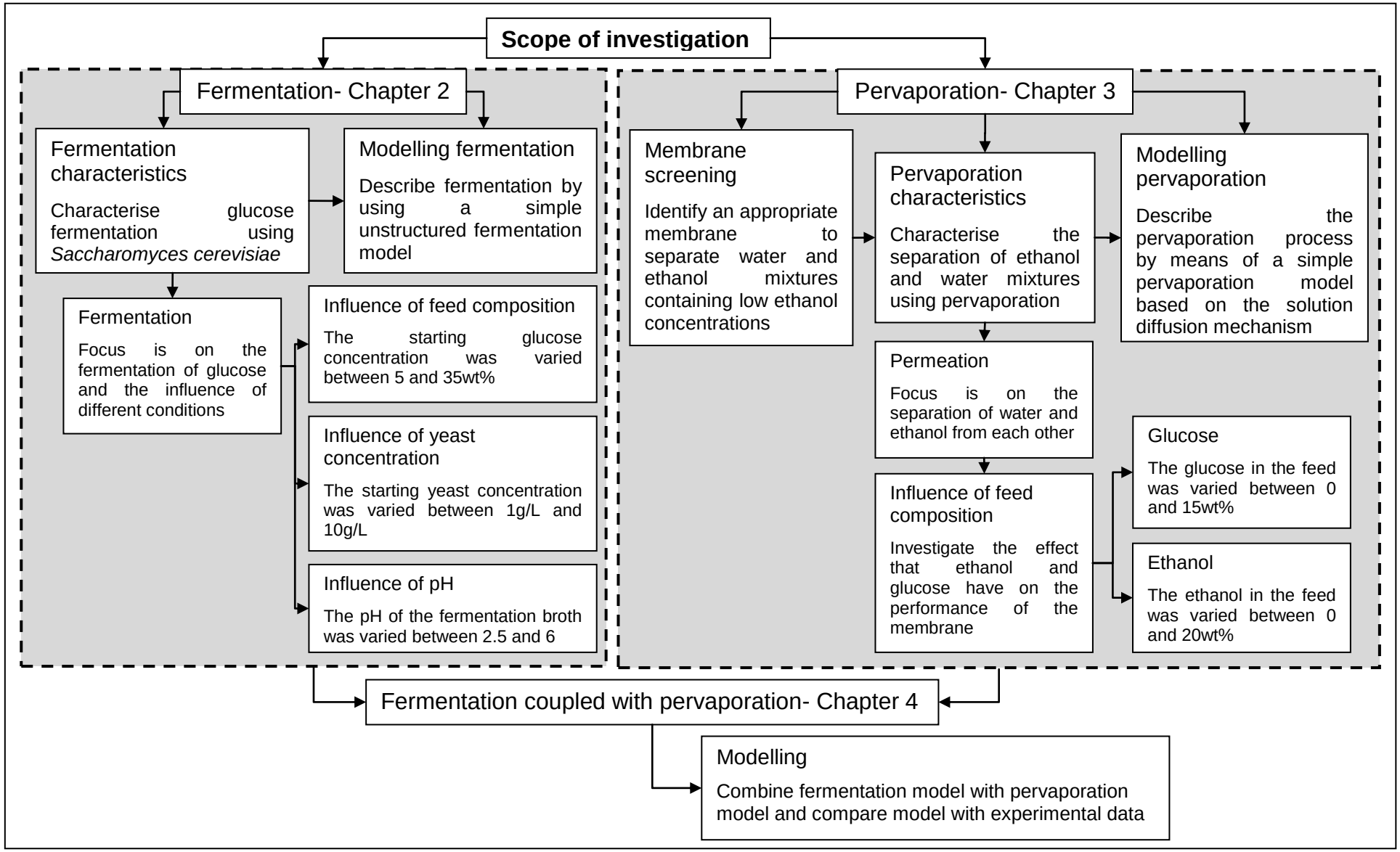

Figure 1.1 Schematic representation of the scope of this investigation

1.4 REFERENCES

BAI, F.W., ANDERSON, W.A. & MOO-YOUNG, M. 2008. Ethanol fermentation technologies from sugar and starch feedstocks. *Biotechnology Advances*, 26: 89-105.

BOMB, C., MCCORMICK, K. & KÅBERGER, T. 2007. Biofuels for transport in Europe: Lessons from Germany and the UK. *Energy Policy*, 35: 2256-2267.

DEMIRBAS, A. 2008. Biofuels sources, biofuel policy, biofuel economy and global biofuel projections. *Energy Conversion and Management*, 49: 2106–2116.

DRESSELHAUS, M.S. & THOMAS, I.L. 2001. Alternative energy technologies. *Nature*, 414: 332-337.

DUNN, I.J., HEINZLE, E., INGHAM, J. & PRENOSIL, J.E. 1992. Biological Reaction Engineering. Weinheim: VCH. 438p.

FADEEV, A.G., KELLEY, S.S., MCMILLAN, J.D., SELINSKAYA, Y.A., KHOTIMSKY, V.S. & VOLKOV, V.V. 2003. Effect of yeast fermentation by-products on poly[1-(trimethylsilyl)-1-propyne] pervaporative performance. *Journal of Membrane Science*, 214: 229-238.

FENG, X. & HUANG, R.Y. M. 1997. Liquid Separation by Membrane Pervaporation: A Review. *Industrial Engineering Chemical Research*, 36:1048-1066.

HUBER, G.W. & DUMESIC, J.A. 2006. An overview of aqueous-phase catalytic processes for production of hydrogen and alkanes in a biorefinery. *Catalysis Today*, 111: 119–132

IKEGAMI, T., YANAGISHITA, H., KITAMOTOA, D., NEGISHI, H., HARAYA, K. & SANO, T. 2002. Concentration of fermented ethanol by pervaporation using silicalite membranes coated with silicone rubber. *Desalination*, 149:49-54.

KASENO, MIYAZAWA, I. &KOKUGAN, T. 1998. Effect of Product Removal by a Pervaporation on Ethanol Fermentation. *Journal of Fermentation and Bioengineering*, 86(5): 488-493.

NOMURA, M., BIN, T. & NAKAO, S. 2002. Selective ethanol extraction from fermentation broth using a silicalite membrane. *Separation and Purification Technology*, 27: 59-66.

O'BRIEN, D. J. & CRAIG, J.C. 1996. Ethanol production in a continuous fermentation/membrane pervaporation system. *Applied Microbiology Biotechnology*, 44:699-704.

O'BRIEN, D.J., SENSKE, G.E., KURANTZ, M.J., CRAIG, J.C. 2004. Ethanol recovery from corn fiber hydrolysate fermentations by pervaporation. *Bioresource Technology*, 92: 15-19.

SA see South Africa

SÁNCHEZ, O.J. & CARDONA, C.A. 2008. Trends in biotechnological production of fuel ethanol from different feedstocks. *Bioresource Technology*, 99: 5270-5295.

SCHMIDT, S.L., MYERS, M.D., KELLEY, S.S, MCMILLAN, J.D. & PADUKONE, N. 1997. Evaluation of PTMSP Membrane in Achieving Enhanced Ethanol Removal from Fermentation by Pervaporation. *Applied Biochemistry and Biotechnology*, 63-65: 469-482.

SOUTH AFRICA. Department of Minerals and Energy. 2007. Biofuels Industrial Strategy of the Republic of South Africa. Pretoria: Government Printer. 29p.

CHAPTER 2: FERMENTATION

OVERVIEW

The recognition of the finite reserves of fossil fuels together with the global rise in energy consumption has sparked new interest in the production of bioethanol by using the age-old technology of fermentation. The focus of Chapter 2 is on the remarkable process of fermentation, including the experimental work of this study.

In the first section of this chapter, Section 2.1, an overview of the concepts, terminology, and literature in the field of fermentation is presented. In addition, an investigation into previous research relating to the field of fermentation kinetics is necessary, shown in Section 2.1.4.

The experimental procedures used for the fermentation experiments follow in Section 2.2. The experimental set-up, experimental planning, analytical equipment and the reproducibility of the experimental work are all presented in this section.

The results of the fermentation experiments are discussed in Section 2.3. More specifically the influence of different feed compositions, yeast concentrations, and experimental conditions are addressed. The experimental data, sample calculations and calculated data for this chapter can be found in Appendix C.

In Section 2.4 a model to represent the fermentation process is developed and finally, in Section 2.5, concluding remarks are given.

2.1 INTRODUCTION TO THE FERMENTATION PROCESS

2.1.1. Introduction to biofuels

Renewable, sustainable, and clean energy sources to replace fossil fuels are becoming increasingly important due to a rising concern surrounding issues such as fossil fuel dependence, global warming, and the depletion of fossil fuels (Singhania *et al.*, 2009:3). Many countries do not possess oil resources and are looking into alternative fuels for fuel security reasons.

Biomass is an alternative energy source from which biofuels such as biogas, biodiesel, and bioethanol can be produced. More environmentally orientated countries are considering biomass fuels to replace fossil fuels as it is generally believed that less carbon dioxide or general pollution is emitted when these fuels are burned, especially if compared to fossil fuels (McGowan, 2009:7). Different biomass feedstocks can be used which make it possible for any country to grow biofuel feedstocks and if managed correctly these fuels would be a renewable and sustainable energy source. Biomass can be directly burnt to produce heat (known as bioenergy) or it can be converted to liquid fuels through chemical means. The major biomass-based liquid fuels are biodiesel and bioethanol and are mainly aimed at the transportation market (McGowan, 2009:37).

Governments have set future targets for the use of biofuels due to various benefits of these fuels (SA, 2007; Schnepf, 2006; NZ, 2007 & BIPP, 2010). These benefits include economic growth, lower carbon emissions, and energy independence. Due to these targets, the biofuel industry is expecting rapid growth in the near future. The Biofuels Industrial Strategy of the Republic of South Africa proposes that the total amount of biofuel used in the transportation sector be 2% by the year 2013, contributing to 30% of the national renewable energy target (SA, 2007:20). This target means that approximately 400 million litres of biofuel will have to be produced per year by this date (SA, 2007:3). The production of this amount of biofuel will create over 25 000 jobs, reducing unemployment by 0.6% and boosting economic growth by 0.05% (SA, 2007:9).

2.1.2. Bioethanol and its application

Currently ethanol production by biomass fermentation is one of the major technologies available to produce liquid fuel from renewable energy sources (Huber and Dumesic,

2006:122). Bioethanol is a major biofuel and mature markets for first generation bioethanol already exist, especially in Brazil and the USA (McGowan, 2009:42).

The two major uses for bioethanol are in the transportation sector and as a heating fuel to replace paraffin and wood. There are two distinct markets for bioethanol as transport fuel (Bergeron, 1996:61). The first and most valuable market is for ethanol as a blending component of petrol, while the other market is for ethanol as a pure fuel. Bioethanol is blended into fuels to oxygenate it, resulting in cleaner and more complete burning (BFAP, 2005:4). Up to 10% ethanol can be blended into transportation fuel without any modification to vehicles. Modified vehicles such as flexible fuel vehicles (FFV) can run on ethanol fuel blends of 85, 95, and even 100% (Bailey, 1996:37).

There are numerous advantages to using alcohol-fuelled engines compared to petrol-fuelled engines (Ghosh & Nag, 2008:199). Bioethanol has a higher octane number than petrol resulting in higher engine efficiency, more power, and high knock resistance. Less carbon dioxide is produced in the engine, i.e. only about 80% of that of a petrol-fuelled engine for the same power output. Bioethanol is also less volatile than petrol and has a higher flash point making ethanol-fuelled engines safer than petrol-fuelled engines.

2.1.3. Bioethanol production through fermentation

Fermentation is a chemical reaction that involves enzymatic hydrolysis of sucrose to glucose and fructose followed by the production of ethanol and carbon dioxide from these simple sugars (Demirbas, 2007:9). The enzyme invertase catalyses the hydrolysis of sucrose to glucose and fructose, as shown in Equation 2.1.

$$\underset{\text{Sucrose}}{C_{12}H_{22}O_{11}} \rightarrow \underset{\text{Glucose}}{C_6H_{12}O_6} + \underset{\text{Fructose}}{C_6H_{12}O_6} \qquad \text{Equation 2.1}$$

The enzyme zymase then converts glucose and fructose to ethanol, as shown in Equation 2.2.

$$\underset{\text{Glucose/Fructose}}{C_6H_{12}O_6} \rightarrow 2\underset{\text{Ethanol}}{C_2H_5OH} + \underset{\text{Carbon dioxide}}{2CO_2} \qquad \text{Equation 2.2}$$

Microorganisms, in which these enzymes are present, are used to produce ethanol through the process of fermentation. There are three types of microorganisms that can be used, i.e. yeast, bacteria and fungi (Naik *et al.*, 2010:585). The essential traits of a microorganism that are used for fermentation are high ethanol yield, high ethanol tolerance, resistance to hydrolysates, low fermentation pH, and a broad substrate utilisation range (Picataggio and

Zhang, 1996:165). Other desirable traits include a high specific growth rate, a high sugar consumption rate, high volumetric productivity, minimal nutrient requirement, high salt tolerance, and thermo tolerance (Picataggio & Zhang, 1996:165).

As mentioned there are various microorganisms able to produce ethanol as a product, but two groups, members of the yeast *Saccharomyces cerevisiae* and of the bacteria *Zymomonas mobilis*, are able to convert sugars such as glucose, fructose and sucrose into ethanol as a major end product. These two microbes have high ethanol yield, high ethanol tolerance, are generally considered safe, and have a variety of other desirable traits. *Saccharomyces cerevisiae* and *Zymomonas mobilis* are thus used industrially to produce ethanol. Traditionally the microorganism most commonly used for ethanol fermentation is *Saccharomyces cerevisiae* and it is still the leading specie used today (Lin & Tanaka, 2006:630 & Bai *et al.*, 2008:90).

Saccharomyces cerevisiae can grow on simple sugars, such a glucose and fructose, as well as on the more complex disaccharide sucrose (Lin & Tanaka, 2006:630). The Embden-Meyerhof (EM) pathway (also called glycolysis) is a model that describes how *Saccharomyces cerevisiae* metabolises glucose (Brock & Madigan, 1991:103 & Pelczar *et al.*, 1977:177-178). The EM pathway is a sequence of enzymatic reactions in the conversion of glucose to pyruvate and then to fermentation products (Brock & Madigan, 1991:103). It can be divided into three parts namely preparatory rearrangement reactions, oxidation-reduction reactions and a second oxidation-reduction reaction. A summarised version of the EM pathway is illustrated in Figure 2.1 (Brock & Madigan, 1991:103, Pelczar *et al.*, 1977:177-178 and Zhang & Chen, 2008:621).

One molecule of glucose is metabolised to produce two molecules of pyruvate. Each pyruvate molecule is then converted into ethanol under anaerobic conditions. Carbon dioxide is released during this process. Therefore, the overall reaction forms two ethanol molecules and two carbon dioxide molecules, as can also be seen in Equation 2.2. The fermentation process, as illustrated in Figure 2.1, takes place under anaerobic conditions.

Ethanol fermentation is a primary microbial metabolite, which means that the product is formed during the primary growth phase (Brock & Madigan, 1991:352). Two ATP molecules are formed during fermentation, which are used for the biosynthesis of yeast cells (Bai *et al.*, 2008:91). This means that yeast cells are produced in parallel with ethanol during fermentation. If the growth of yeast cells is interrupted in any way the glycolysis cycle will be stopped due to the accumulation of ATP (Bai *et al.*, 2008:91). The accumulated ATP inhibits an important regulation enzyme of the glycolysis process, phosphofructokinase (PFK). The fact that ethanol is produced during the growth of yeast cells (that ethanol is a growth

associated product) is especially important when considering the kinetics of ethanol production as will be discussed in Section 2.1.4.

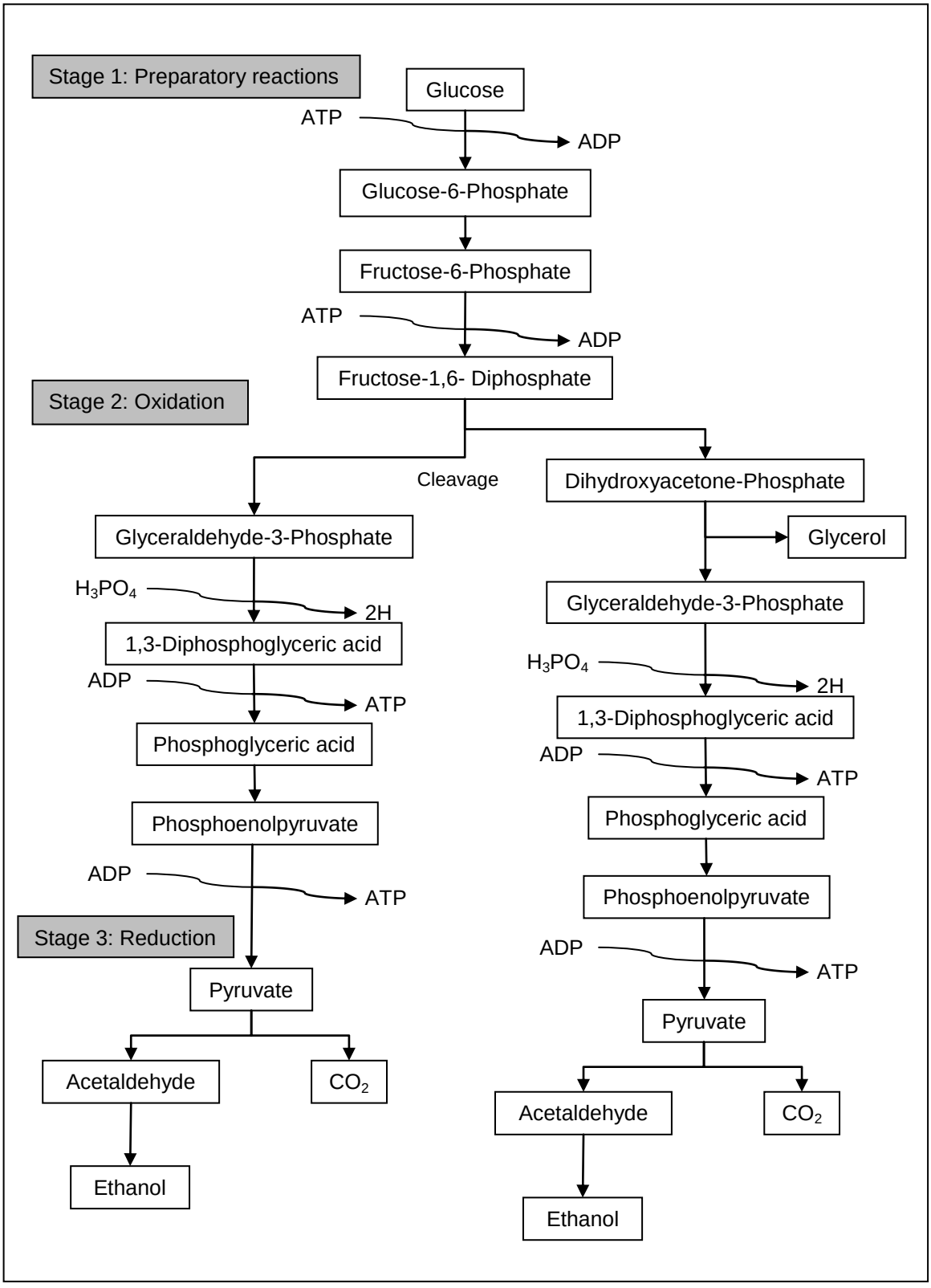

Figure 2.1 The EM pathway

Ethanol is the main product produced when *Saccharomyces cerevisiae* ferments sugars. Theoretically, the amount of ethanol produced will be 51.1wt% and the amount of carbon dioxide will be 48.9wt%. The theoretical ethanol amount will never be achieved, however, as some of the sugar is used for yeast cell production, cell growth, and cell maintenance. Because of this, only about a 40-48% of the glucose is actually converted to ethanol (Naik *et al*., 2010:585). The ethanol yield is also affected by the by-products formed during fermentation.

By-products that can be formed during fermentation are glycerol and organic acids such as acetic acid, pyruvic acid, and succinic acid to name a few (Zhang & Chen, 2008:620). Glycerol is the main by-product of the fermentation process and is formed in a very small amount (about 5% of the carbon source). During growth under osmotic stress conditions or other process conditions such as a high pH the conversion of dihydroxyacetone phosphate to glycerol is stimulated and high amounts of glycerol are produced (as shown in Figure 2.1) (Zhang & Chen, 2008:620).

Inhibition of yeast cell growth and ethanol production can happen during a fermentation process and are the result of various stresses on a yeast cell. Some stresses are environmental such as nutrient deficiency, high temperature, and contamination while other stresses are from the yeast cell metabolism such as high ethanol concentration (Bai *et al.*, 2008:92). Fermentation is inhibited by ethanol and the yeast *Saccharomyces cerevisiae* can usually deal with only 4 to 16wt% ethanol, depending on the specific strain of *Saccharomyces cerevisiae* (Fischer *et al.*, 2008:298). Product inhibition may lead to low yeast cell growth and lower ethanol yield. *In situ* removal of ethanol from the fermentation broth is an effective way to minimise the inhibition effect caused by high ethanol concentrations while good control over the process conditions will minimise environmental inhibition.

Process conditions such as temperature, pH, amount of oxygen and the amount and type of nutrients in the fermentation broth have a large influence on the performance of yeast cells. *Saccharomyces cerevisiae* has an optimum temperature of between 30 and 35°C (Taherzadeh & Karimi, 2008:96). Lower temperatures may reduce the growth and activity of the yeast whereas higher temperatures will kill the yeast cells. The pH range for fermentation by yeast is acidic (Lin & Tanaka, 2006:635). No oxygen should be supplied to the process, as the process is anaerobic. The best possible production of ethanol can be attained by controlling the main process conditions as effectively as possible for a specific process.

2.1.4. Bioethanol production: kinetics

2.1.4.1 Introduction to kinetic modelling

Reaction kinetics deals with how fast a reaction proceeds (also known as the reaction rate) and the effects of different process conditions (such as pressure, temperature, composition, and catalysts) on the reaction rate. A kinetic expression is an algebraic equation that describes the conversion of reactants or the formation of products by relating the rate of the reaction to the concentration of the species present (Fogler, 2006:82). A set of these kinetic expressions (also called a kinetic model) represents the original system and within a limited region, it can predict the kinetic behaviour of the original system (Bellgardt, 2000a:3). The experimental study of the original system can then be replaced by the model. The process of modelling is illustrated in Table 2.1 (Bellgardt, 2000a:5).

Table 2.1 Step sequence of model building

Step	Action
1	Running typical experiments
2	Define the modelling goal
3	Analysis of the system and determination of structural elements
4	Simplifying by assumptions (e.g. about mixing, metabolism, process structure)
5	Choice of important process variables: parameters, input variables and states
6	Establishing the model
7	Simulating the model, parameter identification to fit it to experimental data
8	Evaluation of the model quality; repeat with step 1

Kinetic modelling is an iterative process, which should always start with the most basic equation by way of assumptions (Birol *et al.*, 1998:764 & Bellgardt, 2000a:5). If the model does not sufficiently describe the experimental data of the process, the assumptions should be changed; in this way, the model grows in complexity and accuracy without becoming too complex. Repeating steps 4 to 8 of Table 2.1 leads to a kinetic model that will give a good representation of a particular chemical process. Aspects to be considered when deciding on what represents a good description include the accuracy of the mathematical fit and the range over which the fit extends. Once the model has been established, it can be used to predict performance under different process conditions as well as for process design, process optimisation, and process control, and in doing so reduce research and development time and cost (Dunn *et al.*, 1992:10).

It is the focus of this section to introduce fundamental concepts and theories relevant to the understanding of kinetics specifically applying to fermentation processes and to present a literature review of research in the field of fermentation kinetics.

2.1.4.2 Theoretical background of fermentation kinetics

There is an abundance of publications and reviews available on the topic of fermentation (Bai *et al.*, 2008; Lin & Tanaka, 2006; Naik *et al.*, 2010) and as such, it is the aim of this section to summarise fundamental concepts and theories related to the subject of fermentation kinetics and modelling. Fermentation kinetic studies are concerned with the rate of cell growth, substrate utilisation, and product formation along with the effect of different environmental conditions on these rates (Aiba *et al.*, 1973:92).

The cell mass of yeast increases exponentially with respect to time. This is explained by the fact that each yeast cell has the same probability to multiply. Figure 2.2 illustrates a typical yeast cell growth-curve (Monod, 1949:374).

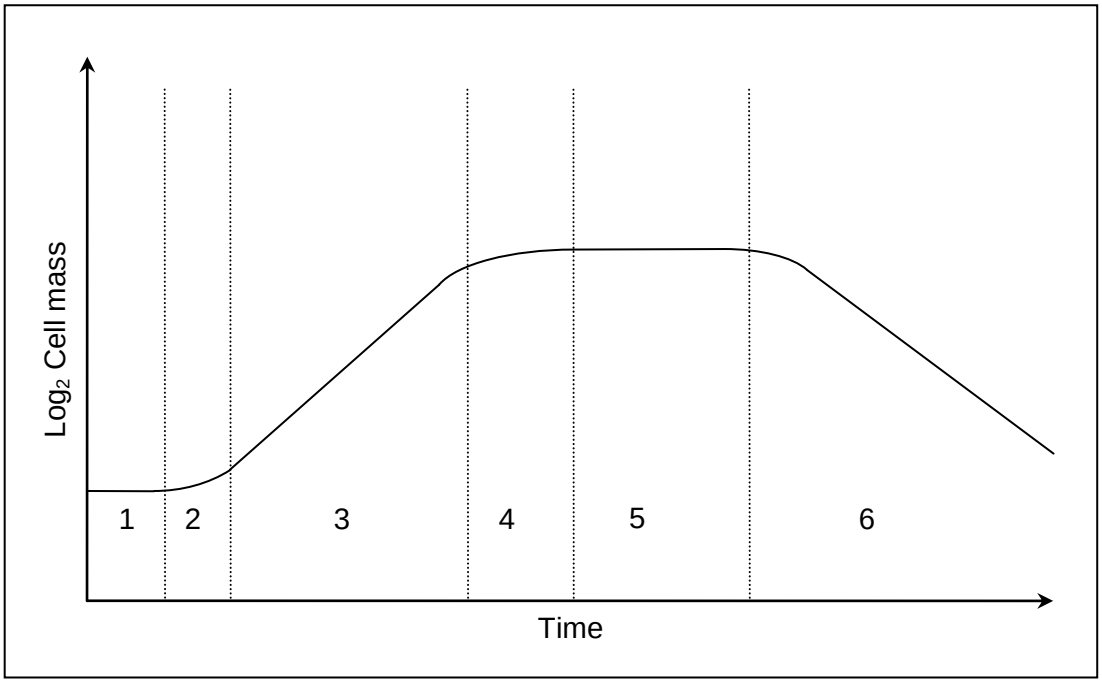

Figure 2.2 Yeast cell growth in a batch system
(1: lag phase; 2: acceleration phase; 3: exponential phase; 4: deceleration phase; 5: stationary phase; 6: death phase)

Yeast cells in a batch system go through various phases of growth; lag, acceleration, exponential growth, deceleration, stationary, and death phase. The lag phase is an adjustment phase directly after the yeast cells have been introduced into a new environment

where no cell growth occurs. The yeast cells needs to manufacture chemicals needed for growth and reproduction and as a result, a time lag is experienced. The lag phase is dependent on the age of the cells and as such, it will be much longer for older yeast cells than for young cells (this is of course dependent on the specific type of microorganism) (Levenspiel, 1999: 625). After the lag phase, exponential growth occurs where the cell mass and cell number increase exponentially. Due to changes in the batch system the growth rate changes and eventually a drop in growth rate is experienced (stationary phase where the growth rate equals the death rate and death phase where the death rate is higher than the growth rate). The drop in growth rate is due to depletion of food, accumulation of materials toxic to the yeast cells or a change in process conditions, such as temperature or pH, that is lethal to the yeast cells. Ethanol is a growth associated product (primary metabolite) during anaerobic alcohol fermentation which means that ethanol is produced during active cell growth. Therefore the product concentration and cell concentration would show a very similar pattern (Bellgardt, 2000b:49).

Determining the reaction kinetics of a reaction taking place homogenously in a single stage is already a complicated matter but the complexity of biological processes that occur in living cells (such as yeast fermentation shown in Figure 2.1 that consists of a series of reactions) means that kinetic modelling of a biological process may be exceptionally difficult (Dunn *et al.*, 1992:63). By not considering any intracellular elements, states or inner balances of the cells (it is assumed that the metabolism is in a balanced state) the biological process can be greatly simplified. Models that do not account for intracellular changes are called unstructured models (Bellgardt, 2000b:52). Structured models consider the internal elements (internal balances and intrinsic reactions) of the cell which means that properties of the cells vary with time. Figure 2.3 shows the difference between unstructured and structured models (Dunn *et al.*, 1992:86).

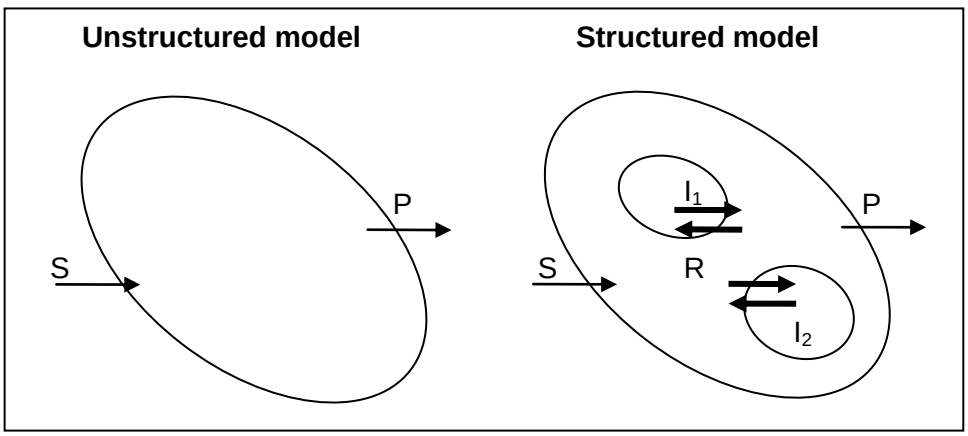

Figure 2.3 Structured and unstructured models

Structured models are seldom used as it is very difficult to obtain sufficient knowledge about cell metabolism experimentally to develop a realistic structured model and if a model has been developed, it is very difficult to determine the values of the model's parameters and to evaluate the model (Dunn *et al.*, 1992:87 & Bellgardt, 2000b:74). Thus, most of the models proposed for fermentation kinetics are unstructured and empirical (Kovárová-kovar & Egli, 1998:650).

Most unstructured models are also nonsegregated models as the cells are considered homogenous biomass, all with the same characteristics at any given time (Bellgardt, 2000b:52). Nonsegregated models assume that all of the cells are at the same state of cell growth or cell division and that there are no interactions between the cells. The biological reactions in unstructured nonsegregated models depend directly and only on the conditions in the bioreactor or shake flask. Therefore, these models are a combination of kinetics describing the influence that process variables such as pH, temperature, initial cell mass, or substrate concentrations.

2.1.4.3 Literature review of unstructured fermentation kinetic modelling

Mathematic modelling of fermentation processes is a widely studied topic in the field of biotechnology and a vast number of kinetic models have been reported in literature (Tan *et al.*, 1996:602; Monod, 1949; Contois, 1959). The most well-known unstructured nonsegregated kinetic model is the Monod model for cell growth, which was introduced to the world in 1949 by a Frenchman named Jacques Monod (Monod, 1949). The Monod model is used as a basis for most recently developed models and as a result, Monod-type models dominate the field.

The differential equations, Equation 2.3 and Equation 2.4, describe cell growth, and product formation as used in most microbial kinetic models.

$$\frac{dX}{dt} = \mu X \qquad \text{Equation 2.3}$$

$$\frac{dP}{dt} = \nu X \qquad \text{Equation 2.4}$$

In Equation 2.3 and 2.4 as well as any subsequent equations X (g cells.L^{-1}) refers to the cell concentration, P (g product.L^{-1}) to the product concentration, μ (h^{-1}) to the specific cell growth rate and v (h^{-1}) to the specific product production rate. Monod's model relates the specific growth rate (μ) of microorganisms to the concentration of a growth controlling

substrate (S (g substrate.L^{-1})) using a relatively simple empirical equation as shown in Equation 2.5 (Monod, 1949:383). Monod studied bacterial cultures in particular in his breakthrough work in 1949.

$$\mu = \mu_{max} \frac{S}{K_{sx} + S} \qquad \text{Equation 2.5}$$

Two parameters namely the maximum specific growth rate (μ_{max} (h^{-1})) and the Monod constant (K_{sx} (g carbon source.m^{-3})) are used in Equation 2.5 to relate growth rate to the substrate concentration. In Monod's original work, the parameters are referred to as R_K and C_1 respectively but μ_{max} and K_s are used by most researchers in more recent literature (for example Blanco *et al.*, 2006 and Birol *et al.*, 1998).

The specific fermentation rate, v, can be related to the concentration of the growth controlling substrate by using Equation 2.6 (Birol *et al.*, 1998:766 & Blanco *et al.*, 2006:366).

$$v = v_{max} \frac{S}{K_{sp} + S} \qquad \text{Equation 2.6}$$

Substrate utilisation and growth associated product formation can be described in terms of cell growth by using yield coefficients. Yield coefficients are a measure of how effectively a growth substrate is converted into cell material, as shown in Equation 2.7 and Equation 2.8.

$$Y_{X/S} = \frac{dX}{dS} \qquad \text{Equation 2.7}$$

$$Y_{P/S} = \frac{dP}{dS} \qquad \text{Equation 2.8}$$

In terms of ethanol production through fermentation, $Y_{X/S}$ is the ratio of cells produced per substrate consumed for growth and $Y_{P/S}$ is the ratio of ethanol produced per substrate consumed for fermentation. Monod's model assumes that substrate utilisation and product formation can be linearly linked to cell formation by these yield coefficients as shown in Equation 2.9 (Birol *et al.*, 1998:766 and Blanco *et al.*, 2006:366).

$$\frac{dS}{dt} = -\left(\frac{1}{Y_{X/S}}\frac{dX}{dt}\right) - \left(\frac{1}{Y_{P/S}}\frac{dP}{dt}\right) \qquad \text{Equation 2.9}$$

The model proposed by Monod was easily accepted by the scientific community, as this relatively simple equation reasonably expressed the growth kinetics of microorganisms. However, Monod's model is too simplified for most biological processes, as it does not

consider that cells may require substrate or produce products while they are not growing. Furthermore, the Monod model considers only one substrate as limiting, it does not include any lag in cell growth, and it does not account for death phase, to name only a few shortcomings. As a result, a range of other models has been suggested over the years.

There are different ways in which a model for growth kinetics is designed. One method often used by researchers is to incorporate additional constants into the original Monod model to describe additional aspects present in the biological system. Some of the models that make use of the original Monod model, therefore called modified Monod models, are presented in Table 2.2.

The Monod model regards the specific growth rate of a microorganism only as a function of the concentration of the limiting substrate. The growth rates of cells are, however, affected by the cell population density as well. Contois (1959) attempted to develop a better model for cell growth by incorporating the effect population density has on the growth rate. Contois studied the growth of the bacteria *Aerobacter aerogenes* in a media that contained ammonium as a nitrogen source and glucose or succinate as a carbon source (Contois, 1959:40). Either the nitrogen source or the carbon source was limiting with all other components present in the media in excess. The Monod model was used as a starting point and by including cell density the Contois model was developed, as shown by Equation 2.11.

$$\mu = \mu_{\max} \frac{S}{B_i X + S} \qquad \text{Equation 2.11}$$

Contois believed that the Contois model represented microbial growth more realistically than previous models presented in literature.

It is well known that during alcoholic fermentation cell growth as well as ethanol production (as it is a growth-associated product) is inhibited by ethanol. Monod's model only accounts for substrate limitations and not for product inhibition. Aiba *et al.* (1968) proposed a model to formulate the inhibitory effect of ethanol on the yeast cell growth as well as on ethanol production. The inhibitory effect of ethanol was studied by doing fermentation experiments with baker's yeast and glucose. An initial glucose concentration of 10 and 20 $g.L^{-1}$ was used at a temperature of 30°C and a pH of 4. Ethanol was added in different concentrations to investigate the inhibition effect on yeast cell growth and ethanol production. The Aiba model for cell growth is shown in Equation 2.12.

$$\mu = \mu_0 e^{-k_1 P} \frac{S}{K_S + S} \qquad \text{Equation 2.12}$$

Table 2.2 Summary of some Monod-based models

Model name	Year	Equation for cell growth	Aspects of cell growth it takes into account
Monod	1949	$\mu = \mu_{\max} \frac{S}{K_{sx} + S}$	Substrate limitation
Moser	1958	$\mu = \mu_{\max} \frac{S^n}{K_{sx} + S^n}$	Substrate limitation
Contois	1959	$\mu = \mu_{\max} \frac{S}{B_i X + S}$	Substrate limitation and cell population density
Aiba	1968	$\mu = \mu_0 e^{-k_1 P} \frac{S}{K_{sx} + S}$	Substrate limitation and product inhibition
Andrews	1968	$\mu = \mu_{\max} \frac{S}{K_{sx} + S + \frac{S^2}{K_i}}$	Substrate limitation and substrate inhibition
Aiba-Edwards	1970	$\mu = \mu_0 e^{-\frac{S}{K_{ix}}} \frac{S}{K_S + S}$	Substrate limitation and substrate inhibition
Ghose and Tyagi	1979	$\mu = \mu_{\max} \left(1 - \frac{P}{P_{x,\max}} \right) X$	Product inhibition
Levenspiel	1980	$\mu = \mu_{\max} \frac{S}{K_{sx} + S} \left(1 - \frac{P}{P_{x,\max}} \right)^n$	Substrate limitation and product inhibition
Luong	1985	$\mu = \mu_{\max} \left(\frac{S}{K_{sx} + S} \right) \left(1 - \frac{S}{S_{s,\max}} \right)^n$	Substrate limitation, substrate inhibition
Ghaly and Taweel	1997	$\mu = \mu_{\max} \frac{S}{K_{sx} + S} \frac{K_p}{K_p + P} \frac{K_s'}{K_s' + S}$	Substrate limitation, substrate inhibition, ethanol inhibition and cell death

Equation 2.13 was derived to account for the inhibitory effect of ethanol on the fermentation activity of the yeast cells.

$$\nu = \nu_0 e^{-k_2 P} \frac{S}{K_S' + S} \qquad \text{Equation 2.13}$$

In the Aiba model subscript "0" refers to the specific growth or fermentation rate where the product concentration is equal to zero, k_1 and k_2 are constants, and K_s and K_s' are the Monod constants for cell growth and ethanol production respectively. The model in Equations 2.12 and 2.13 correlated well to the experimental data obtained by Aiba *et al*. There are two major problems with these models (as discussed by Bai *et al.*, 2008:94). The first problem is that according to these models cell growth is never completely inhibited even if the ethanol concentration approaches infinity, which is an unrealistic statement. Secondly, if the fermentation broth contains a very low sugar concentration and continuous fermentation is done with a very low dilution rate, it is likely that the limiting sugar concentration may be near zero. According to the Aiba model cell growth and ethanol production will be zero as well, which is incorrect since yeast cells and ethanol are continuously produced in practice.

A modification on the Aiba model is the Edwards model, also known as the Aiba-Edwards model as presented by Equation 2.14 and Equation 2.15 (Tan *et al.*, 1996:602). The Aiba model was adapted so that substrate inhibition is taken into account.

$$\mu = \mu_0 e^{-\frac{S}{K_{ix}}} \frac{S}{K_S + S} \qquad \text{Equation 2.14}$$

$$\nu = \nu_0 e^{-\frac{S}{K_{ip}}} \frac{S}{K_S' + S} \qquad \text{Equation 2.15}$$

The constants K_{ix} and K_{ip} are the inhibition constants for cell growth and ethanol production respectively. Tan *et al.* (1996) compared experimental data from literature to the Edwards model as well as two models designed by them. Of the three sets of experimental data tested, the Edwards model only represented one very well (with μ_{max}= 0.569±0.285h^{-1}, K_s=0.122±0.063 mM and K_{ix}=33.35±3.72 mM) while no unique set of parameters could be determined for another one. This verifies the fact that it can never be assumed that any kinetic model will be valid for a real process.

Levenspiel (1999:645) modified the Monod model so that product inhibition would also be accounted for. This model, Equation 2.16, is a more general form of Monod kinetics as the product poisoning term reduces to one when there is no product inhibition.

$$\mu = \mu_{\max} \frac{S}{K_{sx} + S}\left(1 - \frac{P}{P_{x,\max}}\right)^{n} \qquad \text{Equation 2.16}$$

In Equation 2.16 $P_{x,max}$ (g product.L^{-1}) is the product concentration where the fermentation process stops, and n is the order of product poisoning.

More recently, Ghaley and El-Taweel (1997) developed a kinetic model for continuous fermentation of ethanol from cheese whey. Ghaley and El-Taweel used the yeast *Candida Pseudotropicalis*. The model accounts for substrate limitation, substrate inhibition, ethanol inhibition, as well as cell death. A high accuracy has been achieved using Ghaley and El-Taweel's model to predict cell, lactose, and ethanol concentrations. Monod kinetics was modified by adding a term to account for product inhibition and a term to account for substrate inhibition as shown in Equation 2.17.

$$\mu = \mu_{\max} \frac{S}{K_{sx} + S} \frac{K_p}{K_p + P} \frac{K_s'}{K_s' + S} \qquad \text{Equation 2.17}$$

Equation 2.17 is then combined with a mass balance over the system to give Equation 2.18.

$$\frac{dX}{dt} = X\left[\mu_{\max} \frac{S}{K_{sx} + S} \frac{K_p}{K_p + P} \frac{K_s'}{K_s' + S} - \frac{1}{R} - K_d\right] \qquad \text{Equation 2.18}$$

As previously mentioned in this section, it is very difficult to predict which model will fit with which process, as the suitability of each model is dependent on the specific microorganism and process conditions (Tan *et al.*, 1996:602). Roca *et al.* (1996) found that the original Monod model fitted their experimental data well even though it is so simplified. The focus of Roca ***et al.'s*** research was on the use of a pulsing packed column bioreactor and mass transfer but they determined the fermentation kinetics for their system using immobilised *Saccharomyces cerevisiae* and glucose (100 and 200 g.L^{-1}) in batch experiments at 30°C. The kinetic parameters μ_{max} and K_{sx} equalled 1.51h^{-1} and 0.44g.L^{-1} respectively. Another example where the simple Monod model also gave a good representation of the experimental data was with the data of Birol *et al.* (1998). Birol *et al.* fermented glucose using immobilised *Saccharomyces cerevisiae* and studied a variety of different kinetic models. The kinetic parameters varied with different initial glucose levels, at an initial glucose concentration of 2%, μ_{max} and K_{sx} were 0.186h^{-1} and 0.390g.L^{-1} respectively, while at a glucose concentration of 10%, μ_{max} were 0.758h^{-1} and K_{sx} were 362.65g.L^{-1}.

Four factors, namely substrate limitation, substrate inhibition, product inhibition, and cell death, influence cell growth and ethanol fermentation. Most of the models discussed here

account for only one or two of these factors and a model that accounts for all four of these factors will most likely give an improved representation of fermentation. At present, the development of a general kinetic model that is valid for a wide range of fermentation processes and that can provide a theoretical basis for the existing empirical models is required in this field. By studying more fermentation processes and by incorporating more factors that affect fermentation research will get closer to a more general model. The main objective to be addressed within this chapter was to develop a fermentation model to represent glucose fermentation.

2.2 EXPERIMENTAL METHODS AND PROCEDURES

2.2.1. Chemicals used

The chemicals used in the fermentation experiments of this study, as well as the supplier and the purity of the chemical, are listed in Table 2.3.

Table 2.3 Chemicals used in this study

Chemical	Supplier	Purity	Use
Glucose	Associated chemical enterprise (ACE)	Analytical grade	Fermentation feedstock and calibration curve
Sodium hydroxide	Fluka	>98%	pH adjustment
Sulphuric acid	Associated chemical enterprise (ACE)	98%	pH adjustment
Ethanol	Rochelle	99.9%	Calibration curve
Glycerol	Associated chemical enterprise (ACE)	99%	Calibration curve
Buffer solution pH 7	Hanna Instruments	---	pH meter calibration
Buffer solution pH 4	Hanna Instruments	---	pH meter calibration

The chemicals were used as received and no further purification was done. The microorganism used for fermentation was commercial baker's yeast (*Saccharomyces cerevisiae*) obtained from Anchor Yeast in South Africa.

2.2.2. Apparatus and experimental procedure

Traditional batch fermentation was done using glucose as feedstock and baker's yeast as fermenting microorganism. The experimental apparatus used in this study to generate fermentation data is listed in Table 2.4.

Table 2.4 Apparatus used for fermentation

Apparatus	Description	Supplier
Shaker incubator	Used to keep fermentation temperature constant at 30°C	Labcon (model FSIE-SPO 8-35)
Mass balance	All chemicals used were weighed using the mass balance	Scientech
pH meter	Used to measure pH	Hanna Instruments
Autoclave	To sterilise glucose mixture before yeast was added	D & E International Corp

One litre Scott Duran bottles were used as bioreactors for fermentation. The desired amount of glucose and water were measured by using the mass balance. The mixture was transferred to the bioreactor after it had been sterilised using an autoclave at 121°C for 30 minutes. Sterilisation would ensure that no microorganisms other than the yeast cells added would be present in the bioreactor and therefore would prevent contamination. After the glucose mixture had cooled down to about 30°C, the pH was adjusted and a small amount of the mixture was transferred to a separate beaker. The desired amount of baker's yeast was measured by using the mass balance before it was added to the mixture in the separate beaker to activate the dry baker's yeast. The activated yeast was then added to the bioreactor and placed in an incubator at 30°C. The incubator regulated the temperature of the fermentation broth.

The fermentation broth was incubated for 72 hours and samples were collected at various time intervals. Two samples were taken at each time interval; one sample was used to measure the yeast cell concentration by using a spectrophotometer while the other sample was immediately prepared for analysis with a high performance liquid chromatography (HPLC). Glucose, ethanol, and glycerol concentration were measured with the HPLC. The analytical methods and sample preparation are discussed in Section 2.2.5. The pH of the fermentation broth was measured and adjusted before each sample was taken. The pH was measured by using a Hanna pH meter and regulated by adjusting the fermentation broth with either 1M ($mol.dm^{-3}$) sodium hydroxide or 0.1M ($mol.dm^{-3}$) sulphuric acid. The pH meter was calibrated on a regular basis by using buffer solutions.

2.2.3. Experimental design and planning

A classical experimental design was followed where one variable was varied while all the other variables were kept constant. The glucose concentration was varied between 5 and 35wt% while the yeast concentration and the pH were kept constant at $10g.L^{-1}$ and 4 respectively. The glucose concentration used for the experiment with the highest final

ethanol yield when glucose concentration was varied was used for all successive experiments. The yeast concentration was varied between 1 and 10g.L^{-1} while the glucose concentration and pH were kept constant. The optimum yeast concentration was determined which was used for all subsequent experiments. The pH was varied between 2.5 and 6 while the glucose concentration and yeast concentration were kept constant. The reproducibility of the experimental method was validated (as discussed in Section 2.2.4) by repeating experiments at the same conditions.

2.2.4. Reproducibility of experimental method

It is important to determine the reproducibility of the results obtained through experimentation as it confirms the conclusions drawn from the experiments. The reproducibility of results (experimental error) for each type of experiment was determined by conducting at least three experimental runs at the same conditions. The experimental error of the final ethanol yield for the fermentation experiments was found to be 0.75% for the experiments where the yeast concentration was varied, 7.43% where the pH was varied and 9.92% where the starting glucose concentration was varied. The experimental error is discussed in more detail in Appendix A with the calculated statistical parameters of the fermentation experiments shown in Section A.2.

2.2.5. Analytical techniques

2.2.5.1. HPLC analyses

An Agilent technology 1200 series High Performance Liquid Chromatography (HPLC) system fitted with a Shodex sugar column and a refractive index detector was used to analyse all samples collected during fermentation. The operating conditions used in the analysis are listed in Table 2.5.

Samples for HPLC analyses were prepared by filtering through three different sized filters, i.e. a yeast removal filter, a 0.45μm filter, and a 0.2μm filter. The yeast filter stops the fermentation reaction by removing any yeast present while the 0.45μm filter and 0.2μm filter remove any residual solids that may damage the column.

Table 2.5 Operating conditions of HPLC

Operating conditions	
Mobile phase	HPLC grade water
Flow rate	1.00ml/min
Injection volume	2µl
Column temperature	80°C
Detector temperature	55°C
Run time	20 min

It was determined that samples taken from the fermentation broth contained only glucose, ethanol, and/or glycerol. The concentration of each component present in the samples was quantified with a set of standard calibration curves. The calibration curves as well as the method used to quantify components in the samples are given in detail in Appendix B.

2.2.5.2. Spectrophotometer analyses

A spectrophotometer was used to determine the yeast cell concentration. The spectrophotometer measured the optical density of the sample. The sample was transferred to a cuvette and the optical density (absorbance) at a wavelength of 600nm was measured. A calibration curve to relate the absorbance measured by the spectrophotometer to the amount of yeast cells present was prepared by using known amounts of yeast cells, as discussed in Appendix B.

2.3 RESULTS AND DISCUSSION

The specific focus of this section was on the influence of different fermentation variables on the ethanol yield. The fermentation variables of this study were the wt% glucose (5-35wt%), the starting yeast cell concentration (1-10g.L^{-1}), and the pH (2.5-6). All of the fermentation experiments were carried out at 30°C in the absence of nutrients.

Through HPLC analyses, it was found that two products were present in the samples, namely ethanol and glycerol. Glycerol is produced by the yeast cells to equilibrate the intracellular redox balance by converting surplus NADH that is formed during cell formation to NAD^+ (Munene *et al.*, 2002:312, Bakker *et al*. 2001:17 & Bideaux *et al*., 2006:2135). Glycerol production is also linked to osmotic stability in yeast cells as it protects the cells against dehydration. As a result, glycerol production is increased during osmotic stress conditions (Munene *et al.*, 2002:311). Ethanol was the main fermentation product but the amount of glycerol formed can significantly influence the final ethanol yield and therefore

both the ethanol and glycerol yields will be discussed. As it is usually the aim to produce the maximum amount of ethanol, glycerol production by the yeast cells has to be a minimum (Bideaux *et al.*, 2006:2134).

2.3.1. Influence of starting feed composition

The effect that the starting glucose concentration has on the final ethanol yield was investigated. The starting glucose wt% was varied between 5 and 35 wt%. The pH was adjusted to 4 and a starting yeast concentration of 10g.L^{-1} was used. The effect of the starting glucose concentration on the ethanol yield (gram ethanol produced per gram of glucose) during the fermentation process is shown in Figure 2.4.

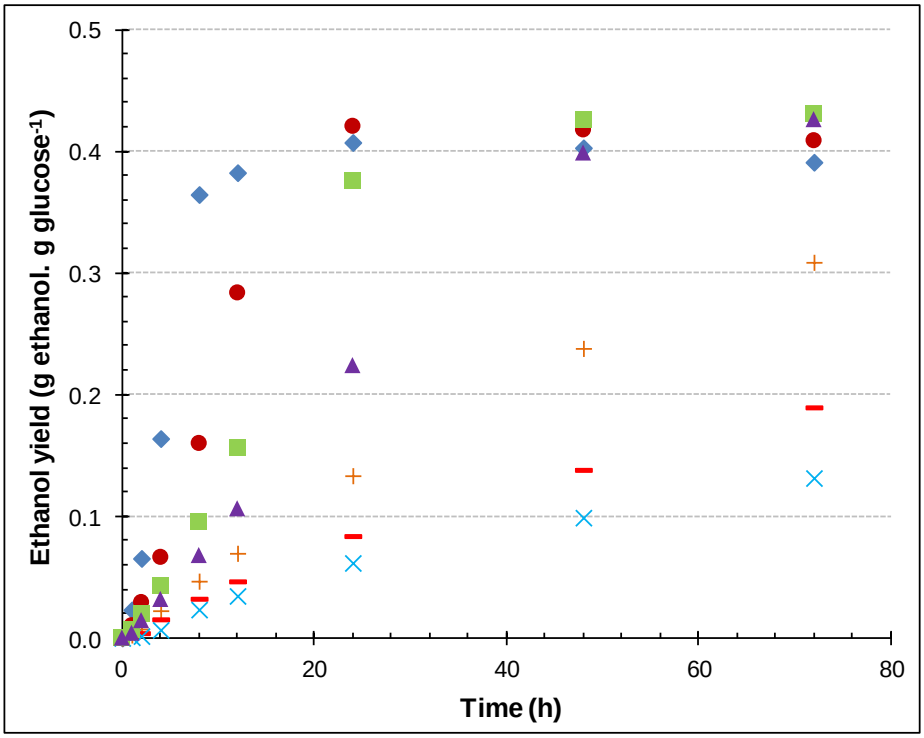

Figure 2.4 Effect of starting glucose on ethanol yield
(♦5wt% glucose, ●10wt% glucose, ■15wt% glucose, ▲20wt% glucose, +25wt% glucose, – 30wt% glucose, x35wt% glucose)

It is clear from Figure 2.4 that the ethanol yield was significantly reduced when a high wt% of glucose was used. Both the fermentation kinetics (the ethanol forms slower) as well as the final ethanol yield obtained during fermentation is affected by a high wt% glucose. Figure 2.5 shows the effect of glucose concentration on the final ethanol yield as well as the final glycerol yield (after 72 hours of fermentation).

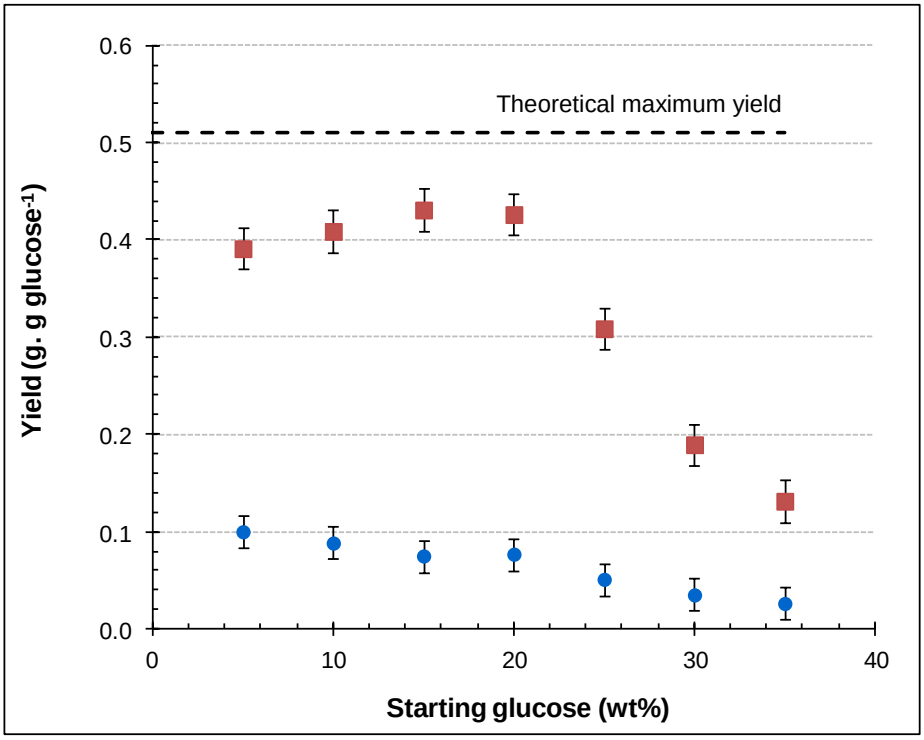

Figure 2.5 Effect of feed composition on final ethanol and glycerol yield (■ ethanol, ● glycerol)

The ethanol yield is relatively higher for glucose concentrations below 20wt%. When the starting glucose concentration is increased above 20wt% the ethanol yield declines sharply. Theoretically, the maximum yield that can be obtained for ethanol is 0.51g.g^{-1} (shown by the dashed line) and for carbon dioxide is 0.49g.g^{-1}. A maximum ethanol yield of 0.43±0.02g.g^{-1} was obtained when 15wt% glucose was used and this value corresponds to approximately 84% of the theoretical maximum. The glycerol yield at 15wt% glucose was 0.08±0.02g.g^{-1} which is the lowest amount of glycerol produced between 5wt% and 20wt% starting glucose.

The amount of glucose that is utilised for ethanol and glycerol production respectively after 72 hours is presented in Table 2.6. Together Figure 2.5 and Table 2.6 show that the total glucose utilisation and the glucose utilisation for ethanol production increase with initial glucose wt% up to a maximum at 15wt% starting glucose. At higher glucose wt%, the glucose utilisation decreases. *Saccharomyces cerevisiae* experiences osmotic pressure when exposed to a very high sugar concentration that interferes with normal cell functions and this hinders cell growth (and therefore ethanol production). Gray (1944:450) found that glucose concentrations above 20wt% caused the yeast cells to plasmolyse while at lower concentrations (13.4% and 6.7%) no effect was observed.

Table 2.6 The effect of initial glucose concentration upon the wt% of glucose utilisation after 72 hours

Initial glucose (wt%)	Total glucose utilization (%)	Glucose utilisation for ethanol production (%)	Glucose utilisation for glycerol production (%)	Ratio (glycerol to ethanol)
5	96	86	10	0.116
10	97	88	9	0.100
15	99	92	8	0.082
20	98	91	8	0.085
25	70	65	5	0.078
30	44	40	4	0.087
35	31	28	3	0.093

It is expected that glycerol production will increase with an increase in starting glucose wt% due to osmotic stress (Munene *et al.*, 2002:311 and D'Amore *et al*., 1988:111). However, as seen in Figure 2.5 and Table 2.6, this is not the case as the glycerol production decreases with an increase in initial glucose. This can be explained by the fact that glycerol production is not dependent on osmotic pressure alone. The main reason that yeast cells produce glycerol is to counterbalance excess NADH that forms during fermentation when yeast cells are produced as shown in Figure 2.6 (Munene *et al*., 2002:312 and Bakker *et al*., 2001:18).

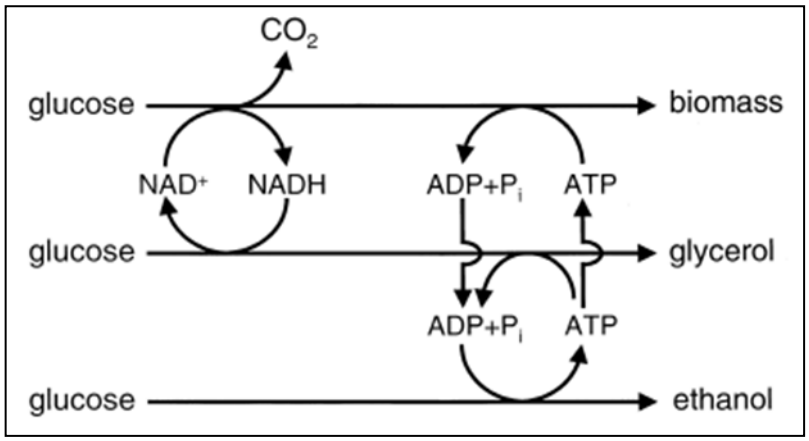

Figure 2.6 Schematic overview of NAD+/NADH turnover in fermentive cultures of Saccharomyces cerevisiae

At high osmotic pressures, the yeast cells do not grow or reproduce normally (Munene *et al*., 2002:311) and a decrease in cell growth will be observed (D'Amore *et al*., 1988:111). A decrease in cell growth will affect the production of glycerol, as the excess amounts of NADH that form under normal circumstances will be reduced. However, it cannot be proven that the cell growth is affected by high osmotic pressures due to the large experimental error on the yeast cell concentration for this set of experiments. It can, however, be said that the ratio of glucose used for ethanol production to glucose used for glycerol production stays relatively the same for starting glucose concentrations from 15wt% to 35wt%, which means

that glycerol production is dependent on ethanol production. Ethanol production is a cell growth associated metabolite (Brock & Madigan, 1991:352), which supports the hypothesis that the decrease in glycerol is due to a decrease in cell growth.

2.3.2. Influence of starting yeast concentration

The effect that the starting yeast concentration would have on the final ethanol yield was investigated. The starting yeast concentration was varied between 1 and 10g.L^{-1}. A 15wt% glucose feed composition (found to be the optimum in the previous set of experiments where wt% glucose was varied) was used for all of the experiments and a constant pH of 4. The effect of the starting yeast concentration on the ethanol yield (gram ethanol produced per gram of glucose) during the fermentation process is shown in Figure 2.7.

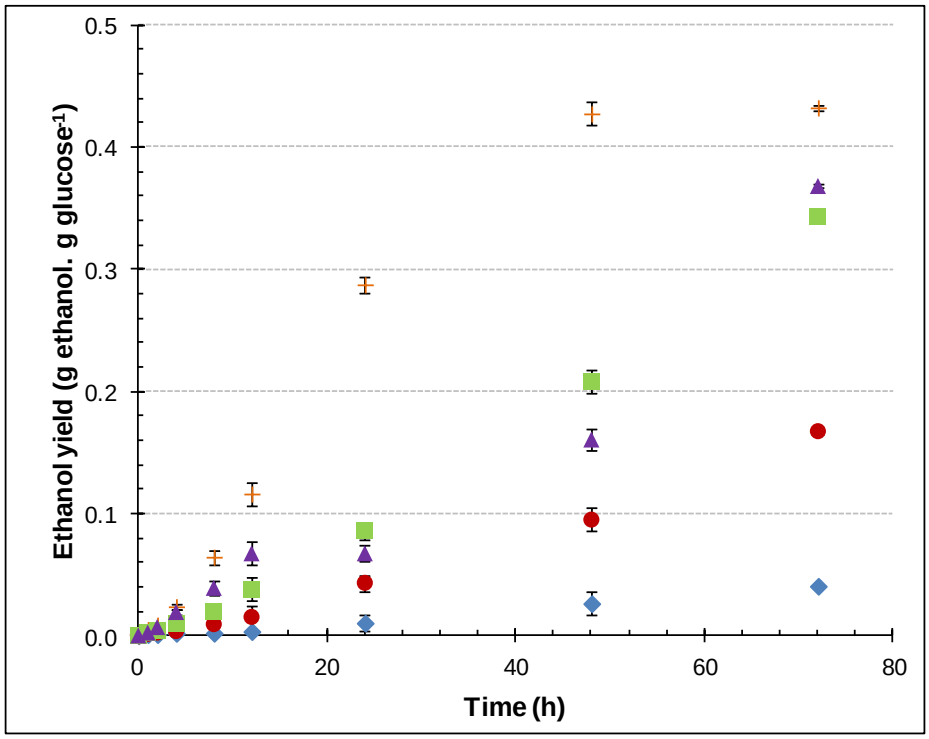

Figure 2.7 Effect of starting yeast concentration on ethanol yield
(♦1g.L^{-1}, ●3g.L^{-1}, ■5g.L^{-1}, ▲7g.L^{-1}, +10g.L^{-1})

The starting yeast concentration has a significant effect on the ethanol yield over time and it is clear that ethanol forms faster (from the slope of the graph) with higher yeast concentrations. A higher yeast concentration means that more yeast cells are available to convert glucose to ethanol, thereby increasing the rate of ethanol formation. The highest ethanol yield (0.432±0.002g.g^{-1}) after 72 hours of fermentation was achieved using 10g.L^{-1} starting yeast concentration. Figure 2.8 shows the final ethanol yield after 72 hours for each different starting yeast concentration.

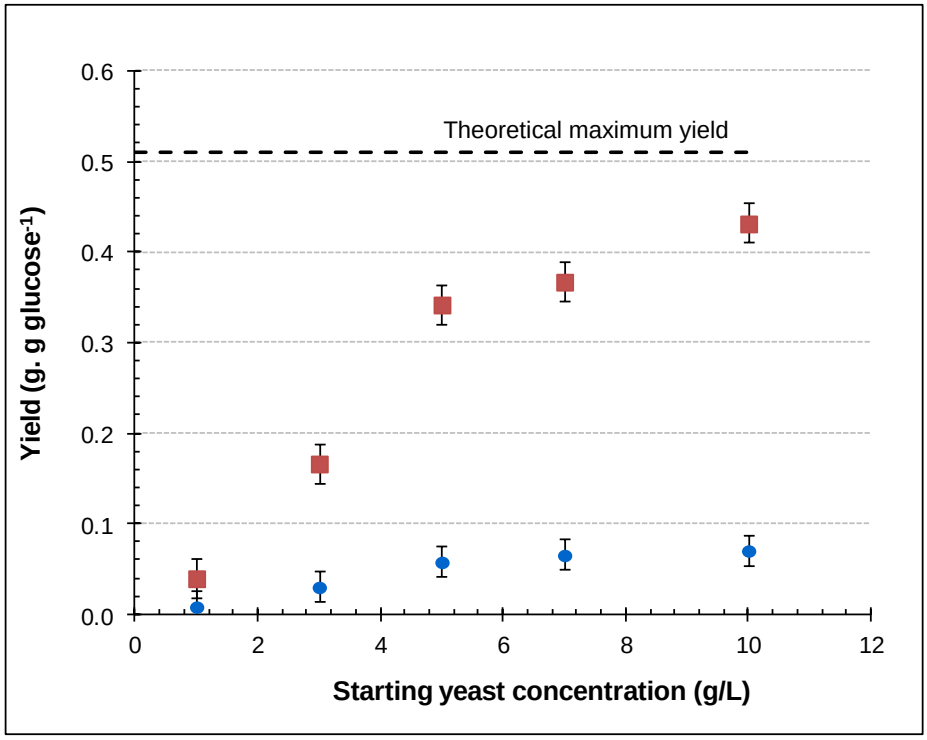

Figure 2.8 Effect of starting yeast concentration on final ethanol and glycerol yield (■ ethanol, ● glycerol)

It is expected that given enough time the same ethanol yield should be reached for all yeast concentrations. Mojović *et al*. (2006:1754) and Cheng *et al.* (2007:71) found that the duration of fermentation decreased with an increase of yeast concentration but the final ethanol yield remained the same after all the substrate had been converted. To extend fermentation for periods longer than 72 hours would, however, not be of much value from an industrial point of view. Table 2.7 shows the amount of glucose that is converted to products and it can be seen that virtually all of the glucose had been converted to products after 72 hours using a starting yeast concentration of 10g.L^{-1}.

Table 2.7 Glucose utilisation after 72 hours using different starting yeast concentrations

Starting yeast concentration (g.L^{-1})	Glucose utilized (wt%)	Glucose utilized for ethanol (wt%)	Glucose utilized for glycerol (wt%)
1	10%	9%	1%
3	39%	36%	3%
5	79%	73%	6%
7	85%	78%	7%
10	98%	91%	7%

2.3.3. Influence of operating pH

The effect of pH was studied by varying the pH of the fermentation broth between 2.5 and 6. A starting yeast concentration of 10g.L^{-1} was used with 15wt% starting glucose concentration, which were the optimum values when wt% glucose was varied (Section 2.3.1) and yeast concentration was varied (Section 2.3.3). Figure 2.9 shows the ethanol yield attained at different pH values over time.

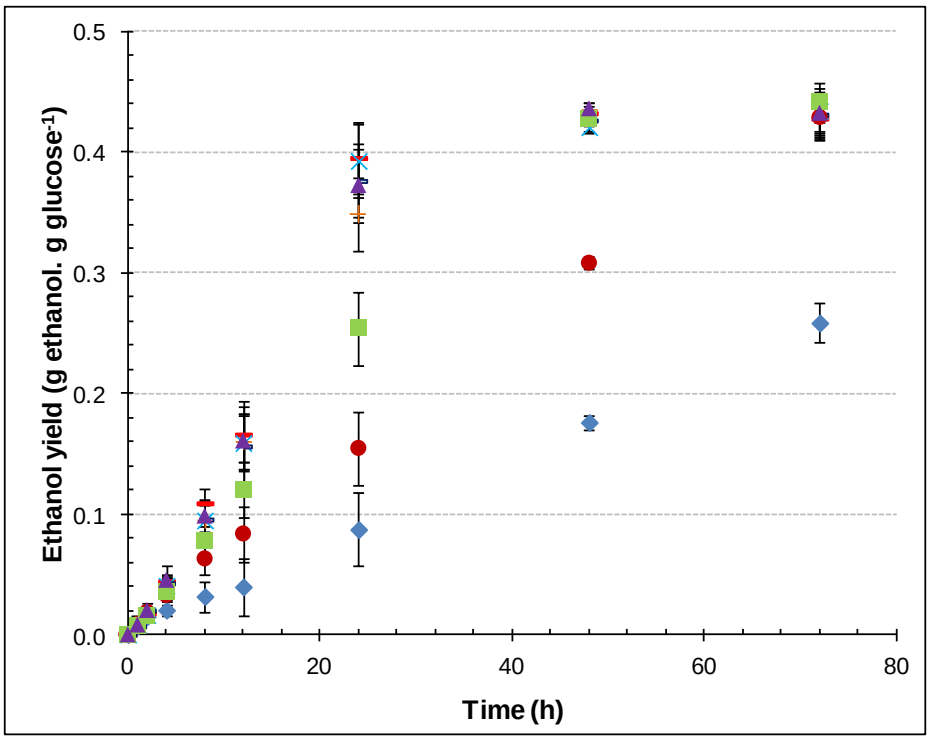

Figure 2.9 Effect of pH on ethanol yield
(♦2.5, ●3, ■3.5, -4, ▲4.5, +5, –5.5, X6)

There was no significant effect on the ethanol yield for pH between 3.5 and 6, especially after 48 hours. After 72 hours, there was almost no difference in ethanol yield except for the experiment at a pH of 2.5. Figure 2.10 shows the effect of pH values on ethanol yield after 72 hours.

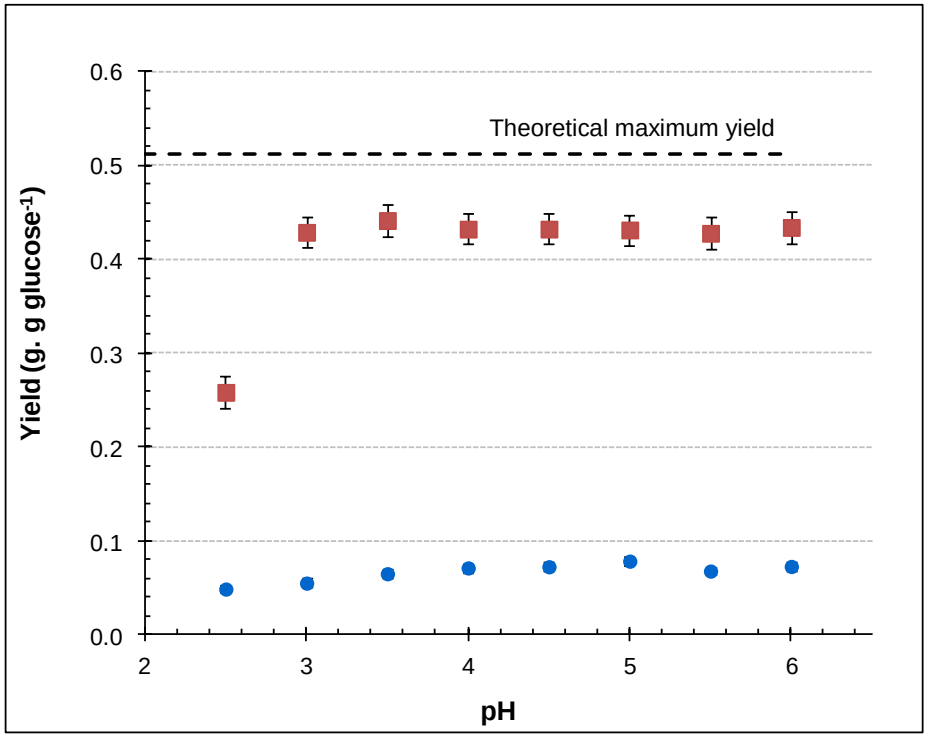

Figure 2.10 Effect of pH on final ethanol and glycerol yield
(■ ethanol, ● glycerol)

There is merely a slight difference in glycerol production with a slightly higher glycerol production as the pH is increased. This means that there would only be a very slight benefit in adjusting the pH between 3.5 and 4.5. It is, however, recommended that the pH be kept low to reduce possible contamination. Verduyn *et al.* (1990:398) found that the optimum pH was between 5 and 5.5 while a pH below 2.7 showed very poor results. Munene *et al*. (2002: 313) confirmed that the optimum range for yeast cell growth, and therefore ethanol production, is between 4.5 and 5.5.

2.4 KINETIC MODEL OF FERMENTATION

Currently most fermentation kinetic models are based on the Monod model, as discussed in Chapter 2.1.4. Therefore, in this study a Monod-type model is used to model the fermentation process.

Most researchers agree that the Monod equation only has numerical meaning for microbial growth, but might not have biological basis other than a regression-based mathematical formula. Even though it is the mathematical analog of the Michaelis–Menten equation for enzyme-catalysed reactions, it is an empirical equation and Monod (1949) noted that there was no relationship between the Monod constant and the Michaelis–Menten constant.

Parameter estimation consists of determining the optimum values of the parameters of a given model with experimental data. Figure 2.11 shows the general approach followed to calculate the parameters of the model.

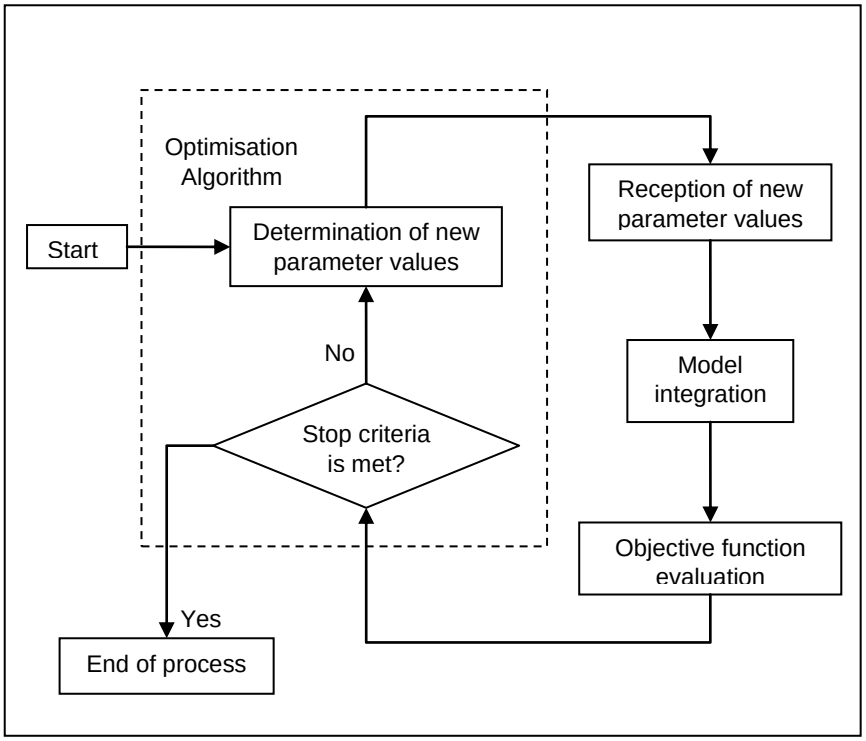

Figure 2.11 Flow diagram of parameter estimation

The fourth order Runge-Kutta method was used to solve the set of differential equations used to model fermentation simultaneously. The Nelder-Mead simplex optimisation method was combined with the Runge-Kutta method to determine the parameters of the equations. The standard error of the parameters was determined with the Bootstrap method. The computer programmes used in this study can be found in Appendix H.

2.4.1. Substrate-limiting kinetics

Usually models proposed to describe fermentation kinetics use a system of nonlinear differential equations to describe cell growth, product formation, and substrate uptake respectively, as shown by Equation 2.19 to 2.21. Two products formed during fermentation, namely ethanol and glycerol and thus the model used had to account for both these products.

$$r_x = \frac{dX}{dt} = \mu X \qquad \text{Equation 2.19}$$

$$r_{P_i} = \frac{dP_i}{dt} = \nu_i X$$ Equation 2.20

$$r_S = \frac{dS}{dt} = -\left(\frac{1}{\sum Y_{P_i/S}} \frac{d\sum P_i}{dt} \right)$$ Equation 2.21

The model presented in Equations 2.19 to 2.21 assumes that substrate consumption over time (dS/dt) is related to both glycerol and ethanol formation.

The Monod model, or Monod-based models, are the most frequently used unstructured type of models to describe cell growth. The Monod equation, shown in Equation 2.22 and Equation 2.23, is used to describe the relation between specific growth rate (μ), the specific product production rate (v) and the substrate concentration respectively.

$$\mu = \mu_{\max} \frac{S}{K_{sx} + S}$$ Equation 2.22

$$\nu_i = \nu_{\max,i} \frac{S}{K_{sp,i} + S}$$ Equation 2.23

Only substrate limitation is considered in these equations, therefore it will only be a good prediction for fermentation processes where no substrate inhibition or product inhibition occurs.

It was found that the initial yeast concentration had a significant effect on the model parameters μ_{max} and $v_{max,i}$. It was therefore necessary to account for the effect of initial yeast concentration on these parameters as shown by the empirical equations, presented in Equation 2.24 to 2.26, which is similar in form to those used by Krishnan *et al.* (1999:377).

$$\mu_{\max} = 0.015 \times X_0^{0.551} - 0.012$$ Equation 2.24

$$\nu_{\max,ethanol} = 9.17 \times 10^{-7} \times X_0^{5.034} + 0.093$$ Equation 2.25

$$\nu_{\max,glycerol} = 8.29 \times 10^{-7} \times X_0^{4.590} + 0.018$$ Equation 2.26

where X_0 is the initial yeast concentration in g/L

Equations 2.24 to 2.26 were determined by finding the u_{max} and $v_{max,i}$ parameters at each different initial yeast concentration and determining an equation that incorporates the effect of cell concentration on these parameters.

Typical results obtained for the ethanol concentration, glycerol concentration, glucose concentration and yeast cell concentration modelled with the Monod-type model given by Equation 2.19 to Equation 2.26 are given in Figures 2.12. The K_{sx}, $K_{sp,ethanol}$ and $K_{sp,glycerol}$ parameters for this model are 21.461±0.005, 0.145±0.016 and 1.413±0.007 respectively.

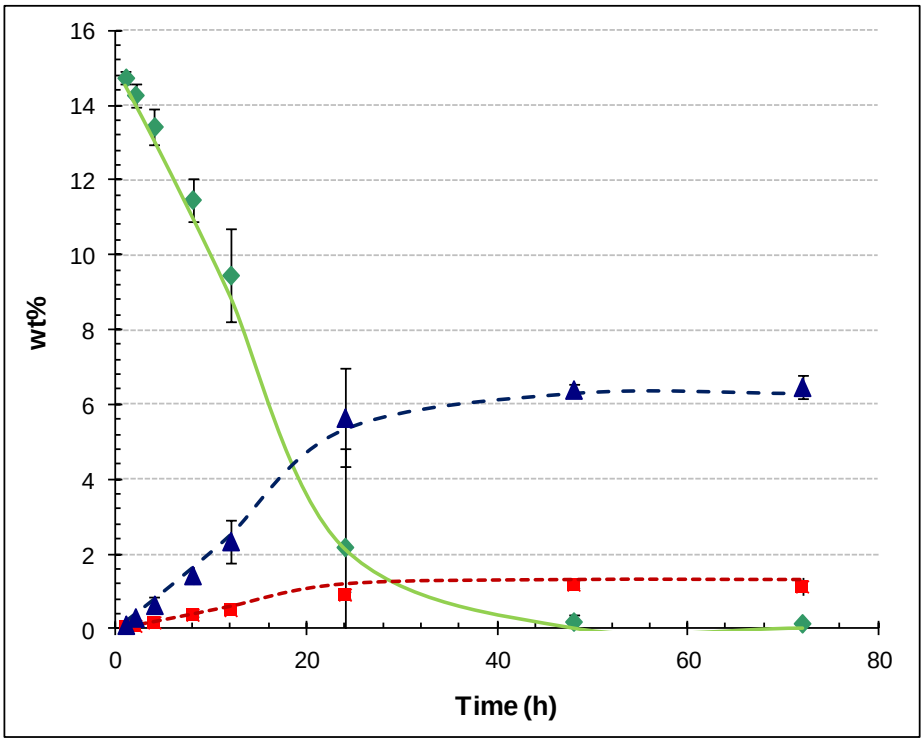

Figure 2.12 Comparison of experimental fermentation with the substrate-limiting model using 15wt% starting glucose and 10g/L starting yeast
(♦ Experimental glucose, ▲ Experimental ethanol, ■ Experimental glycerol, — glucose model, --- ethanol model, ···· glycerol model)

The theoretical values determined by this model led to very accurate results for 15wt% initial glucose, as shown in Figure 2.12, and for glucose concentrations less than 15wt% as shown in Table 2.8. The model failed, however, for initial glucose concentrations higher than 20wt%, as shown in Figure 2.13 and Table 2.8. At high sugar concentration cell growth inhibition occurs due to osmotic pressure that this model does not account for. This phenomenon was discussed in Section 2.3.1.

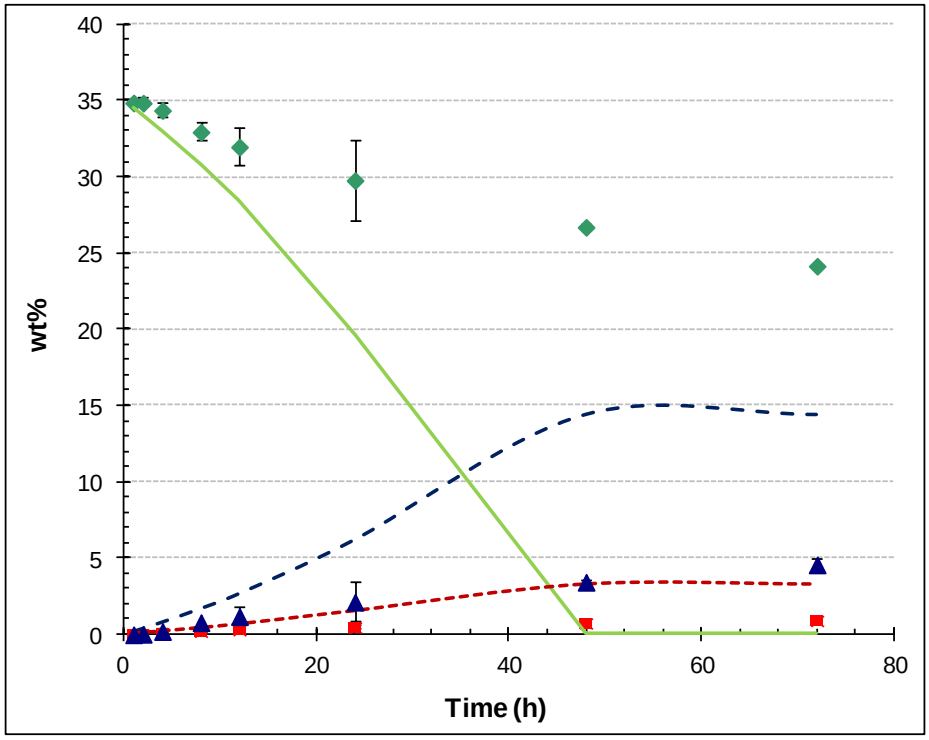

Figure 2.13 Comparison of experimental fermentation with the substrate-limiting model using 35wt% starting glucose and 10g/L starting yeast
(♦Experimental glucose, ▲ Experimental ethanol, ■ Experimental glycerol, — glucose model, --- ethanol model, ···· glycerol model)

The modelling results for other initial sugar concentrations can be found in Appendix I.1. Table 2.8 shows the accuracy of this model for the prediction of ethanol, glucose and glycerol using different initial yeast and glucose concentrations.

Table 2.8 Accuracy of substrate-limiting model

Starting glucose (wt%)	Starting yeast (g/L)	Ethanol R^2	Glycerol R^2	Glucose R^2
5	10	0.994	0.943	0.993
10	10	0.998	0.997	0.999
15	10	0.999	0.986	1.000
20	10	0.995	0.958	0.996
25	10	0.909	0.802	0.967
30	10	0.692	0.613	0.929
35	10	0.533	0.497	0.911
15	1	0.984	0.987	1.000
15	3	0.997	0.998	1.000
15	5	0.996	0.997	1.000
15	7	0.995	0.994	0.999

2.4.2. Substrate-inhibition kinetics

By incorporating the effect of lower product yields caused by high sugar concentration due to osmotic stress, a new model based on the Equations 2.19 to 2.26 could be introduced by

adding a substrate-inhibition term into Equation 2.22 and Equation 2.23. Equation 2.27 and Equation 2.28 show the two equations that replace Equations 2.22 and 2.23 in substrate-inhibition kinetics.

$$\mu = \mu_{max}\left(\frac{S}{K_{sx}+S}\right)\exp\left(\frac{-S}{K_{ix}}\right) \qquad \text{Equation 2.27}$$

$$\nu_i = \nu_{max,i}\left(\frac{S}{K_{sp,i}+S}\right)\exp\left(\frac{-S}{K_{ip,i}}\right) \qquad \text{Equation 2.28}$$

This model is based on a model proposed by Aiba (1968). The parameters K_{ix}, $K_{ip,ethanol}$ and $K_{ip,glycerol}$ represent the substrate-inhibition constants of cell growth, ethanol formation and glycerol formation respectively.

Typical results obtained for the ethanol concentration, glycerol concentration, glucose concentration and yeast cell concentration modelled with the substrate-inhibition model, which incorporate Equation 2.27 and Equation 2.28 are given in Figure 2.14 and Figure 2.15.

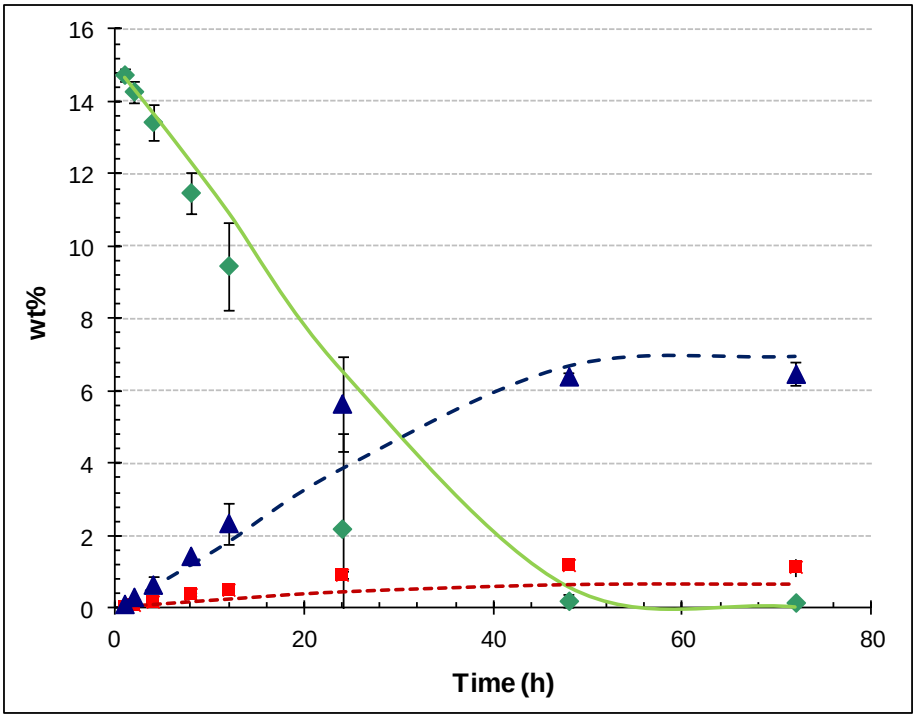

Figure 2.14 Comparison of experimental fermentation with the substrate-inhibition model using 15wt% starting glucose

(♦Experimental glucose, ▲ Experimental ethanol, ■ Experimental glycerol, — glucose model, --- ethanol model, ···· glycerol model)

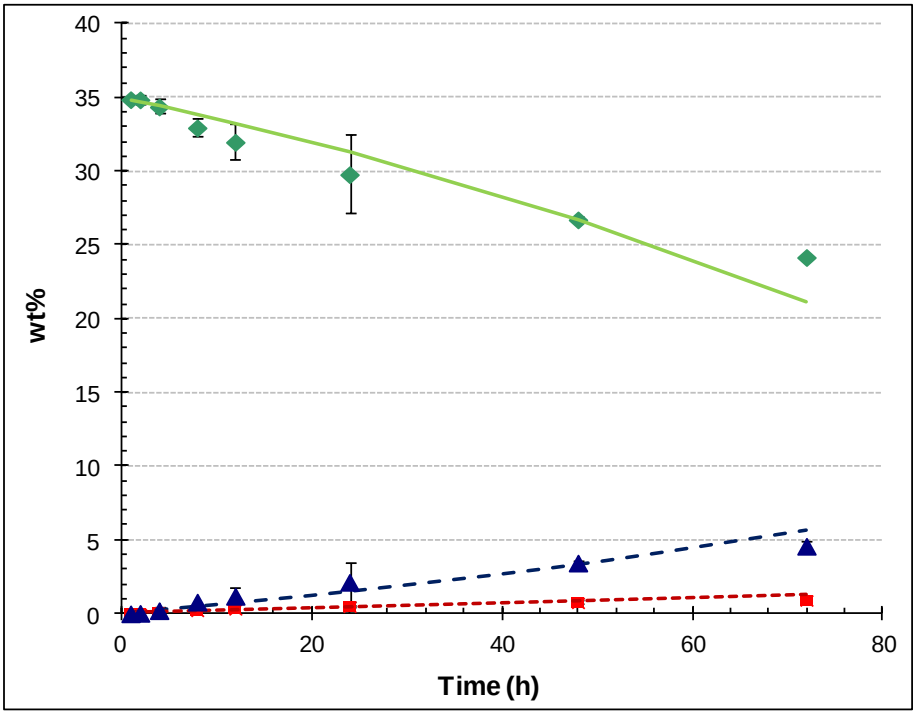

Figure 2.15 Comparison of experimental fermentation with the substrate-inhibition model using 35wt% starting glucose

(♦ Experimental glucose, ▲ Experimental ethanol, ■ Experimental glycerol, — glucose model, --- ethanol model, ···· glycerol model)

The parameters used in this model are shown in Table 2.9. The initial yeast concentration did not have a major effect on the model parameters μ_{max} and $v_{max,glycerol}$, and therefore a constant value was used for these parameters (compared to the empirical equations used in Section 2.4.1). An empirical equation, as shown in Table 2.9, was used for the parameter $v_{max,ethanol}$ as the initial yeast concentration did have a significant influence on this parameter.

Table 2.9 Parameters for substrate-inhibition model

Parameter	Value
K_{ix}	3.569±0.023
$K_{i,ethanol}$	17.468±0.016
$K_{i,glycerol}$	33.829±0.035
K_{sx}	30.953±0.038
$K_{sp,ethanol}$	8.005±0.045
$K_{sp,glycerol}$	23.795±0.029
u_{max}	0.191±0.005
$v_{max,ethanol}$	$0.120 \times X_0^{0.467} + 0.164$
$v_{max,glycerol}$	0.078±0.048

Table 2.10 shows the accuracy of this model when using different initial yeast and glucose concentrations.

Table 2.10 Accuracy of substrate-inhibition model

Starting glucose (wt%)	Starting yeast (g/L)	Ethanol R^2	Glycerol R^2	Glucose R^2
5	10	0.972	0.512	0.958
10	10	0.987	0.674	0.986
15	10	0.984	0.820	0.990
20	10	0.991	0.894	0.996
25	10	0.977	0.988	0.997
30	10	0.962	0.972	0.998
35	10	0.977	0.958	0.999
15	1	0.996	0.997	1.000
15	3	0.996	0.996	1.000
15	5	0.998	0.960	1.000
15	7	0.997	0.899	0.999

This model showed more accurate results than the substrate-limiting model, as discussed in Section 2.4.1, when the initial sugar concentration was higher than 20wt%. At low sugar concentrations the substrate-inhibition model showed results that were less accurate than the substrate-limiting model, as shown in Table 2.10 and Figure 2.14. Substrate inhibition does not take place at low sugar concentrations, which could possibly explain why this model does not fit data with low sugar concentrations. According to Birol *et al*. (1998:770), it is not possible to use a single model to describe the fermentation process within a wide range of initial substrate concentrations, which means that a model may only be accurate within a specific environment.

2.4.3. Comparison of model parameters to literature

It is difficult to compare model parameters of one system to that of another system as each system has its own uniqueness which influences the model parameters. Even so comparative literature values are presented in Table 2.11 for comparison of the magnitude of the values.

Table 2.11 Fermentation model parameters for different systems in literature

System	u_{max}	$v_{max,ethanol}$	K_{sx}	$K_{sp,ethanol}$	Reference
Unstirred batch system, glucose (5-20wt%)	0.003-0.041	0.093-0.192	21.461 ±0.005	0.145 ±0.016	This study
Unstirred batch system, glucose (25-35wt%)	0.191 ±0.005	0.284-0.515	30.953 ±0.038	8.005 ±0.045	This study
Immobilized Saccharomyces cerevisiae in a stirred batch system, glucose (2-10%)	0.186-0.758	0.89-1.83	0.390-362.65	0.39-42.52	Birol *et al.*, 1998
Tequila batch fermentation with Agave juice, sugar = 30-200g/L	0.370	---	20	---	Arellano-Plaza *et al.*, 2007
Wine fermentation with chardonnay juice, sugar = 240g/L	0.160	---	0.010	---	Cramer *et al.*, 2002

It is clear from Table 2.11 that the order of magnitude of the parameters compare very well with those reported in the literature. However, Table 2.11 does show that a wide variety of parameter values can be obtained, as the parameters are dependent on the specific conditions of the fermentation environment i.e. the type of yeast, type of sugar, temperature, agitation to name but a few.

2.5 CONCLUSION

The fermentation process was investigated as described in this chapter. Firstly, the effect that different operating conditions have on fermentation was investigated and experimental data that could be used for the modelling of fermentation were obtained. It was found that the maximum ethanol yield that could be obtained by using the set-up as in this study was 0.441g ethanol per gram glucose. The optimum operational conditions for fermentation were found to be 15wt% glucose, 10g.L^{-1} yeast and a pH of 3.5. Glucose concentrations higher than 20wt% resulted in very low product yields and it was concluded that the low yields were as a result of osmotic stress on the yeast cells caused by high sugar concentrations. The pH did not have a large effect on the ethanol yield and therefore it was not included in the modelling of fermentation kinetics.

In the second part of this chapter, the fermentation data obtained in the first part were used to obtain parameters to model the fermentation process. Two models were proposed. The first model, the substrate-limiting model predicted fermentation very accurately when the initial glucose concentration was below 20wt%, therefore this model can only be used for systems where the starting glucose concentration is below 20wt%. The second model, the substrate-inhibition model, incorporated a term that accounts for osmotic stress experienced by the yeast cells at high glucose concentrations. The substrate-inhibition model predicted fermentation with high initial glucose concentrations more accurately than the substrate-limiting model, but at low glucose concentrations (<20wt%) the substrate-limiting model was more accurate. It was therefore concluded that no single model could be used to predict fermentation within a wide range of initial substrate concentrations as fermentation kinetics are very specific to the experimental environment.

2.6 REFERENCES

AIBA, S., SHODA, M. & NAGATANI, M. 1968. Kinetics of product inhibition in alcohol fermentation. *Biotechnology and Bioengineering*, X(6): 845-864.

ARELLANO-PLAZA, M., HERRERA-LÓPEZ, E. J., DÍAZ-MONTAÑO, D. M., MORAN, A. & RAMÍREZ-CÓRDOVA, J. J. 2007. Unstructured Kinetic Model for Tequila Batch Fermentation. *International journal of mathematics and computers in simulation*, 1(1):1-6.

BAI, F.W., ANDERSON, W.A. & MOO-YOUNG, M. 2008. Ethanol fermentation technologies from sugar and starch feedstocks. *Biotechnology Advances*, 26: 89-105.

BAILEY, B.K. 1996. Performance of ethanol as a transportation fuel. (*In* Wyman, C.E., ed. Handbook on Bioethanol: Production and Utilisation. USA: CRC Press. p. 37-60.)

BAKKER, B.M., OVERKAMP, K.M., VAN MARIS, A.J.A., KOTTER, P., LUTTIK, M.A.H. VAN DIJKEN, J.P. & PRONK, J.T. 2001. Stoichiometry and compartmentation of NADH metabolism in Saccharomyces cerevisiae. *FEMS Microbiology Reviews*, 25:15-37.

BELLGARDT, K.H.. 2000a. Introduction. (*In* Schügerl, K & Bellgardt, K.H., ed. Bioreaction Engineering. Berlin: Springer. p. 1-18.)

BELLGARDT, K.H.. 2000b. Bioprocess models. (*In* Schügerl, K & Bellgardt, K.H., ed. Bioreaction Engineering. Berlin: Springer. p. 44-105.)

BERGERON, P. 1996. Bioethanol market forces. (*In* Wyman, C.E., ed. Handbook on Bioethanol: Production and Utilisation. USA: CRC Press. p. 61-88.)

BFAP (Bureau for Food and Agriculture Policy). 2005. Bioethanol production in South Africa An objective analysis. 37p.

BIDEAUX, C., ALFENORE, S., CAMELEYRE, X., MOLINA-JOUVE, C., URIBELARREA, J. & GUILLOUET, S.E. 2006. Minimization of Glycerol Production during the High-Performance Fed-Batch Ethanolic Fermentation Process in *Saccharomyces cerevisiae*, Using a Metabolic Model as a Prediction Tool. *Applied and Environmental Microbiology*, 72(3): 2134–2140.

BIPP (James A Baker III Institute for Public Policy). 2010. Fundamentals of a Sustainable US Biofuels Policy. 133p.

BIROL, G., DORUKER, P., KARDAR, B., ONSAN, Z.I. & ULGEN, K. 1998. Mathematical description of ethanol fermentation by immobilised *Saccharomyces cerevisiae. Process Biochemistry,* 33(7): 763-771.

BLANCO, M. PEINADO, A.C. & MAS, J. 2006. Monitoring alcoholic fermentation by joint use of soft and hard modelling methods. *Analytica Chimica Acta, 556: 364-373.*

BROCK, T.D. & MADIGAN, M.T. 1991. Biology of microorganisms. 6th ed. USA: Prentice-Hall International. 874p.

CHENG, C.K., HANI, H.H. & ISMAIL, K. 2007. Production of bioethanol from oil palm empty fruit bunch. (*In* Paper read at the ICoSM conference in 2007, accepted for publication on the 15th of May 2007. p69-72).

CONTOIS, D.E. 1959. Kinetics of Bacterial Growth: Relationship between Population Density and Specific Growth Rate of Continuous Cultures. *Journal of gen. Microbial,* 21: 40-50.

CRAMER, A.C., VLASSIDES, S. & BLOCK, D.E. 2002. Kinetic model for nitrogen-limited wine fermentations. *Biotechnology and bioengineering*, 77(1): 49-60.

D'AMORE,T., PANCHAL, C.J. & STEWART, G.G. 1988. Intracellular Ethanol Accumulation in Saccharomyces cerevisiae during Fermentation. *Applied and Environmental Microbiology*, 54(1): 110-114.

DEMIRBAS, A. 2007. Progress and recent trends in biofuels. *Progress in Energy and Combustion Science*, 33:1-18.

DUNN, I.J., HEINZLE, E., INGHAM, J. & PRENOSIL, J.E. 1992. Biological Reaction Engineering. Weinheim: VCH. 438p.

FISCHER, C.R., KLEIN- MARCUSCHAMER, D. & STEPHANOPOULOS, G. 2008. Selection and optimization of microbial hosts for biofuels production. *Metabolic Engineering*, 10: 295–304.

FOGLER, H.S. 2006. Elements of Chemical Reaction Engineering. Prentice Hall. 4th edition. 1080p.

GHALY, A.E. & EL-TAWEEL, A.A. 1997. Kinetic modelling of continuous production of ethanol from cheese whey. *Biomass and Bioenergy,* 12(6): 461-472.

GHOSH, B.B. & NAG, A. 2008. Raw Ethanol and Methanol as Fuels in Internal Combustion Engines. (*In* Nag, A., ed. Biofuels Refining and Performance. New York: McGraw Hill. p. 191-219.)

GRAY, W.D. 1945. The sugar tolerance of four strains of distillers' yeast. *Journal of bacteriology*, 49: 445-452.

HUBER, G.W. & DUMESIC, J.A. 2006. An overview of aqueous-phase catalytic processes for production of hydrogen and alkanes in a biorefinery. *Catalysis Today*, 111: 119–132

KOVÁROVÁ-KOVAR, K & EGLI, T. 1998. Growth Kinetics of Suspended Microbial Cells: From Single-Substrate-Controlled Growth to Mixed-Substrate Kinetics. *Microbiology and molecular biology reviews*, 62(3): 646-666.

KRISHNAN, M.S., HO, N.W.Y. & TSAO, G.T. 1999. Fermentation Kinetics of Ethanol Production from Glucose and Xylose by Recombinant Saccharomyces 1400(pLNH33). *Applied Biochemistry and Biotechnology*, 77-79: 373-388.

LEVENSPIEL, O. 1999. Chemical reaction engineering. Wiley & Sons. 3rd edition. 668p.

LIN, Y. & TANAKA, S. 2006. Ethanol fermentation from biomass resources: current state and prospects. *Applied Microbiology Biotechnology*, 69: 627-642.

MCGOWAN, T.F., *ed.* 2009. Biomass and alternate fuel systems An Engineering and Economic guide. New Jersey: John Wiley & Sons. 264p.

MOJOVIĆ, L., NIKOLIĆ, S., RAKIN, M. & VUKASINOVIĆ, M. 2006. Production of bioethanol from corn meal hydrolyzates. *Fuel*, 85:1750-1755.

MONOD , J. 1949. The growth of bacterial cultures. *Annual Review of Microbiology*, 3: 371-394.

MUNENE, C.N., KAMPEN, W.H. & NJAPAU, H. 2002. Effect of altering fermentation parameters on glycerol and bioethanol production from cane molasses. Journal of the *Science of Food and Agriculture*, 82:309-314.

NAIK, S.N., GOUD, V.V., ROUT, P.K. & Dalai, A.K. 2010. Production of first and second generation biofuels: A comprehensive review. *Renewable and Sustainable Energy Reviews*, 14: 578–597.

NEW ZEALAND. 2007. Ministry of Economic Development. New Zealand Energy Strategy to 2050. Wellington. 107p.

NZ see NEW ZEALAND

PELCZAR, M.J., REID, R.D. & CHAN, E.C.S. 1977. Microbiology. 4th ed. NY: McGraw-Hill. 952p.

PICATAGGIO, S.K. & ZHANG, M. 1996. Biocatalyst development for bioethanol production from hydrolysates. (*In* Wyman, C.E., ed. Handbook on Bioethanol: Production and Utilisation. USA: CRC Press. p. 163-178.)

ROCA, E., FLORES, J., NÚÑEZ, M.J. & LEMA, J. M. 1996. Ethanolic fermentation by immobilized *Saccharomyces cerevisiae* in a semipilot pulsing packed-bed bioreactor. *Enzyme and Microbial Technology*, 19:132-139.

SA see South Africa

SCHNEPF, R. 2006. European Union Biofuels Policy and Agriculture: An Overview. CRS Report for Congress.6p.

SINGHANIA, R.R., PARAMESWARAN, B. & PANDEY, A. 2009. Plant-Based Biofuels An Introduction. (*In* Pandey, A., ed. Handbook of Plant-Based Biofuels. USA: CRC Press. p. 3-12.)

SOUTH AFRICA. Department of Minerals and Energy. 2007. Biofuels Industrial Strategy of the Republic of South Africa. Pretoria: Government Printer. 29p.

TAHERZADEH, M.J. & KARIMI, K. 2008. Bioethanol: Market and Production Processes. (*In* Nag, A., ed. Biofuels Refining and Performance. New York: McGraw Hill. p. 69-106.)

TAN, Y., WANG, Z. & MARSHALL, K.C. 1996. Modelling Substrate Inhibition of Microbial Growth. *Biotechnology and Bioengineering*, 52: 602-608.

VELIZAROV, S. & BESCHKOV, V. 1998. Biotransformation of glucose to free gluconic acid by *Gluconobacter oxydans:* substrate and product inhibition situations. *Process Biochemistry,* 33(5): 527-534.

VERDUYN, C., POSTMA, E., SCHEFFERS, W.A. & VAN DIJKEN, J.P. 1990. Physiology of Saccharomyces cerevisiae in anaerobic glucose-limited chemostat cultures. *Journal of General Microbiology*, 136: 395-403.

ZHANG, A. & CHEN, X. 2008. Improve Ethanol Yield through Minimizing Glycerol Yield in Ethanol Fermentation of *Saccharomyces cerevisiae*. *Chinese Journal of Chemical Engineering*, 16(4): 620-625.

CHAPTER 3: PERVAPORATION

OVERVIEW

Pervaporation can be effectively combined with fermentation to remove ethanol from the fermentation broth continuously. However, before combining fermentation with pervaporation, it is important to explore pervaporation on its own. Therefore, the focus of Chapter 3 is on separation by pervaporation.

This chapter is divided into three main sections. The concepts, terminology, literature, and applications used in the field of membrane technology are presented in the first section (3.1) of this chapter. Pervaporation is discussed extensively in Section 3.1.2 to Section 3.1.8, which presents a general overview of the process of pervaporation, the characteristics of pervaporation as well as the application and advantages of pervaporation, among others. Section 3.1 concludes with an overview of mass transport through a membrane with specific focus on pervaporation.

In the second section of this chapter, Section 3.2, the experimental procedures are discussed in detail. The first part of Section 3.2 gives an overview of the materials and chemicals used in the experimental work followed by a discussion on the membranes and pervaporation set-up used for the experiments. Membrane screening experiments were done on these membranes and the results can be found in this section. In the last part of this section, the reproducibility of the pervaporation and sorption experiments are discussed as well as the analytical techniques used in the experiments.

The results of both the pervaporation and the sorption experiments are presented and discussed in Section 3.3. The membrane's pervaporation characteristics namely the dependence of total flux, partial flux, and selectivity on the ethanol and glucose content of the feed are discussed in this section. The experimental data, sample calculations, and calculated data for this chapter can be found in Appendix D.

In Section 3.4, mass transport through the membrane is modelled and the results of the modelling of the pervaporation data for the ethanol, glucose, and water mixtures are presented. Lastly, concluding remarks are presented in Section 3.5.

3.1 INTRODUCTION TO THE PERVAPORATION PROCESS

3.1.1. Introduction to membrane technology

Membrane technology is exceptionally varied, ranging from age-old separation techniques such as filters made from paper to modern methods, which include nanofiltration, gas separation, and pervaporation (Humphrey & Keller, 1997:226-227). A large amount of energy may be potentially saved if membrane technology is used to replace some of the more common separation techniques such as distillation (Seader & Henley, 2006:493, Wee *et al.*, 2008:515).

Pervaporation is a relatively new membrane separation process (Feng & Huang, 1997:1048). The focus of Section 3.1 is on pervaporation, but membrane separation in general, with specific focus on membrane technology for pervaporation, will be discussed first (Section 3.1.1). This includes a general overview of the terms and concepts used in membrane technology, membrane separation processes, types of membranes, and a discussion on the parameters used to determine the effectiveness of a membrane.

3.1.1.1. Definitions of membrane technology

Membrane separation technology involves the separation of a mixture of two or more components by a semi-permeable barrier, known as a membrane, through which one of the components move faster than the other component (Seader & Henley, 2006:493). The membrane housing with a membrane inside is known as a membrane module (Koros *et al.*, 1996:1482).

Figure 3.1 gives a schematic representation of a membrane separation process (Seader & Henley, 2006:494). The part of the feed that does not pass through the membrane is known as the retentate while the part that does pass through is known as the permeate (Seader & Henley, 2006:493). Mass transfer across a membrane occurs due to a variety of driving forces. Such driving forces can be a concentration difference, a partial pressure difference, electrical potential difference, or a chemical potential difference (Susanto & Ulbricht, 2009:20). A sweep stream may be added to the design to remove the permeate and to ensure that the concentration or partial pressure of the permeating specie remains low on the downstream surface of the membrane.

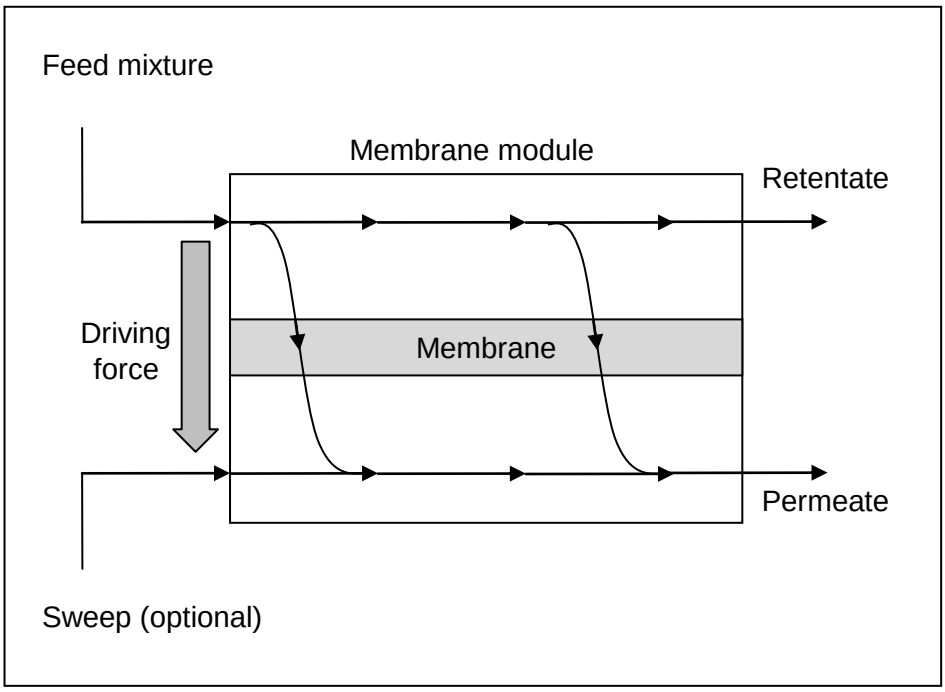

Figure 3.1 General membrane process

3.1.1.2. Membrane separation processes

The use of a semi-permeable barrier such as a membrane for the purification, concentration, and fractionation of liquid mixtures is rapidly expanding (Seader & Henley, 2006:14). Widely used membrane separation operations, the driving force required for separation and examples of commercial applications are summarised in Table 3.1 (Seader & Henley, 2006:14,494, Humphrey & Keller, 1997:229 and Lipnizki *et al.*, 1999:115).

Table 3.1 Membrane separation processes

Separation process	Driving force	Example
Microfiltration	Pressure	Separation of mammalian cells from a liquid
		Concentration of fine solids
Ultrafiltration	Pressure	Pre-concentration of milk before making cheese
		Partial dewatering of clay slurries
Nanofiltration	Pressure	Treatment of electro-plating rinse water
Reverse osmosis	Activity gradient, pressure	Desalination of brackish water
		Treatment of wastewater
Gas separation	Activity gradient	Recovery of helium
Vapour permeation	Activity gradient	Removal of condensable solvents from air
Pervaporation	Activity gradient	Dehydration of ethanol-water azeotrope
		Removal of organics from water
Electro dialysis	Electrical potential	Production of table salt from seawater

Table 3.1 (cont.) Membrane separation processes

Separation process	Driving force	Example
Liquid membranes	Gradient in chemical potential based on solubility	Recovery of nickel from electroplating solutions
		Recovery of zinc from wastewater in the viscose fibre industry
Membrane distillation	Temperature difference across non-wetting pores	Desalination of brine

3.1.1.3. Membrane types

The membrane is the most important factor in a membrane separation process. The following characteristics are essential for an efficient and economical process (Seader & Henley, 2006:496).

- Good permeability.
- High selectivity.
- Chemical and mechanical compatibility with the processing environment.
- Stability (long life).
- Amenability to fabrication and packaging.
- Ability to withstand large pressure differences across the membrane.
- Cost efficiency of membrane.

Membranes can be macro-porous, micro-porous, or nonporous with nonporous membranes normally used for pervaporation (Seader & Henley, 2006:502,505). Nonporous membranes are also known as dense membranes and have no detectable pores (Koros *et al.*, 1996:1482). There are three main categories of membranes (Wee *et al.*, 2008:502). The first category is organic membranes, which broadly covers polymeric membranes. The second category is inorganic membranes with ceramics included in this group. The third category is composite membranes, also known as hybrid membranes, which are membranes made up of inorganic and organic material. The two (or more) different materials each have its own unique characteristics and by combining them, a membrane with very effective performance can be obtained.

The selection of membrane material is determined by the application for which the membrane will be used, the environment in which the membrane must be stable, economic considerations and the separation mechanism. Most industrial membranes are made of natural or synthetic polymers (organic membranes) (Seader & Henley, 2006:496) but ceramics (zeolites) and metals have also been used (inorganic membranes) (Humphrey &

Keller, 1997:247). A comparison between polymer membranes and ceramic membranes (which can both be used for pervaporation) are given in Table 3.2 (Van Der Bruggen, 2009:50).

Table 3.2 Comparison of polymeric and ceramic pervaporation membranes

Polymeric membrane materials	Ceramic membrane materials
Low production cost	High production cost
Easy production up-scaling	Difficult production up-scaling
Variation in module form easy	Variation in module form difficult
Unknown long term stability	Good long term stability
Limited versatility in organics	Good versatility in organics
Vulnerable for unknown components in mixture	Resistance to unknown components in mixture expected good
Thermal regeneration impossible	Thermal regeneration possible
High-temperature applications impossible	High-temperature applications possible

Polymer membranes have the economic and up-scaling advantage but if unknown components are present in the feed mixture or if organic mixtures must be separated it will be beneficial to look at ceramic membranes. Polymer membranes are overwhelmingly utilised for pervaporation processes and will be used in this study, therefore only this type of membranes will be discussed in more detail.

The separation performance of polymer membranes with nonporous barriers, such as required for pervaporation, is directly influenced by the polymer material itself (Susanto & Ulbricht, 2009:25). The polymer should have preferential interaction with one of the components in the feed to ensure selectivity. There are three types of selective polymeric barriers used in pervaporation, namely hydrophilic, organophilic and organoselective membranes. Glassy polymers, such as cross-linked PVA and polyimide, are usually more suitable for water selective (hydrophilic) membranes while rubbery polymers, such as cross-linked silicone rubber (PDMS), are more suitable for organophilic membranes (Feng & Huang, 1997:1055, Susanto & Ulbricht, 2009:37-38). It is not yet clear which type of polymer is more suitable for organoselective (separation of organic mixtures) membranes as both types show some selectivity. Polyacrylonitrile is usually used as a porous support layer for pervaporation membranes as it is resistant to most organic solvents and it is thermally stable (Susanto & Ulbricht, 2009:37).

Some of the membrane materials that can be used for pervaporation are summarised in Figure 3.2 (Lipnizki *et al.*, 1999:114, Susanto & Ulbricht, 2009:38).

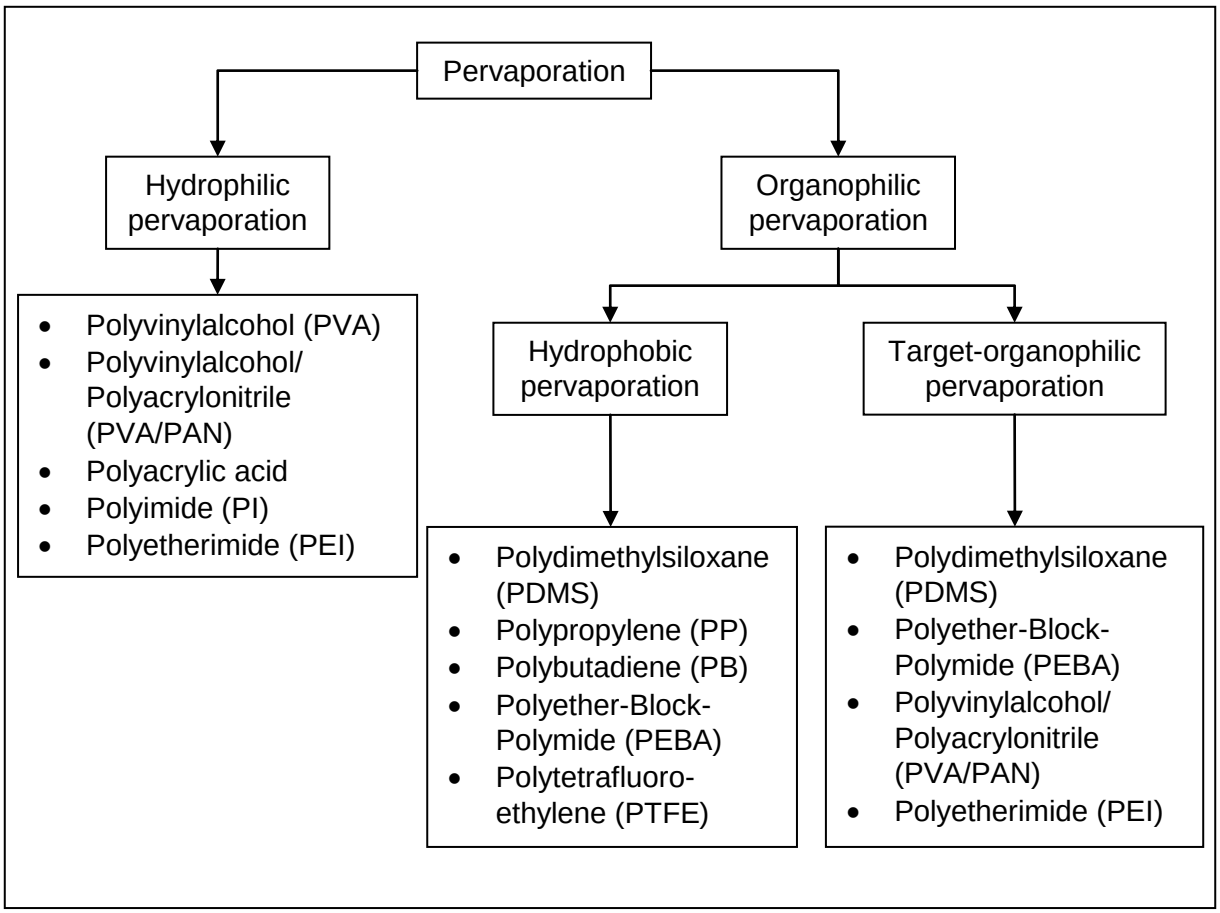

Figure 3.2 Membrane materials for pervaporation

3.1.1.4. Membrane effectiveness parameters

There are three issues that must be addressed in membrane technologies, i.e. the productivity of the membrane, the selectivity of the membrane and the stability of the membrane (Feng & Huang, 1997:1050). These parameters will directly influence the performance of the membrane. The productivity of the membrane is the amount that permeated through a specific area of the membrane in a certain amount of time. Permeation flux (J) is usually used to describe the membrane productivity. The component flux of a membrane is the number of moles, volume, or mass of a specific component passing per unit of time through a unit of membrane surface area (Koros *et al.*, 1996:1482). Equation 3.1 shows how to calculate the flux.

$$J = \frac{m}{At} \qquad \text{Equation 3.1}$$

The enrichment factor (β) is the ratio of the mass or molar fraction of the preferentially permeating specie, i, in the permeate (y) and feed (x), as shown in Equation 3.2.

$$\beta_i = \frac{y_i}{x_i}$$ Equation 3.2

The ability of the membrane to discriminate between the components in the feed mixture to retain or to pass, also known as the extent of separation, is expressed by the separation factor of the membrane. The separation factor is the ratio of the compositions of the components in the permeate relative to the ratio of the compositions of the components in the retentate (Koros *et al.*, 1996:1485). The selectivity (or separation factor) can be calculated using Equation 3.3 (Feng & Huang, 1997:1050).

$$\alpha = \frac{y_i / (1 - y_i)}{x_i / (1 - x_i)} = \frac{(y_i / y_j)}{(x_i / x_j)}$$ Equation 3.3

The preferentially permeating species is i while y and x are the mass or molar fraction of each component in the permeate and in the feed, respectively. If the separation factor is unity, no separation occurs while if the separation factor approaches infinity it becomes perfectly semi-permeable. Membrane permeability and selectivity generally have to be determined experimentally (Feng & Huang, 1997:1050).

The stability of a membrane is the ability of the membrane to maintain the permeability and selectivity under specific process conditions for an extended period of time (Feng & Huang, 1997:1050).

3.1.2. Introduction to pervaporation

Pervaporation is a membrane separation technique in which the phase state on one side of the membrane is different from the other side (Seader & Henley, 2006:527). The feed is in liquid phase and vaporisation occurs as the permeating species passes through the membrane (Humphrey & Keller, 1997:271). The basic concept of pervaporation is shown in Figure 3.3 (Seader & Henley, 2006:527).

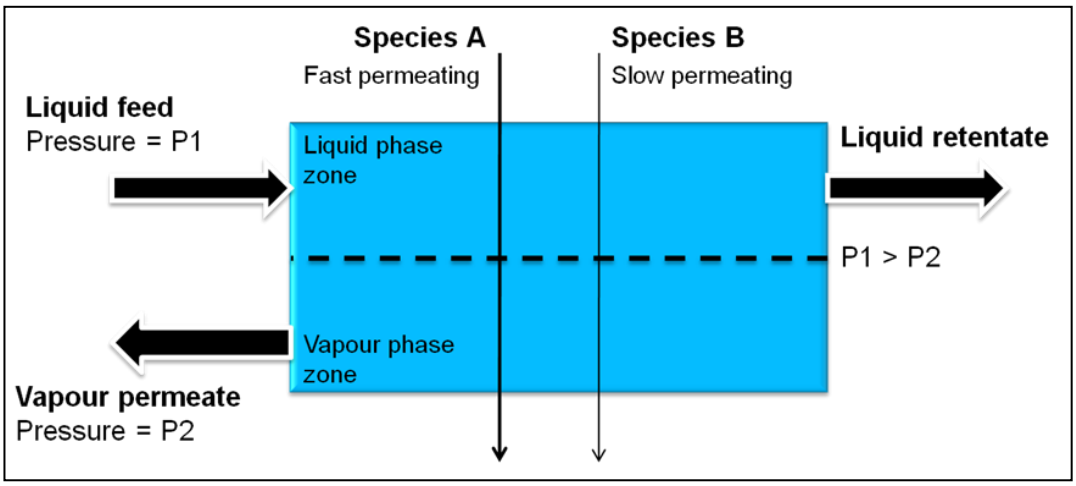

Figure 3.3 Pervaporation

The liquid feed at a higher pressure comes into contact with one side of the membrane and the permeate product is removed as a low pressure vapour from the other side. The driving force that facilitates pervaporation is the chemical potential (difference of partial pressure or activity) between the feed and the permeate side and separation is achieved by different mass transfer rates of the components through the membrane (Lipnizki *et al.*, 1999:116).

3.1.3. Pervaporation in history

Pervaporation is one of the most active areas in membrane research, and the pervaporation process has been shown to be an indispensable component for chemical separations (Feng & Huang, 1997:1048). It all started in 1906 when Kahlenberg observed selective transport of a hydrocarbon and alcohol mixture through a thin rubber sheet (Neel, 1991:2). Kober (1917) defined this transport as pervaporation and many authors consider Kober to be the first observer of pervaporation. The commercial application of pervaporation was first suggested by Binning *et al.* (1961:45) in 1961, but the first commercial plants for the dehydration of alcohol with pervaporation were only installed in the late 1980's (Lipnizki *et al.*, 1999:114, Feng & Huang, 1997:1048).

Pervaporation has come a long way but industrial applications have so far been limited in the number of commercialised systems. Even though pervaporation has been proven as a competitive separation technology and although the process has environmental application and energy saving benefits it appears that due to a lack of knowledge about the capabilities of pervaporation as well as a mistrust of a relatively new technology the application of pervaporation on commercial scale is still relatively limited (Jonquières *et al.*, 2002:105, 106).

3.1.4. Process description

Figure 3.4 shows a typical pervaporation system (adapted from Humphrey & Keller, 1997:272 and Neel, 1991:1).

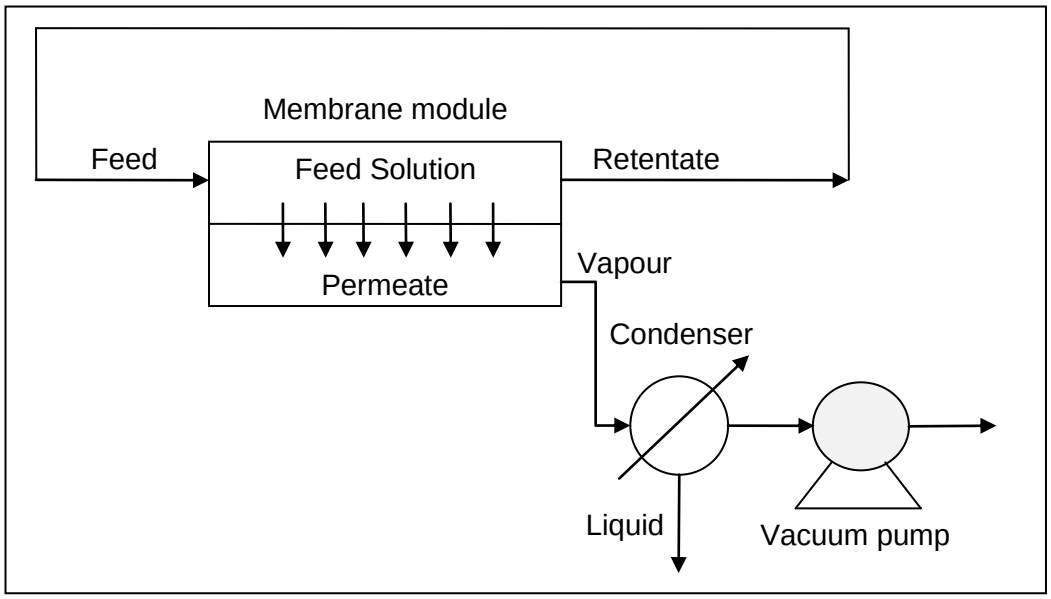

Figure 3.4 Schematic drawing of the pervaporation process

The feed to the membrane module is a liquid mixture, usually at ambient pressure but higher pressures may be necessary to maintain a liquid phase on the feed side (Seader & Henley, 2006:527). The membrane is in contact with the liquid feed. Liquid components are absorbed into the membrane, diffuse through the membrane, and is desorbed at the other side (Seader & Henley, 2006:506). A lower pressure than the dew point of the permeating specie is maintained on the other side of the membrane by using a vacuum pump. A sweep gas can also be used instead of a vacuum pump to maintain a low permeate vapour pressure. The permeating species is recovered by condensing the vapour using a condenser. The retentate can be recycled back to the membrane module depending on the purpose of separation.

As mentioned above, there are different operational modes of pervaporation, vacuum-pervaporation, and sweeping-gas pervaporation. Both of these methods achieve rapid desorption of the permeating species at the downstream surface of the membrane (Neel, 1991:10). Sweeping-gas pervaporation uses a non-permeating gas directed past the downstream membrane surface to reduce the permeate concentration (Koros *et al.*, 1996:1488). The sweeping-gas mode of operation is more complex than vacuum pervaporation and the downstream surface of the membrane is usually not completely dried.

Vacuum pervaporation is most often used but sweeping-gas pervaporation can be used if the permeate can be released without first condensing it (Feng & Huang, 1997:1048).

The product stream of the pervaporation process can be the permeate or retentate stream. The membrane choice and composition of the feed mixture will influence this decision.

3.1.5. Characteristics of pervaporation

3.1.5.1. Swelling of the membrane

One characteristic of pervaporation using polymeric membranes is that the membranes tend to swell. The feed liquid in contact with the membrane dissolves into it, which causes the membrane swelling. This swelling alters the membrane properties and leads to higher permeability and lower selectivity (Feng & Huang, 1997:1049).

The swelling ratio of a membrane is used to describe the swelling of a membrane. It can be measured by bringing a membrane to equilibrium with a liquid by immersing the membrane in the liquid (Freger *et al*., 2000:251). The swelling ratio can be defined as the amount of solution absorbed by the membrane when equilibrium is reached (W_∞-W_0) compared to the dry mass of the membrane (W_0). The degree of swelling (swelling ratio) can be calculated using Equation 3.4 (Mohammadi *et al*., 2005:1876 and Cao *et al*., 1999:378).

$$\text{Swelling ratio } (M_\infty) = \frac{W_\infty - W_0}{W_0} \qquad \text{Equation 3.4}$$

3.1.5.2. Coupling effect

The partial flux of a component in a binary system can change due to the coupling of fluxes. This means that the transport of each permeant is not independent from each other and a change in flux of the component may be observed due to its own movement and the movement of other components through the membrane (Mulder & Smolders, 1984:290). This phenomenon is difficult to measure but indirect information can be obtained through flux and sorption measurements.

3.1.5.3. Fouling

Membrane fouling is caused by undesired interactions between components with the membrane material, which result in the coating or blocking of the membrane surface. The

consequence of fouling is a reduction in membrane flux due to an additional barrier layer that forms or a decrease in the overall selectivity due to the formation of a second non-selective resistance on the membrane (Ulbricht, 2006:2251).

3.1.5.4. Concentration polarisation

Concentration polarisation refers to a difference between the membrane boundary layer composition and the bulk feed composition. Membrane separation leads to an accumulation of the retained species and a depletion of the permeating species in the membrane boundary layer (Bhattacharya & Hwang, 1997:73). This leads to a decrease in the overall efficiency of separation because of a decrease in the driving force of the preferential permeating species across the membrane and an increase in the driving force of the less permeable species. Concentration polarisation can be minimised by maximising mixing at the membrane surface (Wijmans *et al*., 1996:137). The effect of concentration polarisation is often assumed insignificant for pervaporation processes, as the permeating fluxes are usually very small (Feng & Huang, 1997:1053).

3.1.6. Effect of process conditions on pervaporation

It is important to understand the key aspects of a pervaporation process when designing or operating a pervaporation system (Lipnizki *et al.*, 1999:121). Factors that influence the performance of a membrane during pervaporation, apart from the mass transfer through the membrane, are the pervaporation operating parameters. These include the composition of the feed, the temperature of the feed, and the permeate pressure. Understanding the effect of these factors on the membrane will ensure proper operating conditions during the separation process. The influence of the operating parameters on the flux and selectivity of the membrane is discussed in this section.

3.1.6.1. Feed composition

The feed composition affects the sorption of liquid into the membrane, membrane swelling, and diffusion of components through the membrane and therefore the flux and selectivity of the membrane. Permeation takes place when the permeating species is absorbed into and diffused through the membrane. As the feed concentration of the permeating species increases, the quantity of this component absorbed by the membrane also increases (as the affinity by the membrane for a certain component is more than for the other components) and the membrane takes on a swollen state (Baker, 1999:31). It was found by various

researchers that due to the membrane swelling the total flux as well as the specific flux of each component increases with an increase in feed concentration of the preferential permeating component (Baker, 1999:31, Jiraratananon *et al.*, 2002:145, Mohammadi *et al.*, 2005:1877 and Liang & Ruckenstein, 1996:231). The selectivity, however, decreases as the specific flux of the other species in the mixture increases more than the permeating species (Jiraratananon *et al.*, 2002:145, Mohammadi *et al.*, 2005:1877 and Liang & Ruckenstein, 1996:231). The reduction in selectivity can be ascribed to enhanced diffusity of the other components through the membrane as the swollen membrane increases membrane free volume (Mohammadi *et al.*, 2005:1877).

3.1.6.2. Feed temperature

Temperature influences the transport in a membrane in two ways, i.e. firstly by modifying the sorption-diffusion step inside the membrane and secondly by changing the activity driving force across the membrane (Lipnizki *et al.*, 1999:121). Flux is strongly dependent on the feed temperature and the flux usually increases with an increase in temperature (Jiraratananon *et al.*, 2002:147, Weyd *et al.*, 2008:244 and Mohammadi *et al.*, 2005:1877). This is due to an increase in mobility of the permeating molecules and the effect on permeate fluxes because of the strong influence on the vapour pressures of the feed.

The permeation through a membrane is controlled by the amount of sorption into the membrane as well as the diffusion through the membrane. The amount of a component absorbed into a membrane decreases if the temperature increases, but the diffusion rate increases. This means that the flux may increase or decrease if the temperature is increased, depending on the importance of the absorption or diffusion as rate controlling process (Baker, 1999:34). The preferential species usually has a higher affinity for the membrane material than the other components and if the temperature is increased, the permeability of this specie will not increase as much because the decrease in absorption will have a larger influence than with the less permeable components. The diffusity of all the components will increase, however, thereby increasing the flux of the preferential permeating species as well as the non-preferential permeating species. The net effect of an increase in feed temperature will thus most likely be a decrease in membrane selectivity (Baker, 1999:34). A decrease in selectivity was also observed by Jiraratananon *et al.* (2002:147).

Pervaporation involves a phase change from liquid to vapour, as previously discussed. This vaporisation of a portion of the liquid feed requires heat of vaporisation, which is withdrawn from the liquid feed stream (Lipnizki *et al.*, 1999:121). The result is a temperature loss

between the feed entering the membrane module and the retentate leaving the process. If the flux of the membrane is very large, the temperature drop due to the heat loss by vaporisation can be significant.

3.1.6.3. Permeate pressure

The difference between the vapour pressure of the permeating species in the feed and the vapour pressure of the permeate stream is the driving force of the pervaporation process as it is a measure of the chemical potential or activity on the permeate side of the membrane. If the permeate pressure is decreased the driving force of the separation process will increase and thus the permeation rate (total flux) (Baker, 1999:29, Lipnizki *et al.*, 1999:122, Weyd *et al.*, 2008:245 and Jiraratananon *et al.*, 2002:147). It was observed by Jiraratananon *et al.* (2002:147), Weyd *et al.* (2008:245) and Baker (1999:29) that the selectivity also increased if the permeate pressure is decreased. It is not economical to decrease the permeate pressure indefinitely as the energy cost rises sharply with a decrease in pressure (Baker, 1999:29 and Lipnizki *et al.*, 1999:122). An optimum permeate pressure would be a pressure that maximises the driving force of pervaporation, thereby maximising the flux and selectivity of the membrane, while still being economically viable.

3.1.7. Applications for pervaporation

Pervaporation is used in a variety of applications, which include the concentrating, or drying of solvents, purification of solutions, and the separation of mixtures. There are three major commercial applications for pervaporation; dehydration of organic solvents , the removal of organics from water, and the separation of anhydrous organic mixtures (Seader & Henley, 2006:528 and Feng & Huang, 1997:1048).

Dehydration of organic solvents (hydrophilic pervaporation) is especially useful to produce pure products from feed streams that contain azeotropes, such as ethanol and water or isopropanol and water. Water is the targeted component and permeates through the membrane. Specific applications include breaking of azeotropes of binary mixtures and dehydration of multi-component mixtures (Lipnizki *et al.*, 1999:114, Humphrey & Keller, 1997:274).

The removal of organics from water, also known as hydrophobic pervaporation, can be used to purify water contaminated with organic solvents. The organic compound is the target compound, which preferentially permeates through the membrane. Specific industrial

examples include wastewater treatment, the removal of organic traces from ground and drinking water, removal of alcohol from beer and wine, the recovery of aromatics in food technology and separation of compounds from fermentation broths in biotechnology (Lipnizki *et al.*, 1999:114).

The separation of organic mixtures is the least developed of the three categories as problems associated with membrane stability is experienced (Feng & Huang, 1997:1049). One of the organic compounds is the target compound and permeates through the membrane. Examples are the separation of ethanol from ethyl-tert-butyl-ether and the separation of benzene and cyclohexane (Lipnizki *et al.*, 1999:114).

The German company GFT and associated produced over 90% of the commercialised pervaporation systems globally (Jonquiéres *et al.*, 2002:98). Table 3.3 shows the pervaporation systems installed by them between 1984 and 1996 (Jonquiéres *et al.*, 2002:99).

Table 3.3 Installed pervaporation systems

Application	Number of units
Dehydration of organic solvents	
Ethanol	22
Isopropanol	16
Dehydration of other solvents and solvent mixtures	
Esters	4
Ethers	4
Solvent mixtures	3
Dehydration of other solvents and solvent mixtures	
Triethylamine	1
Removal of organics from water	
Tetrachloroethylene	1
Multifunctional systems	
Multifunctional systems	12

Pervaporation can be operated at ambient temperature and low feed pressures and no additional chemicals are required, thereby making it ideal for biotechnology applications where components in the feed may be sensitive to heat, stress or chemicals (Feng & Huang, 1997:1049). Pervaporation is easily integrated with other techniques and a relatively new concept is to combine it with fermentation to remove ethanol continuously from the

fermentation broth. This is to attempt to limit or minimise the inhibitory effect caused by ethanol formed during fermentation.

According to Feng and Huang (1997:1050) there is no significant economy of scale for pervaporation, therefore pervaporation will be suitable for small plants where other separation techniques such as distillation may be too expensive.

3.1.8. Advantages of membrane technology and pervaporation

According to Wee *et al.* (2008:515) pervaporation will become more economical than conventional separation processes such as distillation or adsorption as it is more energy efficient and it is also more environmentally friendly as no other components are required. Pervaporation can also be used to separate azeotropes or other difficult-to-separate mixtures. Less space is required than for other separation techniques, as the process equipment is comparatively small. It is also a simple process, therefore maintenance and control would be fairly easy. It is a very practical and cost-effective separation method especially for smaller plants.

3.1.9. Mass transport through a membrane

There are two extreme approaches to describe mass transport in pervaporation, namely the pore-flow model, and the solution-diffusion model (Wijmans & Baker, 1995:1, Feng & Huang, 1997:1050 and Chen *et al*. 2010:148). According to Wijmans & Baker (1995:1), the pore-flow model describes separation due to pressure-driven convection flow through tiny pores. Separation is achieved because one of the components in the feed is excluded from some of the pores in the membrane through which other components move. In the second model, the solution-diffusion model, the feed components dissolve into the membrane material and then diffuse through the membrane down a concentration gradient. Separation is achieved due to the different amounts of each permeant that dissolve into the membrane and the difference in the rate at which these diffuse through the membrane. Currently the solution-diffusion model is accepted by most researchers to describe pervaporation (Wijmans & Baker, 1995:19, Chen *et al*., 2010:148, Chang *et al*., 2007:43).

The solution-diffusion model consists of three consecutive steps, shown in Figure 3.5 (Feng & Huang, 1997:1051):

1. Sorption of the permeant from the feed to the membrane
2. Diffusion of the permeant in the membrane

3. Desorption of the permeant to the vapour phase on the downstream side of the membrane

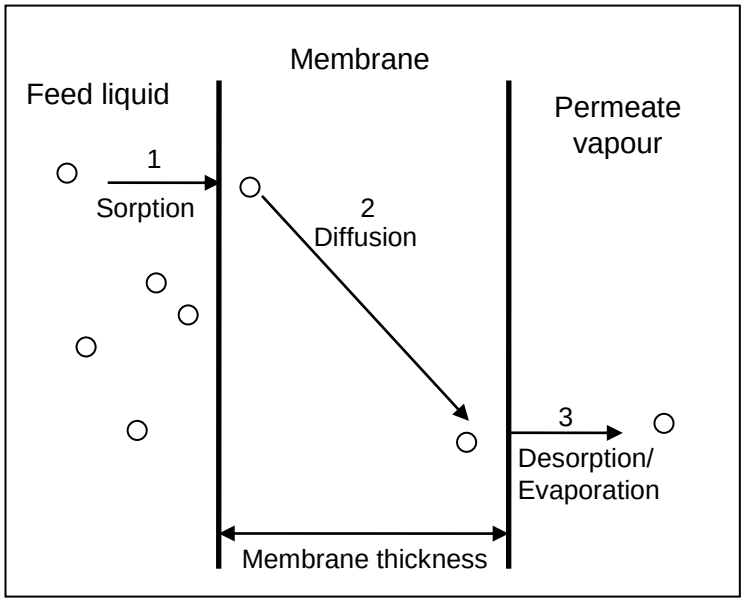

Figure 3.5 Solution-diffusion model

Transport through a membrane during pervaporation involves the transportation of a component of the feed across a membrane from the liquid phase to the vapour phase due to an acting force, i.e. a driving force. The driving force can be the partial pressure difference, the chemical potential difference, or the concentration difference and all three can contribute to the actual driving force for transport. The overall driving force that produces the movement of a permeant is determined by the gradient in chemical potential (Wijmans & Baker, 1995:2). A proportionality relationship exists between the flux and the driving force as shown in Equation 3.5.

$$J_i = -L_i \frac{d\mu_i}{dz} \qquad \text{Equation 3.5}$$

In Equation 3.5 $d\mu_i/dz$ is the gradient in chemical potential of component *i* and L_i is a coefficient of proportionality linking the chemical potential driving force with flux. All the driving forces, such as gradients in concentration, pressure, and temperature, can be reduced to chemical potential gradients, and their effect on flux expressed by Equation 3.5 (Wijmans & Baker, 1995:2). By simply taking into account the driving force produced by the concentration and pressure gradients the chemical potential can be written as shown in Equation 3.6 (Wijmans & Baker, 1995:2).

$$d\mu_i = RTd\ln(\gamma_i c_i) + v_i dp \qquad \text{Equation 3.6}$$

In Equation 3.6 c_i is the molar concentration (mol/mol) of component *i*, γ_i is the activity coefficient linking concentration with activity, p is the pressure and v_i is the molar volume of component *i*. Volume does not change with pressure in incompressible phases such as liquid or solid membranes, and therefore Equation 3.6 can be integrated with respect to concentration and pressure to give Equation 3.7.

$$\mu_i = \mu_i^0 + RT\ln(\gamma_i c_i) + v_i\left(p - p_i^0\right) \qquad \text{Equation 3.7}$$

μ_i^0 is the chemical potential of pure *i* at a reference pressure of p_i^0, defined as the saturation vapour pressure (p_i^{sat}) of *i*.

This model assumes that the fluids on either side of the membrane are in equilibrium with the membrane interface, meaning that there is a continuous chemical potential gradient from one side of the membrane to the other. This assumption also suggests that the rate of absorption and desorption at the membrane interface is much higher than the diffusion rate through the membrane.

The solution-diffusion model assumes that the pressure within the membrane is constant at a high-pressure value p_0, and that the chemical potential gradient across the membrane is a smooth gradient in solvent activity ($\gamma_i c_i$). Equation 3.5 describes the flow that occurs down this gradient (Wijmans & Baker, 1995:4). No pressure gradient exists, therefore Equation 3.5 can be written as Equation 3.8 by combining it with Equation 3.6.

$$J_i = -\frac{RTL_i}{c_i}\frac{dc_i}{dz} \qquad \text{Equation 3.8}$$

Equation 3.8 has the same form as Fick's law (Equation 3.9) where the term RTL_i/c_i can be replaced by the diffusion coefficient D_i.

$$J_i = -D_i\frac{dc_i}{dz} \qquad \text{Equation 3.9}$$

Equation 3.9 can now be used as a starting point (base equation) for pervaporation modelling based on the solution-diffusion model. The basis of the solution-diffusion model is to express diffusion coefficients as a function of concentration, most often linear or exponential equations.

Many versions of the solution-diffusion model have been published, each with its own way of dealing with the non-idealities involved. According to Lipnizki *et al.* (1999:117), Graham (1866) developed the solution-diffusion model to describe gas permeation through rubber septa. In 1961, Binning *et al*. (1961) was the first to propose that the transport of liquids

through homogeneous membranes takes place by a solution-diffusion mechanism. Lee (1975) developed a model that used concentration independent diffusion coefficients and constant solubilities for the permeating species (Feng & Huang, 1997:1051). This model is too oversimplified and will most likely not be a good prediction for pervaporation.

Greenlaw *et al*. proposed a linear relationship between the concentrations of permeants and their diffusion coefficients in 1977, as shown in Equation 3.10.

$$D_i = D_i^0 \left(c_i + \beta_{ij} c_j \right) \qquad \text{Equation 3.10}$$

In Equation 3.10 D_i^0 is the diffusion coefficient at infinite dilution, β_{ij} is the plasticisation coefficient that accounts for the interaction between component *i* and the membrane and the effect thereof on the diffusion of component *j*.

By substituting Equation 3.10 into Equation 3.9 and integrating over the membrane thickness L, Equation 3.11 follows.

$$\int_0^L J_i dz = -D_i^0 \int_{c_{if}}^{c_{ip}} \left(c_i + \beta_{ij} c_j \right) dc_i \qquad \text{Equation 3.11}$$

The concentration of the permeating components on the permeate side is assumed zero due to the very low pressure. Equation 3.11 then simplify as follows:

$$J_i = \frac{D_i^0}{L} \left(\frac{(c_i)^2}{2} + \beta_{ij} c_i (1 - c_i) \right) \qquad \text{Equation 3.12}$$

The parameters D_i^0 and β_{ij} can be determined through non-linear regression.

The Greenlaw model predicts the behaviour of ideal liquid mixtures well but it is uncertain whether it would predict the behaviour of non-ideal mixtures such as ethanol and water (Feng & Huang, 1997:1051, Meuleman *et al*., 1999:2155).

More recently, Mulder and Smolders (1984) developed a solution-diffusion model for the permeation of liquid mixtures through polymeric membranes taking into account coupling of fluxes. They successfully applied this model to the separation by pervaporation of ethanol and water mixtures. Mulder and Smolders (1984) also found that transport of aqueous mixtures could not be described with a concentration independent diffusion coefficient (as proposed by Lee (1975)). Therefore, they proposed an exponential relationship between the diffusion coefficient and concentration.

Long (1965) suggested an exponential concentration dependence of diffusivity, as shown in Equation 3.13. These equations are very sensitive to the permeant concentration in the feed.

$$D_i = D_i^0 \exp\left(\beta_{ij} c_j\right) \qquad \text{Equation 3.13}$$

Equation 3.14 shows substitution of Equation 3.13 into Equation 3.9 and integrating over the membrane thickness L.

$$J_i = \frac{D_i^0}{L}\left(\exp(\beta_{ij} c_i) - 1\right) \qquad \text{Equation 3.14}$$

In 1982, Suzuki and Onozato (1982) proposed an expansion on the Long model (Van der Gryp, 2003).

$$D_i = D_i^0 \exp\left(\beta_{ii} c_i + \beta_{ij} c_j\right) \qquad \text{Equation 3.15}$$

$$J_i = \frac{D_i^0}{L}\left(\frac{-1}{\beta_{ij} - \beta_{ii}}\right)\left(\exp(\beta_{ii} c_i + \beta_{ij}(1 - c_i)) - \exp\beta_{ij}\right) \qquad \text{Equation 3.16}$$

The exponential relationship has been widely used to model pervaporation systems which exhibit large deviations from ideality.

3.2 EXPERIMENTAL METHODS AND PROCEDURES

3.2.1. Chemicals used

The chemicals used in the pervaporation experiments are listed in Table 3.4.

Table 3.4 Chemicals used in this study

Chemical	Supplier	Purity	Use
Glucose	Associated chemical enterprise (ACE)	Analytical grade	Pervaporation experiments and calibration curve
Ethanol	Rochelle	99.9%	Pervaporation experiments and refractometer calibration curve
Liquid nitrogen	Afrox	---	Pervaporation experiments
Yeast (*Saccharomyces cerevisiae*)	Anchor	N/A	Membrane stability experiments

The chemicals were used as received and no further purification was done.

3.2.2. Membranes used

Commercially available membranes were purchased from Sulzer Chemtech in Germany. Four different membranes, PERVAP®2201, PERVAP®2211, PERVAP®4101, and PERVAP®4060, were screened for their efficiency in separating ethanol from water and ethanol mixtures. All of these membranes are crosslinked Polyvinylalcohol (PVA) membranes supported on a Polyacrylonitrile (PAN) support layer coated on a polymer fleece.

A 10wt% ethanol and water mixture was used for the screening experiments as this concentration falls within the ethanol concentration range expected during a traditional batch fermentation process. The membranes were also screened by using pure water and 20wt% ethanol as a minimum and maximum value. A temperature of 30°C was used for all pervaporation experiments including the screening experiments. The pervaporation set-up, as discussed in Section 3.2.3, was used for the screening experiments. The most suitable membrane for ethanol removal was selected on a basis of high flux and high ethanol selectivity, as it is the aim of pervaporation to remove as much ethanol as possible. Good membrane stability was also an important factor in choosing a suitable membrane. The chosen membrane was then used for all subsequent pervaporation experiments, as discussed in Section 3.2.5 and all membrane-reactor system experiments, as discussed in Chapter 4.

3.2.2.1. PERVAP®2201 membrane

A scanning electron microscope (SEM) (Phillips XL30) image of the PERVAP2201® membrane is shown in Figure 3.6. The membrane and the mechanical support separated from each other when the membrane was cut for the SEM photo.

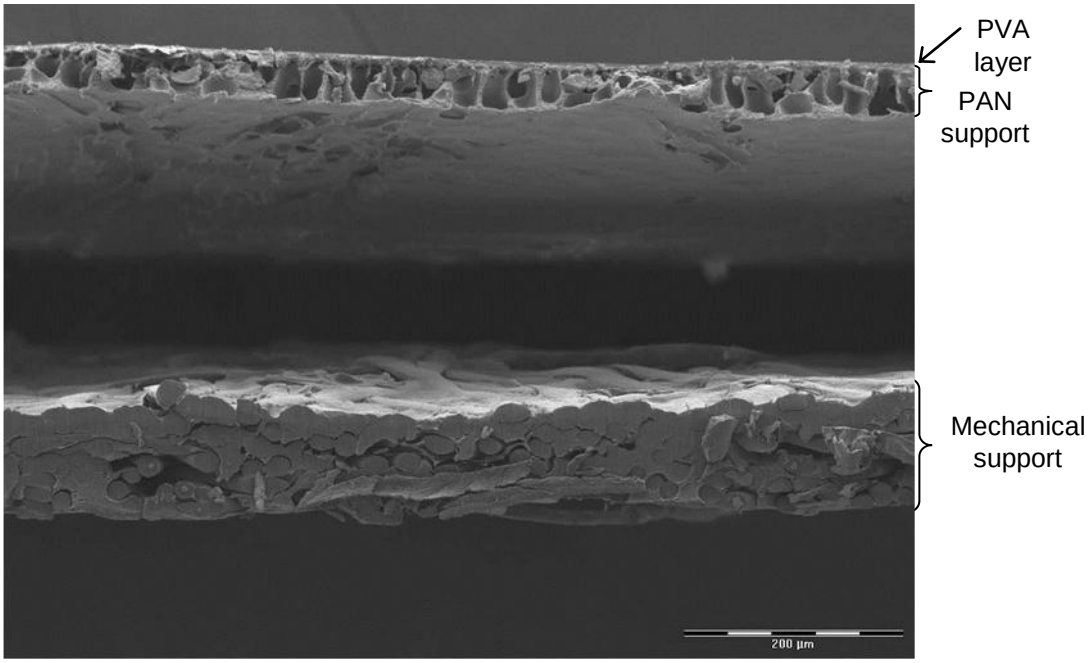

Figure 3.6 SEM image of the PERVAP2201® membrane

Figure 3.7 shows a more detailed SEM image of only the PVA and PAN layers.

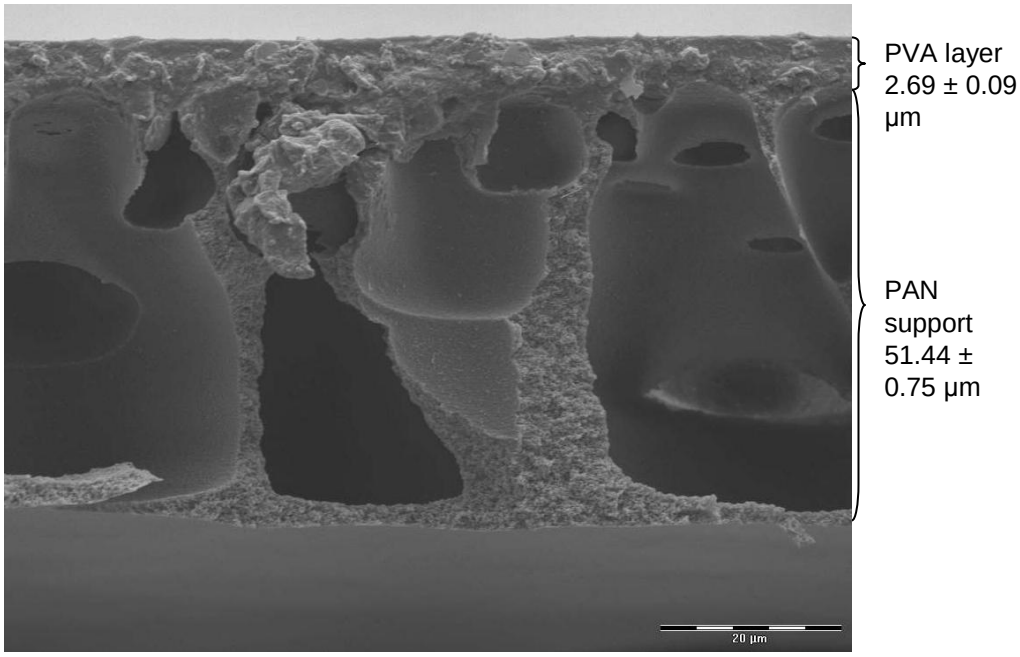

Figure 3.7 SEM image of the PVA and PAN layers of the PERVAP2201® membrane

The thickness of the active PVA layer (the separation layer) was measured as 2.69±0.09µm and the porous PAN support was measured as 51.44±0.75µm. The manufacture's specification sheet for the PERVAP2201® membrane is displayed in Table 3.5.

Table 3.5 Specification sheet for the PERVAP2201® polymeric membrane

Conditions	PERVAP®2201
Main Application	Volatile neutral organics and reaction mixtures
Max Temperature Long Term, °C	95
Max Temperature Short Term, °C	100
Max Water Content in Feed, % b.w.	≤ 50
Major Limitations	
Aprotic Solvents (e.g. DMSO)	≤ 1%
Organic Acids (e.g. acetic acid)	≤ 50%
Formic Acid	≤ 0.5%
Mineral Acids (e.g. H_2SO_4)	≤ 0.1%
Alkali (e.g. NaOH)	<10ppm
Aliphatic Amines (e.g. Triethylamin)	≤ 50%
Aromatic Amines (e.g. Pyridine)	≤ 50%
Aromatic HCs, Ketones, Esters, Cyclic Ethers, Halogenated HCs	no limitations

3.2.2.2. PERVAP®2211 membrane

Figure 3.8 shows an SEM image of the PERVAP2211® membrane.

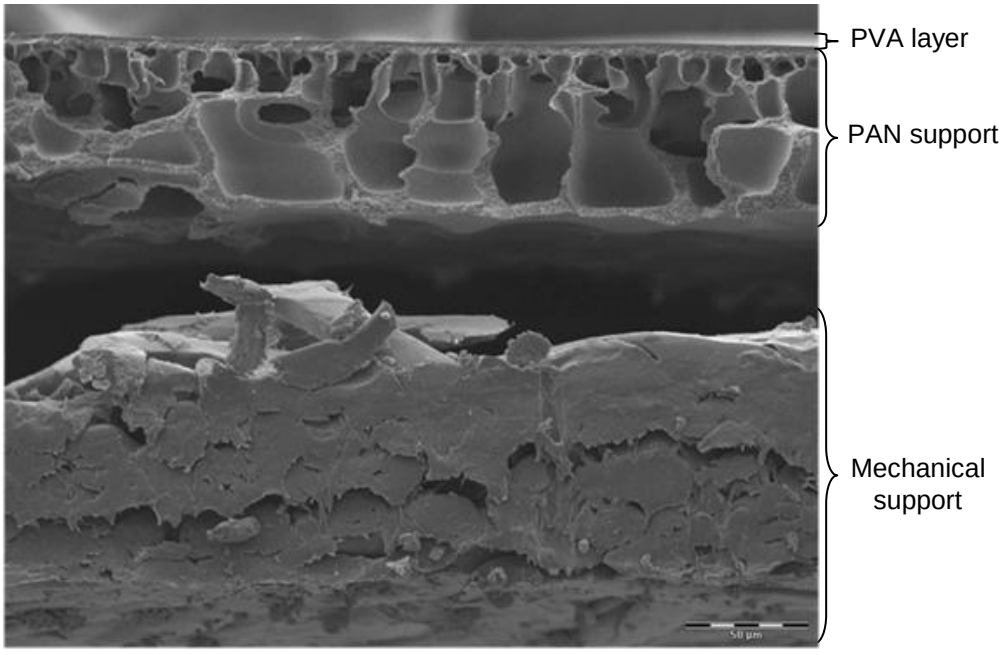

Figure 3.8 SEM image of the PERVAP2211® membrane

A more detailed SEM photo of the PVA and PAN layers is shown in Figure 3.9.

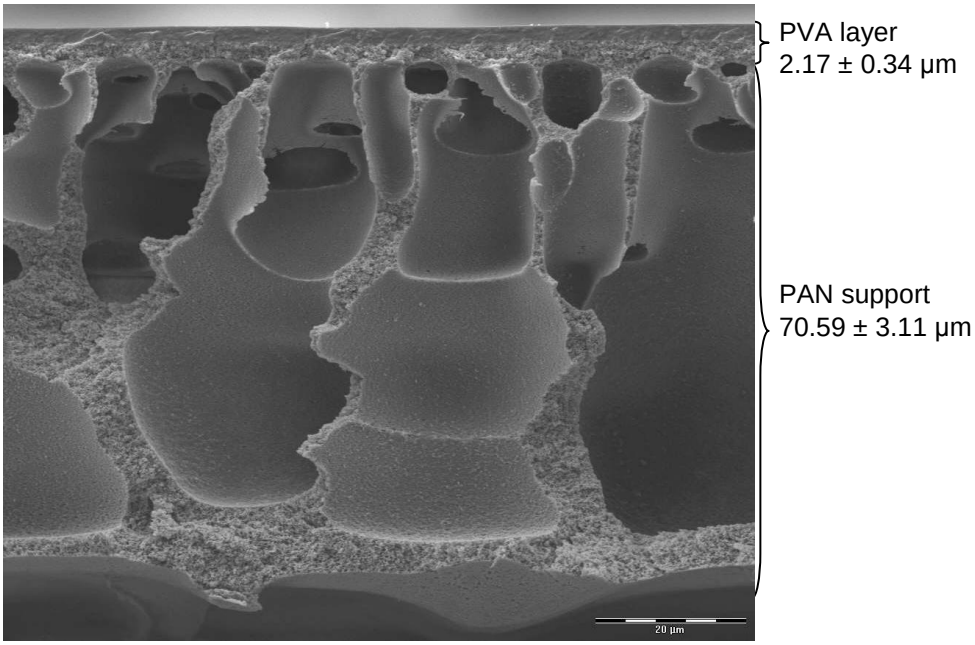

Figure 3.9 SEM image of the PVA and PAN layers of the PERVAP2211® membrane

The thickness of the PVA layer and the PAN layer was measured as 2.17±0.34µm and 70.59±3.11µm respectively. The manufacture's specification sheet for the PERVAP2211® membranes is shown in Table 3.6.

Table 3.6 Specification sheet for the PERVAP2211® polymeric membrane

Conditions	**PERVAP®2211**
Main Application	Volatile neutral organics and their mixtures, EtOH from fermentation processes
Max Temperature Long Term, °C	100 (110 for EtOH)
Max Temperature Short Term, °C	105
Max Water Content in Feed, % b.w.	≤ 40
Major Limitations	
Aprotic Solvents (e.g. DMSO)	≤ 0.1%
Organic Acids (e.g. acetic acid)	≤ 10%
Formic Acid	≤ 0.1%
Mineral Acids (e.g. H_2SO_4)	≤ 0.1%
Alkali (e.g. NaOH)	<10ppm
Aliphatic Amines (e.g. Triethylamin)	≤ 1%
Aromatic Amines (e.g. Pyridine)	≤ 50%
Aromatic HCs, Ketones, Esters, Cyclic Ethers, Halogenated HCs	no limitations

3.2.2.3. PERVAP®4101 membrane

An SEM photo of the PERVAP4101® membrane is shown in Figure 3.10. The three layers, the active PVA layer, the PAN layer, and the mechanical support layer can be clearly seen in Figure 3.10. The PVA and PAN layers, with the thickness of each layer, are shown in Figure 3.11.

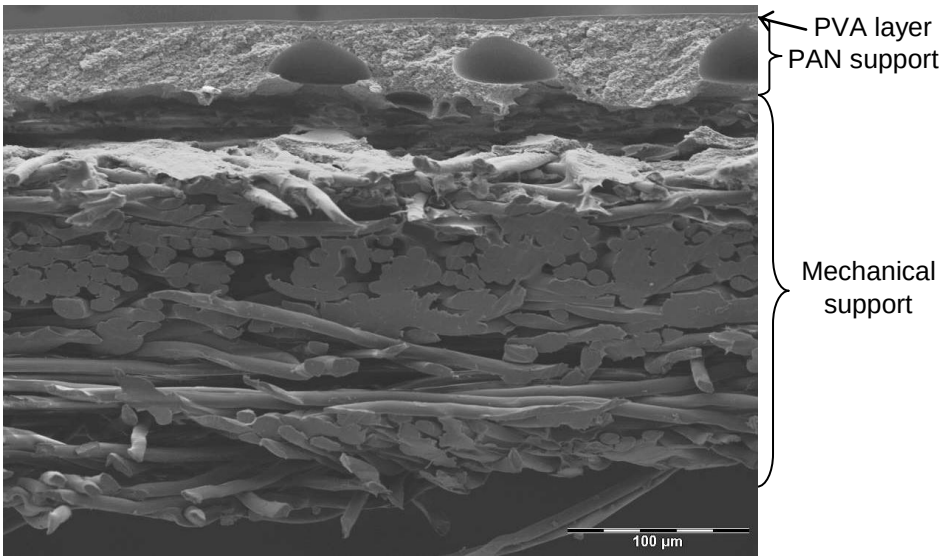

Figure 3.10 SEM image of the PERVAP4101® membrane

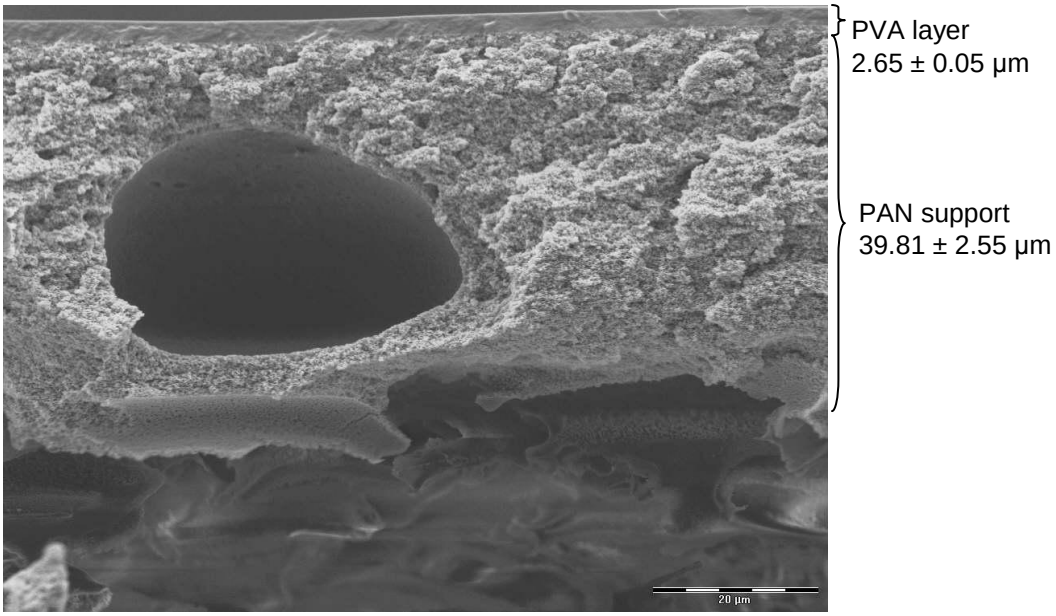

Figure 3.11 SEM image of the PVA and PAN layers of the PERVAP4101® membrane

The PVA layer was measured to be 2.65±0.05µm thick while the porous PAN support was measured as 39.81±2.55µm thick. The specification sheet for the PERVAP4101® membrane, as supplied by the manufacturer, is shown in Table 3.7.

Table 3.7 Specification sheet for the PERVAP4101® polymeric membrane

Conditions	PERVAP®4101
Main Application	Volatile neutral organics and their mixtures, EtOH from fermentation processes
Max Temperature Long Term, °C	100 (110 for EtOH)
Max Temperature Short Term, °C	112
Max Water Content in Feed, % b.w.	≤ 50
Major Limitations	
Aprotic Solvents (e.g. DMSO)	≤ 1%
Organic Acids (e.g. acetic acid)	< 10%
Formic Acid	≤ 0.5%
Mineral Acids (e.g. H_2SO_4)	≤ 1%
Alkali (e.g. NaOH)	<10ppm
Aliphatic Amines (e.g. Triethylamin)	≤ 0.1%
Aromatic Amines (e.g. Pyridine)	≤ 0.1%
Aromatic HCs, Ketones, Esters, Cyclic Ethers, Halogenated HCs	no limitations

3.2.2.4. PERVAP®4060 membrane

Figure 3.12 shows an SEM image of the PERVAP4060® membrane.

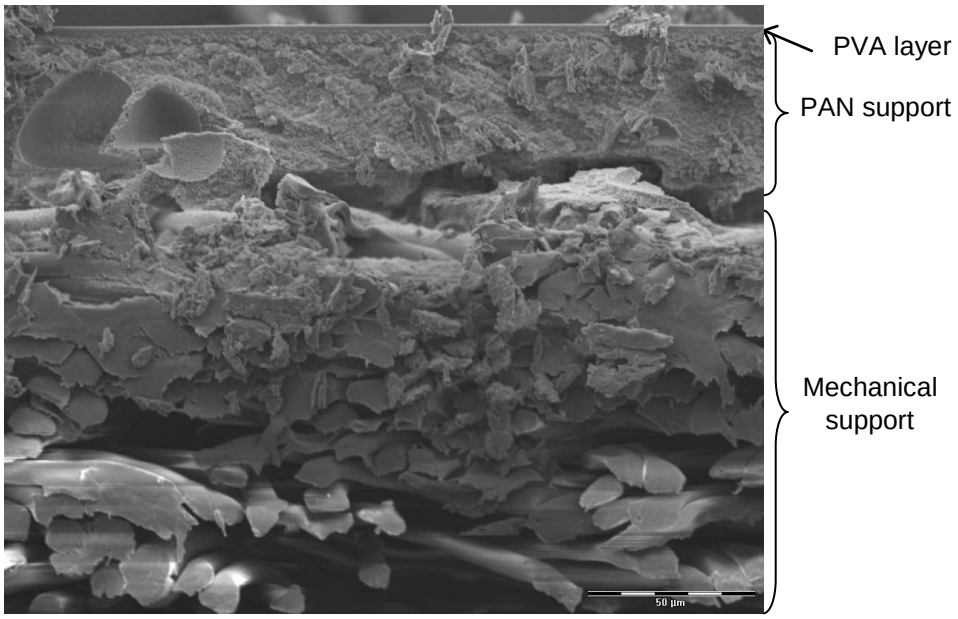

Figure 3.12 SEM image of the PERVAP4060® membrane

Figure 3.13 shows a detailed SEM photo of the PVA and PAN layer of the PERVAP4060® membrane.

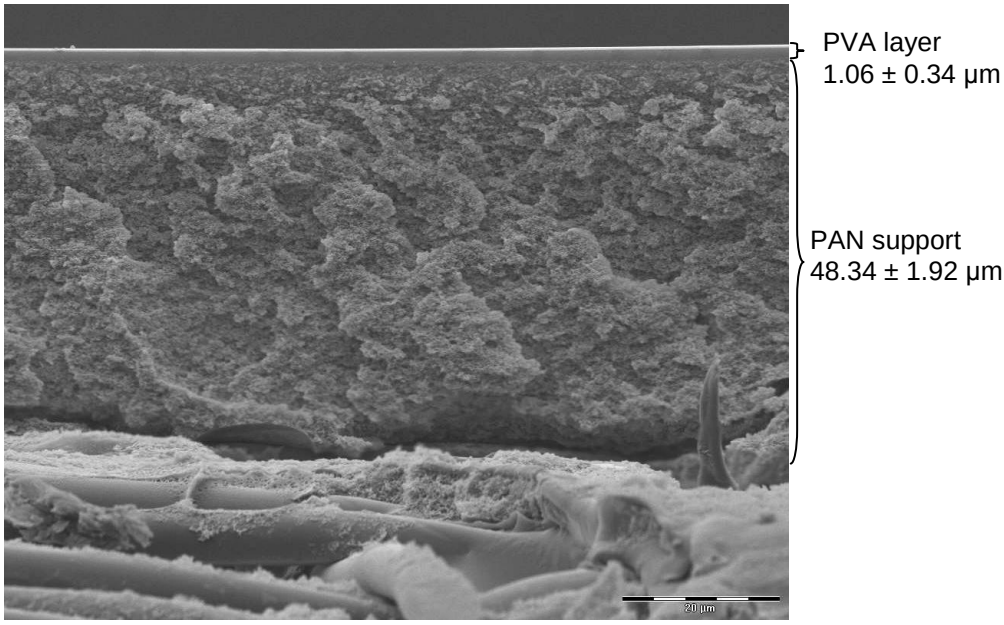

Figure 3.13 SEM image of the PVA and PAN layers of the PERVAP4060® membrane

It was determined that the PVA layer is 1.06±0.34µm thick and that the PAN support layer is 48.34±1.92µm thick. Table 3.8 shows the manufacture's specification sheet for the PERVAP4060® membrane.

Table 3.8 Specification sheet for the PERVAP4060® polymeric membrane

Conditions	PERVAP®4060
Main Application	Removal of volatile organics from water
Max Temperature Long Term, °C	80
Max Temperature Short Term, °C	85
Max Water Content in Feed, % b.w.	N/A
Major Limitations	
Aprotic Solvents (e.g. DMSO)	≤ 0.1%
Organic Acids (e.g. acetic acid)	≤ 1%
Formic Acid	excluded
Mineral Acids (e.g. H_2SO_4)	≤ 0.1%
Alkali (e.g. NaOH)	excluded
Aliphatic Amines (e.g. Triethylamin)	excluded
Aromatic Amines (e.g. Pyridine)	≤ 0.1%
Aromatic HCs, Ketones, Esters, Cyclic Ethers, Halogenated HCs	no limitations

3.2.3. Apparatus and experimental procedure

The standard pervaporation set-up is well described in literature (see for example Schmidt *et al*., 1997; Mohammadi *et al.*, 2005; Weyd *et al.*, 2008 and Wu *et al.*, 2005). The

experimental apparatus used in this study to generate the pervaporation data is shown in Figure 3.14.

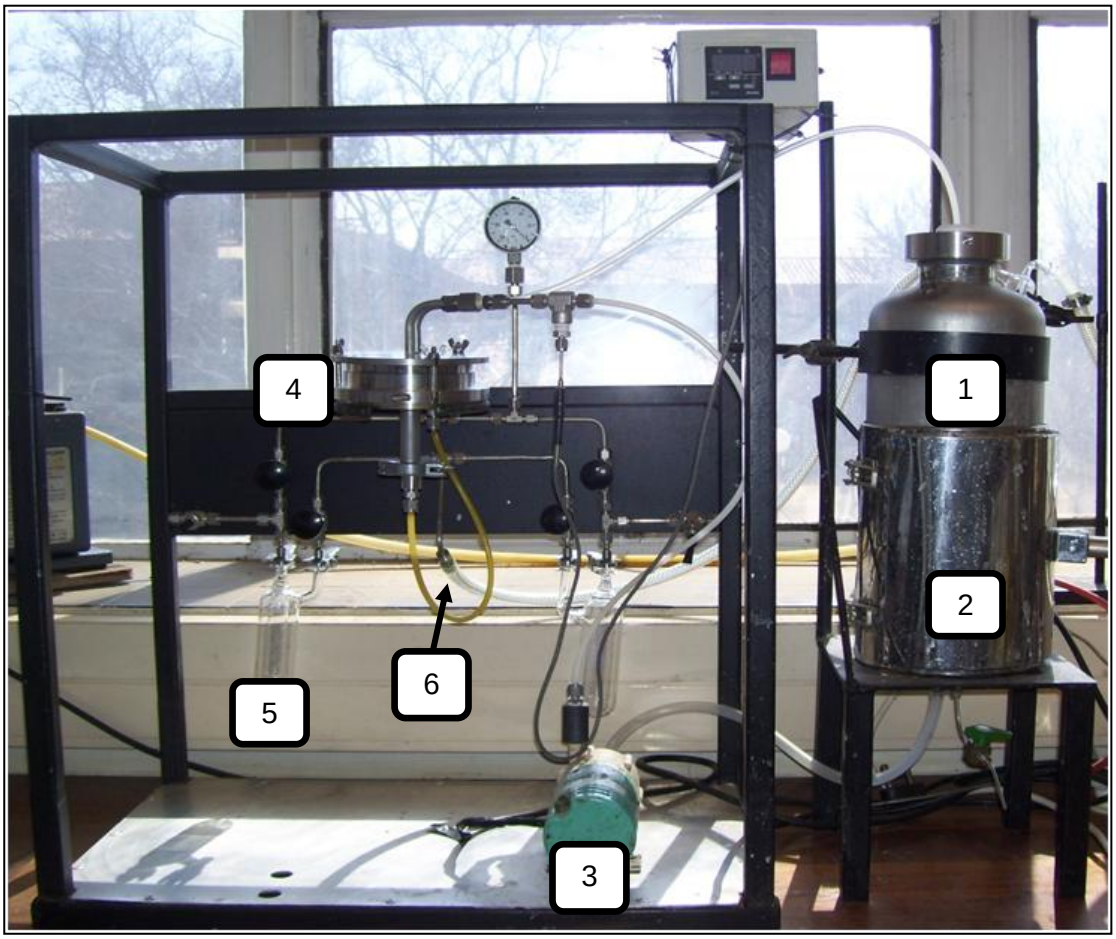

Figure 3.14 Photo of pervaporation apparatus
(1: feed vessel; 2: heating jacket; 3: feed pump; 4: membrane module; 5: cold trap; 6: to vacuum pump)

During pervaporation, the feed mixture in the feed tank (1) was circulated across the membrane module (4) and back to the feed tank using the feed pump (3). The heating jacket (2) kept the temperature in the feed tank at a set temperature. The temperature was also measured just before the feed would reach the membrane module. A vacuum on the permeate side of the membrane was created by a vacuum pump (6). The permeating species was collected in cold traps (5) using liquid nitrogen. The collected fluid in the cold traps was analysed by using a refractometer and confirmed with HPLC analysis and the amount of permeate was measured by using a mass balance. Details of the pervaporation apparatus shown in Figure 3.13 are given in Table 3.9.

Table 3.9 Specifications of pervaporation apparatus

Equipment	Description	Operating conditions
Feed vessel (1)	Stainless steel tank	Total volume of 0.008m^3
Heating jacket (2)	Heats the feed mixture to a set temperature	N/A
Feed pump (3)	Iwaki magnetic pump from Iwaki Co Ltd, Japan	Flow rate of 5.1×10^{-1} $m^3.h^{-1}$
Membrane module (4)	Stainless steel support for membrane	Effective membrane area = $2.54 \times 10^{-2} m^2$
Cold trap (5)	Glass cold trap to collect permeate with liquid nitrogen	---
Vacuum pump (6)	Creates a vacuum on the permeate side of the membrane	Highest vacuum: 0.1mbar

Figure 3.15 shows a detailed three-dimensional drawing of the pervaporation setup.

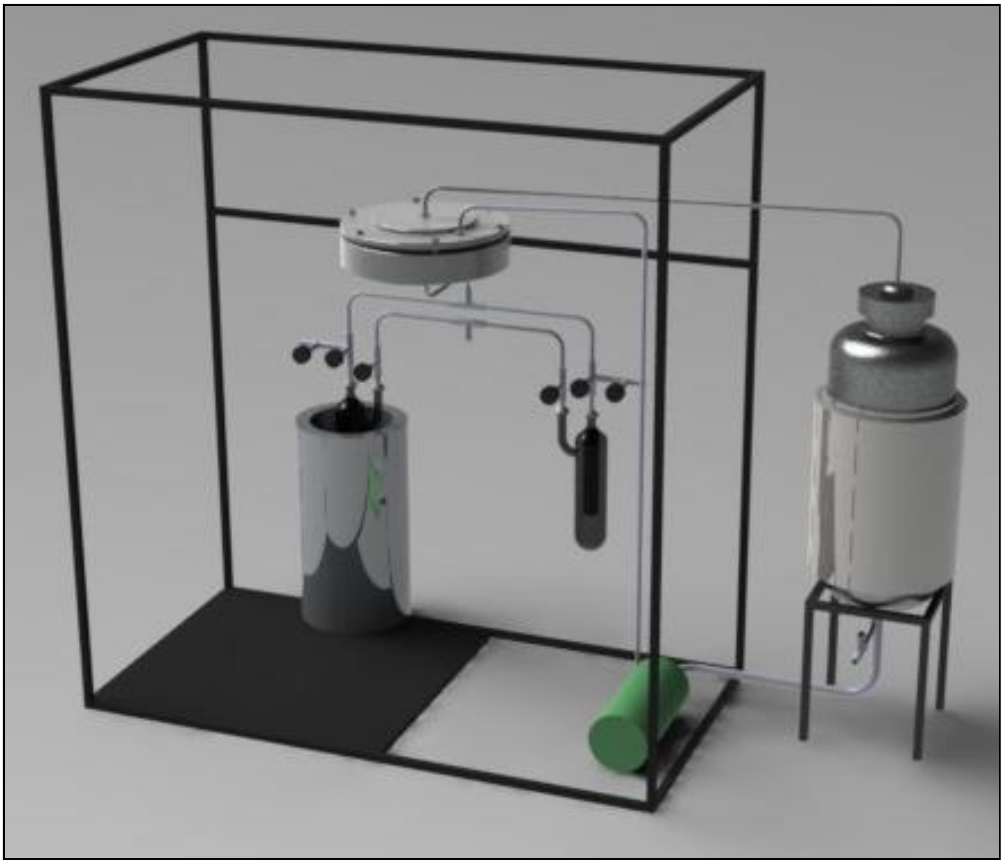

Figure 3.15 Three-dimensional drawing of the pervaporation apparatus

3.2.4. Screening experiments

Screening experiments were necessary to determine the most suitable membrane for ethanol and water separation from the four membranes that were provided. Binary mixtures of ethanol and water were used to test the membranes. All of the membranes were tested at

0, 10, and 20wt% ethanol using the experimental set-up as discussed in Section 3.2.3. The total flux and selectivity of each of these experiments was then calculated and compared. The raw data of the screening experiments can be found in Appendix F. Figure 3.16 shows the total flux over each membrane at the different ethanol concentrations.

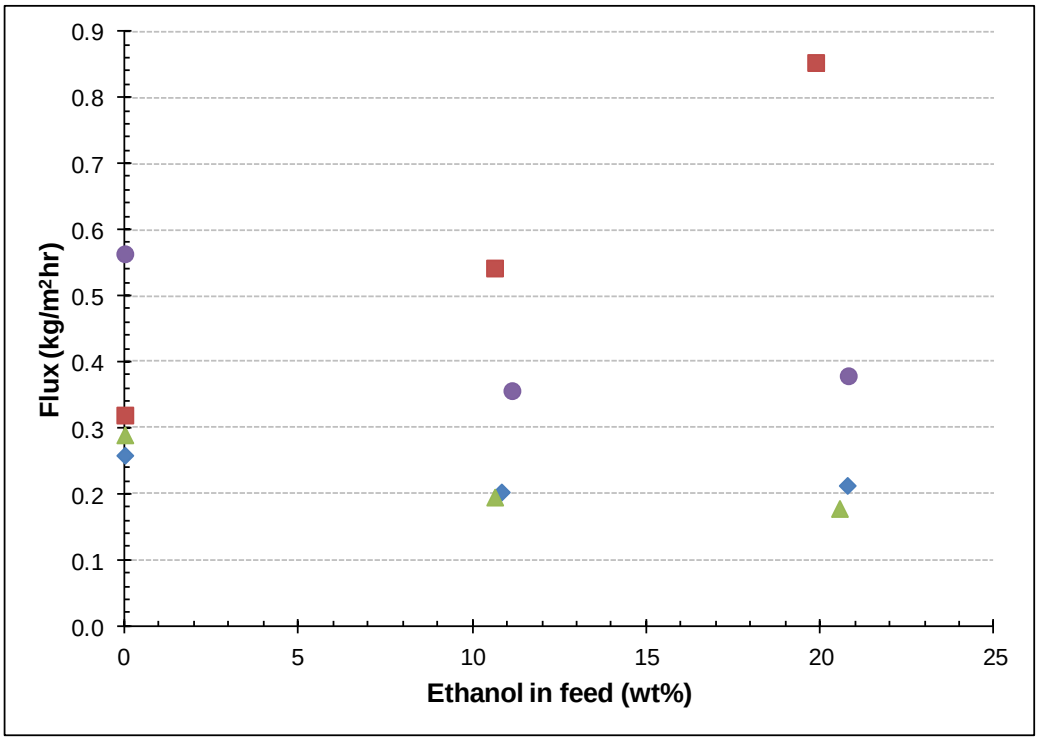

Figure 3.16 Comparison of the flux at different ethanol concentrations for different pervaporation membranes
(♦2211, ■4060, ●2201, ▲4101)

As seen from Figure 3.16 the flux of the PERVAP®2201 membrane was the highest when pure water was used while the flux of the PERVAP®4060 membrane was the highest when 10wt% and 20wt% ethanol was used. The ethanol selectivity of the membranes is shown in Figure 3.17.

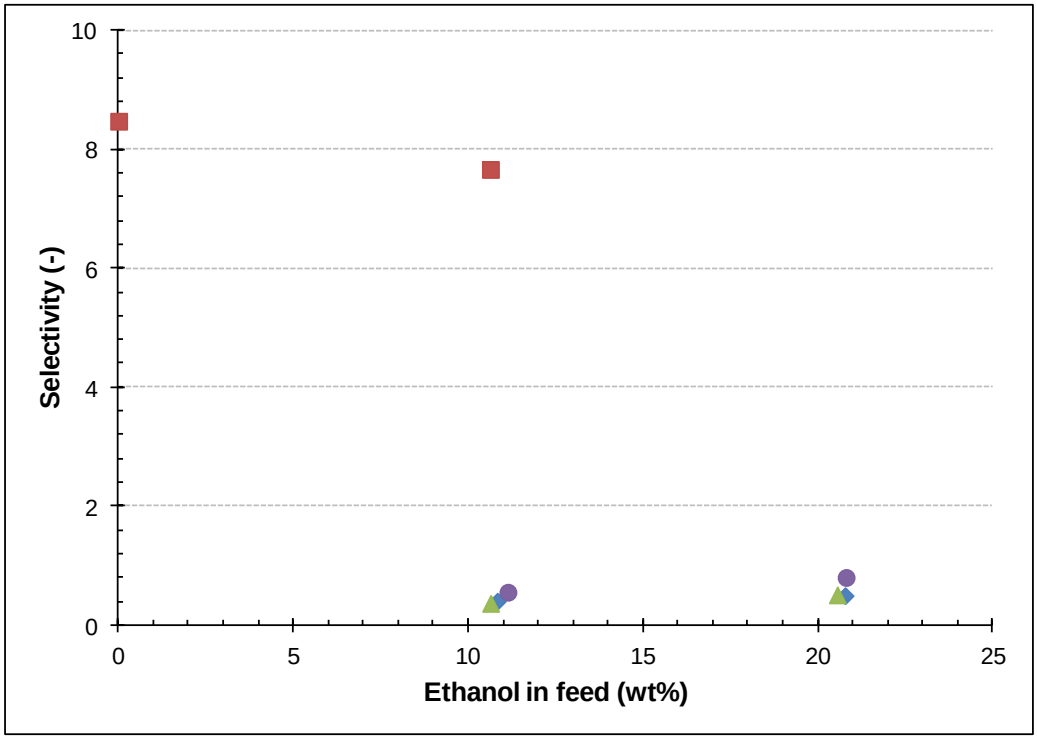

Figure 3.17 Comparison of the ethanol selectivity at different ethanol concentrations for different membranes
(♦2211, ■4060, ●2201, ▲4101)

From Figure 3.17 it is clear that the ethanol selectivity of the PERVAP®4060 membrane is the highest. The ethanol selectivity of the other three membranes (PERVAP®2201, PERVAP®2211, and PERVAP®4101) are all very low and therefore are not suitable to separate ethanol from a fermentation broth.

All four of the membranes showed a stable performance throughout the 3 to 7 hours of operation (time it took to reach steady state). The stability of the membranes in different ethanol concentrations was also verified with a visual stability test. All of the membranes remained stable at different ethanol concentrations, ranging from 30 to 100wt% ethanol, when it was submerged for a minimum of 48 hours. The visual stability test results can be found in Appendix F.3.

It was decided to use the PERVAP®4060 membrane for all subsequent experiments as it compared with the other membranes regarding stability and it had the highest ethanol flux and selectivity of all of the membranes tested. The stability of the PERVAP®4060 membrane was further tested in the pervaporation unit. This stability test was conducted at 30°C with a 10wt% ethanol feed for 48 hours. See Appendix G for the experimental data of this stability test.

3.2.5. Pervaporation experimental planning

The purpose of the pervaporation experiments was to investigate the effect that ethanol and glucose would have on the performance of the membrane.

A traditional experimental design was followed. The ethanol concentration was varied from 0 to 20wt% while the glucose concentration was kept constant at different levels between 0 and 15wt%. The upper limit of 20wt% for ethanol concentration was chosen, as a traditional batch fermentation process will not exceed this concentration of ethanol. An upper boundary of 15wt% glucose was chosen, as it was the optimum glucose concentration for fermentation and therefore fermentation broth combined with pervaporation would not contain more glucose than this optimum. The temperature and permeate pressure was kept constant at 30°C and 0.1mbar respectively for all of the experiments. The reproducibility of the experimental method was validated (as discussed in Section 3.2.7) by repeating experiments at the same conditions.

3.2.6. Sorption experiments

Dry membrane pieces (approximately 0.3g each) were weighed and immersed in solutions of different concentrations of ethanol. The temperature was kept constant at 30°C by placing the flask that contains the membrane piece in an incubator. The membranes were removed from the solutions at fixed time intervals and the adhering solution drops were removed by wiping the membranes with tissue paper. The membranes were then weighed immediately and returned to the solution. This procedure was repeated until no further mass increase was observed as it indicated that sorption equilibrium had been reached. The ethanol concentrations of the solutions were varied from 0 to 20wt% ethanol and each experiment was repeated four times to ensure accurate results. The membrane sorption at 10wt% ethanol was repeated six times to verify the repeatability of the sorption experiments.

3.2.7. Reproducibility of the experimental methods

The reproducibility of results and the experimental error for the pervaporation and sorption experiments were determined by conducting at least three consecutive experimental runs at the same conditions. Details on how the experimental error was calculated are presented in Appendix B.

The pervaporation experimental errors were found to be 3.43% for the total flux response, 24.36% for the ethanol flux response, and 25.10% for the selectivity response. The error on

the enrichment factor was found to be 17.24%. The sorption experimental error was found to be 3.27% for the final swelling ratio.

3.2.8. Analytical techniques

3.2.8.1. Refractive index analyses

A refractometer from Bellingham and Stanley Ltd. (model RFM 340) was used to measure the ethanol concentration in the feed (where only ethanol was present) and the permeate of the pervaporation experiments. A calibration curve relates the refraction measured by the refractometer and the ethanol concentration in the sample. This calibration curve is discussed in Appendix B.

3.2.8.2. Glucose and ethanol analyses

Glucose and ethanol concentrations were determined with an Analox GM8 analyser. The analyser uses an enzyme assay to determine the glucose and ethanol concentrations according to Equation 3.17 and 3.18.

$$\beta\text{-D-Glucose} + O_2 \xrightarrow{\text{Glucose oxidase}} \text{Gluconic Acid} + H_2O_2 \qquad \text{Equation 3.17}$$

$$Ethanol + O_2 \xrightarrow{\text{Alcohol oxidase}} \text{Acetaldehyde} + H_2O_2 \qquad \text{Equation 3.18}$$

3.3 RESULTS AND DISCUSSION

The sorption and pervaporation experimental results will be discussed in this section. Sample calculations related to this section can be found in Appendix D.

3.3.1. Sorption

The sorption characteristics of the PERVAP®4060 membrane are discussed in this section. The active membrane thickness of the PERVAP®4060 membrane was only 1.06±0.34μm as shown in the SEM image in Figure 3.13, meaning that very little liquid had been absorbed into the membrane. The amount that was absorbed was too small to be extracted and analysed by HPLC. Swelling equilibrium was reached very fast with an average time between 2 and 5 minutes for ethanol and water mixtures, depending on the ethanol content. It took longer, about 2 hours, to reach swelling equilibrium when pure water was used.

Scholes *et al.* (2010) used the PERVAP®4060 membrane to study sorption of carbon dioxide, hydrogen sulphide, and carbon monoxide gas mixtures and sorption mass equilibrium was reached within 3 hours for all gases. Water sorption was also studied by Scholes *et al.* (2010) and swelling equilibrium was reached within 2 hours, which compares to the results obtained in this study.

According to Chovau *et al*. (2011:1672), sorption experiments are critical in determining the affinity of a specific component for a membrane and the interaction of the component with the membrane. The final swelling ratio versus the feed composition for the PERVAP®4060 membrane is shown in Figure 3.18.

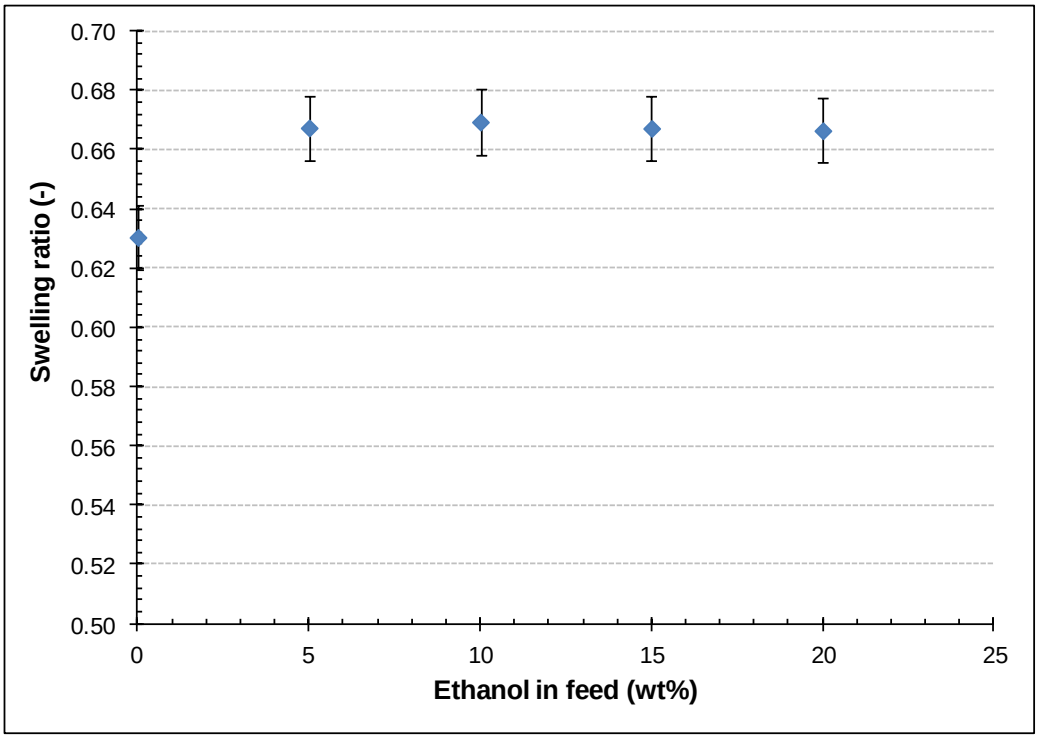

Figure 3.18 Swelling ratio at different feed compositions

For binary mixtures between 5wt% ethanol and 20wt% ethanol the swelling ratio stayed constant. The general rule is that the swelling of the membrane will be higher if the component that interacts with the membrane is higher in the feed (González-Marcos *et al*., 2004:1400). The swelling ratio for pure water is slightly lower than swelling with ethanol mixtures between 5 and 20wt% ethanol, suggesting that the membrane has a higher affinity for ethanol than for water, and will therefore be suitable to separate ethanol and water mixtures. Mohammadi *et al.* (2005) studied sorption of alcohol and water mixtures with a laboratory manufactured PDMS membrane. The degree of swelling of the PDMS membrane using low ethanol concentrations (0.3-5wt%) was investigated and it was found that the equilibrium degree of swelling of 5wt% ethanol was approximately 0.5 which is lower than

the value obtained at the same wt% ethanol in this study using the PERVAP®4060 membrane (0.667±0.011).

3.3.2. Pervaporation: influence of feed composition

The pervaporation characteristics of the PERVAP®4060 membrane in mixtures of different ethanol and glucose concentrations are discussed in this section. The effect of feed composition on total flux, partial flux, and selectivity will be discussed.

3.3.2.1. Total flux and selectivity

The effect of feed composition on the performance of the PERVAP®4060 membrane was investigated by varying the wt% ethanol (0-20wt%) and wt% glucose (0-15wt%) in the feed. All experiments were carried out at a constant temperature of 30°C. The permeate mass as well as the permeate composition was determined in order to calculate the total flux and ethanol selectivity through the membrane. Figure 3.19 shows the effect of feed composition on the total membrane flux.

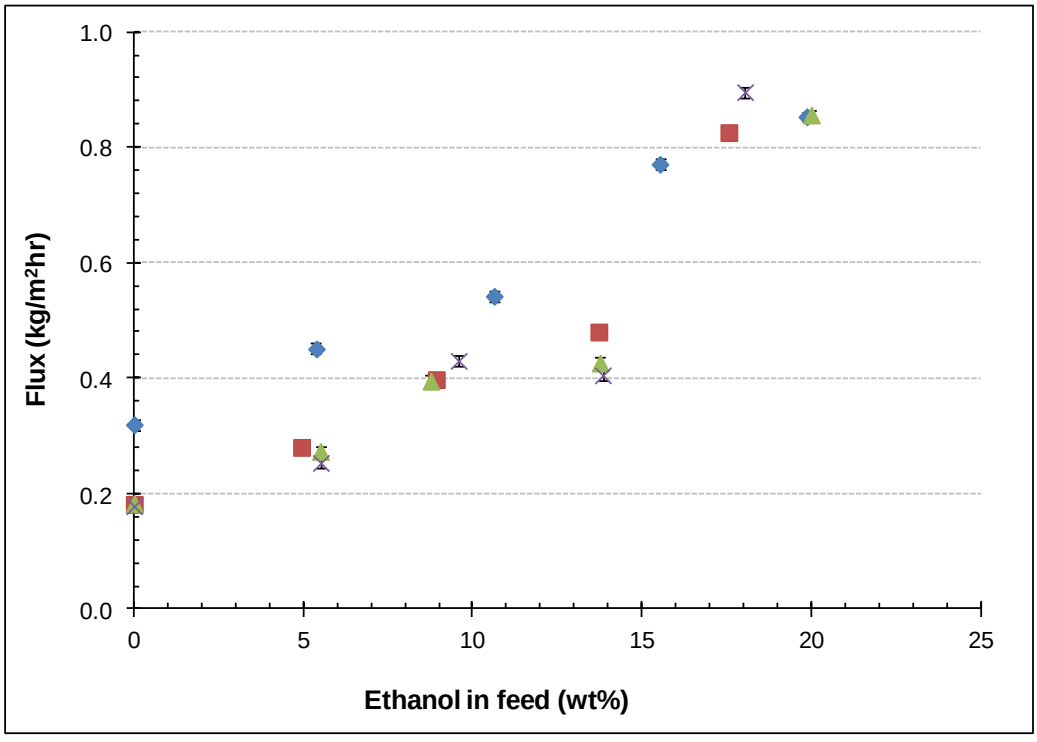

Figure 3.19 Influence of feed composition on total flux
(♦0wt% glucose, ■5wt% glucose, ▲10wt% glucose, X15wt% glucose)

Figure 3.19 shows that the total flux increased with an increase in the wt% ethanol. Various researchers including Zhou *et al*. (2011) and Kaewkannetra *et al*. (2011) also found that the

total flux increased with an increase in the wt% ethanol in the feed. According to Zhou *et al*. (2011:381), this is because an increase in feed concentration results in an increase in activity and partial pressure, thereby increasing the driving force for permeation. Zhou *et al*. (2011) studied the separation of acetone, butanol, ethanol, and water mixtures by pervaporation using a silicalite-1/polydimethylsiloxane (PDMS) hybrid membrane. Kaewkannetra *et al*. (2011) investigated the separation of ethanol from an ethanol and water mixture using flat sheet cellulose acetate membranes. The total flux increased from 3.4 kg/m^{2}h with 10wt% ethanol to 19.1 kg/m^{2}h with 30wt% ethanol which is much higher than the total flux obtained in this study using the PERVAP®4060 membrane. However, the total flux of this study is in the same magnitude as the value obtained by Chovau *et al.* (2011) (0.55 kg/m^{2}h) who used the PERVAP®4060 membrane to separate ethanol from a 5wt% ethanol and water mixtures.

The addition of glucose decreases the total flux but the amount of glucose did not make any difference. The decrease in flux when glucose was present in the feed could be due to fouling of the membrane as a result of the added glucose. At a high wt% of ethanol (20wt%) the addition of glucose did not have an influence on the total flux. No glucose was detected in the permeate during any of the experiments and therefore glucose is considered an impermeable component.

As three components, water, ethanol, and glucose were present in different fractions in the feed Equation 3.3 was used to calculate the selectivity.

$$\alpha = \frac{y_{EtOH} \,/\left(y_{H_2O}\right)}{x_{EtOH} \,/\left(x_{H_2O}\right)} \qquad \text{Equation 3.3}$$

Figure 3.20 shows the selectivity related to the feed composition of the PERVAP®4060 membrane.

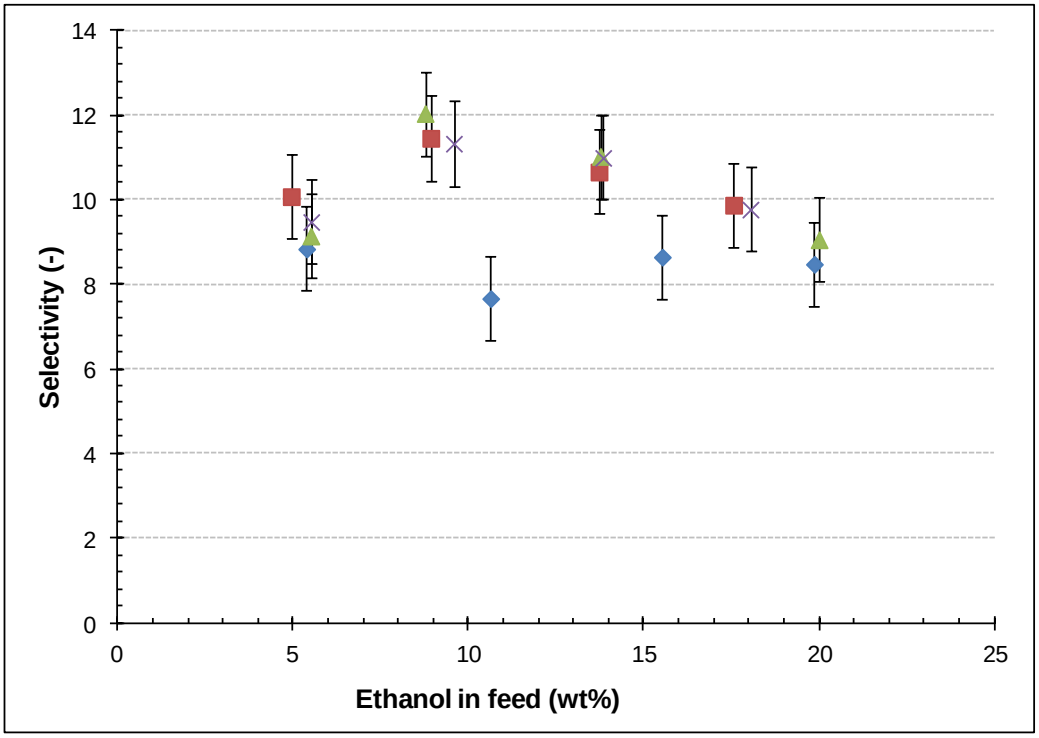

Figure 3.20 Influence of feed composition on selectivity
(♦0wt% glucose, ■5wt% glucose, ▲10wt% glucose, X15wt% glucose)

Again, Figure 3.20 shows that the addition of glucose had an effect on the membrane selectivity but the quantity of glucose present did not have a significant effect on the selectivity. It would, however, be better to make use of an enrichment factor to directly investigate the influence of glucose on the enrichment of ethanol in the permeate compared to the feed composition (Chovau *et al.*, 2011:1671). The enrichment factor was calculated using Equation 3.2.

$$\beta_{EtOH} = \frac{y_{EtOH}}{x_{EtOH}} \qquad \text{Equation 3.2}$$

where y_{EtOH} and x_{EtOH} represent the mass fraction ethanol in the permeate and feed respectively.

Figure 3.21 shows the enrichment factor of the membrane related to the feed composition. The enrichment factor decreases with an increase in ethanol concentration in the feed. This is expected as the ethanol enrichment (related to the selectivity of the membrane) is expected to increase with decreased concentrations of the target component.

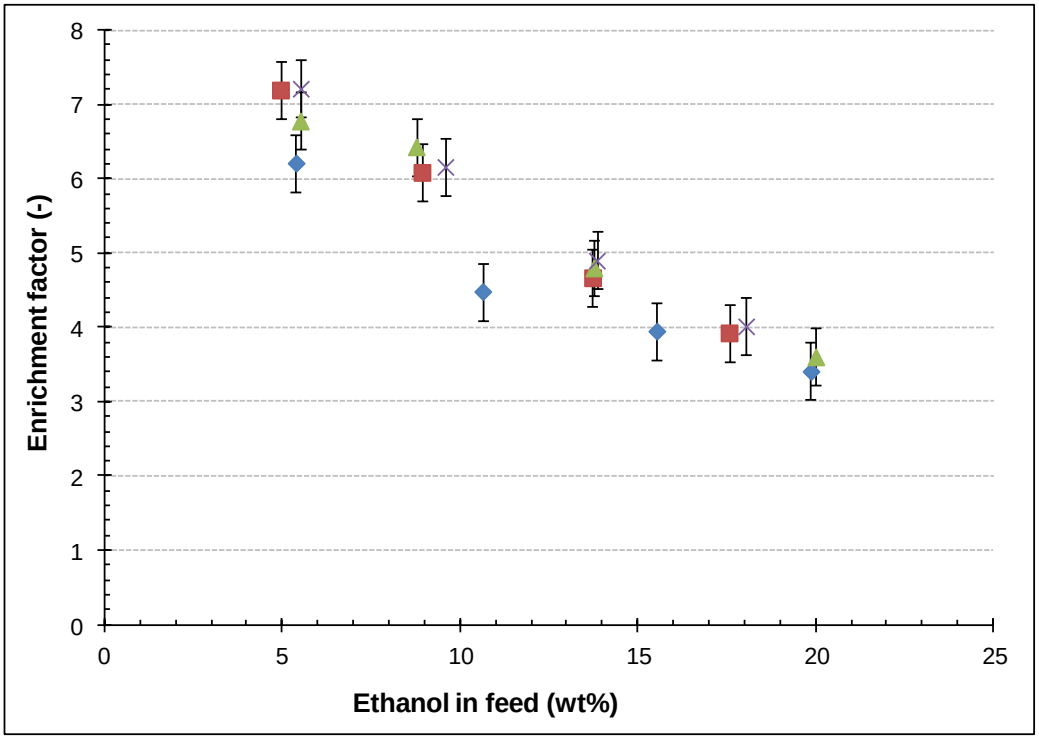

Figure 3.21 Influence of feed composition on enrichment factor
(♦0wt% glucose, ■5wt% glucose, ▲10wt% glucose, X15wt% glucose)

As seen in this study, the total flux increases with an increase in the mass fraction of ethanol while the enrichment factor decreases. This tendency is related to the swelling behaviour of the membrane (Kaewkannetra *et al*., 2011:89, González-Marcos *et al*., 2004:1400). At high concentrations of the preferential permeating component (in this case ethanol), the membrane becomes swollen due to an affinity of the membrane to ethanol. The polymer chains in the membrane become more flexible as the distance between the polymer chains increases as a result of the swelling. This promotes the transport of ethanol and water more freely through the membrane, leading to an increase in total flux. A decrease in enrichment factor is observed as the mobility of both molecules is increased leading to an increase in water flux.

The glucose in the feed leads to a slight increase in enrichment factor (shown in Figure 3.20). The increase in enrichment in the presence of glucose was also observed by Chovau *et al*. (2011). This can be explained by the decrease in partial flux. The partial water flux decreases more than the partial ethanol flux (see Section 3.3.2.2), leading to a higher mass fraction of ethanol in the permeate. Glucose prefers bonding to water rather than ethanol and this decreases the vapour pressure of water and increases the ethanol vapour pressure (Chovau *et al*., 2011:1671) leading to a lower water flux than ethanol flux, thus leading to an increase in enrichment factor.

3.3.2.2. Partial flux

The influence of feed composition on the flux of the single components is shown in Figure 3.22 and Figure 3.23 for ethanol and water respectively.

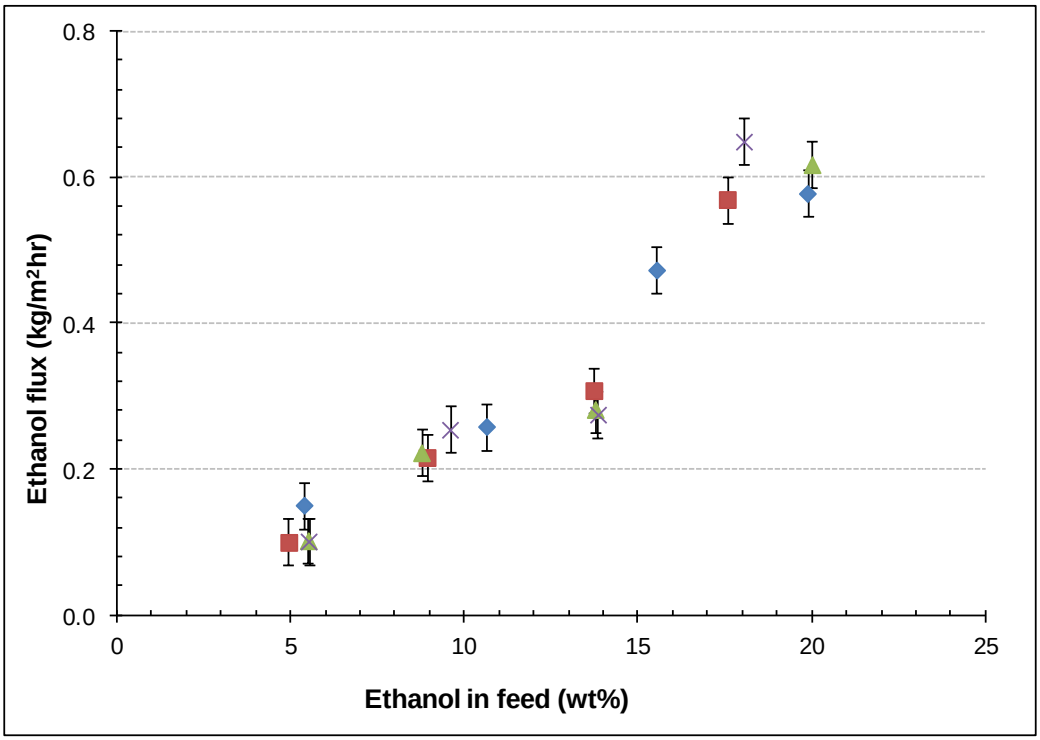

Figure 3.22 Influence of feed composition on ethanol flux
(♦0wt% glucose, ■5wt% glucose, ▲10wt% glucose, X15wt% glucose)

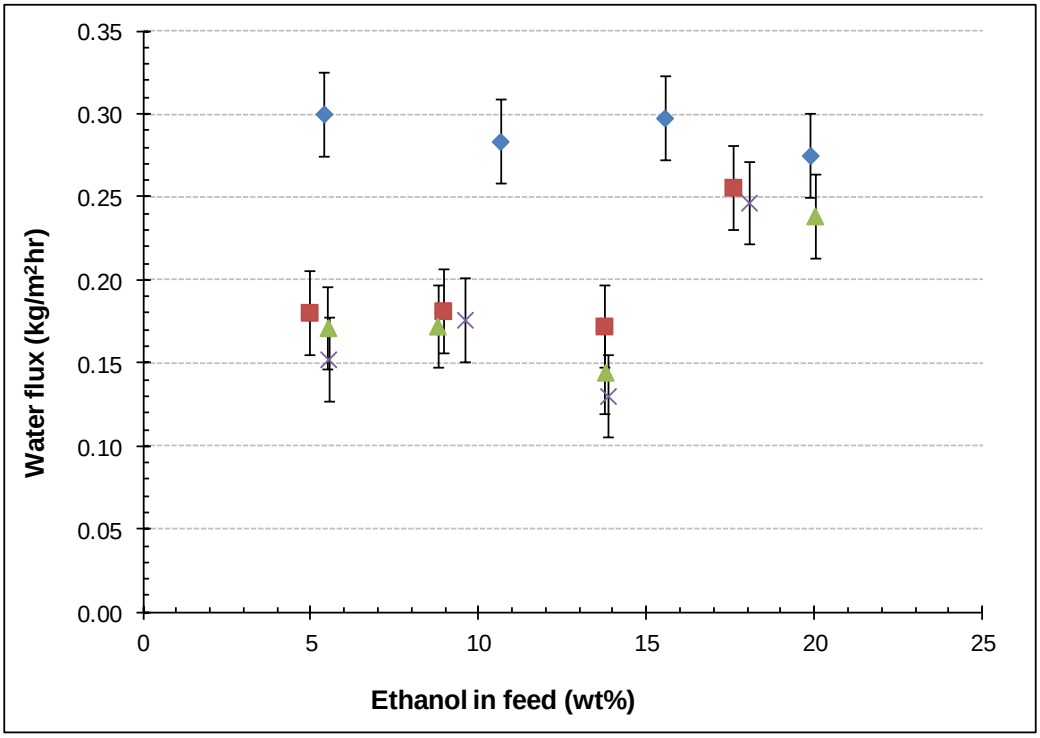

Figure 3.23 Influence of feed composition on water flux
(♦0wt% glucose, ■5wt% glucose, ▲10wt% glucose, X15wt% glucose)

The ethanol flux increases with an increase in ethanol concentration in the feed. This increase in ethanol flux is accompanied by a water flux that stays relatively constant when no glucose is present in the feed or increases when glucose is present in the feed. It does not seem that glucose has a major influence on the ethanol flux but it decreases the water flux significantly except at an ethanol concentration of 20wt%. According to Chovau *et al*. (2011:1671) this is due to the preferential interaction of the hydroxyl groups in the glucose with water and a lower bonding capacity of water molecules to ethanol.

3.4 PERVAPORATION MASS TRANSFER MODEL

Fick's law (Equation 3.9), discussed in Section 3.1.9, was used to model the pervaporation flux.

$$J_i = -D_i \frac{dc_i}{dz} \qquad \text{Equation 3.9}$$

This model (solution-diffusion model) was chosen due to its simplicity and popularity (Chen *et al*., 2010). The models based on the solution-diffusion model vary from each other in the way that the diffusion coefficient varies with concentration. The Greenlaw expression for the

diffusion coefficient was considered, as it is a simple linear model. Equation 3.12 shows the Greenlaw model.

$$J_i = \frac{D_i^0}{L}\left(\frac{(c_i)^2}{2} + \beta_{ij} c_i (1 - c_i)\right) \qquad \text{Equation 3.12}$$

The limiting diffusion coefficient (D_i^0) and plasticisation coefficients (B_{ij}) were determined by using the Nelder-Mead simplex optimisation method discussed in Appendix H and the standard error of the parameters were determined with the Bootstrap method, also discussed in Appendix H. The parameters D_i^0 and B_{ij} for the model are presented in Table 3.10.

Table 3.10 Parameters for Greenlaw partial flux model

	D_i^0 (m^2/s)	B_{ij}
Ethanol flux	$9.55\times10^{-9}\pm1.91\times10^{-10}$	$0.39\pm1.20\times10^{-5}$
Water flux	$6.52\times10^{-10}\pm7.77\times10^{-12}$	$0.75\pm9.69\times10^{-7}$
Water flux in the presence of glucose	$3.79\times10^{-10}\pm6.24\times10^{-11}$	0.5 ± 0.026

The model presented in Equation 3.12 with the parameters presented in Table 3.10 was used to predict theoretical partial flux values for the pervaporation set-up used in this study. Figure 3.24 shows a comparison between the theoretical partial ethanol and water flux and the experimental values obtained in Section 3.3.

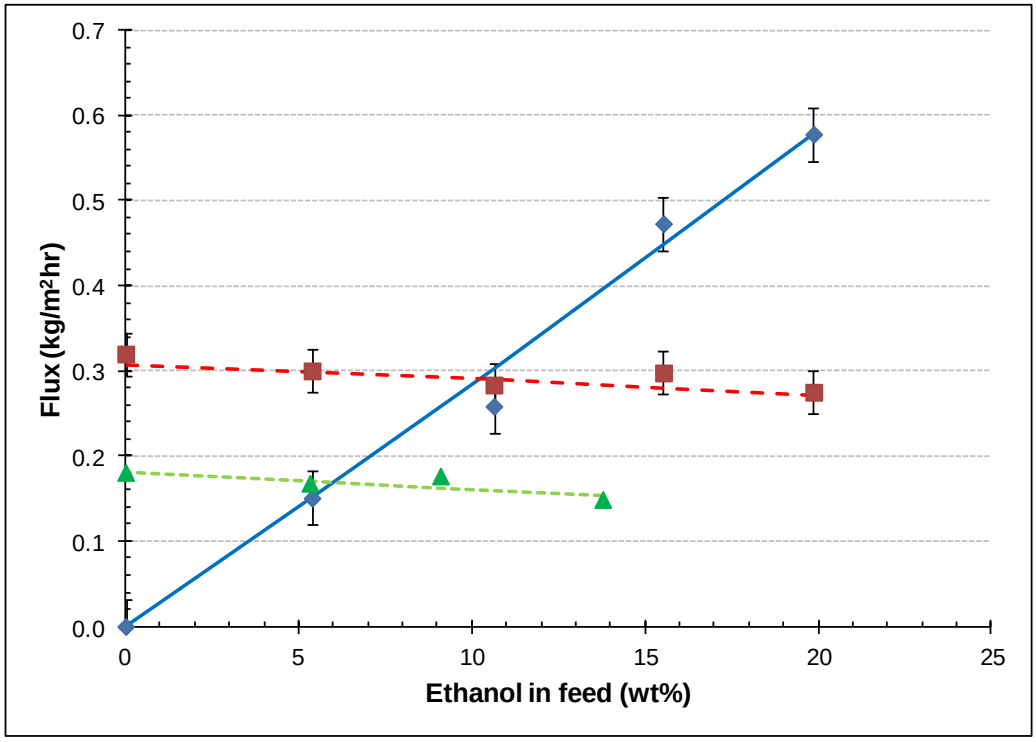

Figure 3.24 Comparison of the experimental partial flux with the Greenlaw model (♦experimental ethanol flux, ■experimental water flux, ▲experimental water flux in the presence of glucose, — ethanol model, --- water model, ···· water model in the presence of glucose)

The solution-diffusion model with the Greenlaw expression for the diffusion coefficient predicted the partial ethanol and partial water flux very accurately. The accuracy of the fit of the model to experimental values is given by the R^2 value and the relative percentage deviation modulus (RPDM) of the different models, shown in Table 3.11.

Table 3.11 Accuracy of the partial flux predictions by the Greenlaw model

Partial flux	R^2	RPDM (%)
Ethanol flux	0.998	5.59
Water flux	0.999	2.78
Water flux in the presence of glucose	0.999	3.01

In Table 3.12 the model parameter values of this study are compared to literature values. However, it is difficult to compare the values of the limiting diffusion coefficient (D_i^0) and plasticisation coefficients (B_{ij}) as each system has its own uniqueness due to the different membranes and chemicals that are used. The values are, however, in relatively the same order of magnitude.

Table 3.12 Limiting diffusion coefficient and plasticisation coefficient for different systems from the literature

System	D_i^0 (m^2/s)	D_j^0 (m^2/s)	B_i	B_j	Reference
Ethanol from ethanol-water mixtures, PERVAP®4060	$D_{ethanol}^0$ 9.55×10^{-9}	D_{water}^0 6.52×10^{-10}	$B_{ethanol}$ 0.39	B_{water} 0.75	This study
Ethanol from ethanol-water mixtures, PDMS membrane	$D_{ethanol}^0$ 4.32×10^{-14}	D_{water}^0 2.75×10^{-14}	$B_{ethanol}$ 1.36×10^{-3}	B_{water} 4.37×10^{-4}	Chang *et al.*, 2007
Ethanol from ethanol-water mixtures, PVA membrane	$D_{ethanol}^0$ 462×10^{-7}	D_{water}^0 1.49×10^{-7}	$B_{ethanol}$ 38.62	B_{water} 22.69	Chen *et al.*, 2010
Ethanol from ethanol–ETBE mixtures, cellulose acetate blended with poly(vinylpyrrolidone-co-vinyl acetate)	$D_{ethanol}^0$ 4.6×10^{-12} 6.9×10^{-12} 5.2×10^{-12}	---	$B_{ethanol}$ 1.5 1.45 0.64	---	Nguyen *et al.*, 1998
Ethanol from ethanol-water mixtures, PVA membrane	$D_{ethanol}^0$ 1.59×10^{-12}	D_{water}^0 1.38×10^{-12}	$B_{ethanol}$ 11.36	B_{water} 11.36	Schaetzel *et al.*, 2010

3.5 CONCLUSION

Both the membrane's sorption and pervaporation characteristics were investigated, and it was found that the PERVAP®4060 membrane is suitable for the separation of ethanol from water and ethanol mixtures that contain glucose. The effect of the ethanol concentration in the feed as well as the influence of glucose was investigated. The total flux increased with an increase in ethanol concentration in the feed and the highest total flux of 0.853±0.006 kg/m^2h was obtained at a feed with 20wt% ethanol. The addition of glucose had almost no effect on the ethanol flux but it lowered the water flux significantly.

The experimental data discussed in Section 3.3 were used to model the pervaporation partial flux. The partial ethanol and water flux through the PERVAP®4060 membrane was modelled based on a solution-diffusion model using the Greenlaw expression for the diffusion coefficient. It was shown that the model could accurately predict the mass transport of ethanol, water, and water in the presence of glucose through the PERVAP®4060 membrane.

3.6 REFERENCES

BAKER, R.W. 1991. Separation of organic azeotropic mixtures by pervaporation. California: Membrane Technology and Research. 40p.

BHATTACHARYA, S. & HWANG, S. 1997. Concentration polarization, separation factor, and Peclet number in membrane processes. *Journal of Membrane Science*, 132: 73-90.

BINNING, R., LEE, R.J., JENNINGS, J.F. & MARTIN, E.C. 1961. Separation of Liquid Mixtures by Permeation. *Industrial and engineering chemistry*, 53(1): 45-50.

CAO, S. SHI, Y. & CHEN, G. 1999. Pervaporation Separation of MeOH/MTBE through CTA Membrane. *Journal of Applied Polymer Science*, 71:377-386.

CHANG, C., CHANG, H. & CHANG, Y. 2007. Pervaporation performance analysis and prediction- using a hybrid solution-diffusion and pore-flow model. *Journal of the Chinese Institute of Chemical Engineers*, 38: 43-51.

CHEN, J., HUANG, J., ZHAN, X. & CHEN, C. 2010. Mass transport study of PVA membranes for the pervaporation separation of water/ethanol mixtures. *Desalination*, 256: 148-153.

CHOVAU, S., GAYKAWAD, S., STRAATHOF, A.J.J. & VAN DER BRUGGEN, B. 2011. Influence of fermentation by-products on purification of ethanol from water using pervaporation. *Bioresource Technology*, 102:1669-1674.

FENG, X. & HUANG, R.Y. M. 1997. Liquid Separation by Membrane Pervaporation: A Review. *Industrial Engineering Chemical Research*, 36:1048-1066.

FREGER, V., KORIN, E., WISNIAK, J. & KORNGOL, E. 2000. Measurement of sorption in hydrophilic pervaporation: sorption modes and consistency of the data. *Journal of Membrane Science*, 164:251-256.

GONZÁLEZ-MARCOS, J.A., LÓPEZ-DEHESA, C., GONZÁLEZ-VELASCO, J.R. 2004. Effect of Operating Conditions in the Pervaporation of Ethanol-Water Mixtures with Poly(1-Trimethylsilyl-1-Propyne) Membranes. Journal of Applied Polymer Science, 94:1395-1403.

HUANG, R.Y.M. & RHIM, J.W. 1991. Separation characteristics of pervaporation membrane separation processes. (*In* Huang, R.Y.M., ed. Pervaporation Membrane Separation Processes. Amsterdam: Elsevier. p. 111-180).

HUMPHREY, J.L. & KELLER, G.E. 1997. Separation Process Technology. NY: McGraw-Hill. 408p.

IKEGAMI, T., YANAGISHITA, H., KITAMOTOA, D., NEGISHI, H., HARAYA, K. & SANO, T. 2002. Concentration of fermented ethanol by pervaporation using silicalite membranes coated with silicone rubber. *Desalination*, 149:49-54.

JIRARATANANON, R., CHANACHAI, A., HUANG, R.Y.M. UTTAPAP, D. 2002. Pervaporation dehydration of ethanol–water mixtures with chitosan/hydroxyethylcellulose (CS/HEC) composite membranes. *Journal of Membrane Science*, 195: 143-151.

JONQUIÈRES, A., CLÉMENT, R., LOCHON, P., NÉEL, J., DRESCH, M. & CHRÉTIEN, B. 2002. Industrial state-of-the-art of pervaporation and vapour permeation in the western countries. *Journal of Membrane Science*, 206: 87-117.

KAEWKANNETRA, P., CHUTINATE, N., MOONAMART, S., KAMSAN, T. & CHIU, T.Y. 2011. Separation of ethanol from ethanol-water mixture and fermented sweet sorghum juice using pervaporation membrane reactor. *Desalination*, 271:88-91.

KOBER, P.A. 1917. Pervaporation, perstillation and percrystallization. *Journal of the American Chemical Society*, 39: 944-948.

KOROS, W.J., MA, Y.H. & SHIMDZU, T. 1996. Terminology for membranes and membrane processes. *Pure and Applied Chemistry*, 68(7):1479-1489.

LIANG, L. & RUCKENSTEIN, E. 1996. Pervaporation of ethanol-water mixtures through polydimethylsiloxane-polystyrene interpenetrating polymer network supported membranes. *Journal of Membrane Science* ,114: 227-234.

LIPNIZKI, F., HAUSMANNS, S., TEN, P., FIELD, R. W. & LAUFENBERG, G. 1999. Organophilic pervaporation: prospects and performance. *Chemical Engineering Journal*, 73: 113-129.

MEULEMAN, E.E.B., BOSCH, B., MULDER, M.H.V. & STRATHMANN, H. 1999. Modelling of liquid/liquid separation by pervaporation: toluene from water. *AIChE Journal,* 45(10):2153-2160.

MOHAMMADI, T., AROUJALIAN, A. & BAKHSHI, A. 2005. Pervaporation of dilute alcoholic mixtures using PDMS membrane. *Chemical Engineering Science*, 60: 1875-1880.

MULDER, M.H.V. & SMOLDERS, C.A.. 1984. On the mechanism of separation of ethanol/ water mixtures by pervaporation I. Calculations of concentration profiles. *Journal of Membrane Science*, 17:289-307.

NEEL, J. 1991. Introduction to pervaporation. (*In* Huang, R.Y.M., ed. Pervaporation Membrane Separation Processes. Amsterdam: Elsevier. p. 111-180).

NGUYEN, T.Q., CLEMENT, R., NOEZAR, I., LOCHON P. 1998. Performance of poly(vinylpyrrolidone-co-vinyl acetate)-cellulose acetate blend membranes in the pervaporation of ethanol-ethyl tert-butyl ether mixtures Simplified model for flux prediction. *Separation and purification technology,* 13:237-245.

SCHAETZEL, P., BOUALLOUCHE, R., AMAR, H. A., NGUYEN, Q. T., RIFFAULT, B. & MARAIS, S. 2010. Mass transfer in pervaporation: The key component approximation for the solution-diffusion model. Desalination, 251: 161-166.

SCHMIDT, S.L., MYERS, M.D., KELLEY, S.S, MCMILLAN, J.D. & PADUKONE, N. 1997. Evaluation of PTMSP Membrane in Achieving Enhanced Ethanol Removal from Fermentation by Pervaporation. *Applied Biochemistry and Biotechnology*, 63-65: 469-482.

SCHOLES, C.A., STEVENS, G.W. & KENTISH, S.E. 2010. The effect of hydrogen sulfide, carbon monoxide and water on the performance of a PDMS membrane in carbon dioxide/nitrogen separation. *Journal of Membrane Science*, 350: 189-199.

SEADER, J.D. & HENLEY, E.J. 2006. Separation Process Principles. 2nd ed. USA: John Wiley & Sons. 756p.

SHAO, P., & HUANG, R.Y.M. 2007. Polymeric membrane pervaporation. *Journal of Membrane Science*, 287: 162-179.

SUSANTO, H. & ULBRICHT, M. 2009. Polymeric Membranes for Molecular Separations. (*In* Drioli, E. & Giorno, L., ed. Membrane Operations. Weinheim: Wiley-VCH. p. 19-43).

ULBRICHT, M. 2006. Advanced functional polymer membranes. *Polymer*, 47: 2217-2262.

VAN DER BRUGGEN, B. 2009. Fundamentals of Membrane Solvent Separation and Pervaporation. (*In* Drioli, E. & Giorno, L., ed. Membrane Operations. Weinheim: Wiley-VCH. p. 45-61).

VAN DER GRYP, P. 2003. Separation by Pervaporation of Methanol from Tertiary Amyl Methyl Ether using a Polymeric Membrane. Potchefstroom: NWU. Potchefstroom campus. (Dissertation – M.Ing)

WEE, S.L., TYE, C.T. & BHATIA, S. 2008. Membrane separation process-Pervaporation through zeolite membrane. *Separation and Purification Technology*, 63:500-516.

WEYD, M., RICHTER, H., PUHLFÜRß, P., VOIGT I., HAMEL, C., & SEIDEL-MORGENSTERN, A. 2008. Transport of binary water-ethanol mixtures through a multilayer hydrophobic zeolite membrane. *Journal of Membrane Science*, 307: 239-248.

WIJMANS, J.G. & BAKER, R.W. 1995. The solution-diffusion model: a review. *Journal of Membrane Science*, 107:1-21

WIJMANS, J.G., ATHAYDE, A.L., DANIELS, R., LY, J.H., KAMARUDDIN, H.D. & PINNAU, I. 1996. The role of boundary layers in the removal of volatile organic compounds from water by pervaporation. *Journal of Membrane Science*, 109: 135-146.

WU, Y., XIAO, Z., HUANG, W. & ZHONG, Y. 2005. Mass transfer in pervaporation of active fermentation broth with a composite PDMS membrane. *Separation and Purification Technology*, 42: 47-53.

ZHOU, H., SU, Y., CHEN, X. & WAN, Y. 2011. Separation of acetone, butanol, and ethanol (ABE) from dilute aqueous solutions by silicalite-1/PDMS hybrid pervaporation membranes. *Separation and Purification technology*, 79:375-384.

CHAPTER 4: FERMENTATION COUPLED WITH PERVAPORATION

OVERVIEW

Fermentation was investigated in Chapter 2 followed by pervaporation, which was investigated in Chapter 3. In Chapter 4, fermentation coupled with pervaporation is investigated.

This chapter is divided into five subsections. In the first section, a literature review regarding the coupling of fermentation with pervaporation is presented. This is followed by Section 4.2 where the experimental procedure used for the coupling of fermentation with pervaporation in this study is discussed. The experimental results are presented and discussed in Section 4.3. The main objective of this study, to model fermentation coupled with pervaporation, is addressed in Section 4.4 where a model based on the fermentation model in Chapter 2 and pervaporation model in Chapter 3 is developed. In the final section, Section 4.5, concluding remarks are given.

4.1 FERMENTATION COUPLED WITH PERVAPORATION

4.1.1. Introduction to fermentation combined with pervaporation processes

Pervaporation is currently one of the methods used commercially to remove excess water from ethanol and water mixtures. Pervaporation can also be used to remove ethanol from water and ethanol mixtures such as a fermentation broth. In this study, the focus is on the use of pervaporation combined with fermentation to remove ethanol continuously from the fermentation broth while the ethanol is produced by the yeast cells.

A review of current literature on the subject of fermentation combined with pervaporation will be presented in Section 4.1.2.

4.1.2. Literature review of fermentation processes coupled with pervaporation

Recovery of ethanol through pervaporation was a widely researched subject in the 1980's. The potential application of recovering bioethanol from fermentation broths together with the water-ethanol system being regarded as a reference system for assessing pervaporation performance sparked this interest (Böddeker & Bengtson, 1991:438). A review of ethanol-water pervaporation from 1981-1988 is presented by Böddeker and Bengtson (1991: 442-445). Silicone rubber (cross-linked PDMS) was found to be the most commonly used membrane polymer and it showed excellent separation qualities for ethanol and water.

More recently, the focus of pervaporation studies with ethanol has shifted from only water and ethanol mixtures to fermentation broths (see Table 4.1) or mixtures demonstrating different features of a fermentation broth (Mohammadi *et al*.; Aroujalian *et al.*, 2006; Aroujalian & Raisi, 2009; Chovau *et al.*, 2011). A summary of some of the recent publications in the field of pervaporation, focusing on the use of fermentation broths as feedstock, is given in Table 4.1.

In 1996, O'Brien and Craig (1996) successfully combined a conventional yeast fermentation system using *Saccharomyces cerevisiae* and glucose with a pervaporation system (with a PDMS membrane) for the recovery of in-situ ethanol. This set-up proved successful at maintaining a relatively low ethanol concentration in the fermentation broth, thereby reducing the inhibition effect of ethanol. A year later, Schmidt and his co-workers (Schmidt *et al.*, 1997), explored the use of a PTMSP (poly[(1-trimethylsilyl)-1-propyne]) membrane in a system similar to O'Brien and Craig (1996) by comparing it to a PDMS membrane.

Table 4.1 Application of pervaporation to separate ethanol from fermentation broths

Year	Membrane	Total flux ($kg.m^{-2}.hr^{-1}$)	Maximum selectivity	Conditions	Reference
1996	PDMS	0.31-0.79	1.8-6.5	35°C, agitation at 100 rpm, pH of 5	O'Brien & Craig, 1996
1997	1.PTMSP 2.PDMS	1. 0.149 2. 0.039	1. 5 2. 13	Pervaporation at ambient temperature (about 25°C), fermentation at 37°C, 150 rpm	Schmidt *et al*., 1997
1998	Hollow fibre micro-porous polypropylene	1.2-1.4	7.5	30°C, pH of 4-5	Kaseno *et al*., 1998
2002	Silicalite coated with silicone rubber	0.08 (ethanol flux)	60	30°C, agitation at 600 rpm	Ikegami *et al.*, 2002
2002	Silicalite	0.5-0.6	85.9-218	30-35°C, agitated at 30–60 rpm, pH of 4	Nomura *et al.*, 2002
2003	PTMSP	not quantified	not quantified	30°C	Fadeev *et al*., 2003
2004	PDMS	0.11	10	34°C , pH of 6.5	O'Brien *et al*., 2004
2005	Composite PDMS	0.566 (ethanol flux)	7.9	35°C, pH of 4.5	Wu *et al.*, 2005
2007	Supported Trioctylamine liquid membrane	0.0012	80	54°C	Thongsukmak & Sirkar, 2007
2007	PDMS–PAN–PV composite membrane	3.5 to 2.6	---	---	Staniszewski *et al*., 2007
2007	PDMS-PAN-PV	2.6-3.5	8	Fermentation at 30°C, pervaporation at 65°C	Lewandowska & Kujawski, 2007
2009	PDMS–PAN–PV composite membrane	2.9	---	30°C, pH of 4.7	Staniszewski *et al*., 2009
2011	Mixed matrix ZSM-5/PDMS	0.203	7.8	50°C	Offerman & Ludvik, 2011
2011	Cellulose acetate	1.2-4.2	9.3-2.2	Between 50°C-70°C for pervaporation	Kaewkannetra *et al*., 2011

The flux and ethanol selectivity was higher with the PTMSP membrane than with the PDMS membrane and it showed increased resistance to fouling. The PTMSP membrane, however, showed a slight deterioration over time, which according to Schmidt *et al.* (1997) was because of it being used unsupported. In another study on a PTMSP membrane, done in 2003 by Fadeev *et al.* (2003) the same deterioration was seen. It was determined that the PTMSP membrane deterioration is due to internal fouling by the by-products formed during fermentation and not through physical degradation as suggested by Schmidt *et al.* (1997).

Glycerol, the main by-product caused the flux to decline by 30%. Other by-products such as *n*-propanol, acetone, and diols (Butanediol) were absorbed into the membrane but diols were absent in the permeate, therefore diols are most likely also affecting the membrane performance by occupying the polymer free volume and reducing mass transport of components across the membrane.

Kaseno *et al.* (1998) conducted a study comparing fed-batch fermentation combined with pervaporation using a micro-porous polypropylene hollow fibre membrane to an ordinary fed-batch process. The focus of Kaseno *et al.* was on the effect that pervaporation would have on fermentation, rather than on the pervaporation membrane performance. With this system, the fermentation performance was two times higher than fermentation without pervaporation, proving that when fermentation is combined with pervaporation the inhibition effect of ethanol can be reduced. The amount of wastewater generated by fermentation was also reduced by 38.5% in the combined process, an important benefit for water scarce countries such as South Africa.

In 2002, two different research groups (Ikegami *et al.*, 2002 and Nomura *et al.*, 2002) both studied the separation of ethanol from fermentation broth using silicalite membranes. These studies did not combine fermentation with pervaporation but fermentation broth was used as feedstock for pervaporation to determine the effect the fermentation broth (opposed to pure water and ethanol mixtures) would have on the membrane. Nomura *et al.* (2002) demonstrated successfully that a silicalite membrane could be used to separate ethanol from a fermentation broth. The selectivity and flux proved to be higher with the fermentation broth than with a water and ethanol mixture. However, the membrane flux did decrease over time. Ikegami *et al.* (2002) observed the same decrease in performance and determined that it was due to succinic acid and glycerol that form as by-products during fermentation that partially coats the membrane. To overcome the problem the silicalite membrane was coated with silicon rubber, thereby effectively preventing the decline in membrane performance and obtaining a more concentrated ethanol solution. The selectivity of the silicalite membranes in both these studies was very high but the flux was much lower than observed in previous studies with other membranes, even with the silicon rubber coating.

The sugar, nutrients, yeast cells, and by-products present in the fermentation broth may have an effect on the performance of the pervaporation membrane if fermentation is directly combined with pervaporation or if pervaporation follows fermentation with these components still present in the mixture. Wu *et al.* (2005) looked at the effect yeast cells have on the performance of a composite polydimethyl-siloxane (PDMS) membrane. In an experiment where inactive yeast cells were used it was observed that the flux and selectivity decreased

with an increase in cell weight, but the performance was still better than with a mixture of pure ethanol and water, suggesting that the inactive cells (particles) in suspension improve ethanol transfer. Fermentation broth containing active yeast cells resulted in a higher flux than with inactive cells indicating that the metabolism of active cells improves ethanol transfer over the membrane. Aroujalian *et al.* (2006) studied the effect of glucose on the flux and selectivity of a polydimethyl-siloxane (PDMS) film on a PVDF-supported membrane. Both the total flux and ethanol selectivity of the membrane decreased with an increase in glucose concentration. The change in flux was very slight while the selectivity was affected slightly more than the flux. No glucose was detected in the permeate and thus it was assumed that glucose is incapable of entering the membrane. Recently Offerman and Ludvik (2011) also looked at the effect of poisoning on PDMS and ZSM-5/PDMS (hydrophobic zeolite ZSM-5 in PDMS) membranes by fermentation components. Offerman and Ludvik used maize as feedstock so there was a variety of different substances present in the fermentation broth. The ZSM-5/PDMS membrane performed better than the pure PDMS membrane in pervaporation with ethanol and water mixtures. However, the performance of the ZSM-5/PDMS membrane was greatly reduced over time when a fermentation broth was used as feed whereas the PDMS membrane showed no significant reduction in performance over time, suggesting that the fermentation broth deactivates the zeolite component in the ZSM-5/PDMS membrane.

Moving away from pure glucose as fermentation feedstock and motivated by the popularity of using maize to produce bioethanol in the USA, O'Brien *et al*. (2004) studied a fermentation-pervaporation coupled system using hydrolysed maize fibre (a by-product from the wet milling of maize) as feedstock. As the hydrolysed maize fibre contained xylose as well as other sugars *Escherichia coli* was used as microorganism for fermentation. O'Brien *et al*. were successful in maintaining a low ethanol concentration in the fermentation broth, thereby allowing sustained fermentation activity without product inhibition. This study demonstrated that the coupling of fermentation with pervaporation is advantageous to processes where the feedstock is not necessarily pure glucose.

Whey is another industrial by-product present in large quantities that can be used to produce bioethanol. A kinetic study of ethanol production from whey, followed by recovery of the product through pervaporation, was done in 2007 by Staniszewski *et al*. (2007). The model that represented fermentation was an extended form of the Monod model, shown in Equation 4.1.

$$\mu = \mu_{\max} \frac{S}{K_{sx} + S} \frac{K_s'}{K_s' + S} \left(\frac{P}{P_{x,\max}} \right)^n \qquad \text{Equation 4.1}$$

Substrate utilisation and growth associated product formation can be described in terms of cell growth by using yield coefficients and a maintenance term (m_s ($kg.kg^{-1}.h^{-1}$)) was added to account for substrate used by the yeast cells for vital processes. Equations 4.2 and 4.3 show the substrate utilisation rate (v_s ($kg.kg^{-1}.h^{-1}$)) and the product formation rate (v_P ($kg.kg^{-1}.h^{-1}$)) as used by Staniszewski *et al*. (2007).

$$v_s = m_s + \frac{\mu}{Y_{XS}} \qquad \text{Equation 4.2}$$

$$v_P = \mu \frac{Y_{PS}}{Y_{XS}} \qquad \text{Equation 4.3}$$

The final model has the form of a set of differential equations, presented in Equation 4.4 to Equation 4.7.

$$\frac{dL}{dt} = -r \qquad \text{Equation 4.4}$$

$$\frac{dX}{dt} = \mu X \qquad \text{Equation 4.5}$$

$$\frac{dS}{dt} = r - v_s X \qquad \text{Equation 4.6}$$

$$\frac{dP}{dt} = v_P X \qquad \text{Equation 4.7}$$

In Equation 4.4 to Equation 4.7, L ($kg.m^{-3}$) is the concentration of lactose, r ($kg.m^{-3}.h^{-1}$) is the rate of enzymatic reaction, X ($kg.m^{-3}$) is the concentration of yeast cells, S ($kg.m^{-3}$) is the concentration of glucose and P ($kg.m^{-3}$) is the ethanol concentration in the broth. The pervaporation model is shown by Equation 4.8 that represents the time derivative of ethanol mass in the feed and Equation 4.9 that represents the time derivative of the mass of the feed.

$$\frac{dm_E}{dt} = -a_1 x_E a_2 A_m \qquad \text{Equation 4.8}$$

$$\frac{dm_F}{dt} = -a_2 A_m \qquad \text{Equation 4.9}$$

The coefficients a_1 (dimensionless) and a_2 ($kg.m^{-2}.h^{-1}$) represent the average selectivity of ethanol separation and the total permeate flux respectively, A_m (m^2) is the area of the membrane and x_E (dimensionless) is the mass ratio of ethanol in the feed. Equations 4.4 to

4.9 (the Staniszewski model) allow for the prediction of ethanol concentration obtained in the bioreactor and the separation time and the concentration of the ethanol removed in the permeate. A drawback of this model is that it was developed for the prediction of fermentation followed by pervaporation on the post-fermentation broth and therefore it cannot be used when fermentation is coupled with pervaporation. The Staniszewski model also does not account for the differences in flux and selectivity due to the feed concentration, as parameters a_1 and a_2 that account for flux and selectivity respectively are constants.

The Staniszewski model did not take the differences in the assimilation rate of glucose and galactose by *Saccharomyces cerevisiae* into account. A follow-up study (Staniszewski *et al*., 2009) that incorporates the glucose repression effect exhibited by *Saccharomyces cerevisiae* was done in 2009.

Sánchez *et al.* (2005) modelled simultaneous saccharification and fermentation coupled with pervaporation. Lignocellulosic biomass was used as feedstock, *Trichoderma reesei* cellulase was used for hydrolyses, and *Saccharomyces cerevisiae* was used for fermentation. Sánchez *et al.* (2005) modelled the simultaneous saccharification and fermentation process when coupled with pervaporation by adding Equations 4.10 to 4.13 to his model for simultaneous saccharification and fermentation. Equations 4.10 to 4.12 simulate the diminish in total volume in the reactor and the change in volume of each individual component in the reactor as a result of the pervaporation outlet stream.

$$\frac{d(VC_i)}{dt} = Vr_i \qquad \text{Equation 4.10}$$

$$\frac{d(VP)}{dt} = -QP_P + Vr_P \qquad \text{Equation 4.11}$$

$$\frac{dV}{dt} = -Q \qquad \text{Equation 4.12}$$

$$\alpha = \frac{[C_{ethanol} / C_{water}]_{permeate}}{[C_{ethanol} / C_{water}]_{water}} \qquad \text{Equation 4.13}$$

In Equations 4.10 to 4.13, V(L) refers to the reaction volume, C_i ($g.L^{-1}$) refers to the concentration of each component except ethanol, r_i ($g/L.h^{-1}$) is the rate of formation of each component, P ($g.L^{-1}$) is the ethanol concentration, Q ($L.h^{-1}$) refers to the output stream for pervaporation and α describes the separation factor of pervaporation. Equation 4.13 was added to the model to describe the separation factor as a result of pervaporation. The value of α was assumed to be constant (88 for a silicate membrane) in this model, which means

that this model does not account for the effect that a change in feed composition will have on the separation efficiency of the membrane.

A recent attempt using sweet sorghum juice for fermentation and a cellulose acetate membrane for pervaporation has been made by Kaewkannetra *et al.* (2011). The cellulose acetate membrane showed promise with ethanol and water mixtures as both the flux and selectivity were very high (a flux of between 5 and 11.4 $kg.m^2.h^{-1}$ and a selectivity of between 7 and 14.2). However, the experiment was deemed unsuccessful as both the flux and selectivity of the membrane decreased significantly when sweet sorghum fermentation broth was used instead of the water and ethanol mixture. However, the study did demonstrate that cellulose acetate membranes could be successfully used to separate ethanol and water mixtures. Furthermore, the cellulose acetate membrane can potentially recover ethanol from fermentation broths other than sweet sorghum juice.

In conclusion, pervaporation coupled with fermentation has been studied in a variety of ways. It has been repeatedly proven that pervaporation is a viable method to recover ethanol from fermentation broths, and thereby to decrease ethanol inhibition, reduce wastewater and increase yeast productivity. Pervaporation has been used with an assortment of membranes and a range of feedstocks has been studied, each process showing a different performance. There are kinetic studies on fermentation and pervaporation when the processes are separate (Staniszewski *et al*. 2007 and Staniszewski *et al*. 2009) as well as where fermentation is directly coupled with pervaporation (Sánchez *et al.*, 2005). There is, however, a definite lack in kinetic studies where fermentation and pervaporation are combined and the model accounts for the change in membrane separation efficiency as a result of change in the feed composition. The objective is thus to improve on the current models by proposing a model for fermentation coupled with pervaporation that would consider the changing feed composition. The model should determine the ethanol and water flux out of the reactor by taking into account the concentration changes in the feed as a result of fermentation as well as the changes due to the removal of ethanol and water.

4.2 EXPERIMENTAL METHODS AND PROCEDURES

4.2.1. Chemicals used

The chemicals used for the fermentation coupled with pervaporation experiments, as well as the supplier and the purity of the chemical, are listed in Table 4.2.

Table 4.2 Chemicals used in this study

Chemical	Supplier	Purity	Use
Glucose	Associated chemical enterprise (ACE)	Analytical grade	Fermentation feedstock and calibration curve
Sodium hydroxide	Fluka	>98%	pH adjustment
Sulphuric acid	Associated chemical enterprise (ACE)	98%	pH adjustment
Ethanol	Rochelle	99.9%	Calibration curve
Glycerol	Associated chemical enterprise (ACE)	99%	Calibration curve
Buffer solution pH 7	Hanna Instruments	---	pH meter calibration
Buffer solution pH 4	Hanna Instruments	---	pH meter calibration
Liquid nitrogen	Afrox	---	Pervaporation experiments
Yeast (*Saccharomyces cerevisiae*)	Anchor	N/A	Fermentation

The chemicals were used as received and no further purification was done.

4.2.2. Apparatus and experimental procedure used for fermentation coupled with pervaporation experiments

The experiments where fermentation was combined with pervaporation used the same set-up as shown in Chapter 3.2.3, Figure 3.13. Fermentation was done directly in the feed vessel.

The desired amounts of glucose and water were measured using the mass balance and transferred to the feed vessel. The feed vessel containing glucose and water was then sterilised using an autoclave at 121°C for 30 minutes to prevent contamination. After the feed mixture had cooled down to approximately 30°C, the pH was adjusted and a small amount of the mixture was transferred to a separate beaker to activate the yeast. The heating jacket was set to 30°C and the activated yeast was added to the feed vessel when the temperature had stabilised.

Samples of the fermentation broth were collected at regular time intervals. Samples were taken to measure the yeast cell concentration using a spectrophotometer and analysed using a HPLC. Before each sample was taken, the pH of the fermentation broth was measured and adjusted.

After a set amount of time, the pervaporation unit was started to remove ethanol continuously from the fermentation broth.

4.2.3. Experimental design and planning

The objective of the fermentation coupled with pervaporation experiments was to test the model proposed from the data in Chapter 2 and Chapter 3. Therefore, it was decided to do one experiment where pervaporation was started after 24 hours of fermentation. The experimental conditions of this experiment are presented in Table 4.3.

Table 4.3 Experimental conditions of fermentation combined with pervaporation experiment

Variable	Value
Temperature (°C)	30
pH	4
Starting sugar (wt%)	15
Starting yeast (g/L)	10
Fermentation time before pervaporation (h)	24

4.2.4. Analytical techniques

HPLC, spectrophotometry, refractometry, glucose analyses, and ethanol analyses, as discussed in Chapter 2.2.5 and Chapter 3.2.8 were used to analyse the samples of the fermentation coupled with pervaporation experiments.

4.3 RESULTS AND DISCUSSION

Fermentation was successfully combined with pervaporation by using the experimental procedure, as discussed in Section 4.2. Table 4.4 shows the ethanol wt% present in the feed vessel and in the permeant at each time interval. The total ethanol yield (ethanol in feed plus the ethanol removed from the system) is also presented in Table 4.4.

The total ethanol yield after 24 hours stayed relatively stable, as most of the glucose had been converted to products at this stage and fermentation was nearly complete. The slight variation in the ethanol yield value measured after each time interval could be due to the error associated with the experimental set-up or the error of the analysis equipment.

Table 4.4 Fermentation combined with pervaporation results

Time (h)	Ethanol in feed (wt%)	Ethanol in permeate (wt%)	Total ethanol yield (g ethanol.g glucose^{-1})
0	0	---	0.000
1	0.031	---	0.002
2	0.052	---	0.003
4	0.073	---	0.005
8	1.822	---	0.121
12	3.690	---	0.246
24	5.886	---	0.392
26	5.935	33.381	0.409
28	5.625	38.791	0.401
30	5.682	37.466	0.416
32	5.272	37.373	0.401
36	5.023	35.494	0.405
38	4.951	34.419	0.410
42	4.583	33.827	0.407
44	4.392	32.344	0.404
46	4.291	30.273	0.406
48	4.050	29.773	0.399

The total ethanol yield is slightly lower than the ethanol yield obtained in the fermentation experiments discussed in Chapter 2 (approximately 0.431±0.022 g.g^{-1}). The lower ethanol yield had a corresponding higher glycerol yield of 0.105 g.g^{-1} compared to 0.075±0.017 g.g^{-1} obtained in Chapter 2 at the same experimental conditions. No osmotic stress due to high glucose concentrations could have been experienced by the yeast cells as the glucose concentration of 15wt% is relatively low. In Figure 4.1, the fermentation experimental data of the membrane-reactor system is compared to traditional fermentation experimental data obtained at the same conditions.

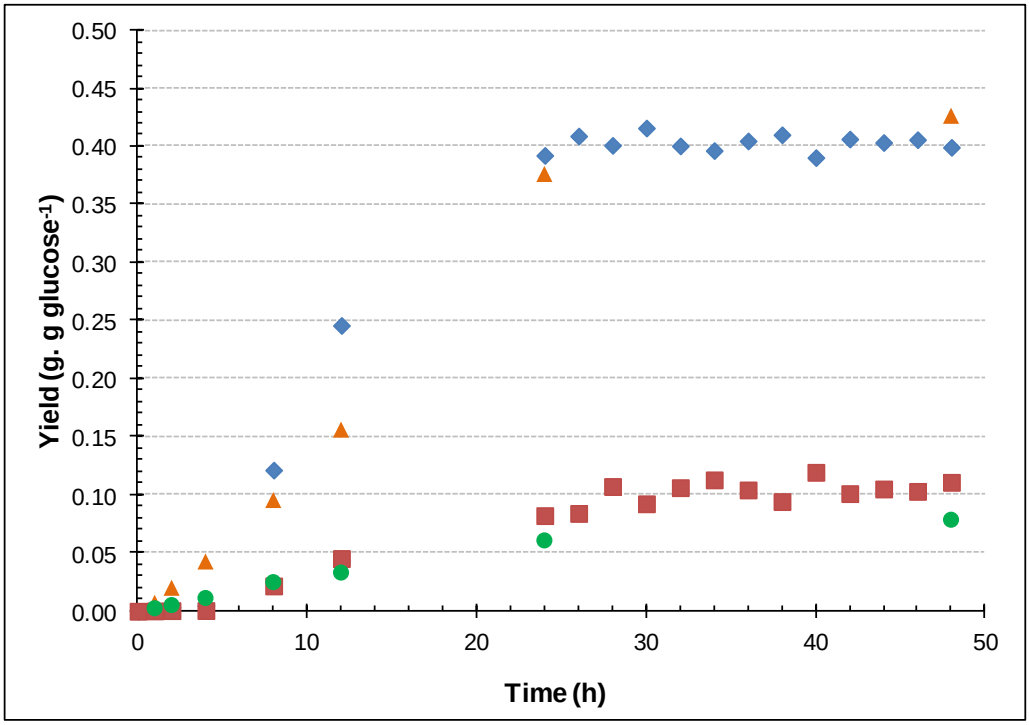

Figure 4.1 Fermentation over time in membrane-reactor system compared to batch data from Chapter 2

(♦Ethanol yield – membrane-reactor system, ▲Ethanol yield - batch experiment, ■Glycerol yield – membrane-reactor system, ●Glycerol yield- batch experiment)

The slightly higher glycerol yield could be the result of stress on the yeast cells due to the membrane-reactor system. The membrane-reactor system was not optimised for fermentation and factors such as mixing in the fermentation vessel can influence the yeast cells and cause a higher production of glycerol (Gardner *et al*., 1993).

The partial flux of the PERVAP®4060 membrane in the membrane-reactor system is graphically presented in Figure 4.1. The raw data can be found in Appendix E. In Figure 4.1, it can be seen that a steady state is reached after approximately 4 hours of pervaporation. The ethanol flux decreased over the time, as was expected, due to the decreasing ethanol concentration in the feed vessel as a result of the continuous removal of ethanol. The water flux stayed constant after a steady state had been reached. These results are comparable to the ethanol-water pervaporation results obtained in Chapter 3 with regard to the feed composition.

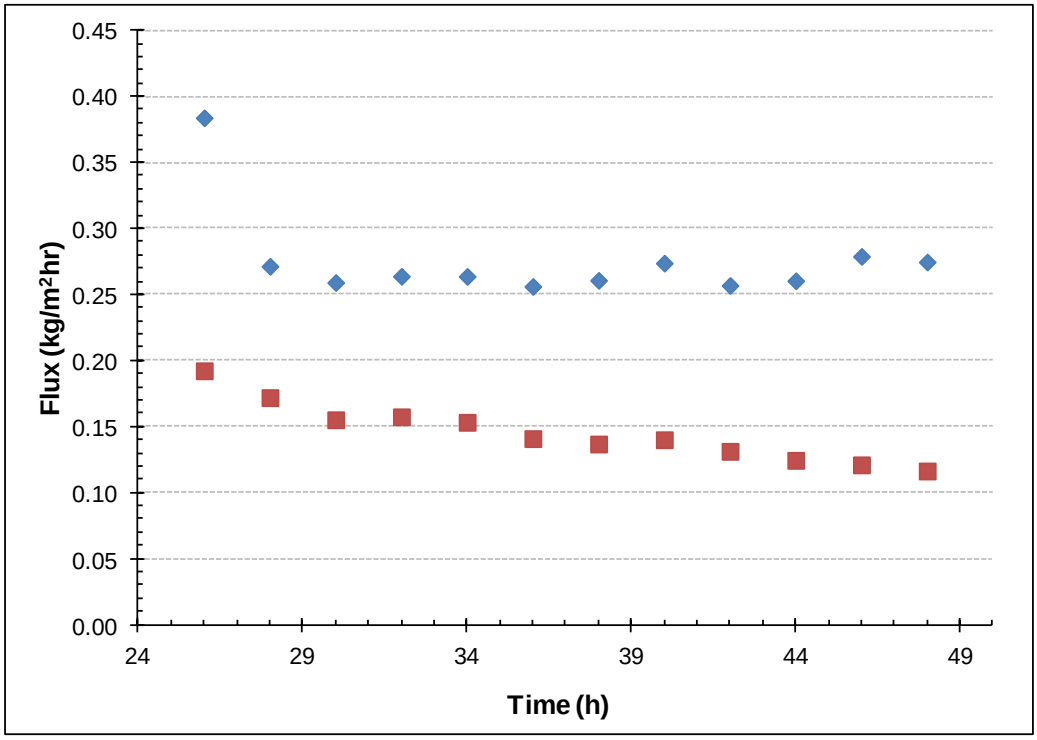

Figure 4.2 Flux over time
(♦Water flux, ■Ethanol flux)

The results discussed in this section are compared to the kinetic model proposed for fermentation coupled with pervaporation in Section 4.4.

4.4 FERMENTATION COUPLED WITH PERVAPORATION MODEL

The main objective of this study was to propose a model to represent fermentation when it is combined with pervaporation. The fermentation kinetic models proposed in Chapter 2 were combined with the pervaporation model presented in Chapter 3 to propose a combined model to represent the membrane-reactor system. This model is expected to represent the process where fermentation is coupled with pervaporation and will be presented in this section.

In Chapter 2, it was shown that the substrate-limiting model showed the best fit with data that do not exhibit substrate inhibition while the substrate inhibition model showed the best fit for data that exhibit substrate inhibition. It was therefore decided to use the substrate-limiting model for the combined model, as the combined experiment, discussed in Section 4.3, does not exhibit substrate inhibition.

The rate of ethanol separation from the fermentation broth (ethanol partial flux) depends on both the instantaneous composition of the feed and on the membrane properties. The mass

transport model based on Fick's law and the Greenlaw expression for diffusion coefficient, discussed in Chapter 3, represents the ethanol separation from the fermentation broth as a result of change in the feed composition.

A continuous stream of ethanol and water was removed from the system by means of pervaporation. This caused a decrease in the total reaction mass, which influences all of the components in the feed vessel, as shown by Equations 4.14 to 4.16. In the model M refers to the total mass in the reactor (kg), y_i refers to the weight fraction of each component and r_i is the reaction rate of each component as described in Chapter 2.4.

$$\frac{d\left(My_x\right)}{dt} = Mr_x \qquad \text{Equation 4.14}$$

$$\frac{d\left(My_{glycerol}\right)}{dt} = Mr_{glycerol} \qquad \text{Equation 4.15}$$

$$\frac{d\left(My_S\right)}{dt} = Mr_S \qquad \text{Equation 4.16}$$

As ethanol was removed from the system, it influenced the ethanol concentration in the reactor, shown by Equations 4.17 and 4.18. Q (kg/h) is the stream leaving the reactor (mass flow of permeate stream) while $P_{ethanol,permeate}$ is the weight fraction ethanol in the permeate stream.

$$\frac{d\left(MP_{ethanol}\right)}{dt} = Mr_{ethanol} - QP_{ethanol,permeate} \qquad \text{Equation 4.17}$$

$$\frac{d\left(M\right)}{dt} = -Q \qquad \text{Equation 4.18}$$

Equations 4.19 to 4.21 complete the fermentation side of the model.

$$\mu = \mu_{\max}\frac{S}{K_{sx} + S} \qquad \text{Equation 4.19}$$

$$\nu_{ethanol} = \nu_{\max,ethanol}\frac{S}{K_{sp,ethanol} + S} \qquad \text{Equation 4.20}$$

$$\nu_{glycerol} = \nu_{\max,glycerol}\frac{S}{K_{sp,glycerol} + S} \qquad \text{Equation 4.21}$$

To model the removal of ethanol by pervaporation Equations 4.22 and 4.23, discussed in Chapter 3.4 were added. Equation 4.22 describes the ethanol flux while Equation 4.23 describes the water flux and these equations were used to determine Q and $P_{ethanol,permeate}$ of the system depending on the ethanol and glucose concentrations of the feed.

$$J_{ethanol}(t) = \frac{D^0_{ethanol}\rho_{ethanol}}{L}\left(\frac{(y_{ethanol}(t))^2}{2} + \beta_{ethanol} y_{ethanol}(t)(1 - y_{ethanol}(t))\right) \quad \text{Equation 4.22}$$

$$J_{water}(t) = \frac{D^0_{water}\rho_{water}}{L}\left(\frac{(y_{water}(t))^2}{2} + \beta_{water} y_{water}(t)(1 - y_{water}(t))\right) \quad \text{Equation 4.23}$$

The parameters used for Equations 4.14 to 4.23 are shown in Table 4.5.

Table 4.5 Parameters for membrane-reactor system model

Parameter	Value
Fermentation	
u_{max}	$0.015 \times X_0^{0.551} - 0.012$
$v_{max,ethanol}$	$9.17 \times 10^{-7} \times X_0^{5.034} + 0.093$
$v_{max,glycerol}$	$8.29 \times 10^{-7} \times X_0^{4.590} + 0.018$
K_{sx}	21.461±0.005
$K_{sp,\ ethanol}$	0.145±0.016
$K_{sp,\ glycerol}$	1.413±0.007
Ethanol flux	
$D_{ethanol}^0$	$9.55 \times 10^{-9} \pm 1.91 \times 10^{-10}$
$B_{ethanol}$	$0.39 \pm 1.20 \times 10^{-5}$
Water flux	
D_{water}^0	$6.52 \times 10^{-10} \pm 7.77 \times 10^{-12}$
B_{water}	$0.75 \pm 9.69 \times 10^{-7}$
Water flux in the presence of glucose	
D_{water}^0	$3.79 \times 10^{-10} \pm 6.24 \times 10^{-11}$
B_{water}	0.5±0.026

A classic Runge-Kutta method of order 4 was used to solve the set of differential equations presented by Equations 4.14 to 4.21, which represents the fermentation process. The parameters presented in Table 4.5 were entered into these equations. The Runge-Kutta programme was written in Excel using Visual Basic. See Appendix H for more detail on the Runge-Kutta numerical method. The Runge-Kutta programme was adapted to incorporate Equations 4.22 and 4.23, that represent the ethanol and water flux out of the system. After each step size taken by the Runge-Kutta programme, the programme did a test to determine

whether pervaporation had started (a simple if-function, as the time after which pervaporation had been started was entered into the programme by the user). If pervaporation had started, the programme did another test to determine whether any glucose was left in the system to determine which parameters to use to calculate the water flux. The parameters for ethanol and water flux were then entered into Equations 4.22 and 4.23 by the programme. The programme then determined both the water and ethanol flux based on the feed composition determined by the Runge-Kutta programme and Q and $P_{ethanol,permeate}$ could be calculated. The model was then solved for each step size (a step size of 0.1 hour was used) until the total fermentation time, also entered into the programme by the user, had been reached.

The membrane-reactor system model was compared to experimental data and it can be seen in Figure 4.3 that the model predicts the experimental data fairly well. The variables that were entered into the model included the initial yeast concentration ($10g.L^{-1}$) the initial glucose concentration (15wt%), the total initial feed mass (4kg), the fermentation time before pervaporation was started (24h) and the total experiment time (72h).

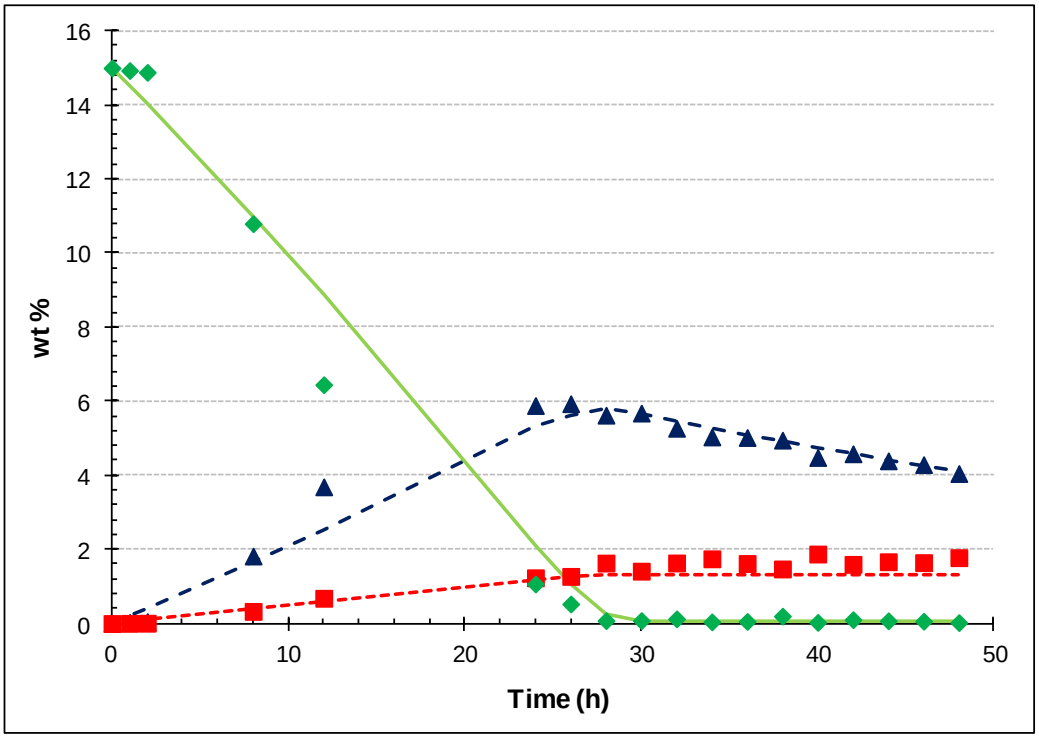

Figure 4.3 Comparison of the membrane-reactor system model with experimental data
(♦Experimental glucose yield, ▲ Experimental ethanol yield, ■ Experimental glycerol yield, — glucose yield model, --- ethanol yield model, ···· glycerol yield model)

The accuracy of the fit of the membrane-reactor system model, given by the R^2 value, is 0.997 for the ethanol data, 0.972 for the glycerol data and 0.993 for the glucose data. In this

study, the fermentation experiments used to develop the fermentation model were done in Scott Duran bottles whereas when fermentation was combined with pervaporation fermentation took place directly in the membrane-reactor feed vessel. This might account for the small differences in the experimental data and the model predictions.

As presented in this section the membrane-reactor system model describes the feed side of the membrane-reactor system relatively accurately. The water and ethanol flux could also be well predicted with the model, except where a steady state had not been reached (first 6 hours), as this model assumes a steady state of the flux. Therefore, Figure 4.4 shows the water and ethanol flux, as predicted by the model and determined experimentally after 30 hours of fermentation.

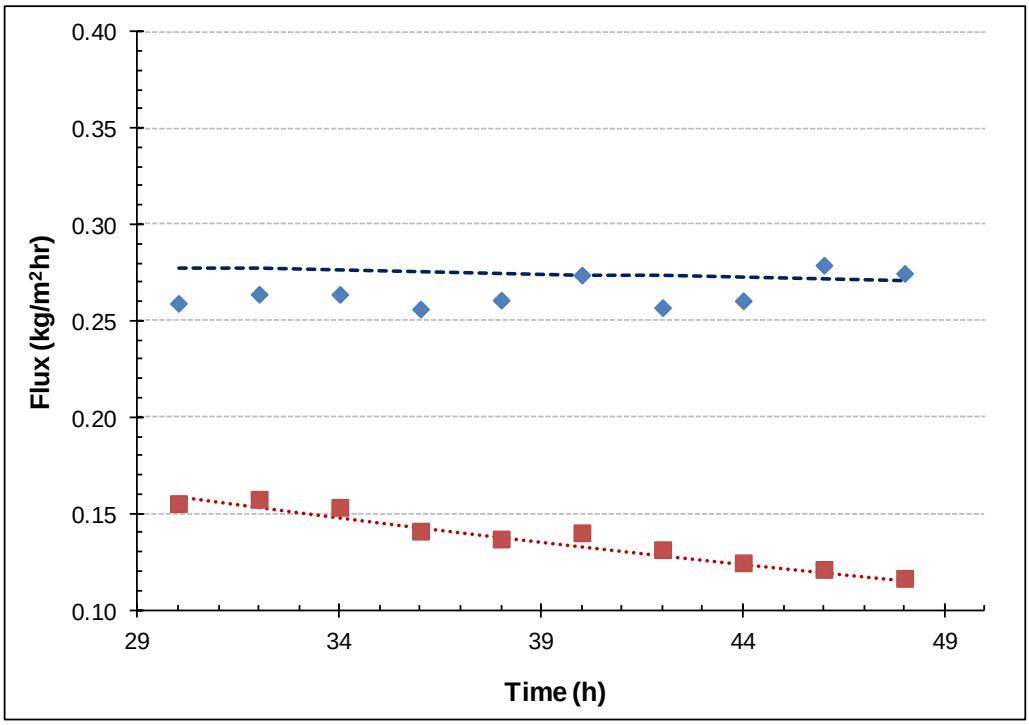

Figure 4.4 Comparison of the experimental partial flux with the membrane-reactor system model

(♦experimental water flux, ■experimental ethanol flux, ···· ethanol model, --- water model)

4.5 CONCLUSION

Fermentation was successfully coupled with pervaporation. The total ethanol yield was slightly lower than the batch fermentation experiments while the glycerol yield was slightly higher. It was concluded that the lower ethanol yield could be due to stress factors such as mixing in the fermentation vessel, which can influence the yeast cells and cause a lower ethanol production and a higher glycerol production.

Fermentation coupled with pervaporation was then modelled. A Monod-type kinetic model of fermentation was combined with a mass transport model based on Fick's law and Greenlaw's expression for diffusion coefficients. The removal of ethanol and water was modelled by taking into account the concentration changes in the feed vessel as a result of fermentation as well as the removal of ethanol and water by pervaporation. The fermentation coupled with pervaporation model was relatively accurate in predicting the experimental values.

4.6 REFERENCES

AROUJALIAN, A. & RAISI, A. 2009. Pervaporation as a means of recovering ethanol from lignocellulosic bioconversions. *Desalination*, 247: 509-517.

AROUJALIAN, A., BELKACEMI, K., DAVIDS, S.J., TURCOTTE, G. & POULIOT, Y. 2006. Effect of residual sugars in fermentation broth on pervaporation flux and selectivity for ethanol. *Desalination*, 193: 103-108.

BÖDDEKER, K.W. & BENGTSON, G. 1991. Selective pervaporation of organics from water. (*In* Huang, R.Y.M., ed. Pervaporation Membrane Separation Processes. Amsterdam: Elsevier. p. 437-490).

CHOVAU, S., GAYKAWAD, S., STRAATHOF, A.J.J. & VAN DER BRUGGEN. 2011. Influence of fermentation by-products on the purification of ethanol from water using pervaporation. *Bioresource Technology*, 102: 1669-1674.

DRESSELHAUS, M.S. & THOMAS, I.L. 2001. Alternative energy technologies. *Nature*, 414: 332-337.

FADEEV, A.G., KELLEY, S.S., MCMILLAN, J.D., SELINSKAYA, Y.A., KHOTIMSKY, V.S. & VOLKOV, V.V. 2003. Effect of yeast fermentation by-products on poly[1-(trimethylsilyl)-1-propyne] pervaporative performance. *Journal of Membrane Science*, 214: 229-238.

GARDNER,N., RODRIGUE, N. & CHAMPAGNE, C.P. 1993. Combined Effects of Sulfites, Temperature, and Agitation Time on Production of Glycerol in Grape Juice by *Saccharomyces cerevisiae. Applied and environmental microbiology*, 59(7): 2022-2028.

IKEGAMI, T., YANAGISHITA, H., KITAMOTOA, D., NEGISHI, H., HARAYA, K. & SANO, T. 2002. Concentration of fermented ethanol by pervaporation using silicalite membranes coated with silicone rubber. *Desalination*, 149:49-54.

KAEWKANNETRA, P., CHUTINATE, N., MOONAMART, S., KAMSAN, T. & CHIU, T.Y. 2011. Separation of ethanol from ethanol–water mixture and fermented sweet sorghum juice using pervaporation membrane reactor. *Desalination*. In Press.

KASENO, MIYAZAWA, I. &KOKUGAN, T. 1998. Effect of Product Removal by a Pervaporation on Ethanol Fermentation. *Journal of Fermentation and Bioengineering*, 86(5): 488-493.

LEWANDOWSKA, M. & KUJAWSKI, W.. 2007. Ethanol production from lactose in a fermentation/pervaporation system. *Journal of Food Engineering*, 79: 430–437.

MOHAMMADI, T., AROUJALIAN, A. & BAKHSHI, A. 2005. Pervaporation of dilute alcoholic mixtures using PDMS membrane. *Chemical Engineering Science*, 60: 1875-1880.

NOMURA, M., BIN, T. & NAKAO, S. 2002. Selective ethanol extraction from fermentation broth using a silicalite membrane. *Separation and Purification Technology*, 27: 59-66.

O'BRIEN, D. J. & CRAIG, J.C. 1996. Ethanol production in a continuous fermentation/membrane pervaporation system. *Applied Microbiology Biotechnology*, 44:699-704.

O'BRIEN, D.J., SENSKE, G.E., KURANTZ, M.J., CRAIG, J.C. 2004. Ethanol recovery from corn fiber hydrolysate fermentations by pervaporation. *Bioresource Technology*, 92: 15-19.

OFFEMAN, R.D. & LUDVIK, C.N. 2011. Poisoning of mixed matrix membranes by fermentation components in pervaporation of ethanol. *Journal of Membrane Science*, 367: 288-295.

SÁNCHEZ, O.J, CARDONA, C.A., CUBIDES, D.C. 2005. Modelling of simultaneous saccharification and fermentation process coupled with pervaporation for fuel ethanol production. (*In:* second mercosur congress on chemical engineering and fourth mercosur congress on process systems engineering, Rio de Janeiro, Brazil.)

SCHMIDT, S.L., MYERS, M.D., KELLEY, S.S, MCMILLAN, J.D. & PADUKONE, N. 1997. Evaluation of PTMSP Membrane in Achieving Enhanced Ethanol Removal from Fermentation by Pervaporation. *Applied Biochemistry and Biotechnology*, 63-65: 469-482.

STANISZEWSKI, M., KUJAWSKI, W. & LEWANDOWSKA, M. 2007. Ethanol production from whey in bioreactor with co-immobilized enzyme and yeast cells followed by

pervaporative recovery of product – Kinetic model predictions. Journal of Food Engineering, 82: 618–625.

STANISZEWSKI, M., KUJAWSKI, W. & LEWANDOWSKA, W. 2009. Semi-continuous ethanol production in bioreactor from whey with co-immobilized enzyme and yeast cells followed by pervaporative recovery of product-Kinetic model predictions considering glucose repression. *Journal of Food Engineering*, 91: 240–249.

THONGSUKMAK, A. & SIRKAR, K.K. 2007. Pervaporation membranes highly selective for solvents present in fermentation broths. *Journal of Membrane Science*, 302: 45-58

WU, Y., XIAO, Z., HUANG, W. & ZHONG, Y. 2005. Mass transfer in pervaporation of active fermentation broth with a composite PDMS membrane. *Separation and Purification Technology*, 42: 47-53.

CHAPTER 5: CONCLUSIONS AND RECOMMENDATIONS

OVERVIEW

This study consisted of the investigation of the kinetics of fermentation coupled with pervaporation. In this chapter, the main conclusions drawn from this study and recommendations for further study will be discussed. In the first section, Section 5.1, conclusions drawn from each part of this study will be discussed. This is followed by the second section, Section 5.2, where recommendations regarding fermentation coupled with pervaporation research will be discussed.

5.1 CONCLUSIONS

5.1.1. Main objective

By means of a literature review, it was shown that there is a lack in kinetic studies with regard to fermentation coupled with pervaporation. The models proposed by Staniszewski *et al*. (2007) and Staniszewski *et al*. (2009) represented the separate process but did not represent fermentation coupled with pervaporation directly. On the other hand, the model proposed by Sánchez *et al*. (2005) was for fermentation combined directly with pervaporation but it assumes that the separation factor as a result of pervaporation is constant and it does not account for the changes in separation due to the changes in feed concentration.

The main objective of this study was to propose a model that would represent the membrane-reactor kinetics when fermentation is coupled with pervaporation. It was demonstrated in Chapter 4 that fermentation could be successfully coupled with pervaporation to remove ethanol from the system. A model that predicted the membrane-reactor kinetics, the membrane-reactor system model, was proposed in Chapter 4.4 and it was shown that this model could accurately predict the ethanol, glycerol, and glucose contents of the feed as well as the ethanol and water flux of the system. The proposed model took into account changes in the feed composition as a result of fermentation as well as the removal of ethanol and water by pervaporation.

5.1.2. Fermentation

The effect of different operating conditions on fermentation was investigated in the first part of this study. The reproducibility of the fermentation experiments were deemed as acceptable as the experimental error varied between 0.75% and 9.92% for each different set of data. The starting glucose and starting yeast content of the fermentation broth had a remarkable effect on the final ethanol yield and it was found that the optimum ethanol yield was achieved by using 15wt% glucose and 10g.L^{-1} yeast. Glucose concentrations higher than 15wt% resulted in low yields due to inhibition of the yeast. The pH of the fermentation broth did not have a large effect on the ethanol yield, as long as it was above 3.5. This made the modelling of the fermentation kinetics remarkably simpler as the effect of pH could be ignored.

5.1.3. Fermentation modelling

Simplified models based on the Monod model were developed by using the fermentation data obtained in the first part of this study. The first model only incorporated substrate limitation and this model showed very accurate results for low (<20 wt%) initial sugar concentrations. At high sugar concentrations, where substrate inhibition had an effect, this model did not accurately predict the fermentation process. The second model accounted for the inhibition effect of the sugar. The second model (substrate-inhibition model) showed more accurate results than the first model at high sugar concentrations, but it did not predict fermentation with low initial sugar concentrations as accurately.

5.1.4. Pervaporation

Four membranes were obtained from Sulzer Chemtech in Germany and tested to determine whether they were appropriate for ethanol removal from a fermentation broth. It was found that the PERVAP®4060 membrane would be the best choice for this study due to its selectivity and flux related to the separation of ethanol and water.

The effect of the ethanol concentration in the feed as well as the influence of glucose on the flux and selectivity of the membrane was investigated. The total flux varied with ethanol content of the feed and the highest total flux of 0.853±0.009 kg/m^{2}h was obtained with a feed containing 20wt% ethanol. The water flux was not influenced by the ethanol concentration in the feed but an increase in ethanol in the feed resulted in an increase in ethanol flux. Glucose did not have an effect on the ethanol flux but it significantly lowered the water flux.

5.1.5. Pervaporation modelling

A model based on the solution-diffusion model was developed by using the pervaporation data obtained with the PERVAP®4060 membrane. Fick's first law was used to describe the transport of the permeating species through the membrane. A concentration-dependent diffusion coefficients model namely the Greenlaw model was used together with Fick's law to describe the mass transport of ethanol and water through the PERVAP®4060 membrane. The water and ethanol flux could be predicted very accurately by this model with R^2 values above 0.998.

5.2 RECOMMENDATIONS FOR FUTURE RESEARCH

The following research, which did not fall within the scope of this investigation, is recommended for future research.

The main reason for combining fermentation with pervaporation is to reduce product inhibition, therefore it is recommended to expand the fermentation model to incorporate product inhibition. Further experimental work, where high ethanol concentrations are present in the fermentation broth will be required to determine the product inhibition constants.

The second reason for combining fermentation with pervaporation is to be able to produce ethanol continuously from fermentation. It would thus be interesting to see the effect of changing the batch fermentation system used in this study to a fed-batch system where glucose is added at different intervals. This would be done in order to prevent substrate inhibition and increase the final ethanol concentration in the feed. Obviously, optimisation of the sugar addition timing and concentrations would be necessary as well.

Optimisation of the membrane module as well as testing other pervaporation membranes is also recommended as this might result in better selectivity and higher flux.

APPENDIX A: EXPERIMENTAL ERROR

OVERVIEW

An overview of the terminology and methods used in calculating the experimental error and reproducibility of an experiment will be discussed in Section A.1. Sections A.2 to A.4 focuses on determining the experimental error and reproducibility of the fermentation experiments, pervaporation experiments and the analytical equipment, respectively.

A.1 REPRODUCIBILITY AND EXPERIMENTAL ERROR

The experimental error, also known as the reproducibility of the experiments, is important for the researcher as it validates the experimental results and conclusions (Moffat, 1988). The experimental error associated with each variable was calculated using the method as described below.

First, the average value ($\bar{x}$) is calculated by adding all the individual values (x_i) together and dividing the number by the amount of data points (N) as shown in Equation A.1 (Ross, 2009:216).

$$\bar{x} = \frac{1}{N}\sum_{i=1}^{N} x_i \qquad \text{Equation A.1}$$

The next step is to calculate the standard deviation (δ) of the data set. The standard deviation shows how much the data varies from the average value. Equation A.2 is used to calculate the standard deviation (Ross, 2009:216).

$$\delta = \sqrt{\frac{\sum_{i=1}^{N}\left(x_i - \bar{x}\right)^2}{(N-1)}} \qquad \text{Equation A.2}$$

A 95% confidence level is used which means that there is a 95% probability that the data from the experiments lies within the range of the confidence level. The confidence level is calculated with Equation A.3

$$95\%\ \text{confidence level} = \bar{x} \pm z \times \frac{\delta}{\sqrt{N}} \qquad \text{Equation A.3}$$

The area under the normal curve (z) is calculated using the t-distribution function (tinv) function in Excel®.

Finally, the experimental error is calculated using Equation A.4.

$$\text{Experimental error} = 2 \times \frac{\text{Confidence level}}{\bar{x}} \times 100\% \qquad \text{Equation A.4}$$

A.2 FERMENTATION EXPERIMENTAL ERROR

The experimental error for each fermentation variable (initial glucose concentration, initial yeast concentration, and pH) was determined by using Equations A.1 to A.4, as discussed in Section A.1. The reproducibility of the experiments where the initial glucose concentration was varied was determined by repeating an experiment four times using 15wt% glucose, 10g.L^{-1} yeast, a pH of 4, and at 30°C. The ethanol yield (g.g^{-1}) of each experiment at different time intervals is presented in Table A.1 (as well as the confidence level calculated for each time interval) and the statistical parameters calculated from this data for the final ethanol yield are shown in Table A.2.

Table A.1 Ethanol yield (g.g^{-1}) of fermentation- starting glucose concentration varied

Time (h)	Run 1	Run 2	Run 3	Run 4	Average	Standard deviation
1	0.007	0.005	0.005	0.011	0.007	0.003
2	0.020	0.014	0.011	0.021	0.017	0.005
4	0.043	0.034	0.025	0.049	0.038	0.011
8	0.095	0.078	0.068	0.084	0.081	0.012
12	0.156	0.136	0.115	0.178	0.146	0.027
24	0.376	0.333	0.276	0.425	0.353	0.063
48	0.426	0.422	0.421	0.436	0.426	0.007
72	0.431	0.424	0.427	0.458	0.435	0.016

Table A.2 Statistical parameters of final ethanol yield for fermentation- starting glucose concentration varied

Repeat number	Ethanol yield (g.g^{-1})
1	0.431
2	0.424
3	0.427
4	0.458
Average ($\bar{x}$)	0.435
Standard deviation (δ)	0.016
Experimental error (%)	9.92

The experimental error and reproducibility related to the experiments where the initial yeast concentration was varied was determined by repeating an experiment four times. The experimental conditions for these repeats were an initial yeast concentration of 5g.L^{-1}, an initial glucose concentration of 15wt%, a pH of 4 and a temperature of 30˚C. Table A.3 shows the ethanol yield (g.g^{-1}) and the confidence level for each repeat at different time intervals.

Table A.3 Ethanol yield ($g.g^{-1}$) of fermentation- starting yeast concentration varied

Time (h)	Run 1	Run 2	Run 3	Run 4	Average	Standard deviation
1	0.006	0.004	0.007	0.005	0.005	0.001
2	0.010	0.011	0.010	0.009	0.010	0.001
4	0.021	0.024	0.022	0.021	0.022	0.001
8	0.046	0.052	0.049	0.042	0.047	0.004
12	0.073	0.083	0.073	0.066	0.074	0.007
24	0.150	0.152	0.159	0.147	0.152	0.005
48	0.357	0.365	0.362	0.350	0.358	0.007
72	0.446	0.449	0.448	0.448	0.448	0.001

The statistical parameters calculated from the data in Table A.3 data for the final ethanol yield are presented in Table A.4.

Table A.4 Statistical parameters of final ethanol yield for fermentation- starting yeast concentration varied

Repeat number	Ethanol yield ($g.g^{-1}$)
1	0.446
2	0.449
3	0.448
4	0.448
Average ($\bar{x}$)	0.448
Standard deviation (δ)	0.001
Experimental error (%)	0.75

The fermentation experiments associated with varying the pH was repeated four times to determine the reproducibility and experimental error. A pH of 5.5, a temperature of 30°C, an initial glucose concentration of 15wt%, and an initial yeast concentration of $10g.L^{-1}$ was used. In Table A.5, the Ethanol yield for each time interval is shown together with the average value and the confidence level. In Table A.6, the statistical parameters of the final ethanol yield for the pH experiments are shown.

Table A.5 Ethanol yield ($g.g^{-1}$) of fermentation- pH varied

Time (h)	Run 1	Run 2	Run 3	Run 4	Average	Standard deviation
1	0.011	0.007	0.012	0.009	0.010	0.002
2	0.017	0.019	0.019	0.017	0.018	0.001
4	0.042	0.042	0.045	0.040	0.042	0.002
8	0.103	0.111	0.102	0.095	0.103	0.007
12	0.160	0.184	0.155	0.165	0.166	0.013
24	0.401	0.436	0.411	0.401	0.412	0.016
48	0.442	0.440	0.440	0.446	0.442	0.003
72	0.437	0.449	0.455	0.437	0.444	0.009

Table A.6 Statistical parameters of final ethanol yield for fermentation- pH varied

Repeat number	Ethanol yield ($g.g^{-1}$)
1	0.437
2	0.449
3	0.455
4	0.437
Average ($\bar{x}$)	0.444
Standard deviation (δ)	0.009
Experimental error (%)	7.43

A.3 PERVAPORATION EXPERIMENTAL ERROR

A.3.1. Sorption experiments

A mixture of 10wt% ethanol at 30°C was used to determine the reproducibility and experimental error for the sorption experiments. Six experiments were repeated and the results obtained are summarized in Table A.7.

Table A.7 Reproducibility of the sorption experiments

Repeat number	M∞ (-)
1	0.659
2	0.674
3	0.661
4	0.689
5	0.665
6	0.669
Average ($\bar{x}$)	0.669
Standard deviation (δ)	0.011
Experimental error (%)	3.27

A.3.2. Pervaporation experiments

The reproducibility and the experimental error of the pervaporation experiments were determined by repeating three pervaporation experiments at the same conditions. A feed mixture of 10wt% ethanol at 30°C was used for the three experiments. The results obtained as well as the reproducibility parameters are summarised in Table A.8. The steady state flux, selectivity, enrichment factor and ethanol flux values were used to determine the statistical parameters.

Table A.8 Reproducibility of the pervaporation experiments

Repeat number	Flux ($kg/m^2.h$)	Selectivity (-)	Enrichment factor (-)	Ethanol flux ($kg/m^2.h$)	Water flux ($kg/m^2.h$)
1	0.533	7.558	4.238	0.244	0.289
2	0.542	7.664	4.486	0.259	0.284
3	0.542	8.544	4.654	0.279	0.263
Average ($\bar{x}$)	0.539	7.922	4.459	0.260	0.279
Standard deviation (δ)	0.005	0.541	0.209	0.017	0.014
Experimental error (%)	3.43	25.10	17.24	24.36	18.01

A.4 THE ANALYTICAL EQUIPMENT EXPERIMENTAL ERROR

The experimental error associated with the analytical equipment used in this study was calculated by analysis the same sample three times. This was done for the HPLC, the refractometer, the spectrophotometer, the glucose analyser. In Table A.9 and Table A.10 the statistical parameters for each of the analytical equipment is presented.

Table A.9 Statistical parameters for the refractometer, spectrophotometer, and glucose analyser

Repeat number	Refractometer	Spectrophotometer	Glucose analyser
1	1.377	0.600	4.850
2	1.373	0.598	4.890
3	1.377	0.602	4.880
Average ($\bar{x}$)	1.376	0.600	4.873
Standard deviation (δ)	0.002	0.002	0.021
Experimental error (%)	0.57	1.22	1.57

Table A.10 Statistical parameters for the HPLC

Repeat number	Glucose area (A_2)	Ethanol area (A_1)	Area Ratio (A_2/A_1)
1	1.91×10^6	1.94×10^6	0.983
2	1.98×10^6	1.94×10^6	1.019
3	1.96×10^6	1.95×10^6	1.009
Average ($\bar{x}$)	1.95	1.94×10^6	1.004
Standard deviation (δ)	3.70×10^4	4.95×10^3	0.019
Experimental error (%)	6.96	0.94	6.79

A.5 REFERENCES

MOFFAT, R.J. 1988. Describing the uncertainties in experimental results. *Experimental thermal and fluid science*, 1(1): 3-17.

ROSS, S. Introduction to probability and statistics for engineers and scientists. 4th ed. London: Academic Press. 664p.

APPENDIX B: CALIBRATION CURVES

OVERVIEW

The focus of this appendix is on the calibration curves required for each analytical technique. In Section B.1, the calibration curve used with the spectrophotometer to determine the yeast cell concentration is discussed. The calibration curves used for the HPLC and how the composition of the sample was determined using this calibration curve is presented in Section B.2. Section B.3 focuses on the refractometer calibration curve which was used to determine the ethanol fraction in the feed and the permeate of the pervaporation experiments.

B.1 SPECTROPHOTOMETER CALIBRATION CURVE

The biomass concentration (yeast cell concentration) is a critical measurement in fermentation studies. A variety of methods to measure the cell concentration of a fermentation broth can be used, but a simple and fast method is to monitor the optical density of the sample. The optical density of a sample can be related to the cell density by a calibration curve. The advantage of using this method is that feedback is available immediately. The optical density of a sample is measured in a cuvette at a visible wavelength such as 600 nm using a spectrophotometer. The sample must be diluted until its optical density falls within the linear regime of the spectrophotometer (optical density < 1A). The calibration curve showing the relationship of absorbance to yeast cell concentration is presented in Figure B.1.

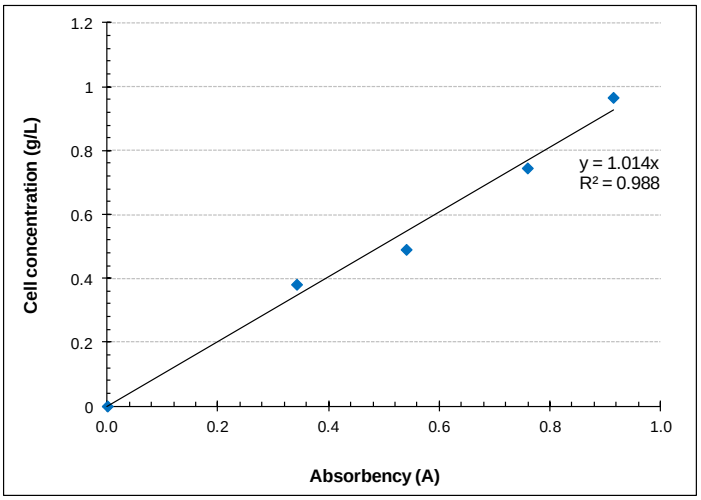

Figure B.1 Spectrophotometer calibration curve

As most samples needs to be diluted to fall within the range of the calibration curve, the calculated cell concentration must be multiplied by the dilution factor for the correct cell concentration.

B.2 THE HPLC

B.2.1. Calibration Curve of glucose, glycerol and ethanol

The HPLC was used to determine the content and composition of the fermentation broth in the fermentation experiments. The retention time for each of these components were determined by injecting a known component (i.e. glucose, glycerol, or ethanol) into the HPLC. Table B.1 shows the retention times of the fermentation broth components.

Table B.1 Retention times of the components in fermentation broth

Fermentation broth component	Retention time (min)
Ethanol	12.311-13.951
Glucose	9.417-9.514
Glycerol	14.366-16.190

Calibration curves are required to determine the content of each sample using the HPLC. Standard mixtures were prepared that contained known amounts of two components each. The wt% of each component in the mixture was varied so that the range fit in with the wt% of each component that is expected in the results. Table B.2 shows the wt% of each component used for the standard mixtures.

Table B.2 Preparation of standard mixtures

Calibration curve	Ethanol (wt %)	Glycerol (wt %)	Glucose	Water (wt %)
Ethanol/Glycerol	5.062	30.214	0	64.724
Ethanol/Glycerol	9.833	26.110	0	64.057
Ethanol/Glycerol	14.292	24.123	0	61.584
Ethanol/Glycerol	19.941	15.761	0	64.298
Ethanol/Glycerol	24.046	13.678	0	62.276
Ethanol/Glycerol	29.973	5.075	0	64.952
Ethanol/Glucose	28.811	0	5.222	65.967
Ethanol/Glucose	24.205	0	10.031	65.764
Ethanol/Glucose	18.503	0	14.216	67.281
Ethanol/Glucose	14.451	0	19.355	66.195
Ethanol/Glucose	9.811	0	24.846	65.343
Ethanol/Glucose	5.340	0	30.045	64.615
Glycerol/Glucose	0	6.650	29.349	64.002
Glycerol/Glucose	0	9.925	24.174	65.902
Glycerol/Glucose	0	15.263	19.631	65.106
Glycerol/Glucose	0	19.922	14.939	65.140
Glycerol/Glucose	0	24.085	10.188	65.727
Glycerol/Glucose	0	29.822	4.798	65.381

These standard mixtures were then analysed by the HPLC. The peak areas of the two components present in each standard were compared and a peak area ratio was calculated. For the calibration curve, the peak area ratio was then plotted against the ratio of the wt% of each component. Figure B.2 to Figure B.4 shows the calibration curves for glucose, ethanol, and glycerol.

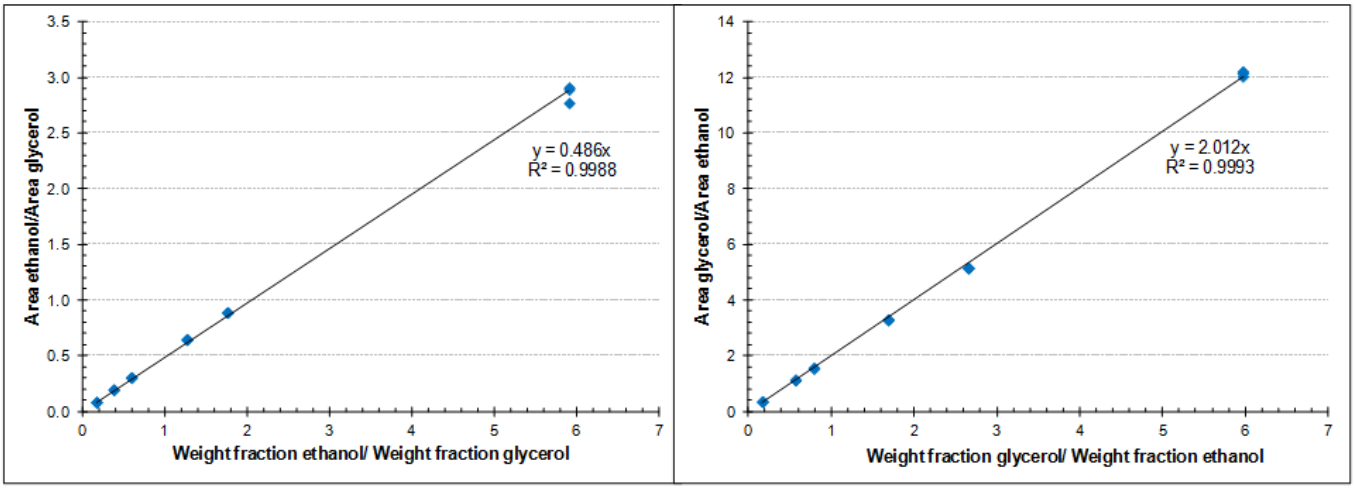

Figure B.2 Glycerol/Ethanol calibration curve

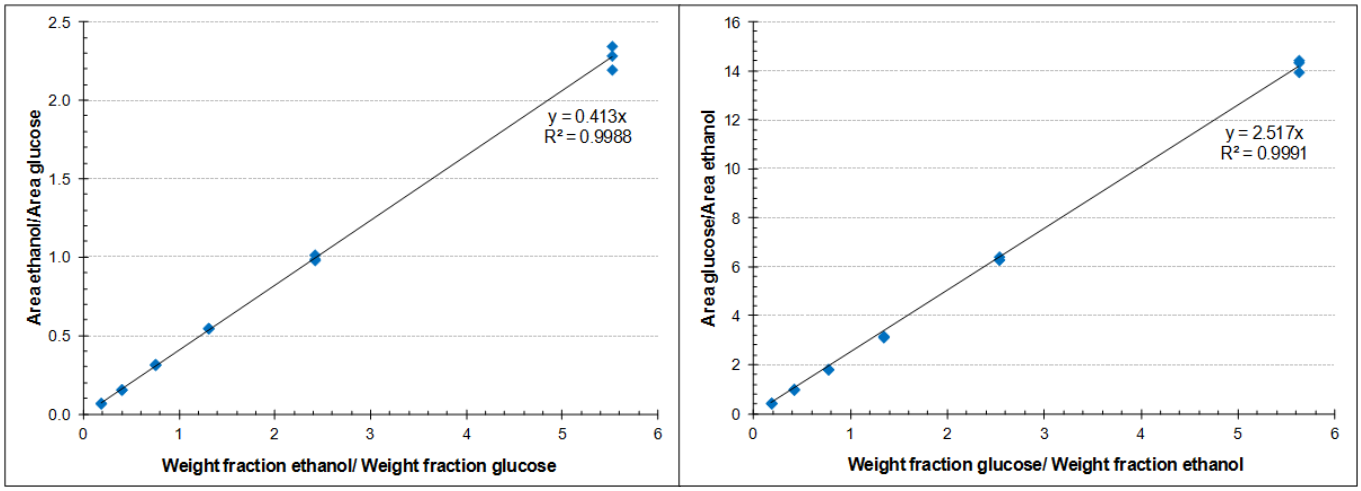

Figure B.3 Ethanol/Glucose calibration curve

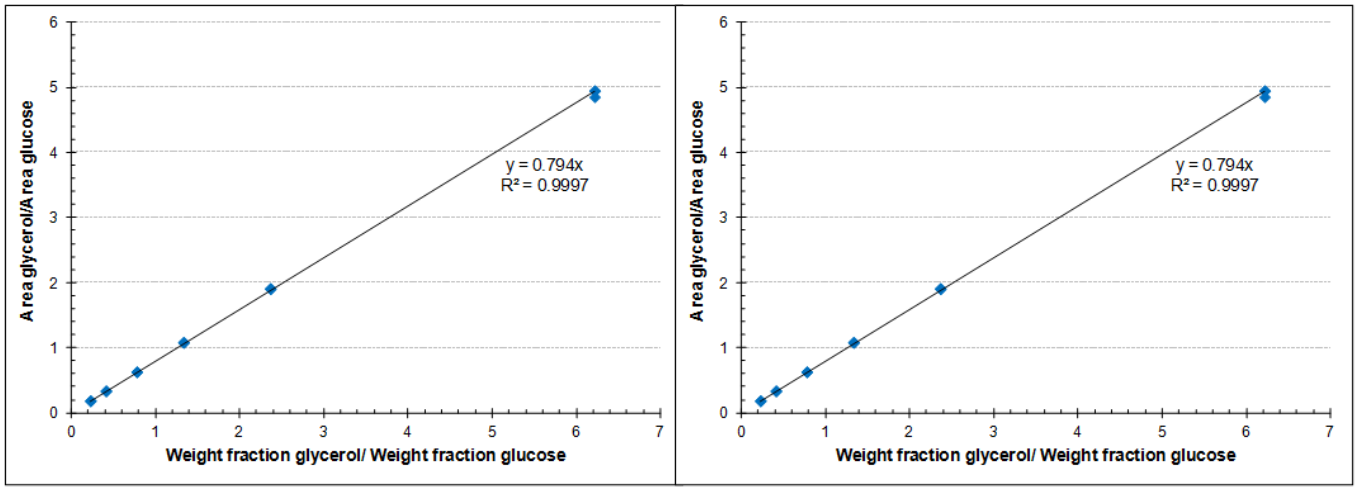

Figure B.4 Glycerol/Glucose calibration curve

A straight line was fitted to the data to obtain a constant, which was used to determine the glycerol and ethanol yields as well as the glucose consumption for the fermentation

experiments (See Chapter 2 and Appendix C). In Table B.3, the constants obtained from the calibration curves are summarised.

Table B.3 Constants from calibration curves

Standard	Constant
Ethanol/Glycerol	0.4867
Glycerol/Ethanol	2.0117
Ethanol/Glucose	0.4131
Glucose/Ethanol	2.5174
Glycerol/Glucose	0.7941
Glucose/Glycerol	1.2272

B.2.2. Determination of composition from calibration curve

Equation B.1 is used to determine the ethanol glycerol and sugar content of each sample.

$$x_1 + x_2 + x_3 = 1 \qquad \text{Equation B.1}$$

In Equation B.1, x_1 is the mass fraction of ethanol plus the mass fraction of carbon dioxide, x_2 is the mass fraction of glucose, and x_3 is the mass fraction of glycerol. Equation B.1 can be rearranged to determine each individual component, as follows (showing glycerol as an example).

$$\frac{x_1}{x_3} + \frac{x_2}{x_3} + \frac{x_3}{x_3} = \frac{1}{x_3} \qquad \text{Equation B.2}$$

$$\frac{1}{1 + \frac{x_1}{x_3} + \frac{x_2}{x_3}} = x_2 \qquad \text{Equation B.3}$$

From the calibration curves, Equation B.4 follows:

$$\frac{x_1}{x_3} = \frac{1}{k_1} \times \frac{\text{Peak area of ethanol}}{\text{Peak area of glycerol}} \qquad \text{Equation B.4}$$

Therefore

$$x_2 = \frac{1}{1 + \frac{1}{k_1} \times \frac{\text{Peak area of ethanol}}{\text{Peak area of glycerol}} + \frac{x_2}{x_3}} \qquad \text{Equation B.5}$$

The same principle applies to the other ratios thus:

$$x_2 = \frac{1}{1 + \frac{1}{k_1} \times \frac{\text{Peak area of ethanol}}{\text{Peak area of glycerol}} + \frac{1}{k_2} \times \frac{\text{Peak area of glucose}}{\text{Peak area of glycerol}}} \qquad \text{Equation B.6}$$

The ethanol yield can then be determined (as x_1 is the ethanol mass fraction plus the carbon dioxide fraction), using Equation B.7:

$$\text{Ethanol yield} = \text{Mass fraction} \times \frac{Mw_{\text{Ethanol}}}{Mw_{\text{Ethanol}} + Mw_{CO_2}} \qquad \text{Equation B.7}$$

where $Mw_{Ethanol}$ = molecular weight of ethanol (46 g.mol^{-1}) and Mw_{CO2} = molecular weight of carbon dioxide (44 g.mol^{-1})

B.3 REFRACTOMETER CALIBRATION CURVE

The refractometer is used to measure the ethanol concentration of water and ethanol mixtures. This was used to measure the ethanol weight fraction in the feed of the pervaporation unit as well as in the permeate during the pervaporation experiments. The samples had to be diluted to ensure that the refractometer readings fall within the range of the calibration curve. The refractometer calibration curve is shown in Figure B.5.

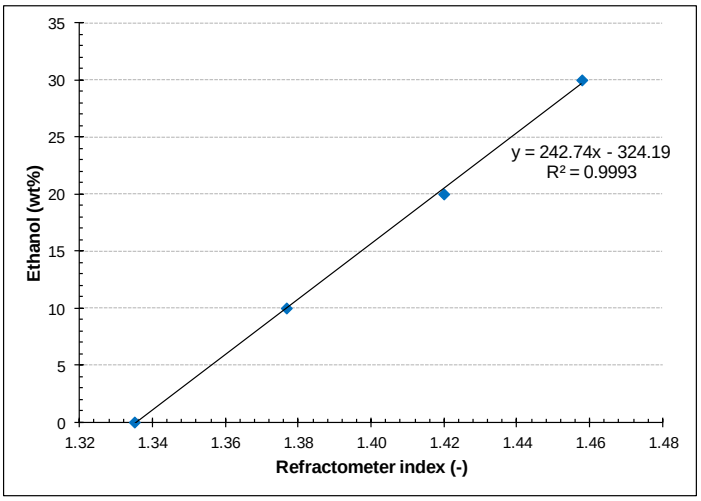

Figure B.5 Refractometer calibration curve

APPENDIX C: FERMENTATION EXPERIMENTS

OVERVIEW

The results obtained from the fermentation experiments, at each different set of conditions, are presented in Appendix C. In Section C.1, the calculations for determining the glucose utilization presented in Chapter 2 is discussed. In Section C.2, the results (obtained through HPLC analysis as discussed in Appendix B) of the experiments where the starting glucose concentration was varied is presented. In Section C.3, the result of the fermentation experiments where the starting yeast concentration was varied is presented. The result from the experiments where the pH was varied is presented in the final section of this Appendix, Section C.4.

C.1 SAMPLE CALCULATIONS

The method used to determine the glucose utilization for ethanol production, glucose utilization for glycerol production, total glucose utilization, and ratio of glycerol to ethanol utilization presented in Chapter 2 is discussed in this section.

Sample calculation are done using the data obtained from an experiment using 15wt% starting glucose, 10g.L^{-1} yeast and a pH of 4. The glucose utilized for glycerol production is determined by the glycerol yield after 72 hours. The glucose utilized for ethanol production is then determined by subtracting the glycerol yield after 72 hours from the amount of glucose that was converted.

$$\text{Glucose utilization for ethanol production (\%)} = \left(\text{Glucose converted-Glycerol yield}\right) \times 100\%$$
$$= \left(\left(1 - 0.009\right) - 0.075\right) \times 100\% = 91.6\%$$

The total glucose utilization is determined by adding the amount of glucose utilized for ethanol production and the amount of glucose utilized for glycerol production after 72 hours of fermentation.

$$\text{Total glucose utilized (\%)} = \text{\% utilized for ethanol +\% utilized for glycerol}$$
$$= 91.60\% + 7.52\% = 99.12\%$$

The ratio of glucose utilization for glycerol to ethanol is then determined:

$$\text{Ratio (glycerol to ethanol)} = \frac{\text{\% glucose utilized for glycerol production}}{\text{\% glucose utilized for ethanol production}}$$
$$= \frac{7.52\%}{91.60\%} = 0.08$$

C.2 EFFECT OF STARTING GLUCOSE CONCENTRATION

Table C.1 Yields and yeast cell concentration using a 5wt% starting glucose

Time (h)	Ethanol (g.g^{-1})	Glycerol (g.g^{-1})	Glucose (g.g^{-1})	Yeast cells (g.L^{-1})
1	0.023±0.004	0.005±0.002	0.945±0.010	10.203±0.216
2	0.065±0.007	0.022±0.004	0.829±0.020	9.689±0.501
4	0.164±0.015	0.041±0.002	0.600±0.032	10.757±1.225
8	0.365±0.016	0.086±0.004	0.119±0.039	11.587±2.073
12	0.383±0.038	0.076±0.005	0.102±0.082	12.325±2.142
24	0.407±0.088	0.091±0.007	0.025±0.177	12.460±2.654
48	0.403±0.009	0.107±0.006	0.002±0.013	13.596±1.865
72	0.391±0.022	0.100±0.017	0.039±0.010	10.335±1.697

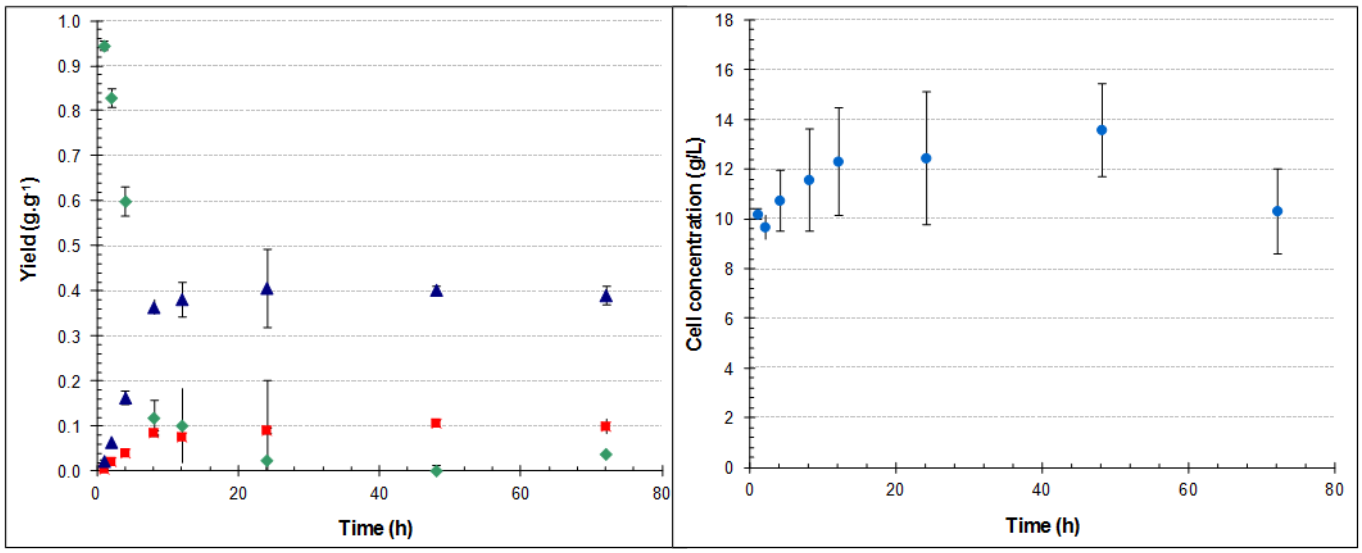

Figure C.1 Fermentation using 5wt% starting glucose

(♦Glucose yield, ▲Ethanol yield, ■Glycerol yield, ●yeast cell concentration)

Table C.2 Yields and yeast cell concentration using a 10wt% starting glucose

Time (h)	Ethanol ($g.g^{-1}$)	Glycerol ($g.g^{-1}$)	Glucose ($g.g^{-1}$)	Yeast cells ($g.L^{-1}$)
1	0.010±0.004	0.003±0.002	0.974±0.010	9.649±0.216
2	0.029±0.007	0.009±0.004	0.924±0.020	10.084±0.501
4	0.066±0.015	0.018±0.002	0.835±0.032	10.414±1.225
8	0.160±0.016	0.043±0.004	0.603±0.039	11.244±2.073
12	0.284±0.038	0.059±0.005	0.329±0.082	12.312±2.142
24	0.421±0.088	0.085±0.007	0.009±0.177	13.612±2.654
48	0.418±0.009	0.083±0.006	0.020±0.013	11.714±1.865
72	0.409±0.022	0.088±0.017	0.027±0.010	12.265±1.697

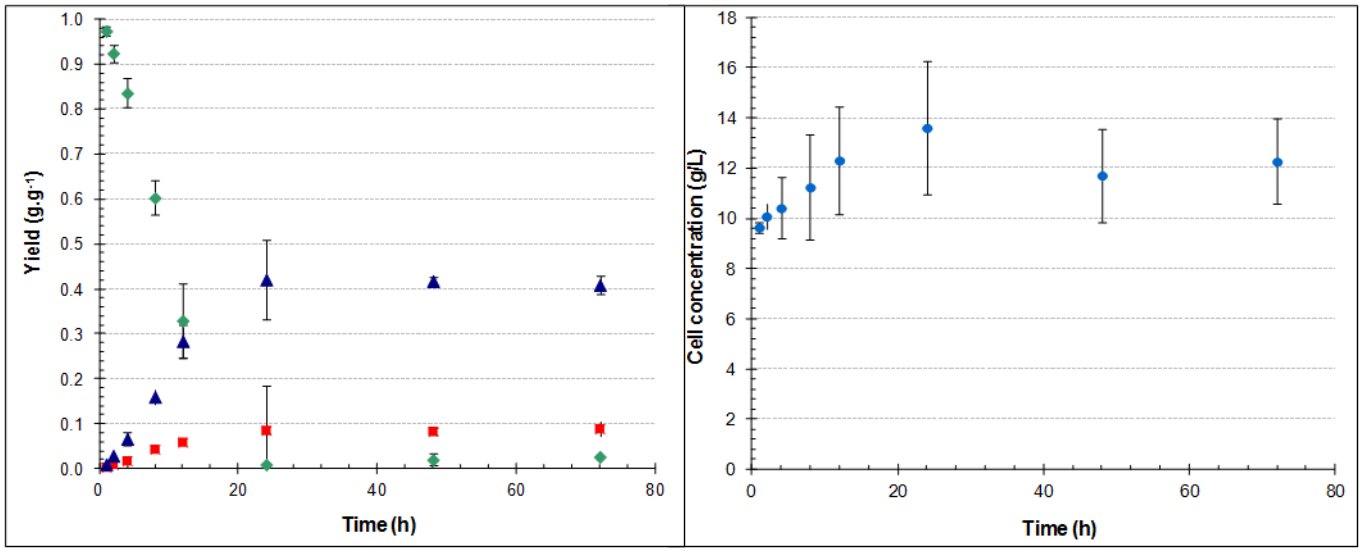

Figure C.2 Fermentation using 10wt% starting glucose

(♦Glucose yield, ▲Ethanol yield, ■Glycerol yield, ●yeast cell concentration)

Table C.3 Yields and yeast cell concentration using a 15wt% starting glucose

Time (h)	Ethanol ($g.g^{-1}$)	Glycerol ($g.g^{-1}$)	Glucose ($g.g^{-1}$)	Yeast cells ($g.L^{-1}$)
1	0.007±0.004	0.002±0.002	0.982±0.010	9.320±0.216
2	0.020±0.007	0.005±0.004	0.951±0.020	10.071±0.501
4	0.043±0.015	0.011±0.002	0.895±0.032	10.757±1.225
8	0.095±0.016	0.025±0.004	0.765±0.039	11.112±2.073
12	0.156±0.038	0.033±0.005	0.630±0.082	12.035±2.142
24	0.376±0.088	0.061±0.007	0.145±0.177	13.417±2.654
48	0.426±0.009	0.078±0.006	0.013±0.013	12.736±1.865
72	0.431±0.022	0.075±0.017	0.009±0.010	12.152±1.697

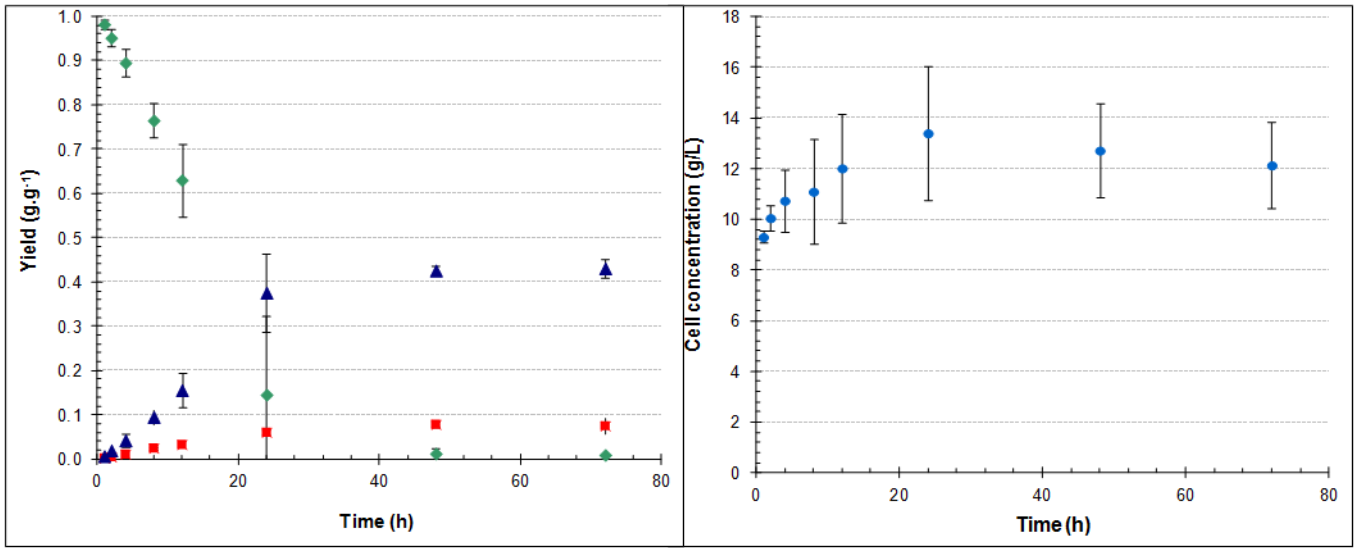

Figure C.3 Fermentation using 15wt% starting glucose

(♦Glucose yield, ▲Ethanol yield, ■Glycerol yield, ●yeast cell concentration)

Table C.4 Yields and yeast cell concentration using a 20wt% starting glucose

Time (h)	Ethanol ($g.g^{-1}$)	Glycerol ($g.g^{-1}$)	Glucose ($g.g^{-1}$)	Yeast cells ($g.L^{-1}$)
1	0.004±0.004	0.000±0.002	0.991±0.010	9.939±0.216
2	0.014±0.007	0.003±0.004	0.966±0.020	11.561±0.501
4	0.032±0.015	0.007±0.002	0.924±0.032	10.704±1.225
8	0.068±0.016	0.015±0.004	0.837±0.039	11.917±2.073
12	0.106±0.038	0.023±0.005	0.748±0.082	12.114±2.142
24	0.224±0.088	0.038±0.007	0.487±0.177	13.936±2.654
48	0.399±0.009	0.070±0.006	0.083±0.013	14.407±1.865
72	0.426±0.022	0.077±0.017	0.015±0.010	13.093±1.697

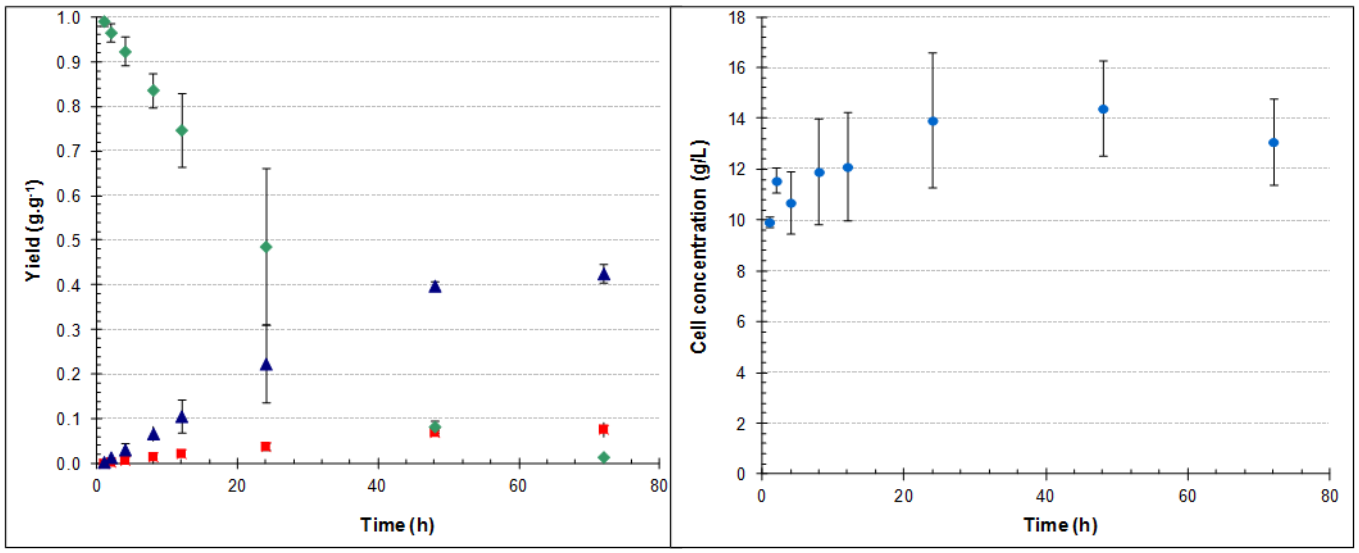

Figure C.4 Fermentation using 20wt% starting glucose

(♦Glucose yield, ▲Ethanol yield, ■Glycerol yield, ●yeast cell concentration)

Table C.5 Yields and yeast cell concentration using a 25wt% starting glucose

Time (h)	Ethanol ($g.g^{-1}$)	Glycerol ($g.g^{-1}$)	Glucose ($g.g^{-1}$)	Yeast cells ($g.L^{-1}$)
1	0.002±0.004	0.000±0.002	0.994±0.010	8.550±0.216
2	0.007±0.007	0.002±0.004	0.982±0.020	11.276±0.501
4	0.022±0.015	0.005±0.002	0.946±0.032	11.195±1.225
8	0.047±0.016	0.011±0.004	0.887±0.039	11.957±2.073
12	0.070±0.038	0.016±0.005	0.833±0.082	13.077±2.142
24	0.133±0.088	0.024±0.007	0.691±0.177	13.255±2.654
48	0.238±0.009	0.043±0.006	0.450±0.013	14.001±1.865
72	0.309±0.022	0.051±0.017	0.295±0.010	14.504±1.697

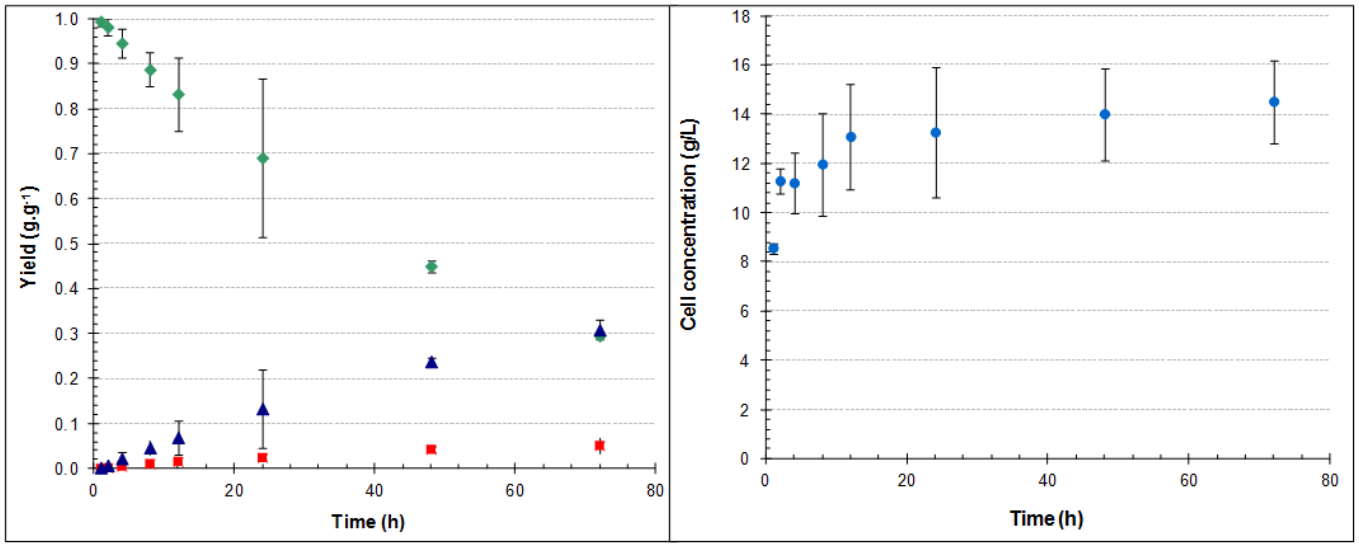

Figure C.5 Fermentation using 25wt% starting glucose

(♦Glucose yield, ▲Ethanol yield, ■Glycerol yield, ●yeast cell concentration)

Table C.6 Yields and yeast cell concentration using a 30wt% starting glucose

Time (h)	Ethanol ($g.g^{-1}$)	Glycerol ($g.g^{-1}$)	Glucose ($g.g^{-1}$)	Yeast cells ($g.L^{-1}$)
1	0.001±0.004	0.001±0.002	0.996±0.010	9.523±0.216
2	0.004±0.007	0.001±0.004	0.991±0.020	10.108±0.501
4	0.015±0.015	0.003±0.002	0.963±0.032	9.929±1.225
8	0.032±0.016	0.008±0.004	0.921±0.039	10.708±2.073
12	0.047±0.038	0.011±0.005	0.887±0.082	10.870±2.142
24	0.084±0.088	0.018±0.007	0.802±0.177	12.006±2.654
48	0.138±0.009	0.027±0.006	0.676±0.013	13.450±1.865
72	0.190±0.022	0.035±0.017	0.560±0.010	12.801±1.697

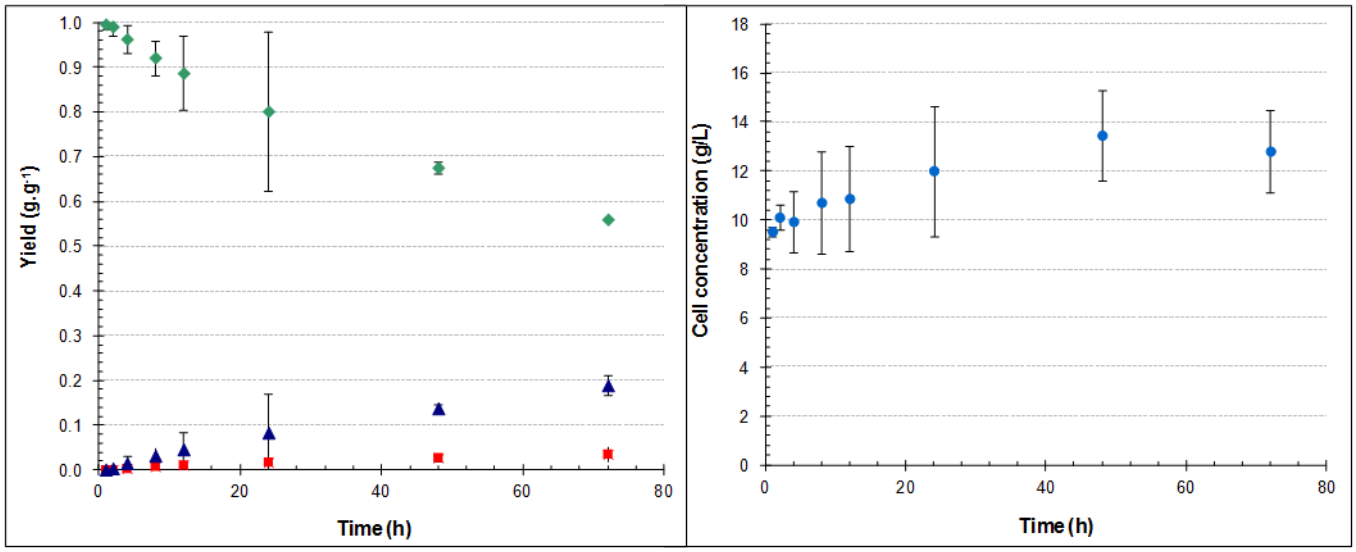

Figure C.6 Fermentation using 30wt% starting glucose

(♦Glucose yield, ▲Ethanol yield, ■Glycerol yield, ●yeast cell concentration)

Table C.7 Yields and yeast cell concentration using a 35wt% starting glucose

Time (h)	Ethanol ($g.g^{-1}$)	Glycerol ($g.g^{-1}$)	Glucose ($g.g^{-1}$)	Yeast cells ($g.L^{-1}$)
1	0.001±0.004	0.001±0.002	0.997±0.010	10.481±0.216
2	0.002±0.007	0.000±0.004	0.997±0.020	10.919±0.501
4	0.007±0.015	0.002±0.002	0.983±0.032	10.043±1.225
8	0.023±0.016	0.006±0.004	0.942±0.039	11.049±2.073
12	0.035±0.038	0.009±0.005	0.914±0.082	12.541±2.142
24	0.062±0.088	0.014±0.007	0.852±0.177	13.206±2.654
48	0.099±0.009	0.022±0.006	0.764±0.013	13.304±1.865
72	0.132±0.022	0.026±0.017	0.691±0.010	13.904±1.697

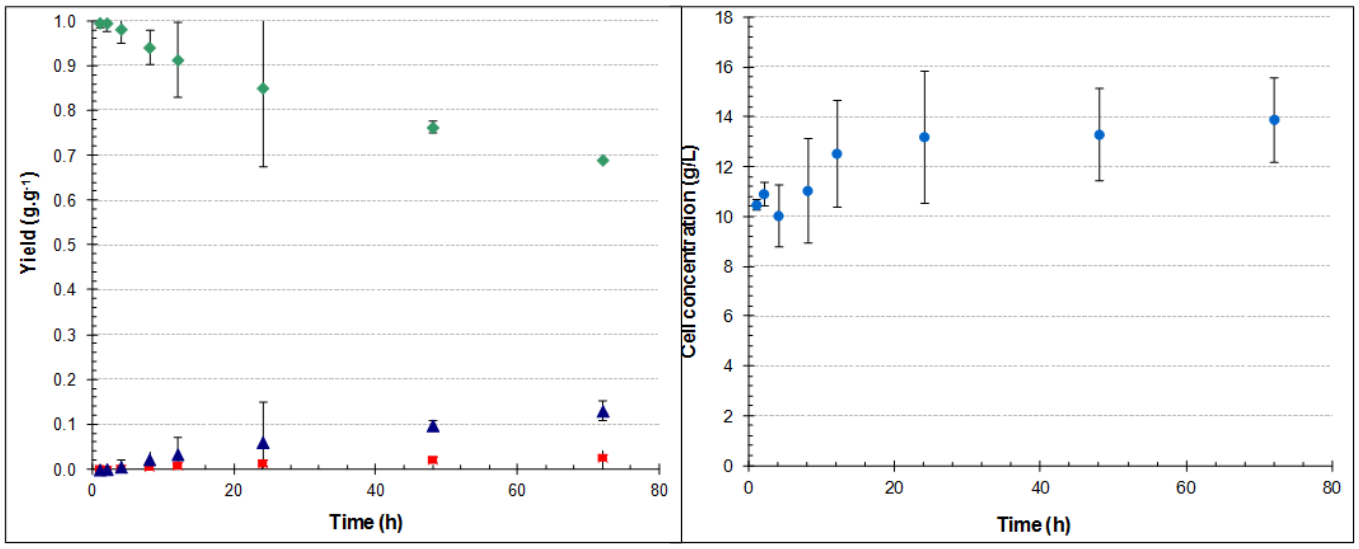

Figure C.7 Fermentation using 35wt% starting glucose
(♦Glucose yield, ▲Ethanol yield, ■Glycerol yield, ●yeast cell concentration)

C.3 EFFECT OF STARTING YEAST CONCENTRATION

Table C.8 Yields using a 1g.L^{-1} starting yeast concentration

Time (h)	Ethanol (g.g^{-1})	Glycerol (g.g^{-1})	Glucose (g.g^{-1})	Yeast cells (g.L^{-1})
1	0.001±0.002	0.000±0.001	0.998±0.003	0.751±0.278
2	0.001±0.001	0.000±0.000	0.998±0.003	1.265±0.085
4	0.002±0.002	0.001±0.001	0.995±0.006	1.379±0.349
8	0.002±0.006	0.001±0.002	0.994±0.016	1.785±0.416
12	0.003±0.009	0.001±0.005	0.990±0.022	1.590±0.516
24	0.010±0.007	0.003±0.003	0.975±0.014	1.752±0.427
48	0.026±0.009	0.007±0.008	0.935±0.033	1.979±0.429
72	0.041±0.002	0.009±0.005	0.903±0.011	2.109±0.287

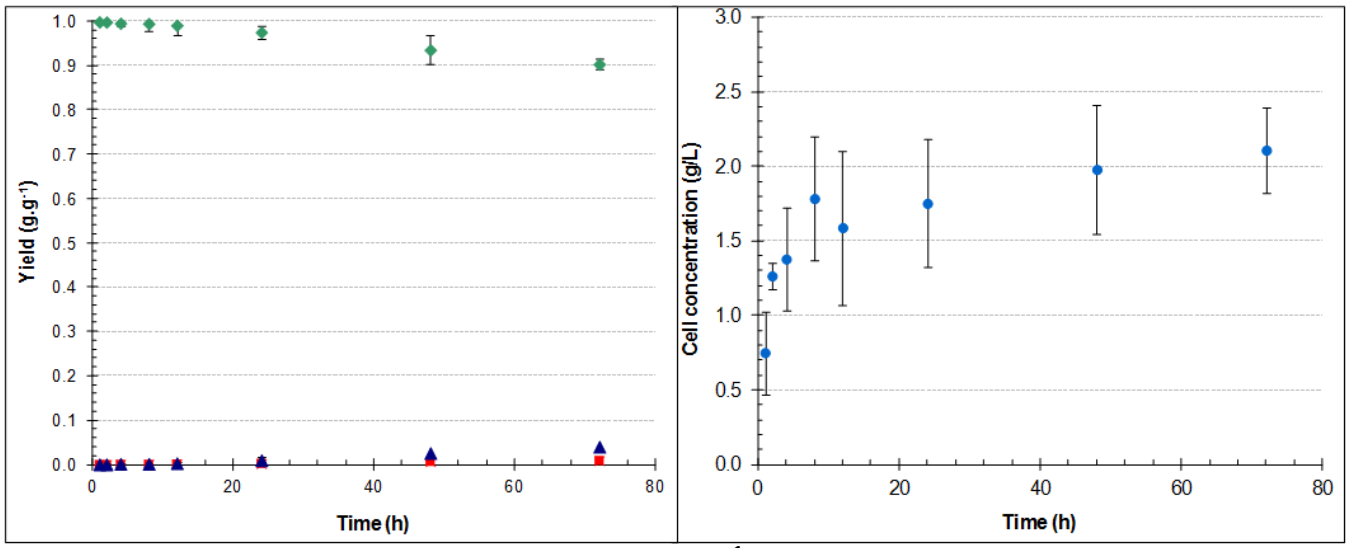

Figure C.8 Fermentation using a 1 g.L^{-1} starting yeast concentration
(♦Glucose yield, ▲Ethanol yield, ■Glycerol yield, ●yeast cell concentration)

Table C.9 Yields using a 3 g.L^{-1} starting yeast concentration

Time (h)	Ethanol (g.g^{-1})	Glycerol (g.g^{-1})	Glucose (g.g^{-1})	Yeast cells (g.L^{-1})
1	0.001±0.002	0.000±0.001	0.997±0.003	3.335±0.278
2	0.002±0.001	0.001±0.000	0.994±0.003	3.602±0.085
4	0.004±0.002	0.002±0.001	0.990±0.006	4.153±0.349
8	0.009±0.006	0.002±0.002	0.977±0.016	4.802±0.416
12	0.015±0.009	0.004±0.005	0.963±0.022	5.111±0.516
24	0.043±0.007	0.009±0.003	0.897±0.014	5.922±0.427
48	0.095±0.009	0.018±0.008	0.778±0.033	6.490±0.429
72	0.167±0.002	0.031±0.005	0.612±0.011	6.928±0.287

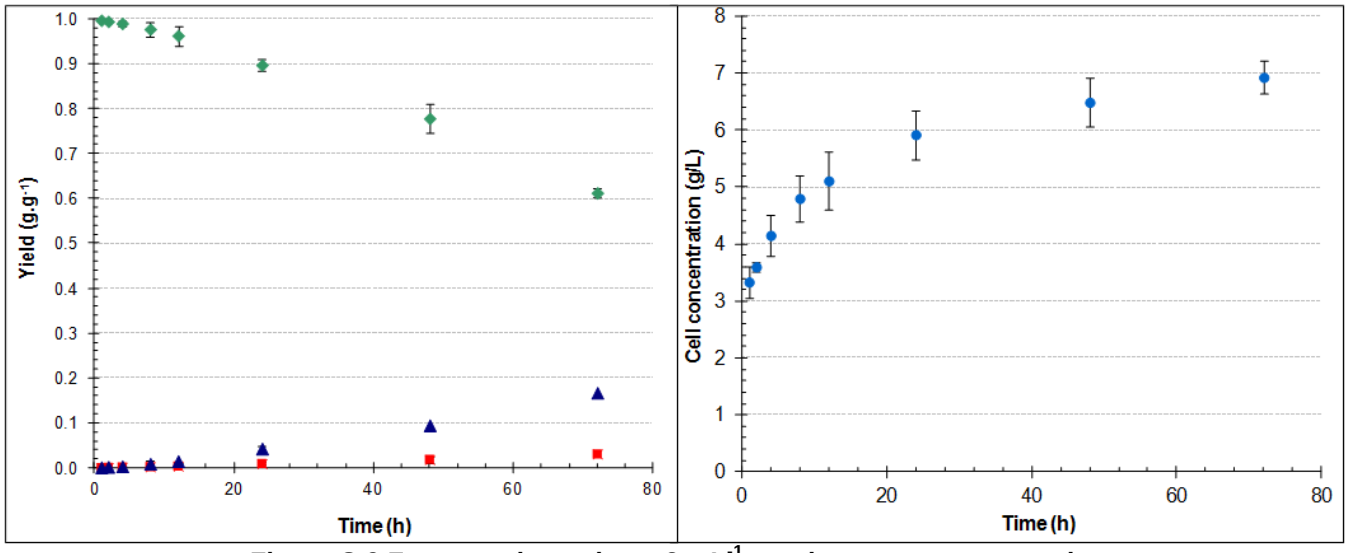

Figure C.9 Fermentation using a 3 g.L^{-1} starting yeast concentration
(♦Glucose yield, ▲Ethanol yield, ■Glycerol yield, ●yeast cell concentration)

Table C.10 Yields using a 5 g.L^{-1} starting yeast concentration

Time (h)	Ethanol (g.g^{-1})	Glycerol (g.g^{-1})	Glucose (g.g^{-1})	Yeast cells (g.L^{-1})
1	0.002±0.002	0.000±0.001	0.995±0.003	5.309±0.278
2	0.004±0.001	0.001±0.000	0.990±0.003	5.792±0.085
4	0.010±0.002	0.003±0.001	0.975±0.006	6.506±0.349
8	0.019±0.006	0.005±0.002	0.952±0.016	7.804±0.416
12	0.038±0.009	0.011±0.005	0.905±0.022	8.501±0.516
24	0.086±0.007	0.018±0.003	0.798±0.014	10.318±0.427
48	0.208±0.009	0.036±0.008	0.522±0.033	9.913±0.429
72	0.343±0.002	0.059±0.005	0.215±0.011	8.907±0.287

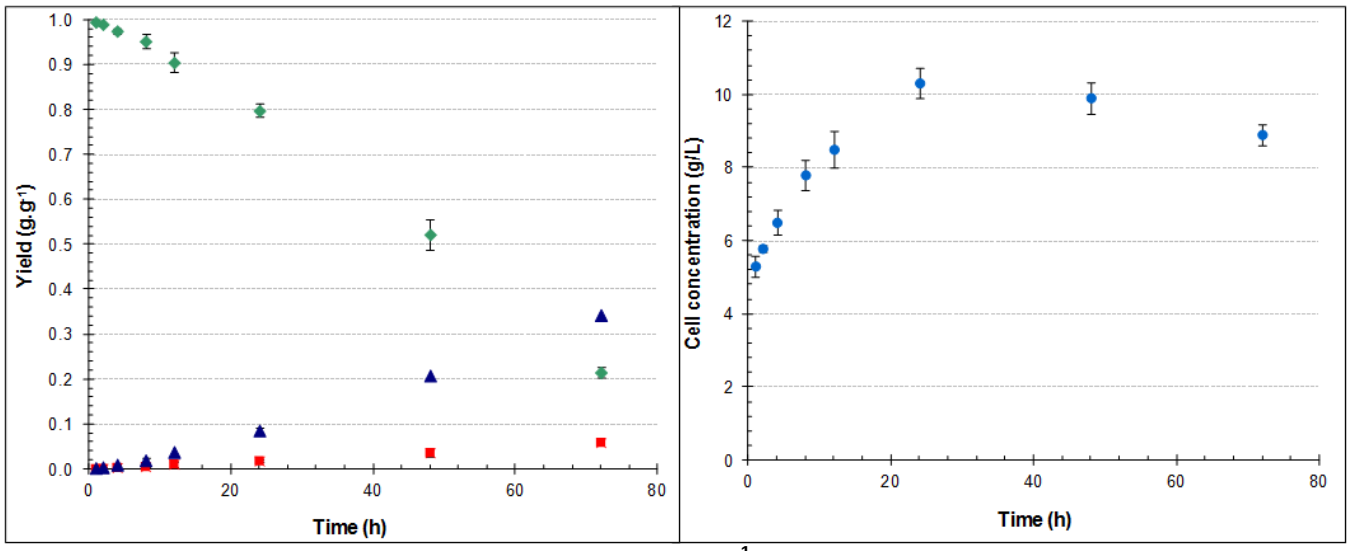

Figure C.10 Fermentation using a 5 g.L^{-1} starting yeast concentration
(♦Glucose yield, ▲Ethanol yield, ■Glycerol yield, ●yeast cell concentration)

Table C.11 Yields using a 7 g.L^{-1} starting yeast concentration

Time (h)	Ethanol (g.g^{-1})	Glycerol (g.g^{-1})	Glucose (g.g^{-1})	Yeast cells (g.L^{-1})
1	0.002±0.002	0.001±0.001	0.994±0.003	6.915±0.278
2	0.007±0.001	0.002±0.000	0.983±0.003	7.982±0.085
4	0.019±0.002	0.006±0.001	0.952±0.006	9.037±0.349
8	0.039±0.006	0.010±0.002	0.905±0.016	11.032±0.416
12	0.067±0.009	0.017±0.005	0.836±0.022	11.876±0.516
24	0.160±0.007	0.035±0.003	0.618±0.014	13.369±0.427
48	0.368±0.009	0.066±0.008	0.151±0.033	11.925±0.429
72	0.423±0.002	0.068±0.005	0.038±0.011	10.708±0.287

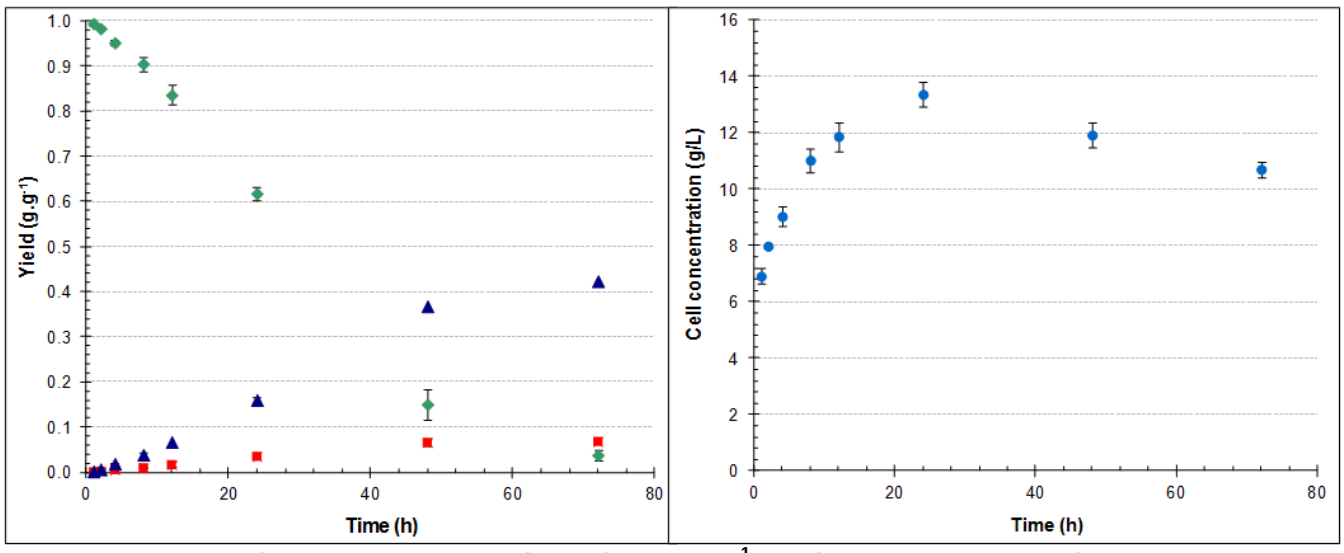

Figure C.11 Fermentation using a 7 g.L^{-1} starting yeast concentration
(♦Glucose yield, ▲Ethanol yield, ■Glycerol yield, ●yeast cell concentration)

Table C.12 Yields using a 10 g.L^{-1} starting yeast concentration

Time (h)	Ethanol (g.g^{-1})	Glycerol (g.g^{-1})	Glucose (g.g^{-1})	Yeast cells (g.L^{-1})
1	0.005±0.002	0.001±0.001	0.988±0.003	9.659±0.278
2	0.009±0.001	0.003±0.000	0.978±0.003	10.984±0.085
4	0.024±0.002	0.007±0.001	0.940±0.006	11.762±0.349
8	0.064±0.006	0.017±0.002	0.841±0.016	13.547±0.416
12	0.116±0.009	0.027±0.005	0.721±0.022	14.959±0.516
24	0.287±0.007	0.056±0.003	0.327±0.014	17.540±0.427
48	0.427±0.009	0.076±0.008	0.015±0.033	15.025±0.429
72	0.432±0.002	0.071±0.005	0.015±0.011	14.302±0.287

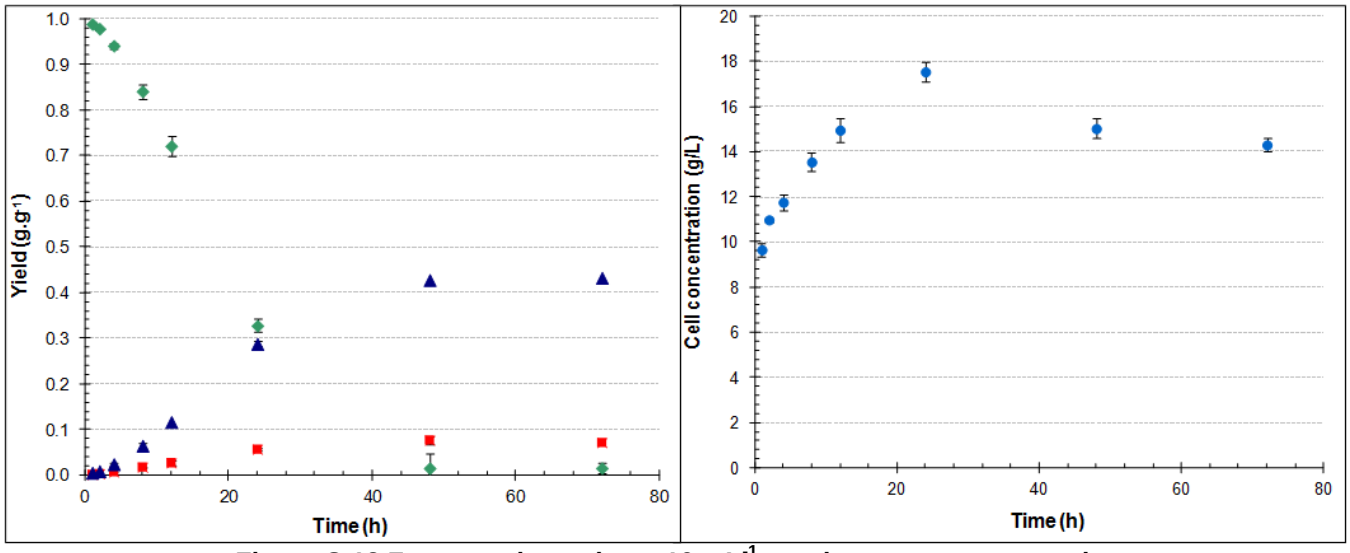

Figure C.12 Fermentation using a 10 g.L^{-1} starting yeast concentration
(♦Glucose yield, ▲Ethanol yield, ■Glycerol yield, ●yeast cell concentration)

C.4 EFFECT OF PH

Table C.13 Yields and cell concentration at a pH of 2.5

Time (h)	Ethanol (g.g^{-1})	Glycerol (g.g^{-1})	Glucose (g.g^{-1})	Yeast cells (g.L^{-1})
1	0.007±0.004	0.004±0.004	0.979±0.011	9.523±0.088
2	0.015±0.002	0.005±0.003	0.961±0.006	10.821±0.484
4	0.020±0.004	0.011±0.003	0.938±0.014	10.675±0.889
8	0.032±0.012	0.015±0.006	0.910±0.018	10.610±1.073
12	0.040±0.023	0.017±0.004	0.889±0.048	10.140±0.240
24	0.087±0.030	0.024±0.004	0.782±0.068	10.075±0.296
48	0.176±0.005	0.039±0.005	0.580±0.008	9.491±0.504
72	0.258±0.017	0.049±0.004	0.399±0.029	9.880±0.291

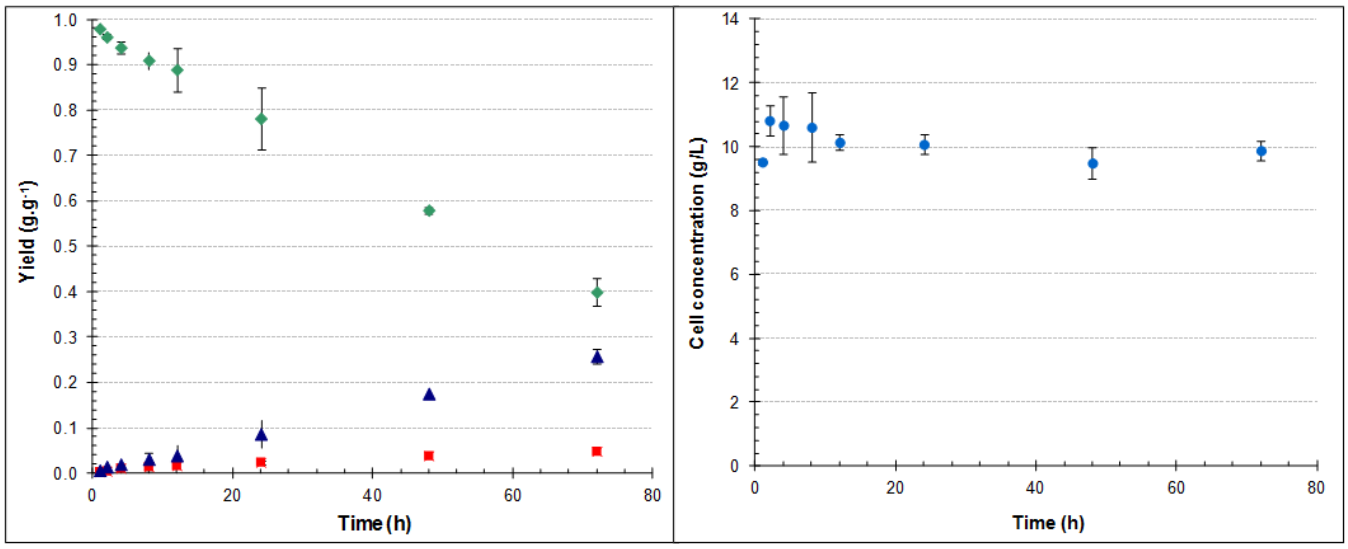

Figure C.13 Fermentation at a pH of 2.5

(♦Glucose yield, ▲Ethanol yield, ■Glycerol yield, ●yeast cell concentration)

Table C.14 Yields and cell concentration at a pH of 3

Time (h)	Ethanol ($g.g^{-1}$)	Glycerol ($g.g^{-1}$)	Glucose ($g.g^{-1}$)	Yeast cells ($g.L^{-1}$)
1	0.009±0.004	0.005±0.004	0.974±0.011	8.988±0.088
2	0.019±0.002	0.004±0.003	0.956±0.006	9.945±0.484
4	0.033±0.004	0.009±0.003	0.919±0.014	10.821±0.889
8	0.063±0.012	0.014±0.006	0.850±0.018	11.178±1.073
12	0.084±0.023	0.020±0.004	0.797±0.048	11.730±0.240
24	0.155±0.030	0.031±0.004	0.638±0.068	12.720±0.296
48	0.308±0.005	0.046±0.005	0.308±0.008	11.243±0.504
72	0.429±0.017	0.055±0.004	0.053±0.029	10.692±0.291

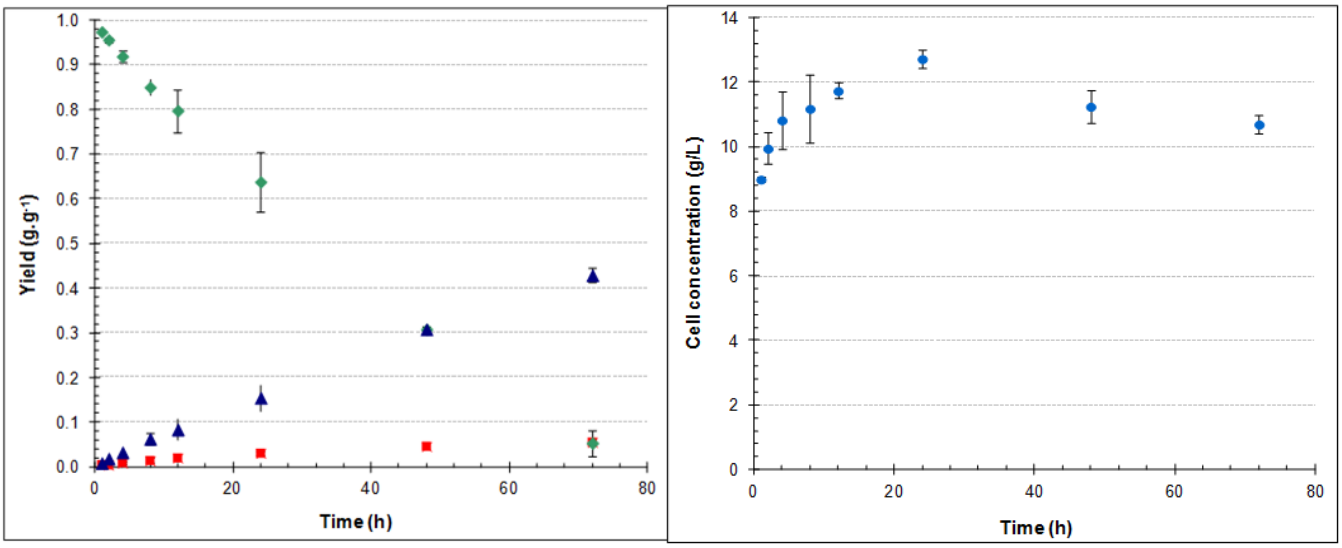

Figure C.14 Fermentation at a pH of 3

(♦Glucose yield, ▲Ethanol yield, ■Glycerol yield, ●yeast cell concentration)

Table C.15 Yields and cell concentration at a pH of 3.5

Time (h)	Ethanol ($g.g^{-1}$)	Glycerol ($g.g^{-1}$)	Glucose ($g.g^{-1}$)	Yeast cells ($g.L^{-1}$)
1	0.007±0.004	0.003±0.004	0.979±0.011	9.702±0.088
2	0.016±0.002	0.017±0.003	0.936±0.006	9.897±0.484
4	0.035±0.004	0.010±0.003	0.912±0.014	11.519±0.889
8	0.077±0.012	0.019±0.006	0.812±0.018	12.752±1.073
12	0.120±0.023	0.026±0.004	0.715±0.048	12.801±0.240
24	0.254±0.030	0.036±0.004	0.432±0.068	13.109±0.296
48	0.427±0.005	0.054±0.005	0.058±0.008	12.346±0.504
72	0.441±0.017	0.065±0.004	0.009±0.029	10.562±0.291

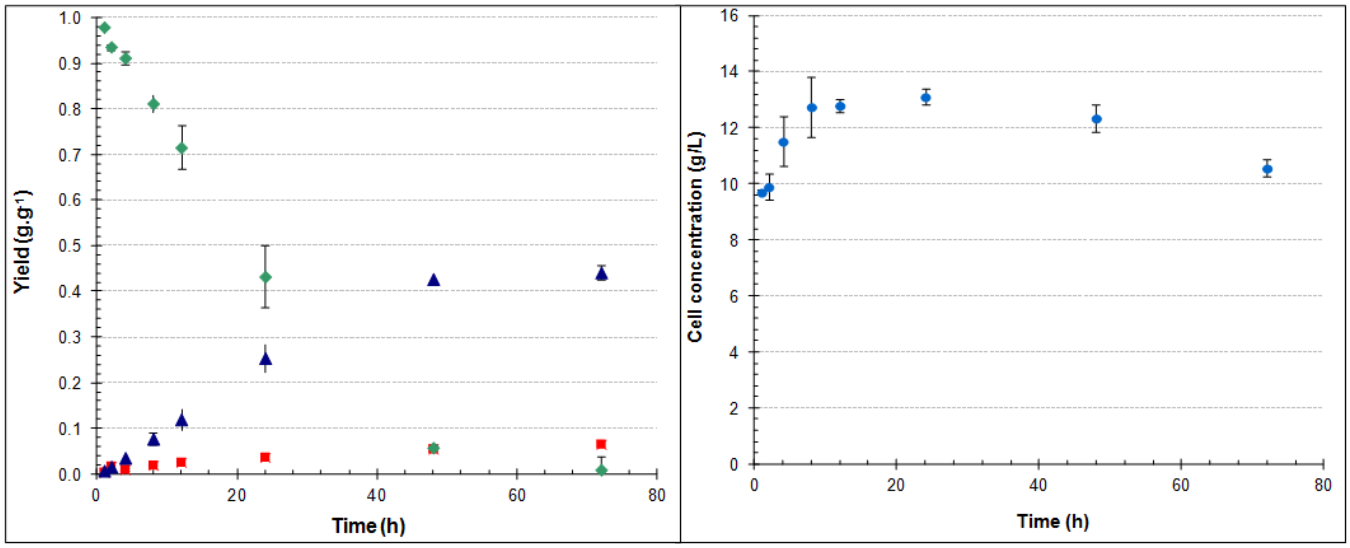

Figure C.15 Fermentation at a pH of 3.5

(♦Glucose yield, ▲Ethanol yield, ■Glycerol yield, ●yeast cell concentration)

Table C.16 Yields and cell concentration at a pH of 4.5

Time (h)	Ethanol ($g.g^{-1}$)	Glycerol ($g.g^{-1}$)	Glucose ($g.g^{-1}$)	Yeast cells ($g.L^{-1}$)
1	0.008±0.004	0.003±0.004	0.977±0.011	9.686±0.088
2	0.020±0.002	0.007±0.003	0.947±0.006	10.675±0.484
4	0.045±0.004	0.010±0.003	0.891±0.014	11.551±0.889
8	0.098±0.012	0.022±0.006	0.764±0.018	13.255±1.073
12	0.161±0.023	0.036±0.004	0.614±0.048	13.596±0.240
24	0.372±0.030	0.064±0.004	0.146±0.068	14.845±0.296
48	0.436±0.005	0.066±0.005	0.017±0.008	13.369±0.504
72	0.432±0.017	0.072±0.004	0.013±0.029	12.054±0.291

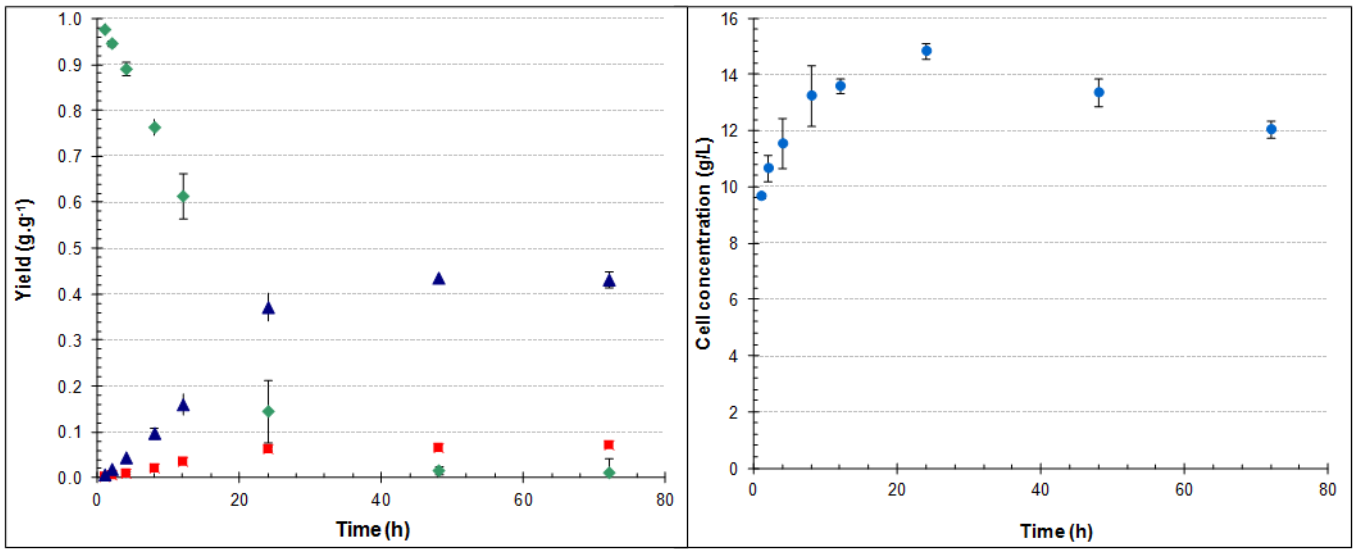

Figure C.16 Fermentation at a pH of 4.5

(♦Glucose yield, ▲Ethanol yield, ■Glycerol yield, ●yeast cell concentration)

Table C.17 Yields and cell concentration at a pH of 5

Time (h)	Ethanol ($g.g^{-1}$)	Glycerol ($g.g^{-1}$)	Glucose ($g.g^{-1}$)	Yeast cells ($g.L^{-1}$)
1	0.010±0.004	0.003±0.004	0.975±0.011	9.621±0.088
2	0.017±0.002	0.006±0.003	0.956±0.006	10.270±0.484
4	0.043±0.004	0.010±0.003	0.895±0.014	11.324±0.889
8	0.095±0.012	0.024±0.006	0.768±0.018	13.352±1.073
12	0.160±0.023	0.031±0.004	0.627±0.048	14.261±0.240
24	0.348±0.030	0.077±0.004	0.169±0.068	15.429±0.296
48	0.435±0.005	0.065±0.005	0.022±0.008	12.346±0.504
72	0.431±0.017	0.078±0.004	0.003±0.029	11.795±0.291

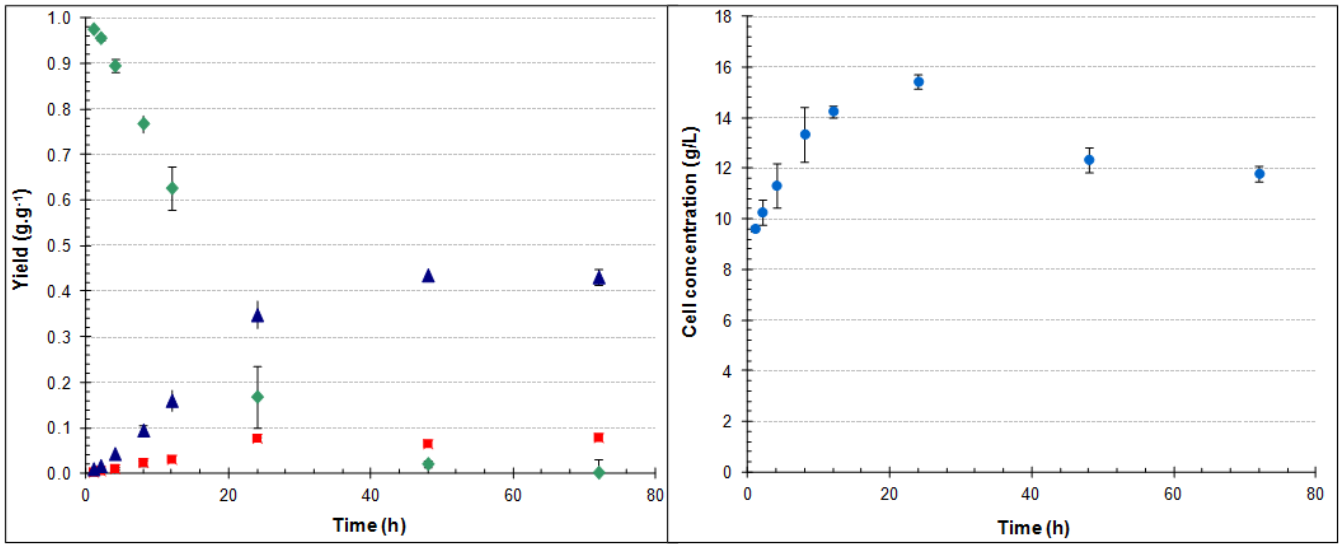

Figure C.17 Fermentation at a pH of 5

(♦Glucose yield, ▲Ethanol yield, ■Glycerol yield, ●yeast cell concentration)

Table C.18 Yields and cell concentration at a pH of 5.5

Time (h)	Ethanol ($g.g^{-1}$)	Glycerol ($g.g^{-1}$)	Glucose ($g.g^{-1}$)	Yeast cells ($g.L^{-1}$)
1	0.012±0.004	0.009±0.004	0.960±0.011	8.939±0.088
2	0.018±0.002	0.006±0.003	0.953±0.006	10.156±0.484
4	0.044±0.004	0.014±0.003	0.886±0.014	10.821±0.889
8	0.109±0.012	0.026±0.006	0.736±0.018	13.417±1.073
12	0.166±0.023	0.039±0.004	0.598±0.048	13.661±0.240
24	0.395±0.030	0.066±0.004	0.099±0.068	15.429±0.296
48	0.432±0.005	0.069±0.005	0.020±0.008	11.049±0.504
72	0.428±0.017	0.068±0.004	0.030±0.029	11.259±0.291

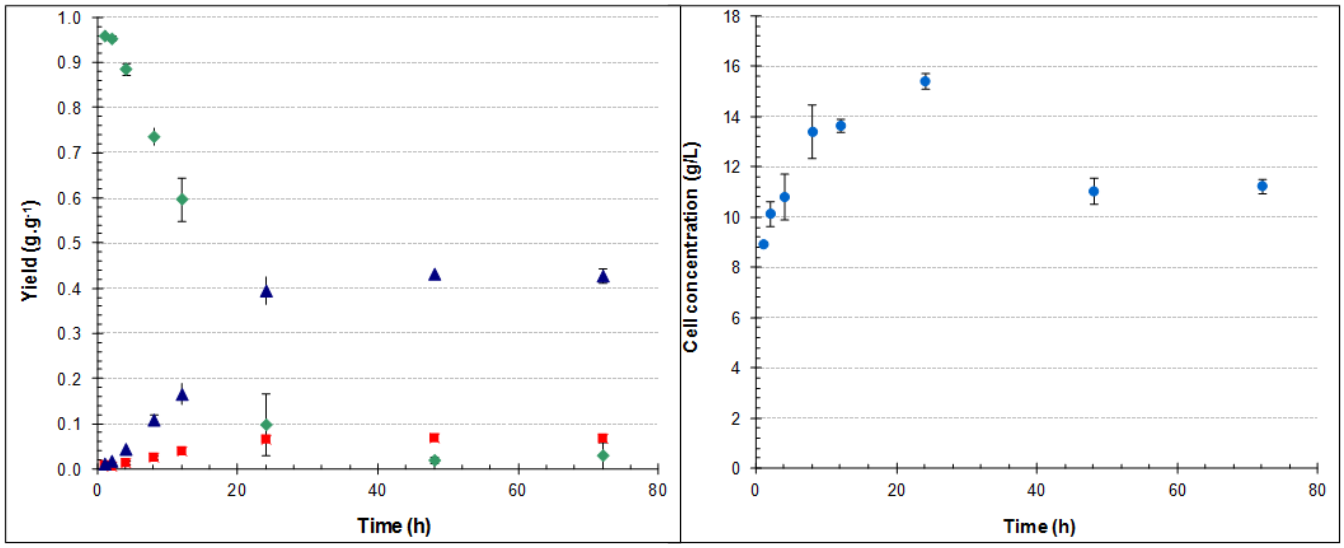

Figure C.18 Fermentation at a pH of 5.5

(♦Glucose yield, ▲Ethanol yield, ■Glycerol yield, ●yeast cell concentration)

Table C.19 Yields and cell concentration at a pH of 6

Time (h)	Ethanol ($g.g^{-1}$)	Glycerol ($g.g^{-1}$)	Glucose ($g.g^{-1}$)	Yeast cells ($g.L^{-1}$)
1	0.008±0.004	0.003±0.004	0.977±0.011	8.696±0.088
2	0.016±0.002	0.012±0.003	0.945±0.006	10.400±0.484
4	0.041±0.004	0.011±0.003	0.899±0.014	10.886±0.889
8	0.095±0.012	0.024±0.006	0.769±0.018	12.492±1.073
12	0.159±0.023	0.033±0.004	0.625±0.048	13.644±0.240
24	0.393±0.030	0.065±0.004	0.104±0.068	15.754±0.296
48	0.421±0.005	0.074±0.005	0.032±0.008	11.178±0.504
72	0.434±0.017	0.073±0.004	0.008±0.029	10.578±0.291

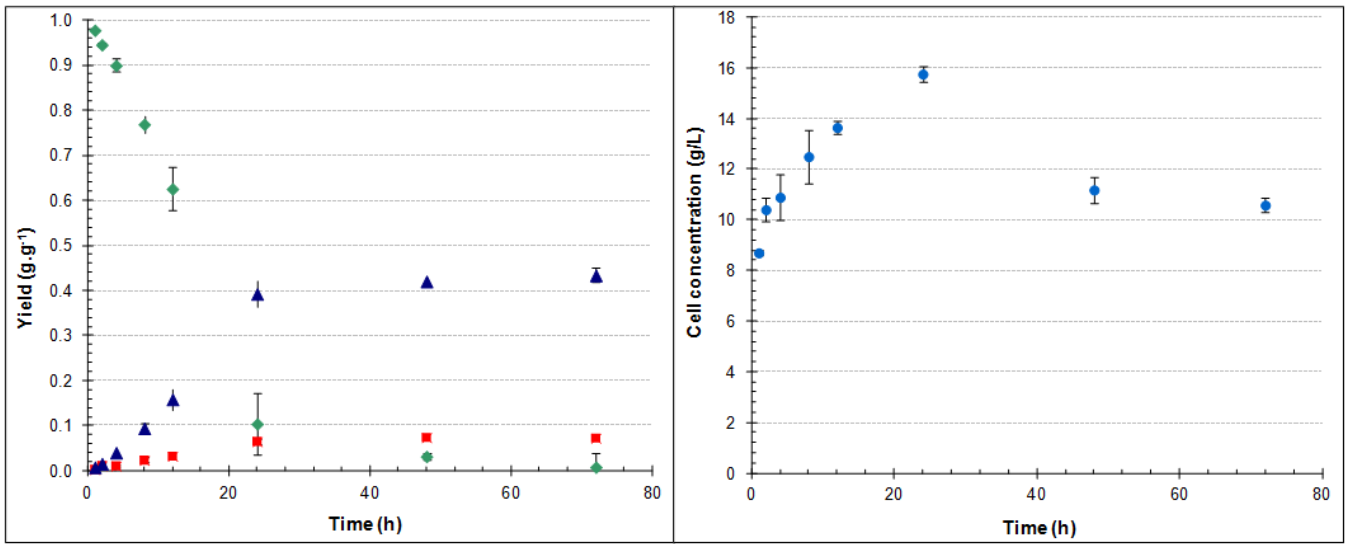

Figure C.19 Fermentation at a pH of 6

(♦Glucose yield, ▲Ethanol yield, ■Glycerol yield, ●yeast cell concentration)

APPENDIX D: PERVAPORATION EXPERIMENTS

OVERVIEW

The results obtained from the pervaporation experiments are presented in this appendix. Appendix D is subdivided into five subsections. The measured and calculated results of the sorption experiments are presented in Section D.1. This section also includes a graphical representation of the sorption results. The mass permeated through the membrane at each different feed composition as well as the composition of the permeate are shown in Section D.2. The calculations used to determine the membrane swelling, total flux, partial flux, selectivity and enrichment factor are discussed in Section D.3. In Section D.4, the calculated results of the pervaporation experiments are shown and finally in Section D.5 these results are graphically presented.

D.1 MEASURED AND CALCULATED RESULTS OF SORPTION EXPERIMENTS

The results for the sorption experiments are presented in Table D.1 and Figure D.1.

Table D.1 Results for the sorption experiments

Ethanol (wt%)	W_0 (g)	W_∞ (g)	M_∞ (-)
0	0.291	0.475	0.630±0.011
5	0.301	0.501	0.667±0.011
10	0.307	0.512	0.669±0.011
15	0.308	0.514	0.667±0.011
20	0.305	0.508	0.666±0.011
30	0.291	0.483	0.660±0.011
40	0.293	0.491	0.676±0.011
50	0.278	0.463	0.665±0.011
60	0.263	0.43	0.635±0.011
70	0.293	0.478	0.631±0.011
80	0.308	0.496	0.610±0.011
90	0.278	0.448	0.612±0.011
100	0.287	0.440	0.532±0.011

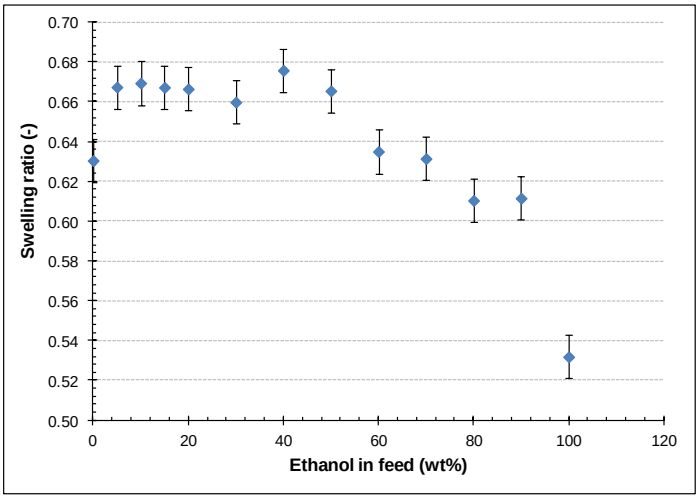

Figure D.1 Swelling ratio versus wt% ethanol of PERVAP®4060 membrane

Sample calculations for the sorption experiments are presented in Section D.3.1.

D.2 RAW DATA FROM PERVAPORATION EXPERIMENTS

D.2.1. Ethanol and water mixtures

Table D.2 Measured data for pervaporation - 20wt% ethanol and 0wt% glucose

Cumulative time (min)	Time (min)	Mass permeate (g)	Fraction ethanol permeate
30	30	15.573	0.483
90	60	21.023	0.684
120	30	11.740	0.689
150	30	10.893	0.605
180	30	10.954	0.674
210	30	10.856	0.675
240	30	10.855	0.680

Table D.3 Measured data for pervaporation - 15wt% ethanol and 0wt% glucose

Cumulative time (min)	Time (min)	Mass permeate (g)	Fraction ethanol permeate
45	45	18.716	0.612
75	30	10.528	0.628
135	60	21.396	0.661
165	30	10.029	0.633
195	30	9.229	0.624
225	30	9.848	0.617
255	30	9.812	0.616
285	30	9.764	0.608

Table D.4 Measured data for pervaporation - 10wt% ethanol and 0wt% glucose

Cumulative time (min)	Time (min)	Mass permeate (g)	Fraction ethanol permeate
75	75	15.992	0.391
120	45	13.306	0.461
180	60	13.842	0.492
240	60	13.932	0.481
300	60	13.861	0.474
360	60	13.733	0.480

Table D.5 Measured data for pervaporation - 5wt% ethanol and 0wt% glucose

Cumulative time (min)	Time (min)	Mass permeate (g)	Fraction ethanol permeate
60	60	12.345	0.331
120	60	12.385	0.334
180	60	13.142	0.331
240	60	11.157	0.339
300	60	12.095	0.329
360	60	11.171	0.335

Table D.6 Measured data for pervaporation - pure water

Cumulative time (min)	Time (min)	Mass permeate (g)
50	50	8.069
110	60	6.781
170	60	6.040
230	60	8.154
290	60	8.117

D.2.2. Ethanol, glucose and water mixtures

Table D.7 Measured data for pervaporation - 20wt% ethanol and 5wt% glucose

Cumulative time (min)	Time (min)	Mass permeate (g)	Fraction ethanol permeate
20	20	12.230	0.643
50	30	10.862	0.734
80	30	11.070	0.728
110	30	10.371	0.724
140	30	11.007	0.718
170	30	11.222	0.706
200	30	10.170	0.710
230	30	10.641	0.690
260	30	10.373	0.690

Table D.8 Measured data for pervaporation - 15wt% ethanol and 5wt% glucose

Cumulative time (min)	Time (min)	Mass permeate (g)	Fraction ethanol permeate
30	30	8.972	0.569
60	30	6.107	0.696
90	30	6.291	0.711
120	30	6.204	0.676
150	30	6.254	0.663
180	30	6.158	0.664
210	30	6.041	0.652
240	30	6.155	0.640
270	30	6.048	0.647
300	30	6.159	0.633
330	30	6.085	0.644

Table D.9 Measured data for pervaporation - 10wt% ethanol and 5wt% glucose

Cumulative time (min)	Time (min)	Mass permeate (g)	Fraction ethanol permeate
30	30	5.094	0.511
60	30	5.509	0.543
90	30	4.980	0.547
120	30	5.037	0.542
150	30	7.608	0.542
180	30	5.403	0.533
210	30	5.004	0.552
240	30	5.263	0.541
270	30	5.130	0.543
300	30	4.985	0.542
330	30	5.070	0.545

Table D.10 Measured data for pervaporation - 5wt% ethanol and 5wt% glucose

Cumulative time (min)	Time (min)	Mass permeate (g)	Fraction ethanol permeate
60	60	5.944	0.330
120	60	6.991	0.353
180	60	7.160	0.355
240	60	7.668	0.354
300	60	7.123	0.360
360	60	7.152	0.351

Table D.11 Measured data for pervaporation - 0wt% ethanol and 5wt% glucose

Cumulative time (min)	Time (min)	Mass permeate (g)
30	30	2.689
60	30	2.198
90	30	2.114
120	30	2.041
150	30	1.902
180	30	2.035
210	30	2.303
240	30	1.854
270	30	2.246
300	30	2.309
330	30	2.384

Table D.12 Measured data for pervaporation - 20wt% ethanol and 10wt% glucose

Cumulative time (min)	Time (min)	Mass permeate (g)	Fraction ethanol permeate
30	30	18.232	0.578
60	30	11.156	0.722
90	30	11.982	0.723
120	30	11.081	0.698
150	30	11.533	0.718
180	30	11.019	0.717
210	30	10.966	0.718
240	30	10.782	0.728
270	30	11.026	0.717
300	30	10.804	0.721

Table D.13 Measured data for pervaporation - 15wt% ethanol and 10wt% glucose

Cumulative time (min)	Time (min)	Mass permeate (g)	Fraction ethanol permeate
30	30	7.481	0.599
60	30	5.790	0.695
90	30	5.813	0.701
120	30	5.571	0.696
150	30	5.685	0.685
180	30	5.804	0.680
210	30	5.691	0.683
240	30	5.364	0.670
270	30	5.439	0.675
300	30	5.479	0.658
330	30	5.374	0.664

Table D.14 Measured data for pervaporation - 10wt% ethanol and 10wt% glucose

Cumulative time (min)	Time (min)	Mass permeate (g)	Fraction ethanol permeate
30	30	6.670	0.549
60	30	5.667	0.596
90	30	5.028	0.591
120	30	5.183	0.590
150	30	5.155	0.577
180	30	5.574	0.567
210	30	5.475	0.573
240	30	4.989	0.574
270	30	5.192	0.561
300	30	5.001	0.549
330	30	4.922	0.571

Table D.15 Measured data for pervaporation - 5wt% ethanol and 10wt% glucose

Cumulative time (min)	Time (min)	Mass permeate (g)	Fraction ethanol permeate
60	60	7.339	0.344
120	60	8.344	0.373
180	60	7.164	0.379
240	60	6.942	0.368
300	60	7.061	0.383
360	60	6.877	0.369

Table D.16 Measured data for pervaporation - 0wt% ethanol and 10wt% glucose

Cumulative time (min)	Time (min)	Mass permeate (g)
60	60	3.952
120	60	4.636
180	60	4.599
240	60	4.076
300	60	4.676
360	60	4.657

Table D.17 Measured data for pervaporation - 20wt% ethanol and 15wt% glucose

Cumulative time (min)	Time (min)	Mass permeate (g)	Fraction ethanol permeate
30	30	16.750	0.697
60	30	12.006	0.738
90	30	11.713	0.750
120	30	13.142	0.739
150	30	11.783	0.721
180	30	12.140	0.716
210	30	11.533	0.732
240	30	10.021	0.730
270	30	11.460	0.718
300	30	11.366	0.730
330	30	11.371	0.726

Table D.18 Measured data for pervaporation - 15wt% ethanol and 15wt% glucose

Cumulative time (min)	Time (min)	Mass permeate (g)	Fraction ethanol permeate
30	30	6.811	0.610
60	30	5.247	0.682
90	30	5.254	0.638
120	30	5.138	0.664
150	30	5.744	0.672
180	30	5.210	0.773
205	25	3.563	0.698
240	35	5.023	0.677
270	30	5.000	0.680
300	30	5.285	0.675
330	30	5.182	0.680

Table D.19 Measured data for pervaporation - 10wt% ethanol and 15wt% glucose

Cumulative time (min)	Time (min)	Mass permeate (g)	Fraction ethanol permeate
30	30	6.087	0.564
60	30	5.417	0.637
90	30	5.719	0.621
150	60	10.461	0.609
180	30	5.878	0.602
210	30	5.576	0.617
240	30	5.788	0.607
270	30	5.415	0.591
300	30	5.678	0.594
330	30	5.335	0.586

Table D.20 Measured data for pervaporation - 5wt% ethanol and 15wt% glucose

Cumulative time (min)	Time (min)	Mass permeate (g)	Fraction ethanol permeate
60	60	7.288	0.322
120	60	6.444	0.360
180	60	6.544	0.428
240	60	5.934	0.370
300	60	6.927	0.403
360	60	6.485	0.420

Table D.21 Measured data for pervaporation - 0wt% ethanol and 15wt% glucose

Cumulative time (min)	Time (min)	Mass permeate (g)
60	60	5.719
120	60	4.046
180	60	4.712
240	60	4.216
300	60	4.569
360	60	4.513

D.3 SAMPLE CALCULATIONS

D.3.1. Sorption experiments

The swelling ratio (uptake of solution by membrane) can be calculated using Equation D.1.

$$\text{Swelling ratio } (M_t) = \frac{W_t - W_0}{W_0} \qquad \text{Equation D.1}$$

In Equation D.1 W_0 is the dry mass of the membrane and W_t is the membrane mass after being soaked in a solution for a certain amount of time.

A sample calculation of the swelling ratio at equilibrium (M_∞) is:

$$M_\infty = \frac{W_\infty - W_0}{W_0} = \frac{0.475 - 0.291}{0.291} = 0.630$$

D.3.2. Pervaporation experiments

The flux and selectivity of each experiment was calculated from the raw data presented in Section D.2. The data used in the sample calculation is taken from an experiment with a feed composition of 15wt% ethanol and 0wt% glucose as shown in Table D.22. The calculated values obtained for the other data sets are presented in Section D.4.

Table D.22 Pervaporation data used for sample calculations (15wt% ethanol, 0wt% glucose)

Cumulative time (min)	Time (min)	Mass permeate (g)	Fraction ethanol permeate
45	45	18.716	0.612
75	30	10.528	0.628
135	60	21.396	0.661
165	30	10.029	0.633
195	30	9.229	0.624
225	30	9.848	0.617
255	30	9.812	0.616
285	30	9.764	0.608

The total flux (*J*) is expressed as the total amount (mass) of permeate (m) collected through a certain area (A) during a certain time unit (t), as shown in Equation 4.1.

$$J = \frac{m}{At} \quad (\text{kg/m}^2\text{h}) \qquad \text{Equation 4.1}$$

with $A = \pi \times r^2$

A sample calculation of the total flux is as follows:

$$J_{total} = \frac{18.716\text{g} \times \frac{1\text{kg}}{1000\text{g}}}{2.544 \times 10^{-2}\text{m}^2 \times 45\,\text{min} \times \frac{1\text{h}}{60\,\text{min}}} = 0.981 \frac{\text{kg}}{\text{m}^2\text{h}}$$

The partial fluxes are calculated by multiplying the total flux with the mass fractions of the component in the permeate ($J_{ethanol} = J_{total} \times y_i$ with y_i the fraction ethanol in the permeate). A sample calculation of the ethanol flux:

$$J_{ethanol} = 0.981 \frac{\text{kg}}{\text{m}^2\text{h}} \times 0.612 = 0.600 \frac{\text{kg}}{\text{m}^2\text{h}}$$

The pervaporation selectivity is defined as:

$$\alpha = \frac{y_{EtOH} / \left(y_{H_2O}\right)}{x_{EtOH} / \left(x_{H_2O}\right)} \qquad \text{Equation 4.3}$$

A sample calculation of the selectivity:

$$\alpha = \frac{0.612 / (1 - 0.612)}{0.155 / (1 - 0.155)} = \frac{0.612 / (0.388)}{0.155 / (0.845)} = 8.594$$

The enrichment factor was calculated by dividing the mass fraction ethanol in the permeate by the mass fraction ethanol in the feed, as shown in Equation 4.2.

$$\beta_{EtOH} = \frac{y_{EtOH}}{x_{EtOH}}$$ Equation 4.2

A sample calculation of the enrichment factor:

$$\beta_{EtOH} = \frac{0.612}{0.155} = 3.944$$

The total flux, partial flux, selectivity, and enrichment factor of each experiment is calculated at steady state by averaging the values obtained after steady state has been reached. As an example, after four hours steady state has been reached for the data shown in Table D.22, the values are 0.774, 0.771, and 0.767, giving a steady state flux of 0.771.

$$\text{Steady state total flux} = \frac{0.774 + 0.771 + 0.767}{3} = 0.771 \frac{\text{kg}}{\text{m}^2\text{h}}$$

D.4 CALCULATED RESULTS OF PERVAPORATION EXPERIMENTS

The results for the pervaporation experiments, calculated as shown in Section D.3 are presented in this section.

Table D.23 Calculated results for pervaporation - 20wt% ethanol and 0wt% glucose

Cumulative time (min)	Total flux (kg/m^{2}h)	Selectivity (-)	Enrichment factor (-)	Ethanol flux (kg/m^{2}h)	Water flux (kg/m^{2}h)
30	1.224	3.762	2.429	0.591	0.633
90	0.826	8.745	3.445	0.565	0.261
120	0.923	8.949	3.470	0.636	0.287
150	0.856	6.185	3.047	0.518	0.338
180	0.861	8.328	3.391	0.580	0.281
210	0.853	8.364	3.396	0.576	0.278
240	0.853	8.585	3.425	0.580	0.273
Steady state	0.853	8.475	3.410	0.578	0.275

Table D.24 Calculated results for pervaporation - 15wt% ethanol and 0wt% glucose

Cumulative time (min)	Total flux (kg/m^{2}h)	Selectivity (-)	Enrichment factor (-)	Ethanol flux (kg/m^{2}h)	Water flux (kg/m^{2}h)
45	0.981	8.594	3.944	0.601	0.380
75	0.827	9.200	4.047	0.520	0.307
135	0.841	10.621	4.259	0.556	0.285
165	0.788	9.391	4.078	0.499	0.289
195	0.725	9.037	4.020	0.453	0.273
225	0.774	8.770	3.975	0.478	0.296
255	0.771	8.710	3.964	0.475	0.296
285	0.767	8.450	3.918	0.467	0.301
Steady state	0.771	8.643	3.952	0.473	0.298

Table D.25 Calculated results for pervaporation - 10wt% ethanol and 0wt% glucose

Cumulative time (min)	Total flux (kg/m^2h)	Selectivity (-)	Enrichment factor (-)	Ethanol flux (kg/m^2h)	Water flux (kg/m^2h)
75	0.503	5.404	3.681	0.197	0.306
120	0.697	7.193	4.337	0.321	0.376
180	0.544	8.144	4.629	0.268	0.276
240	0.547	7.776	4.520	0.263	0.284
300	0.545	7.581	4.461	0.258	0.286
360	0.540	7.746	4.511	0.259	0.281
Steady state	0.542	7.664	4.486	0.259	0.284

Table D.26 Calculated results for pervaporation - 5wt% ethanol and 0wt% glucose

Cumulative time (min)	Total flux (kg/m^2h)	Selectivity (-)	Enrichment factor (-)	Ethanol flux (kg/m^2h)	Water flux (kg/m^2h)
60	0.485	8.713	6.158	0.161	0.324
120	0.487	8.814	6.205	0.162	0.324
180	0.516	8.711	6.157	0.171	0.345
240	0.438	9.030	6.305	0.149	0.290
300	0.475	8.609	6.108	0.156	0.319
360	0.439	8.867	6.230	0.147	0.292
Steady state	0.451	8.835	6.214	0.151	0.300

Table D.27 Calculated results for pervaporation - pure water

Cumulative time (min)	Total flux (kg/m^2h)
50	0.381
110	0.266
170	0.237
230	0.320
290	0.319
Steady state	0.320

Table D.28 Calculated results for pervaporation - 20wt% ethanol and 5wt% glucose

Cumulative time (min)	Total flux (kg/m^2h)	Selectivity (-)	Enrichment factor (-)	Ethanol flux (kg/m^2h)	Water flux (kg/m^2h)
20	1.442	7.990	3.661	0.927	0.515
50	0.854	12.254	4.181	0.627	0.227
80	0.870	11.859	4.14	0.633	0.237
110	0.815	11.633	4.122	0.590	0.225
140	0.865	11.281	4.087	0.621	0.244
170	0.882	10.665	4.022	0.623	0.259
200	0.799	10.856	4.042	0.567	0.232
230	0.836	9.889	3.931	0.577	0.259
260	0.815	9.855	3.927	0.562	0.253
Steady state	0.826	9.872	3.929	0.570	0.256

Table D.29 Calculated results for pervaporation - 15wt% ethanol and 5wt% glucose

Cumulative time (min)	Total flux (kg/m^2h)	Selectivity (-)	Enrichment factor (-)	Ethanol flux (kg/m^2h)	Water flux (kg/m^2h)
30	0.705	7.874	4.146	0.401	0.304
60	0.480	13.660	5.072	0.334	0.146
90	0.494	14.699	5.184	0.352	0.143
120	0.488	12.474	4.930	0.330	0.158
150	0.492	11.753	4.834	0.326	0.166
180	0.484	11.774	4.837	0.321	0.163
210	0.475	11.205	4.755	0.310	0.165
240	0.484	10.613	4.665	0.310	0.174
270	0.475	10.927	4.714	0.307	0.168
300	0.484	10.292	4.613	0.306	0.178
330	0.478	10.787	4.692	0.308	0.170
Steady state	0.480	10.655	4.671	0.308	0.173

Table D.30 Calculated results for pervaporation - 10wt% ethanol and 5wt% glucose

Cumulative time (min)	Total flux (kg/m^2h)	Selectivity (-)	Enrichment factor (-)	Ethanol flux (kg/m^2h)	Water flux (kg/m^2h)
30	0.400	10.079	5.732	0.205	0.196
60	0.433	11.423	6.082	0.235	0.198
90	0.391	11.638	6.134	0.214	0.177
120	0.396	11.399	6.076	0.215	0.181
150	0.598	11.420	6.081	0.324	0.274
180	0.425	10.980	5.972	0.226	0.198
210	0.393	11.875	6.190	0.217	0.176
240	0.414	11.348	6.064	0.224	0.190
270	0.403	11.427	6.083	0.219	0.184
300	0.392	11.412	6.079	0.212	0.179
330	0.398	11.518	6.105	0.217	0.181
Steady state	0.398	11.452	6.089	0.216	0.182

Table D.31 Calculated results for pervaporation - 5wt% ethanol and 5wt% glucose

Cumulative time (min)	Total flux (kg/m^2h)	Selectivity (-)	Enrichment factor (-)	Ethanol flux (kg/m^2h)	Water flux (kg/m^2h)
60	0.234	9.001	6.686	0.077	0.156
120	0.275	9.968	7.151	0.097	0.178
180	0.281	10.063	7.194	0.100	0.181
240	0.301	9.984	7.158	0.107	0.195
300	0.280	10.278	7.293	0.101	0.179
360	0.281	9.868	7.104	0.099	0.182
Steady state	0.280	10.073	7.198	0.100	0.181

Table D.32 Calculated results for pervaporation - 0wt% ethanol and 5wt% glucose

Cumulative time (min)	Total flux (kg/m^2h)
30	0.211
60	0.173
90	0.166
120	0.160
150	0.149
180	0.160
210	0.181
240	0.146
270	0.177
300	0.181
330	0.187
Steady state	0.182

Table D.33 Calculated results for pervaporation - 20wt% ethanol and 10wt% glucose

Cumulative time (min)	Total flux (kg/m^{2}h)	Selectivity (-)	Enrichment factor (-)	Ethanol flux (kg/m^{2}h)	Water flux (kg/m^{2}h)
30	1.433	4.792	2.889	0.828	0.605
60	0.877	9.072	3.608	0.633	0.244
90	0.942	9.120	3.613	0.681	0.261
120	0.871	8.093	3.490	0.608	0.263
150	0.906	8.912	3.590	0.651	0.256
180	0.866	8.877	3.586	0.621	0.245
210	0.862	8.926	3.592	0.619	0.243
240	0.847	9.387	3.642	0.617	0.230
270	0.867	8.866	3.585	0.621	0.245
300	0.849	9.040	3.604	0.612	0.237
Steady state	0.856	9.055	3.606	0.617	0.239

Table D.34 Calculated results for pervaporation - 15wt% ethanol and 10wt% glucose

Cumulative time (min)	Total flux (kg/m^{2}h)	Selectivity (-)	Enrichment factor (-)	Ethanol flux (kg/m^{2}h)	Water flux (kg/m^{2}h)
30	0.588	8.452	4.354	0.352	0.236
60	0.455	12.867	5.048	0.316	0.139
90	0.457	13.257	5.094	0.320	0.137
120	0.438	12.972	5.061	0.305	0.133
150	0.447	12.311	4.980	0.306	0.141
180	0.456	12.034	4.944	0.310	0.146
210	0.447	12.184	4.963	0.305	0.142
240	0.422	11.463	4.867	0.282	0.139
270	0.427	11.749	4.906	0.289	0.139
300	0.431	10.867	4.780	0.283	0.147
330	0.422	11.180	4.826	0.280	0.142
Steady state	0.426	11.024	4.803	0.282	0.145

Table D.35 Calculated results for pervaporation - 10wt% ethanol and 10wt% glucose

Cumulative time (min)	Total flux (kg/m^{2}h)	Selectivity (-)	Enrichment factor (-)	Ethanol flux (kg/m^{2}h)	Water flux (kg/m^{2}h)
30	0.524	11.338	6.268	0.288	0.236
60	0.445	13.763	6.809	0.266	0.180
90	0.395	13.443	6.744	0.233	0.162
120	0.407	13.398	6.734	0.240	0.167
150	0.405	12.700	6.586	0.234	0.171
180	0.438	12.213	6.477	0.249	0.190
210	0.430	12.501	6.542	0.247	0.184
240	0.392	12.523	6.547	0.225	0.167
270	0.408	11.885	6.400	0.229	0.179
300	0.393	11.327	6.265	0.216	0.177
330	0.387	12.416	6.523	0.221	0.166
Steady state	0.395	12.038	6.434	0.223	0.172

Table D.36 Calculated results for pervaporation - 5wt% ethanol and 10wt% glucose

Cumulative time (min)	Total flux (kg/m^{2}h)	Selectivity (-)	Enrichment factor (-)	Ethanol flux (kg/m^{2}h)	Water flux (kg/m^{2}h)
60	0.288	8.043	6.247	0.099	0.189
120	0.328	9.161	6.791	0.122	0.205
180	0.282	9.383	6.893	0.107	0.175
240	0.273	8.931	6.683	0.100	0.173
300	0.277	9.525	6.957	0.106	0.171
360	0.270	8.973	6.703	0.100	0.171
Steady state	0.274	9.143	6.781	0.102	0.171

Table D.37 Calculated results for pervaporation - 0wt% ethanol and 10wt% glucose

Cumulative time (min)	Total flux (kg/m^{2}h)
60	0.155
120	0.182
180	0.181
240	0.160
300	0.184
360	0.183
Steady state	0.183

Table D.38 Calculated results for pervaporation - 20wt% ethanol and 15wt% glucose

Cumulative time (min)	Total flux (kg/m^{2}h)	Selectivity (-)	Enrichment factor (-)	Ethanol flux (kg/m^{2}h)	Water flux (kg/m^{2}h)
30	1.316	8.521	3.861	0.917	0.399
60	0.944	10.453	4.091	0.696	0.247
90	0.921	11.119	4.156	0.690	0.230
120	1.033	10.499	4.095	0.763	0.270
150	0.926	9.610	3.999	0.668	0.258
180	0.954	9.363	3.970	0.683	0.271
210	0.906	10.128	4.057	0.663	0.243
240	0.788	10.012	4.044	0.575	0.213
270	0.901	9.429	3.977	0.646	0.254
300	0.893	10.051	4.048	0.652	0.241
330	0.894	9.827	4.023	0.649	0.245
Steady state	0.896	9.769	4.016	0.649	0.247

Table D.39 Calculated results for pervaporation - 15wt% ethanol and 15wt% glucose

Cumulative time (min)	Total flux (kg/m^{2}h)	Selectivity (-)	Enrichment factor (-)	Ethanol flux (kg/m^{2}h)	Water flux (kg/m^{2}h)
30	0.535	8.163	4.411	0.327	0.209
60	0.412	11.168	4.928	0.281	0.131
90	0.413	9.189	4.612	0.264	0.149
120	0.404	10.271	4.794	0.268	0.136
150	0.451	10.657	4.854	0.303	0.148
180	0.409	17.708	5.583	0.316	0.093
205	0.336	12.057	5.046	0.235	0.101
240	0.338	10.927	4.893	0.229	0.109
270	0.393	11.069	4.913	0.267	0.126
300	0.415	10.825	4.878	0.280	0.135
330	0.407	11.075	4.914	0.277	0.130
Steady state	0.405	10.989	4.902	0.275	0.130

Table D.40 Calculated results for pervaporation - 10wt% ethanol and 15wt% glucose

Cumulative time (min)	Total flux (kg/m^{2}h)	Selectivity (-)	Enrichment factor (-)	Ethanol flux (kg/m^{2}h)	Water flux (kg/m^{2}h)
30	0.478	10.176	5.891	0.270	0.208
60	0.426	13.781	6.648	0.271	0.155
90	0.449	12.846	6.477	0.279	0.171
150	0.411	12.222	6.354	0.250	0.161
180	0.462	11.896	6.287	0.278	0.184
210	0.438	12.682	6.446	0.271	0.168
240	0.455	12.143	6.338	0.276	0.179
270	0.426	11.361	6.171	0.252	0.174
300	0.446	11.481	6.198	0.265	0.181
330	0.419	11.135	6.120	0.246	0.173
Steady state	0.430	11.325	6.163	0.254	0.176

Table D.41 Calculated results for pervaporation - 5wt% ethanol and 15wt% glucose

Cumulative time (min)	Total flux (kg/m^2h)	Selectivity (-)	Enrichment factor (-)	Ethanol flux (kg/m^2h)	Water flux (kg/m^2h)
60	0.286	6.801	5.846	0.092	0.194
120	0.253	8.051	6.534	0.091	0.162
180	0.257	10.696	7.763	0.110	0.147
240	0.233	8.401	6.713	0.086	0.147
300	0.272	9.663	7.315	0.110	0.162
360	0.255	10.358	7.620	0.107	0.148
Steady state	0.253	9.474	7.216	0.101	0.152

Table D.42 Calculated results for pervaporation - 0wt% ethanol and 15wt% glucose

Cumulative time (min)	Total flux (kg/m^2h)
60	0.225
120	0.159
180	0.185
240	0.166
300	0.180
360	0.177
Steady state	0.178

D.5 GRAPHICAL REPRESENTATION OF THE PERVAPORATION RESULTS

D.5.1. Total flux

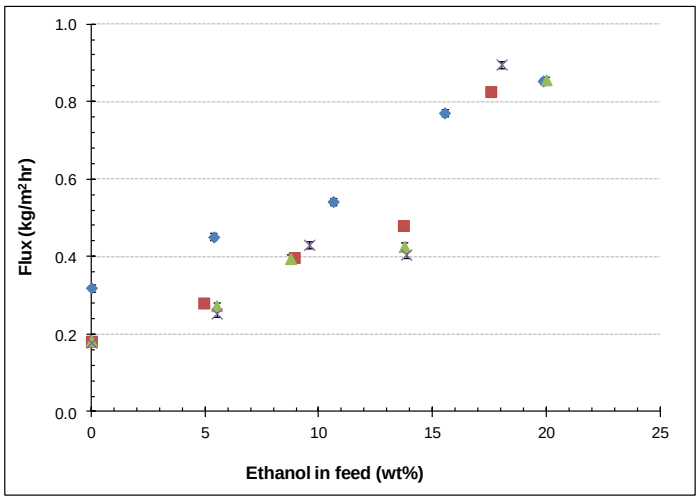

Figure D.2 Influence of feed composition on total flux
(♦0wt% glucose, ■5wt% glucose, ▲10wt% glucose, X15wt% glucose)

D.5.2. Selectivity

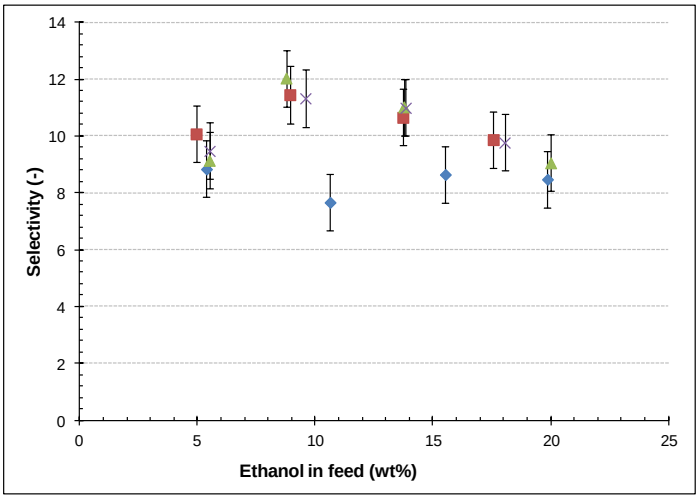

Figure D.3 Influence of feed composition on selectivity
(♦0wt% glucose, ■5wt% glucose, ▲10wt% glucose, X15wt% glucose)

D.5.3. Enrichment factor

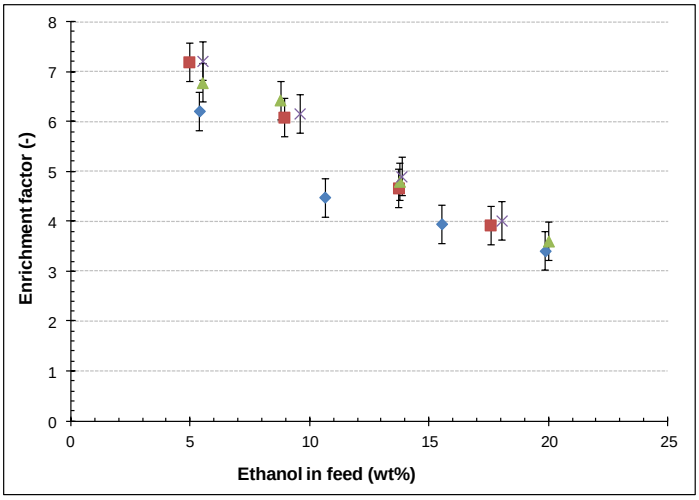

Figure D.4 Influence of feed composition on enrichment factor
(♦0wt% glucose, ■5wt% glucose, ▲10wt% glucose, X15wt% glucose)

D.5.4. Partial flux

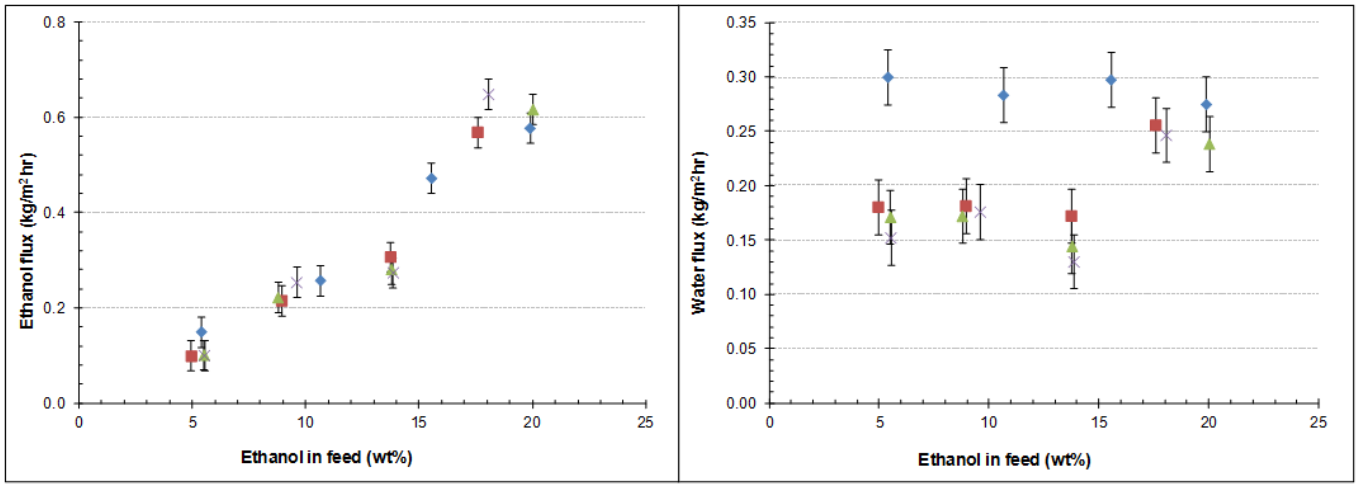

Figure D.5 Influence of feed composition on partial flux
(♦0wt% glucose, ■5wt% glucose, ▲10wt% glucose, X15wt% glucose)

APPENDIX E: FERMENTATION COUPLED WITH PERVAPORATION EXPERIMENTS

OVERVIEW

The results obtained from the experiment where fermentation is combined with pervaporation are presented in this appendix. This Appendix is subdivided into two subsections. Section E.1 is divided into two parts with the measured and calculated data obtained from fermentation presented in the first part. The mass permeated through the membrane at each different feed composition as well as the composition of the permeate are shown in the second part of Section E.1. The pervaporation data is used to determine the total flux, partial flux, and selectivity of the membrane, as shown in Section D.3.2, and is presented in Section E.1.2. In Section E.4, the results from both parts of this experiment are graphically presented.

E.1 EXPERIMENTAL DATA FROM FERMENTATION COMBINED WITH PERVAPORATION EXPERIMENTS

E.1.1. Fermentation measured and calculated data

The results of the fermentation part in the membrane-reactor system are presented in this section.

Table E.1 Yields and yeast cell concentration in membrane-reactor system

Time (h)	Ethanol ($g.g^{-1}$)	Glycerol ($g.g^{-1}$)	Glucose ($g.g^{-1}$)	Yeast cells ($g.L^{-1}$)
1	0.002	0.000	0.995	12.416
2	0.003	0.001	0.992	13.139
4	0.005	0.001	0.989	14.931
8	0.121	0.022	0.720	16.943
12	0.246	0.045	0.430	18.483
24	0.392	0.082	0.071	17.037
26	0.409	0.084	0.035	19.018
28	0.401	0.107	0.005	18.326
30	0.416	0.093	0.005	17.666
32	0.401	0.106	0.008	18.420
34	0.397	0.113	0.003	19.049
36	0.405	0.104	0.004	19.300
38	0.410	0.094	0.013	19.049
40	0.391	0.120	0.002	18.955
42	0.407	0.101	0.007	19.112
44	0.404	0.105	0.005	18.357
46	0.406	0.103	0.004	18.075
48	0.399	0.111	0.002	16.660

E.1.2. Pervaporation measured and calculated data

The measured and calculated results of the pervaporation part in the membrane-reactor system are presented in this section. The calculated results were determined using the method as discussed in Section D.3.2.

Table E.2 Measured data for pervaporation in membrane-reactor system

Cumulative time (h)	Time (min)	Mass permeate (g)	Fraction ethanol permeate
26	120	29.326	0.334
28	120	22.570	0.388
30	120	21.092	0.375
32	120	21.443	0.374
34	120	21.228	0.368
36	120	20.213	0.355
38	120	20.240	0.344
40	120	21.067	0.339
42	120	19.761	0.338
44	120	19.595	0.323
46	120	20.36	0.303
48	120	19.907	0.298

Table E.3 Calculated results for pervaporation in membrane-reactor system

Cumulative time (h)	Total flux (kg/m^{2}h)	Selectivity (-)	Enrichment factor (-)	Ethanol flux (kg/m^{2}h)	Water flux (kg/m^{2}h)
26	0.576	7.103	5.624	0.192	0.384
28	0.443	9.494	6.896	0.172	0.271
30	0.414	8.898	6.593	0.155	0.259
32	0.421	9.568	7.089	0.157	0.264
34	0.417	9.765	7.297	0.153	0.264
36	0.397	9.314	7.089	0.141	0.256
38	0.398	9.024	6.974	0.137	0.261
40	0.414	9.733	7.577	0.140	0.274
42	0.388	9.522	7.407	0.131	0.257
44	0.385	9.305	7.392	0.125	0.260
46	0.400	8.660	7.083	0.121	0.279
48	0.391	8.971	7.382	0.116	0.275

E.2 GRAPHICAL REPRESENTATION

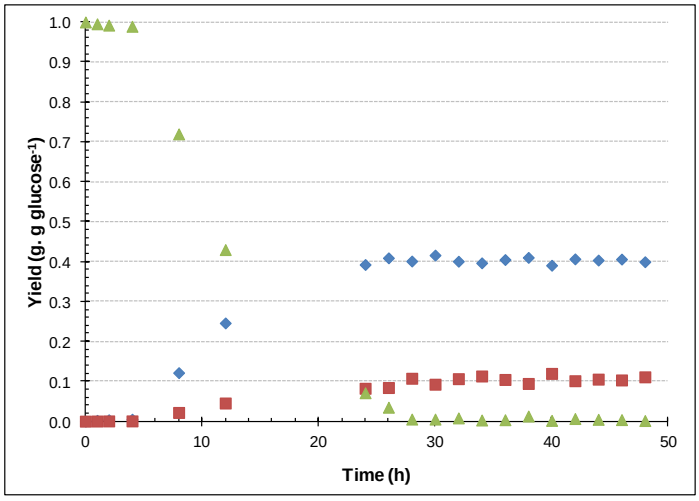

Figure E.1 Fermentation over time in membrane-reactor system
(▲Glucose yield, ♦Ethanol yield, ■Glycerol yield)

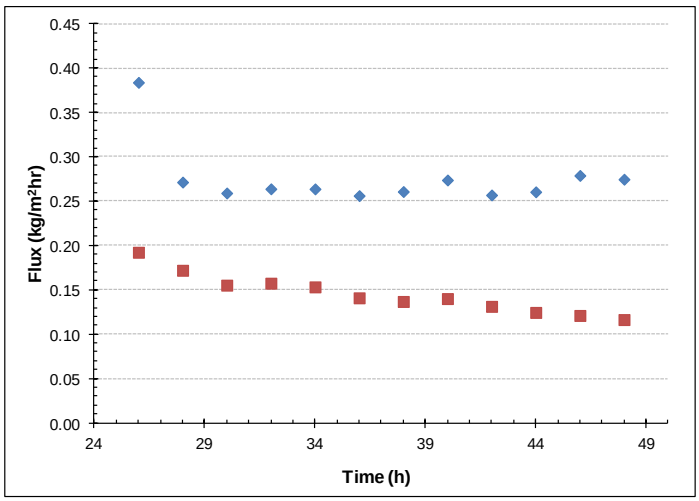

Figure E.2 Membrane flux over time in membrane-reactor system
(♦Water flux, ■Ethanol flux)

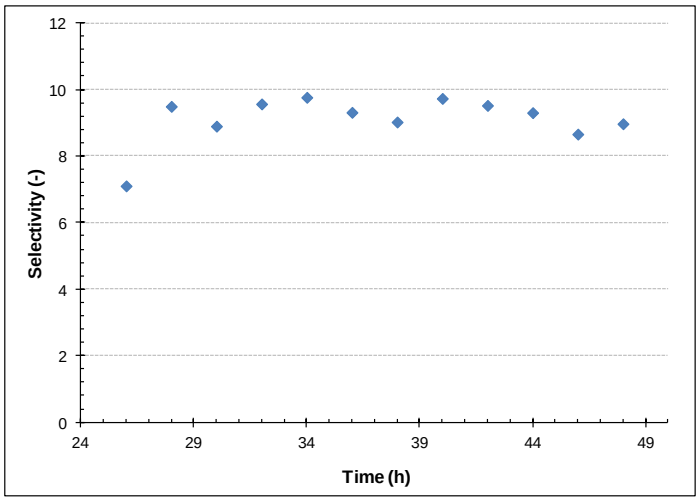

Figure E.3 Membrane selectivity over time in membrane-reactor system

APPENDIX F: MEMBRANE SCREENING

OVERVIEW

The results of the membrane screening experiments, as discussed in Section 4.2.4, are presented in Appendix F.

F.1 MEMBRANE SCREENING RESULTS

The separation efficiency of ethanol from a water and ethanol mixture was tested using four different membranes namely PERVAP®2201, PERVAP®2211, PERVAP®4101, and PERVAP®4060.

F.1.1. PERVAP®2201 membrane

Table F.1 Screening results of PERVAP®2201 membrane using pure water

Time (h)	Mass permeate (g)	Flux (kg/m^2.h)
1	14.424	0.567
2	13.781	0.542
3	17.028	0.669
4	15.222	0.598
5	14.249	0.560
6	14.442	0.568

Table F.2 Screening results of PERVAP®2201 membrane using 10wt% ethanol

Time (h)	Mass permeate (g)	Fraction ethanol in permeate	Flux (kg/m^2.h)	Selectivity
1	18.163	0.102	0.714	0.922
2	12.290	0.091	0.483	0.820
3	6.240	0.101	0.245	0.935
4	11.584	0.104	0.455	0.972
5	9.209	0.087	0.362	0.789
6	9.014	0.079	0.354	0.724
7	9.003	0.062	0.354	0.556

Table F.3 Screening results of PERVAP®2201 membrane using 20wt% ethanol

Time (h)	Mass permeate (g)	Fraction ethanol in permeate	Flux (kg/m^2.h)	Selectivity
0.5	13.569	0.206	1.066	0.989
1	5.357	0.178	0.421	0.823
1.5	5.144	0.189	0.404	0.878
2	4.814	0.183	0.378	0.842
2.5	4.817	0.175	0.379	0.792
3	4.790	0.177	0.376	0.807
3.5	4.897	0.187	0.385	0.857
4	4.801	0.177	0.377	0.804

F.1.2. PERVAP®2211 membrane

Table F.4 Screening results of PERVAP®2211 membrane using pure water

Time (h)	Mass permeate (g)	Flux (kg/m^2.h)
1	9.703	0.381
2	7.129	0.280
3	6.946	0.273
4	6.508	0.256
5	6.669	0.262
6	6.504	0.256

Table F.5 Screening results of PERVAP®2211 membrane with 10wt% ethanol

Time (h)	Mass permeate (g)	Fraction ethanol in permeate	Flux (kg/m^2.h)	Selectivity
1	8.418	0.046	0.331	0.395
2	5.123	0.045	0.201	0.385
3	5.272	0.047	0.207	0.402
4	5.124	0.048	0.201	0.406

Table F.6 Screening results of PERVAP®2211 membrane with 20wt% ethanol

Time (h)	Mass permeate (g)	Fraction ethanol in permeate	Flux (kg/m^2.h)	Selectivity
1	19.522	0.203	0.767	0.986
2	6.354	0.107	0.250	0.468
3	5.169	0.123	0.203	0.556
4	5.166	0.126	0.203	0.576
5	5.345	0.129	0.210	0.598
6	5.451	0.110	0.214	0.501
7	5.479	0.108	0.215	0.493

F.1.3. PERVAP®4101 membrane

Table F.7 Screening results of PERVAP®4101 membrane using pure water

Time (h)	Mass permeate (g)	Flux (kg/m^2.h)
1	18.155	0.713
2	8.732	0.343
3	8.450	0.332
4	7.379	0.290
5	7.460	0.293
6	7.285	0.286

Table F.8 Screening results of PERVAP®4101 membrane using 10wt% ethanol

Time (h)	Mass permeate (g)	Fraction ethanol in permeate	Flux (kg/m^2.h)	Selectivity
1	20.743	0.055	0.815	0.488
2	5.017	0.042	0.197	0.364
3	4.745	0.043	0.186	0.374
4	5.167	0.042	0.203	0.366

Table F.9 Screening results of PERVAP®4101 membrane using 20wt% ethanol

Time (h)	Mass permeate (g)	Fraction ethanol in permeate	Flux (kg/m^2.h)	Selectivity
0.5	28.784	0.176	2.262	0.825
1	4.064	0.115	0.319	0.503
1.5	2.579	0.121	0.203	0.535
2	2.262	0.118	0.178	0.516
2.5	2.275	0.119	0.179	0.520
3	2.271	0.114	0.178	0.493

F.1.4. PERVAP®4060 membrane

Table F.10 Screening results of PERVAP®4060 membrane using pure water

Time (h)	Mass permeate (g)	Flux (kg/m^2.h)
1	8.069	0.381
2	6.781	0.266
3	6.040	0.237
4	8.154	0.320
5	8.117	0.319

Table F.11 Screening results of PERVAP®4060 membrane using 10wt% ethanol

Time (h)	Mass permeate (g)	Fraction ethanol in permeate	Flux (kg/m^2.h)	Selectivity
1	13.454	0.487	0.529	7.644
2	15.369	0.504	0.604	8.168
3	15.074	0.525	0.592	8.881
4	13.422	0.536	0.527	9.297
5	14.361	0.502	0.564	8.095
6	13.574	0.506	0.533	8.239

Table F.12 Screening results of PERVAP®4060 membrane using 20wt% ethanol

Time (h)	Mass permeate (g)	Fraction ethanol in permeate	Flux (kg/m^2.h)	Selectivity
0.5	15.573	0.483	1.224	3.396
1.5	21.023	0.684	0.826	7.896
2	11.740	0.689	0.923	8.079
2.5	10.893	0.605	0.856	5.584
3	10.954	0.674	0.861	7.519
3.5	10.856	0.675	0.853	7.551
4	10.855	0.680	0.853	7.751

F.2 GRAPHICAL REPRESENTATION OF THE MEMBRANE SCREENING RESULTS

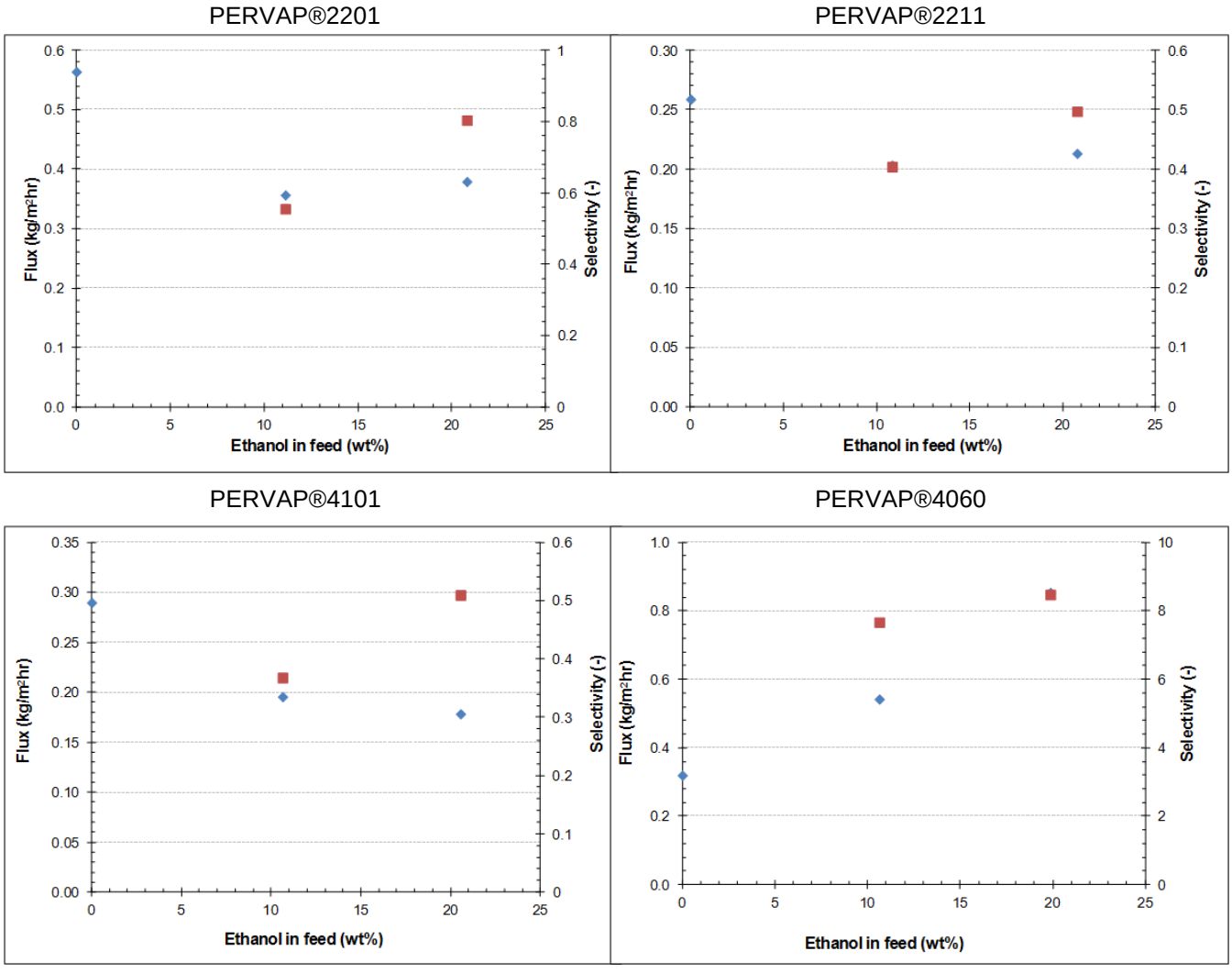

Figure F.1 Graphical representation of the membrane screening results
(♦Total flux, ■Selectivity)

F.3 STABILITY SCREENING TEST

The physical stability of all four membranes was tested by soaking the membrane in solutions of different ethanol concentrations. A membrane was classified as stable if the active layer did not visually change over time. All four of the membranes were stable at high ethanol concentrations and a typical observation of each membrane is shown in Figure F.2 to Figure F.5.

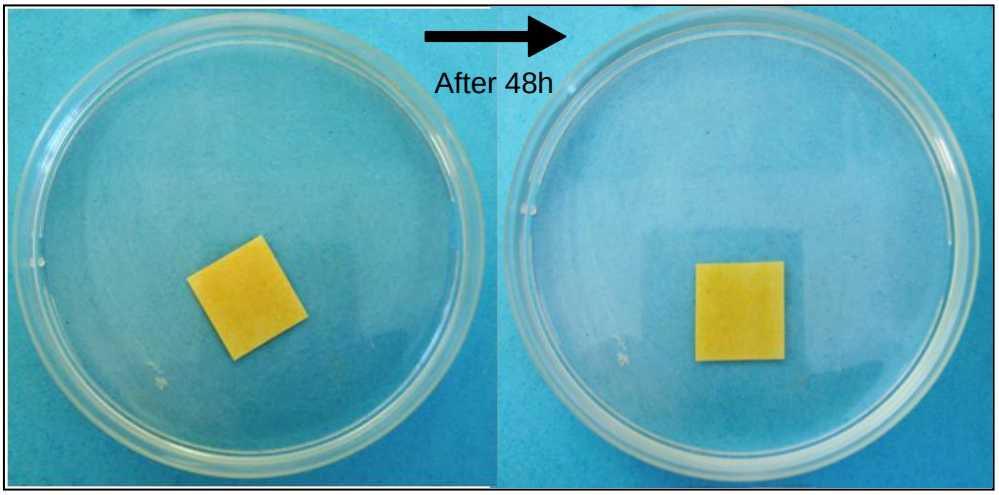

Figure F.2 Visual stability test of membrane PERVAP®2201 in 90wt% ethanol

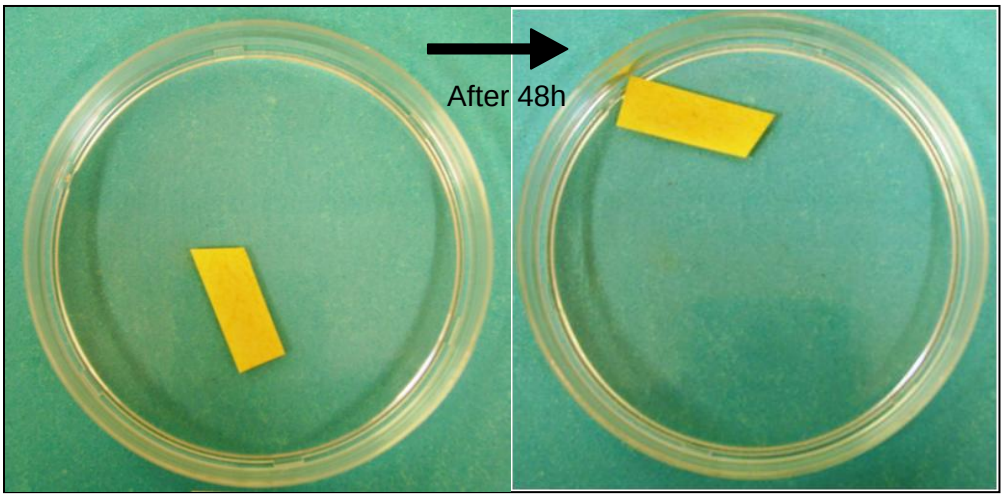

Figure F.3 Visual stability test of membrane PERVAP®2211 in 90wt% ethanol

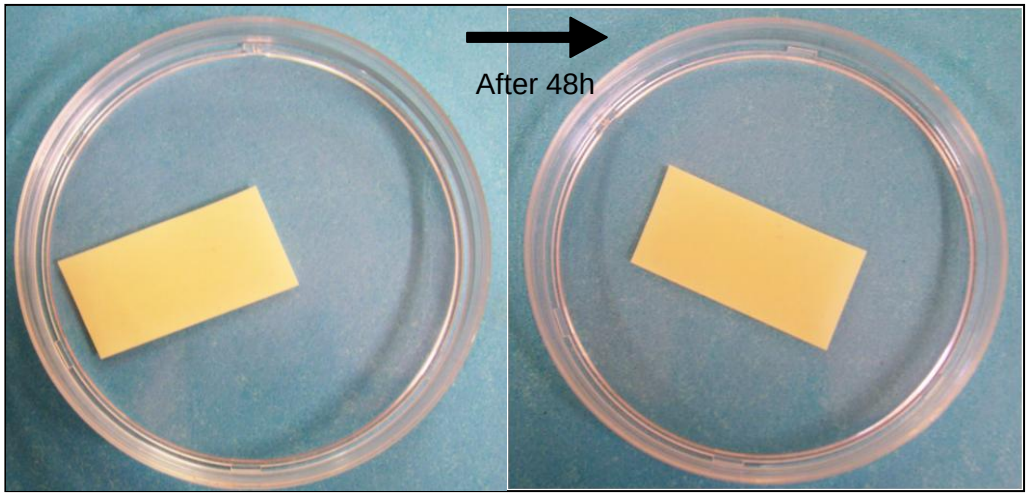

Figure F.4 Visual stability test of membrane PERVAP®4101 in 90wt% ethanol

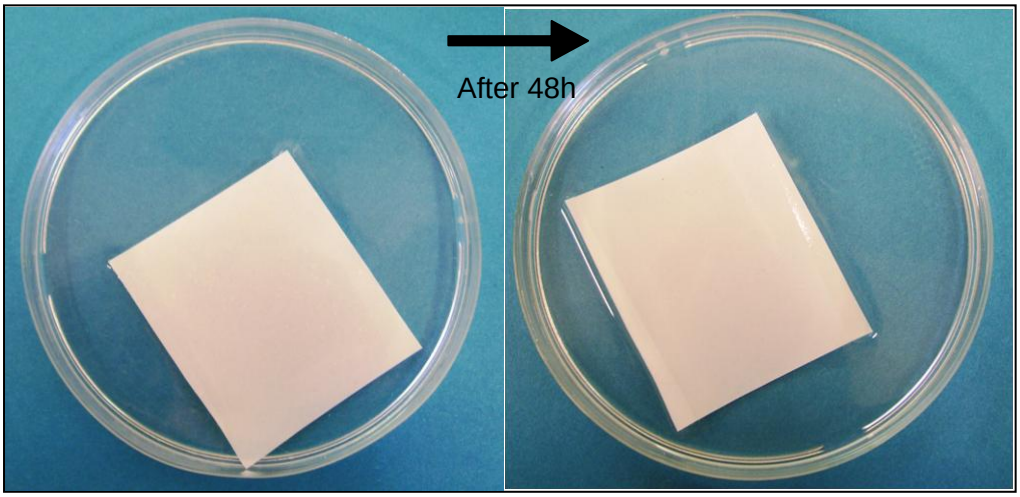

Figure F.5 Visual stability test of membrane PERVAP®4060 in 90wt% ethanol

APPENDIX G: MEMBRANE SYSTEM STABILITY

OVERVIEW

The stability of the membrane system was tested to ensure that it would be suitable for coupling with fermentation. First of all the chosen membrane (PERVAP®4060) was tested for stability over time. The results of the time test are shown in Section G.1. In Section G.2, the effect that yeast has on the membrane is shown.

G.1 MEMBRANE STABILITY OVER TIME

The stability of the PERVAP®4060 membrane was tested over 40 hours, as shown in Figure G.1. The starting ethanol concentration of 10wt% ethanol was chosen and this concentration was kept constant over the 40 hours.

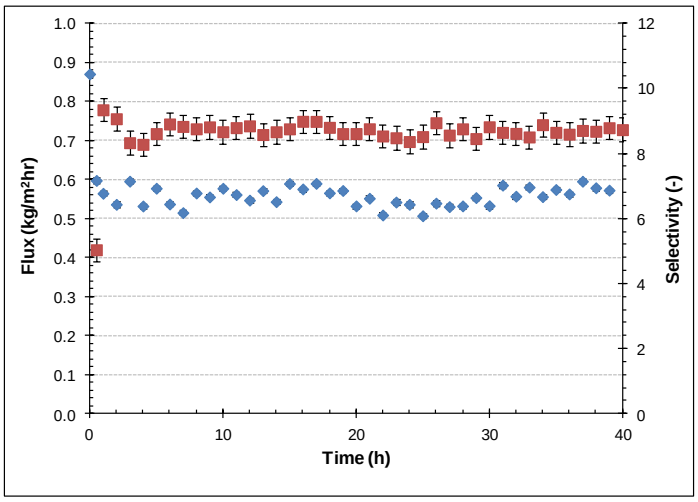

Figure G.1 Membrane stability over time flux
(♦Flux, ■Selectivity)

G.2 MEMBRANE STABILITY WITH YEAST

To observe the effect that yeast cells have on the membrane system 10g/L yeast was added to a feed of 10wt% ethanol. Figure G.2 and Table G.1 shows the results of the addition of yeast.

Table G.1 Membrane stability with the addition of yeast cells

Time (h)	Mass permeate (g)	Fraction ethanol in permeate	Flux (kg/m^2.h)	Selectivity
1	16.195	0.39	0.636	5.089
2	17.540	0.45	0.551	6.656
3	12.674	0.46	0.498	6.885
4	12.953	0.45	0.509	6.734

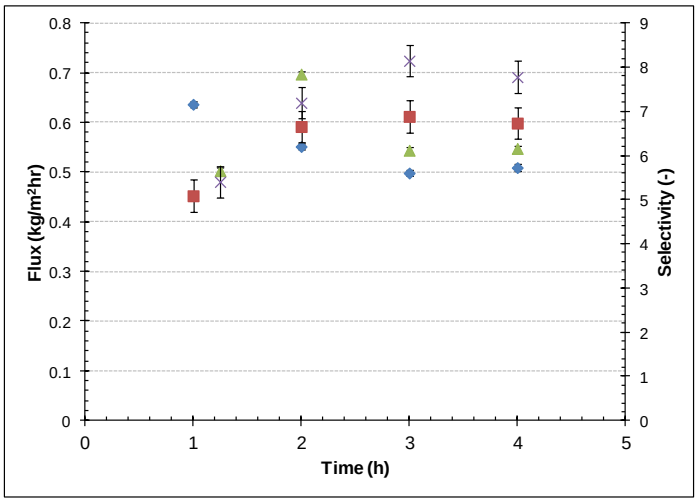

Figure G.2 Membrane stability with the addition of yeast cells flux
(♦Flux with yeast cells, ▲ Flux without yeast cells, ■Selectivity with yeast cells, XSelectivity without yeast cells)

Figure G.2 shows a slight decrease in flux (from 0.573kg/m^2.h to 0.509kg/m^2.h) and a slight decrease in ethanol selectivity (8.731 to 6.734) when yeast cells are added to the feed. As the decrease is only minor, this is not a major concern.

APPENDIX H: COMPUTER PROGRAMMES

OVERVIEW

The computer programmes written in this investigation, in order to solve the differential equations during modelling, are presented in this chapter. Three programmes were used namely Runge-Kutta discussed in Section H.1, the Nelder-Mead Simplex method, described in Section H.2 and the bootstrap method, as presented in Section H.3. In this appendix, the method is discussed followed by the procedure flow diagram and sample computer code of each programme.

H.1 THE RUNGE-KUTTA METHOD

H.1.1. Background

The Runge-Kutta method is a widely used numerical scheme to solve differential equations due to its simplicity and accuracy. In this study a classic Runge-Kutta method of order 4 was used to solve the system of differential equations.

The standard fourth-order Runge-Kutta method takes the following form (Cheney & Kincaid, 2004:461):

$$x(t+h) = x(t) + \frac{1}{6}(k_1 + 2k_2 + 2k_3 + k_4)$$

$$k_1 = h.f(t, x)$$

$$k_2 = h.f\left(t + \frac{1}{2}h, x + \frac{1}{2}k_1\right)$$

$$k_3 = h.f\left(t + \frac{1}{2}h, x + \frac{1}{2}k_2\right)$$

$$k_4 = h.f(t + h, x + k_3)$$

with h the step size.

The solution at x(t+h) is obtained by evaluation the function *f* four times. The Runge-Kutta method can extend to systems of differential equations. Consider the following system of *m* equations:

$$\frac{dx_1}{dt} = f_1(t, x_1, x_2, ..., x_m),$$

$$\frac{dx_2}{dt} = f_2(t, x_1, x_2, ..., x_m),$$

…

$$\frac{dx_m}{dt} = f_2(t, x_1, x_2, ..., x_m)$$

with $a \le t \le b$ and initial conditions $x_1(a)=\alpha_1$, $x_2(a)=\alpha_2$,…, $x_m(a)=\alpha_m$.

To solve the system of differential equations using Runge-Kutta the following four steps are used (van der Gryp, 2008: A-3 & Cheney & Kincaid, 2004:492-493).

1. Let an integer N>0 be chosen, let $h = \frac{b-a}{N}$ and partition [a,b] into N subintervals with the mesh points

   $t_j = a + j.h$ for each j =0,1,…,N Equation H.1

2. Set the initial conditions $x_1(a)=\alpha_1$, $x_2(a)=\alpha_2,\ldots$, $x_m(a)=\alpha_m$.
3. Calculate the different k-values using the following set of equations for each i=1,2,…,m.

   $$k_{1,i} = h.f_i\left(t_j, x_{1,j}, x_{2,j}, ..., x_{m,j}\right)$$

   $$k_{2,i} = h.f_i\left(t_j + \frac{1}{2}h, x_{1,j} + \frac{1}{2}k_{1,1}, x_{2,j} + \frac{1}{2}k_{1,2}, ..., x_{m,j} + \frac{1}{2}k_{1,m}\right)$$

   $$k_{3,i} = h.f_i\left(t_j + \frac{1}{2}h, x_{1,j} + \frac{1}{2}k_{2,1}, x_{2,j} + \frac{1}{2}k_{2,2}, ..., x_{m,j} + \frac{1}{2}k_{2,m}\right)$$

   $$k_{4,i} = h.f_i\left(t_j + h, x_{1,j} + k_{3,1}, x_{2,j} + k_{3,2}, ..., x_{m,j} + k_{3,m}\right)$$ Equations H.2-H.5

   All the values of $k_{l,i}$ must be computed before $k_{l+1,i}$.

4. Combine the k-values

   $$x_{i,j} = x_{i,j} + \frac{1}{6}(k_{1,i} + 2k_{2,i} + 2k_{3,i} + k_{4,i})$$ Equation H.6

   for each i=1,2,…,m.

H.1.2. Flow diagram

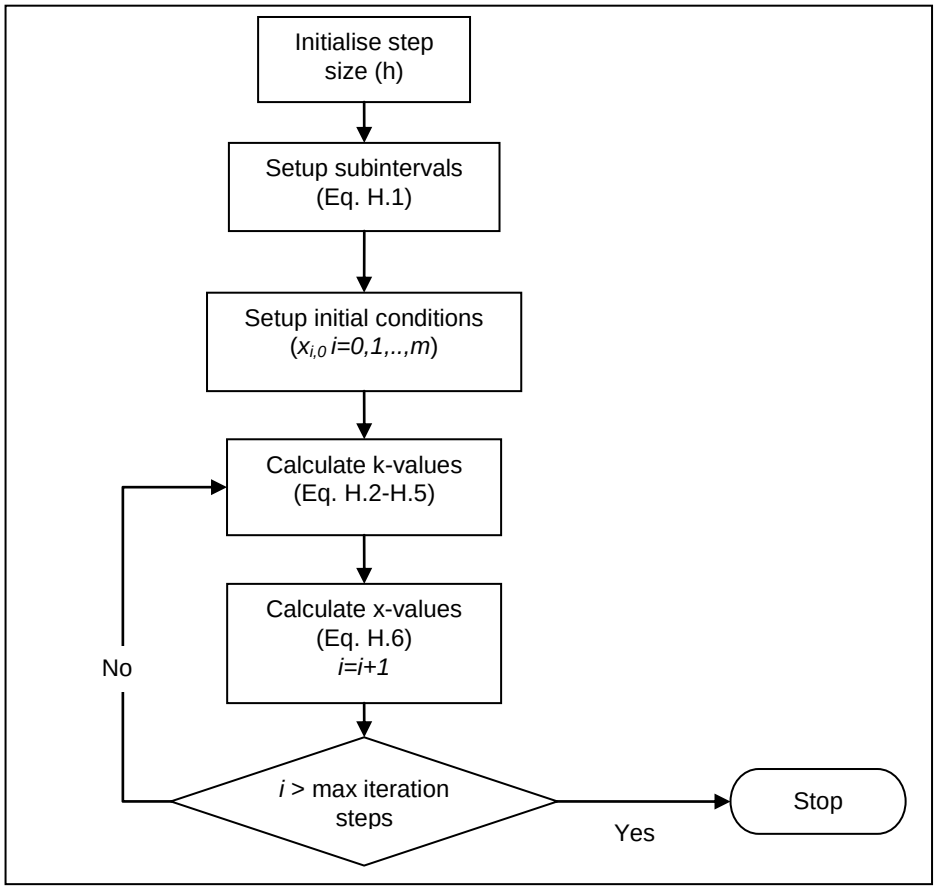

Figure H.1 Flow diagram of the Runge-Kutta method for systems of equations (van der Gryp, 2008)

H.1.3. Sample code

The Runge-Kutta programme was written in Excel using Visual Basic.

```
Do
    KPe1 = h * Ethanol(vmaxe, S, x, Kspe)
    KPg1 = h * Glycerol(vmaxg, S, x, Ksge)
    Kx1 = h * Cells(umax, S, x, Ksx)
    KS1 = h * (-((Ethanol(vmaxe, S, x, Kspe)) - (Glycerol(vmaxg, S, x, Ksge))) / (YPes - YPgS))

    KPe2 = h * Ethanol(vmaxe, S + 0.5 * KS1, x + 0.5 * Kx1, Kspe)
    KPg2 = h * Glycerol(vmaxg, S + 0.5 * KS1, x + 0.5 * Kx1, Ksge)
    Kx2 = h * Cells(umax, S + 0.5 * KS1, x + 0.5 * Kx1, Ksx)
    KS2 = h * (-((Ethanol(vmaxe, S + 0.5 * KS1, x + 0.5 * Kx1, Kspe)) - (Glycerol(vmaxg, S + 0.5 *
KS1, x + 0.5 * Kx1, Ksge))) / (YPes - YPgS))

    KPe3 = h * Ethanol(vmaxe, S + 0.5 * KS2, x + 0.5 * Kx2, Kspe)
    KPg3 = h * Glycerol(vmaxg, S + 0.5 * KS2, x + 0.5 * Kx2, Ksge)
    Kx3 = h * Cells(umax, S + 0.5 * KS2, x + 0.5 * Kx2, Ksx)
    KS3 = h * (-((Ethanol(vmaxe, S + 0.5 * KS2, x + 0.5 * Kx2, Kspe)) - (Glycerol(vmaxg, S + 0.5 *
KS2, x + 0.5 * Kx2, Ksge))) / (YPes - YPgS))
```

```
    KPe4 = h * Ethanol(vmaxe, S + KS3, x + Kx3, Kspe)
    KPg4 = h * Glycerol(vmaxg, S + KS3, x + Kx3, Ksge)
    Kx4 = h * Cells(umax, S + KS3, x + Kx3, Ksx)
    KS4 = h * (-((Ethanol(vmaxe, S + KS3, x + Kx3, Kspe)) - (Glycerol(vmaxg, S + KS3, x + Kx3,
Ksge))) / (YPes - YPgS))

    Pe = Pe + (1 / 6) * (KPe1 + 2 * KPe2 + 2 * KPe3 + KPe4)
    Pg = Pg + (1 / 6) * (KPg1 + 2 * KPg2 + 2 * KPg3 + KPg4)
    x = x + (1 / 6) * (Kx1 + 2 * Kx2 + 2 * Kx3 + Kx4)
    S = S + (1 / 6) * (KS1 + 2 * KS2 + 2 * KS3 + KS4)

    Z = Z + 1
    t = Z * h
Loop Until t > 72
End Function
```

H.2 THE NELDER-MEAD SIMPLEX METHOD

H.2.1. Background

The simplex method was used to estimate the parameters of the system of differential equations used for modelling. The simplex method compares objective function values at the (n+1) vertices of a general simplex with n dimensions and moves this simplex to an optimum point by using three basic actions namely, reflection, contraction, and expansion as shown below (Jacoby *et al*, 1974:79, Koekemoer, 2004).

- Reflection: x^h is replaced by

  $$x^r = (1+\alpha)x^0 - \alpha x^h$$ Equation H.7

- Expansion: x^r is expanded in the direction along which a further improvement of the function may be expected

  $$x^e = \gamma x^r + (1-\gamma)x^0$$ Equation H.8

- Contraction: The simplex is contracted by

  $$x^c = \beta x^h + (1-\beta)x^0$$ Equation H.9

Nelder and Mead found that useful values for the coefficients α, β, γ are $\alpha = 1$, $\beta = 0.5$ and $\gamma = 2$.

In Equation H.7 to Equation H.9 and the flow diagram shown in Figure H.2 the following notation is used:

- x^h is the vertex corresponding to the highest value of the objective function

  $$M\left(x^h\right) = \max_i\left(x^i\right),\ i = 1,2,...,(n+1)$$ Equation H.10

- x^l is the vertex with the lowest value of M
- x^s is the vertex with the second highest value of M
- x^0 is the centroid of al x^i except i=h given by

$$x^0 = \frac{1}{n}\sum_{\substack{i=1 \\ i\neq h}}^{n+1} x^i \qquad \text{Equation H.11}$$

To use the simplex method, the first step is to estimate the minimum $x^l=(x_1,x_2,\ldots,x_n)$ and to form an initial simplex using Equations H.12 and H.13.

$$p_n = \frac{\sqrt{n+1}-1+n}{n\sqrt{2}}S \qquad \text{Equation H.12}$$

$$q_n = \frac{\sqrt{n+1}-1}{n\sqrt{2}}S \qquad \text{Equation H.13}$$

with S the scaling factor.

The n+1 vertices of a regular simplex with edge of length S are given by

$$\begin{aligned} x^1 &= \left(x_1, x_2, x_3, \ldots, x_n\right)^T \\ x^2 &= \left(p_n + x_1, q_n + x_2, q_n + x_3, \ldots, q_n + x_n\right)^T \\ x^3 &= \left(q_n + x_1, p_n + x_2, q_n + x_3, \ldots, q_n + x_n\right)^T \\ &\vdots \\ x^{n+1} &= \left(q_n + x_1, q_n + x_2, q_n + x_3, \ldots, p_n + x_n\right)^T \end{aligned} \qquad \text{Equation H.14}$$

The construction of the initial simplex ensures that its vertices span the full n-dimensional space.

The vertices x^h, x^s, x^l, and the centroid x^0 of the current simplex are determined and a convergence test is performed. x^h is then reflected and the value of $M(x^r)$ is determined. If $M(x^s) \geq M(x^r) \geq M(x^l)$ then x^h is replaced by x^r and the process is restarted. If $M(x^r)<M(x^l)$ the simplex is expanded in the direction of x^r-x^0. If the expansion is successful, if $M(x^e)<M(x^l)$, x^h is replaced by x^e, otherwise x^h is replaced by x^r. The process is then restarted. If the reflection step produces a x^r such that $M(x^h)>M(x^r)>M(x^s)$, x^h is replaced by x^r followed by the contraction step. Contraction is also done if $M(x^r) \geq M(x^h)$. If $M(x^h)>M(x^c)$ then x^h is replaced by x^c and the whole procedure is restarted. If $M(x^h) \leq M(x^c)$, the current simplex is shrunk about the point x^l as shown in Equation H.15, before the whole procedure is restarted.

$$x^i = \frac{1}{2}\left(x^i + x^l\right), \quad i = 1,\ldots,n+1 \qquad \text{Equation H.15}$$

The test for convergence is shown in Equation H.16.

$$\left\{\sum_{i=1}^{n+1}\frac{\left[M\left(x^{i}\right)-M\left(x^{0}\right)\right]^{2}}{n}\right\}^{\frac{1}{2}} \leq \tau \qquad \text{Equation H.16}$$

The standard deviation of the function at the (n+1) vertices of the current simplex is compared with a preselected tolerance τ. The process is terminated when Equation H.16 is satisfied.

H.2.2. Flow diagram

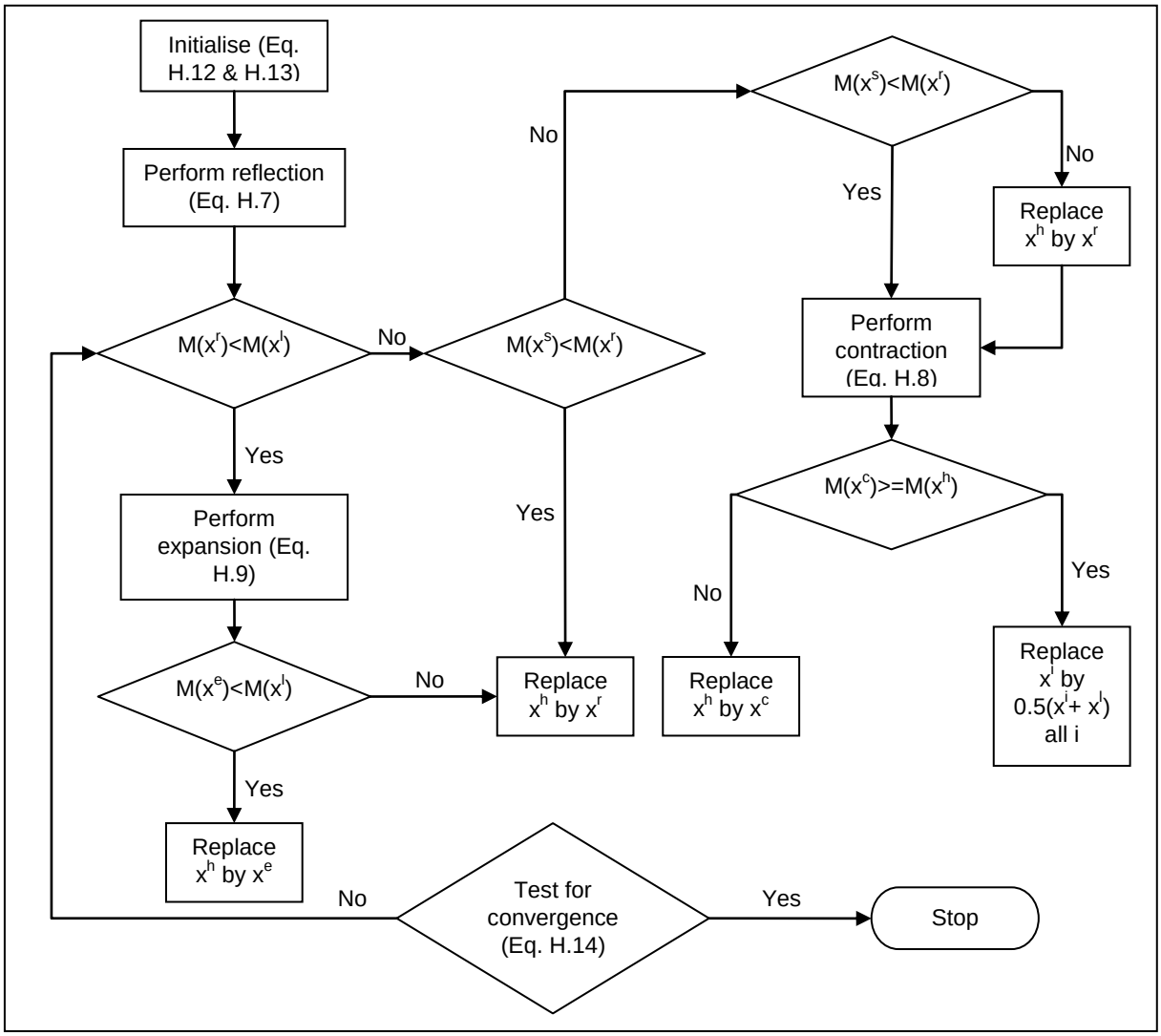

Figure H.2 Flow diagram of the Simplex method (Koekemoer, 2004:D5 & Jacoby *et al*, 1972:81)

H.2.3. Sample code

The Nelder-Mead Simplex programme was written in Excel using Visual Basic, as shown below.

```
Do
    If M(I) > high Then
       high = M(I)
       h = I
    ElseIf (M(I) > sec) And (M(I) < high) Then
       sec = M(I)
       S = I
    ElseIf M(I) < low Then
       low = M(I)
       L = I
    End If
 I = I + 1
 Loop Until I > n + 1

 {Centerpoint without h}
 For I = 0 To n
    Sum = 0
    For J = 0 To (n + 1)
       If J <> h Then
          Sum = Sum + Worksheets("sheet2").Cells(5 + I, 2 + J)
       End If
    Next J
    Worksheets("Sheet2").Cells(5 + I, x0) = Sum / (n + 1)
 Next I

 {Reflection}
 For I = 0 To n
    Worksheets("Sheet2").Cells(5 + I, Xr) = 2 * Worksheets("Sheet2").Cells(5 + I, x0) -
Worksheets("Sheet2").Cells(5 + I, 2 + h)
 Next I

 If M(Xr - 2) < M(L) Then
    For I = 0 To n
       Worksheets("Sheet2").Cells(5 + I, Xe) = 2 * Worksheets("Sheet2").Cells(5 + I, Xr) -
Worksheets("Sheet2").Cells(5 + I, x0)
    Next I

 {Expansion}
    If M(Xe - 2) < M(L) Then
       For I = 0 To n
          Worksheets("Sheet2").Cells(5 + I, 2 + h) = Worksheets("Sheet2").Cells(5 + I, Xe)
       Next I

    Else
       For I = 0 To n
          Worksheets("Sheet2").Cells(5 + I, 2 + h) = Worksheets("Sheet2").Cells(5 + I, Xr)
       Next I
    End If

 Else
    If M(S) >= M(Xr - 2) Then
       For I = 0 To n
          Worksheets("Sheet2").Cells(5 + I, 2 + h) = Worksheets("Sheet2").Cells(5 + I, Xr)
```

```
        Next I

      Else

        If M(Xr - 2) < M(h) Then
          For I = 0 To n
            Worksheets("Sheet2").Cells(5 + I, 2 + h) = Worksheets("Sheet2").Cells(5 + I, Xr)
          Next I
        End If

  {Contraction}
          For I = 0 To n
            Worksheets("Sheet2").Cells(5 + I, Xc) = 0.5 * Worksheets("Sheet2").Cells(5 + I, 2 + h) +
0.5 * Worksheets("Sheet2").Cells(5 + I, x0)
          Next I

        If M(Xc - 2) < M(h) Then
          For I = 0 To n
            Worksheets("Sheet2").Cells(5 + I, 2 + h) = Worksheets("Sheet2").Cells(5 + I, Xc)
          Next I

        Else
          For J = 0 To (n + 1)
            For I = 0 To (n + 1)
              Worksheets("Sheet2").Cells(5 + J, 2 + I) = 0.5 * (Worksheets("Sheet2").Cells(5 + I, 2 +
J) + Worksheets("Sheet2").Cells(5 + L, 2 + J))
            Next I
          Next J
         End If

      End If
  End If

  tsi = 0
  For I = 0 To n + 1
    tsi = tsi + (M(I) + M(x0 - 2)) ^ 2
    tsi = (tsi / (n + 1)) ^ 0.5
  Next I
  Loop Until tsi < con
```

H.3 THE BOOTSTRAP METHOD

H.3.1. Background

The bootstrap method was used to determine the confidence levels and standard errors of the parameters obtained through the non-linear simplex regression method discussed in Section H.2. The bootstrap method is a statistical method that resample from the original data set to determine the error associated with each parameter. The procedure is as follows (Chernick, 1999:9):

1. Generate a bootstrap sample with replacement from the empirical distribution

2. Compute the values of interest by using the bootstrap sample in place of the original sample.
3. Repeat steps 1 and 2 k times.

The procedure for bootstrapping the residuals of a regression, as discussed by Chernick (1999:80), Koekemoer (2004:D14) and van der Gryp (2008:A-12) will be discussed below.

Consider a general regression model as given by Equation H.17.

$$y_i = f_i(x, c_i) + \varepsilon_i \text{ for } i = 1,2,...,n \qquad \text{Equation H.17}$$

The functions f_i are of a known form and may depend on a fixed vector of covariates c_i. The vector x is a $p \times 1$ vector of unknown parameters. The error of each data point, ε_i, is independent. The value of x is usually calculated by minimizing the distance measured with the least squares method, shown by Equation H.18.

$$M(y, x, c) = \sum_{i=1}^{n} \left[y_i - f_i(x, c_i) \right]^2 \qquad \text{Equation H.18}$$

The parameters (x') of x are acquired when M is minimized. The residuals are obtained by Equation H.19.

$$\varepsilon_i ' = y_i - f(x', c_i) \qquad \text{Equation H.19}$$

Bootstrapping the residuals y_i^* for i=1,2,…n where y_i^* are obtained by random sampling from y_i', a bootstrap sample data set can be generated by using y_i^* and $f(x', c_i)$, as shown in Equation H.20.

$$y_i^* = f(x', c_i) + \varepsilon_i^* \text{ for } i = 1,2,...,n \qquad \text{Equation H.20}$$

Each bootstrap data set (y_i^*) can then be used to obtain x^* with parameters so that M is minimized.

This procedure is repeated k times to determine the confidence level and error.

H.3.2. Flow diagram

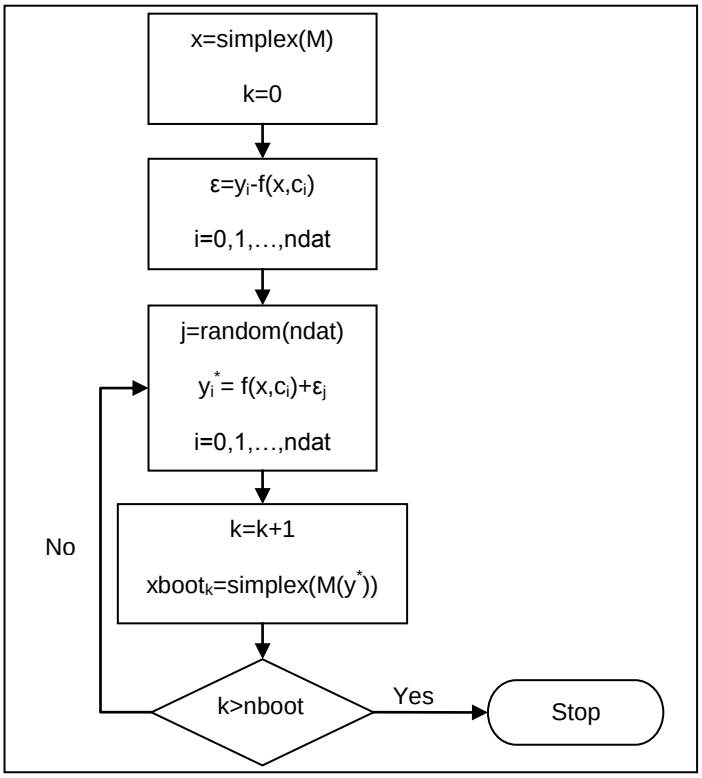

Figure H.3 Flow diagram of the Bootstrap method (Koekemoer, 2004:D15)

H.3.3. Sample code

The Bootstrap programme was written in Excel using Visual Basic. This programme uses the Simplex programme discussed in Section H.2.

```
Sub Button3_Click()

For k = 0 To (nboot - 1)
   Worksheets("Sheet2").Cells(13, 2).Value = Round(((ndat - 1) * Rnd() + 0))
   nrandom = (Worksheets("Sheet2").Cells(13, 2).Value)
      For i = 0 To (ndat - 1)
       Worksheets("Sheet2").Cells(24 + i, 2).Value = Worksheets("Sheet2").Cells(24 + i, 6).Value + Worksheets("Sheet2").Cells(24 + nrandom, 10).Value
       Worksheets("Sheet2").Cells(24 + i, 3).Value = Worksheets("Sheet2").Cells(24 + i, 7).Value + Worksheets("Sheet2").Cells(24 + nrandom, 11).Value
       Worksheets("Sheet2").Cells(24 + i, 4).Value = Worksheets("Sheet2").Cells(24 + i, 8).Value + Worksheets("Sheet2").Cells(24 + nrandom, 12).Value
```

```
        Worksheets("Sheet2").Cells(24 + i, 5).Value = Worksheets("Sheet2").Cells(24 + i, 9).Value +
Worksheets("Sheet2").Cells(24 + nrandom, 13).Value
      Next i

   p = (((n + 2) ^ 0.5) - 1 + (n + 1)) / ((n + 1) * (2 ^ 0.5)) * Sf
   q = (((n + 2) ^ 0.5) - 1) / ((n + 1) * (2 ^ 0.5)) * Sf

   For i = 1 To n + 1
      For j = 0 To n
         If i = (j + 1) Then
            Worksheets("Sheet2").Cells(4 + i, 3 + j).Value = p + Worksheets("Sheet2").Cells(4 + i,
2).Value
         Else
            Worksheets("Sheet2").Cells(4 + i, 3 + j).Value = q + Worksheets("Sheet2").Cells(4 + i,
2).Value
         End If
      Next j
   Next i
   SimplexM (k)
Next k
End Sub
```

The error of each parameter was calculated directly in Excel using the data generated by the bootstrap programme and the method described in Appendix A.

H.4 REFERENCES

CHENEY, W. & KINCAID, D. 2004. Numerical Mathematics and Computing. 5th ed. USA: Thomson. 817p.

CHERNICK, M.R. 1999. Bootstrap Methods. 2nd ed. New York: John Wiley & Sons. 369p.

JACOBY, S.L.S., KOWALIK, J.S. & PIZZO, J.T. 1972. Iterative methods for nonlinear optimization problems. New Jersey: Prentice-hall. 274p.

KOEKEMOER, L.R. 2004. The evaluation of the mechanism involved in the extraction of nickel from low concentration effluents by means of supported liquid membrane. Potchefstroom: NWU. Potchefstroom campus. (Thesis – Ph.D)

VAN DER GRYP, P. 2008. Separation of Grubbs-based catalysts with nanofiltration. Potchefstroom: NWU. Potchefstroom campus. (Thesis – Ph.D)

APPENDIX I: MODELLING

OVERVIEW

In this appendix, the details related to the modelling of the fermentation process, the pervaporation process and fermentation coupled with pervaporation is presented. The appendix is subdivided into three sections, namely fermentation modelling (Section I.1), pervaporation modelling (Section I.2), and fermentation coupled with pervaporation modelling (Section I.3). The method and calculations that was used to model each different process as well as the calculated result and a graphical representation of each model will also be given in each section.

I.1 FERMENTATION MODELLING

I.1.1. Method and calculations

The fermentation process was modelled using the Monod model as basis, shown by Equations I.1 to I.8.

$$\frac{dX}{dt} = \mu X \qquad \text{Equation I.1}$$

$$\frac{dP_i}{dt} = \nu_i X \qquad \text{Equation I.2}$$

$$\frac{dS}{dt} = -\left(\frac{1}{Y_{P_i/S}}\frac{dP_i}{dt}\right) \qquad \text{Equation I.3}$$

$$\mu = \mu_{\max}\frac{S}{K_{sx}+S} \qquad \text{Equation I.4}$$

$$\nu_i = \nu_{\max,i}\frac{S}{K_{sp,i}+S} \qquad \text{Equation I.5}$$

$$\mu_{\max} = 0.015 \times X_0^{0.551} - 0.012 \qquad \text{Equation I.6}$$

$$\nu_{\max,ethanol} = 9.17 \times 10^{-7} \times X_0^{5.034} + 0.093 \qquad \text{Equation I.7}$$

$$\nu_{\max,glycerol} = 8.29 \times 10^{-7} \times X_0^{4.590} + 0.018 \qquad \text{Equation I.8}$$

This model did not consider substrate inhibition so Equation I.4 and Equation I.5 was changed to Equation I.9 and Equation I.10 by adding a term to account for the inhibition effect of glucose.

$$\mu = \mu_{\max}\left(\frac{S}{K_{sx}+S}\right)\exp\left(\frac{-S}{K_{ix}}\right) \qquad \text{Equation I.9}$$

$$\nu_i = \nu_{\max,i}\left(\frac{S}{K_{sp,i}+S}\right)\exp\left(\frac{-S}{K_{ip,i}}\right) \qquad \text{Equation I.10}$$

The fourth order Runge-Kutta method was used to solve the set of differential equations simultaneously. The Nelder-Mead simplex optimisation method was combined with the Runge-Kutta method to determine the parameters of the equations. The Bootstrap method

was used to determine the standard error of the parameters. The computer programmes used are presented in Appendix H.

The parameters determined for fermentation models are shown in Table I.1.

Table I.1 Fermentation model parameters

Parameter	Substrate-limiting model	Substrate inhibition model
u_{max}	$0.015 \times X_0^{0.551} - 0.012$	0.191±0.005
$v_{max,ethanol}$	$9.17 \times 10^{-7} \times X_0^{5.034} + 0.093$	$0.120 \times X_0^{0.467} + 0.164$
$v_{max,glycerol}$	$8.29 \times 10^{-7} \times X_0^{4.590} + 0.018$	0.078±0.048
K_{sx}	21.461±0.005	30.953±0.038
$K_{sp,\ ethanol}$	0.145±0.016	8.005±0.045
$K_{sp,\ glycerol}$	1.413±0.007	23.795±0.029
K_{ix}	---	3.569±0.023
$K_{ip,\ ethanol}$	---	17.468±0.016
$K_{ip,\ glycerol}$	---	33.829±0.035

The accuracy of the models was determined through the R^2 value (van der Gryp, 2003:179), as shown by Equation I.1. These values are presented in Chapter 2.4.

$$R^2 = \frac{\text{Sum of squares differences}}{\text{Sum of squares}} = 1 - \frac{\sum (x-y)^2}{\sum \left(x^2 - y^2\right)} \qquad \text{Equation I.11}$$

where x is the experimental value and y the theoretical model value

I.1.2. Calculated results

Table I.2 Theoretical fermentation data using 5wt% starting glucose and 10g/L yeast

	Experimental				Substrate-limiting model				Substrate inhibition model			
time (h)	Cells (wt%)	Ethanol (wt%)	Glycerol (wt%)	Glucose (wt%)	Cells (wt%)	Ethanol (wt%)	Glycerol (wt%)	Glucose (wt%)	Cells (wt%)	Ethanol (wt%)	Glycerol (wt%)	Glucose (wt%)
1	1.020	0.116	0.025	4.724	1.001	0.019	0.004	4.955	1.007	0.148	0.012	4.686
2	0.969	0.327	0.109	4.147	1.008	0.187	0.039	4.553	1.014	0.293	0.023	4.377
4	1.076	0.820	0.203	2.998	1.015	0.375	0.077	4.106	1.028	0.573	0.043	3.781
8	1.159	1.823	0.428	0.594	1.027	0.753	0.151	3.214	1.058	1.085	0.079	2.701
12	1.233	1.913	0.382	0.509	1.043	1.501	0.279	1.482	1.088	1.508	0.106	1.811
24	1.246	2.037	0.455	0.124	1.049	2.129	0.346	0.109	1.144	2.188	0.145	0.391
48	1.360	2.015	0.536	0.009	1.049	2.182	0.348	0	1.161	2.371	0.154	0.010
72	1.033	1.956	0.501	0.193	1.049	2.182	0.348	0	1.161	2.376	0.154	0

Table I.3 Theoretical fermentation data using 10wt% starting glucose and 10g/L yeast

	Experimental				Substrate-limiting model				Substrate inhibition model			
time (h)	Cells (wt%)	Ethanol (wt%)	Glycerol (wt%)	Glucose (wt%)	Cells (wt%)	Ethanol (wt%)	Glycerol (wt%)	Glucose (wt%)	Cells (wt%)	Ethanol (wt%)	Glycerol (wt%)	Glucose (wt%)
1	0.965	0.102	0.032	9.737	1.001	0.019	0.004	9.954	1.003	0.162	0.017	9.646
2	1.008	0.293	0.094	9.243	1.013	0.191	0.044	9.536	1.006	0.325	0.034	9.290
4	1.041	0.664	0.177	8.354	1.026	0.384	0.089	9.067	1.013	0.654	0.067	8.575
8	1.124	1.601	0.430	6.026	1.050	0.776	0.178	8.114	1.031	1.318	0.130	7.139
12	1.231	2.839	0.589	3.294	1.094	1.584	0.358	6.162	1.053	1.978	0.187	5.720
24	1.361	4.209	0.854	0.094	1.130	2.416	0.533	4.172	1.145	3.681	0.311	2.109
48	1.171	4.179	0.830	0.199	1.165	4.251	0.809	0	1.225	4.660	0.367	0.066
72	1.227	4.090	0.885	0.266	1.165	4.251	0.809	0	1.228	4.690	0.369	0.001

Table I.4 Theoretical fermentation data using 15wt% starting glucose and 10g/L yeast

	Experimental				Substrate-limiting model				Substrate inhibition model			
time (h)	Cells (wt%)	Ethanol (wt%)	Glycerol (wt%)	Glucose (wt%)	Cells (wt%)	Ethanol (wt%)	Glycerol (wt%)	Glucose (wt%)	Cells (wt%)	Ethanol (wt%)	Glycerol (wt%)	Glucose (wt%)
1	0.932	0.104	0.034	14.731	1.002	0.019	0.005	14.953	1.001	0.143	0.019	14.679
2	1.007	0.298	0.075	14.270	1.017	0.192	0.046	14.529	1.002	0.288	0.039	14.354
4	1.076	0.638	0.166	13.427	1.034	0.387	0.093	14.051	1.004	0.583	0.077	13.696
8	1.111	1.432	0.371	11.473	1.067	0.787	0.189	13.072	1.010	1.192	0.153	12.341
12	1.204	2.341	0.494	9.453	1.132	1.622	0.387	11.030	1.018	1.828	0.227	10.939
24	1.342	5.642	0.910	2.182	1.193	2.504	0.591	8.884	1.064	3.842	0.428	6.561
48	1.274	6.393	1.177	0.189	1.317	5.333	1.182	2.125	1.228	6.673	0.628	0.569
72	1.215	6.466	1.128	0.142	1.328	6.295	1.295	0	1.253	6.942	0.643	0.012

Table I.5 Theoretical fermentation data using 20wt% starting glucose and 10g/L yeast

	Experimental				Substrate-limiting model				Substrate inhibition model			
time (h)	Cells (wt%)	Ethanol (wt%)	Glycerol (wt%)	Glucose (wt%)	Cells (wt%)	Ethanol (wt%)	Glycerol (wt%)	Glucose (wt%)	Cells (wt%)	Ethanol (wt%)	Glycerol (wt%)	Glucose (wt%)
1	0.994	0.080	0.008	19.828	1.002	0.019	0.005	19.953	1.000	0.118	0.020	19.728
2	1.156	0.287	0.061	19.319	1.020	0.193	0.047	19.526	1.001	0.237	0.040	19.453
4	1.070	0.636	0.145	18.473	1.040	0.389	0.096	19.042	1.001	0.480	0.079	18.896
8	1.192	1.358	0.306	16.744	1.080	0.794	0.195	18.047	1.003	0.983	0.159	17.744
12	1.211	2.127	0.452	14.954	1.162	1.648	0.403	15.947	1.005	1.511	0.238	16.543
24	1.394	4.482	0.766	9.733	1.243	2.564	0.623	13.702	1.018	3.257	0.472	12.631
48	1.441	7.978	1.395	1.662	1.452	5.639	1.334	6.218	1.124	7.239	0.859	3.997
72	1.309	8.527	1.541	0.302	1.525	8.330	1.790	0	1.255	9.058	0.973	0.175

Table I.6 Theoretical fermentation data using 25wt% starting glucose and 10g/L yeast

	Experimental				Substrate-limiting model				Substrate inhibition model			
time (h)	Cells (wt%)	Ethanol (wt%)	Glycerol (wt%)	Glucose (wt%)	Cells (wt%)	Ethanol (wt%)	Glycerol (wt%)	Glucose (wt%)	Cells (wt%)	Ethanol (wt%)	Glycerol (wt%)	Glucose (wt%)
1	0.855	0.062	0.008	24.862	1.002	0.019	0.005	24.953	1.000	0.094	0.019	24.777
2	1.128	0.184	0.044	24.554	1.022	0.193	0.048	24.523	1.000	0.188	0.038	24.552
4	1.119	0.561	0.127	23.654	1.045	0.391	0.097	24.036	1.000	0.381	0.077	24.095
8	1.196	1.169	0.271	22.183	1.091	0.799	0.198	23.030	1.001	0.779	0.155	23.155
12	1.308	1.741	0.390	20.831	1.186	1.668	0.413	20.888	1.001	1.196	0.233	22.177
24	1.326	3.337	0.610	17.278	1.283	2.609	0.645	18.569	1.004	2.567	0.470	18.997
48	1.400	5.953	1.069	11.260	1.566	5.869	1.428	10.580	1.028	5.978	0.940	11.328
72	1.450	7.723	1.280	7.385	1.748	10.358	2.292	0	1.159	9.914	1.295	2.847

Table I.7 Theoretical fermentation data using 30wt% starting glucose and 10g/L yeast

	Experimental				Substrate-limiting model				Substrate inhibition model			
time (h)	Cells (wt%)	Ethanol (wt%)	Glycerol (wt%)	Glucose (wt%)	Cells (wt%)	Ethanol (wt%)	Glycerol (wt%)	Glucose (wt%)	Cells (wt%)	Ethanol (wt%)	Glycerol (wt%)	Glucose (wt%)
1	0.952	0.040	0.019	29.885	1.002	0.019	0.005	29.953	1.000	0.073	0.018	29.820
2	1.011	0.120	0.017	29.731	1.024	0.194	0.049	29.522	1.000	0.147	0.036	29.638
4	0.993	0.461	0.105	28.894	1.049	0.392	0.098	29.032	1.000	0.297	0.072	29.269
8	1.071	0.968	0.236	27.643	1.099	0.802	0.201	28.017	1.000	0.606	0.145	28.515
12	1.087	1.397	0.338	26.606	1.205	1.683	0.421	25.842	1.000	0.927	0.219	27.736
24	1.201	2.515	0.525	24.052	1.316	2.646	0.660	23.466	1.001	1.969	0.446	25.229
48	1.345	4.148	0.822	20.277	1.662	6.053	1.496	15.081	1.005	4.508	0.916	19.281
72	1.280	5.690	1.055	16.804	1.993	12.382	2.798	0	1.027	7.884	1.387	11.679

Table I.8 Theoretical fermentation data using 35wt% starting glucose and 10g/L yeast

	Experimental				Substrate-limiting model				Substrate inhibition model			
time (h)	Cells (wt%)	Ethanol (wt%)	Glycerol (wt%)	Glucose (wt%)	Cells (wt%)	Ethanol (wt%)	Glycerol (wt%)	Glucose (wt%)	Cells (wt%)	Ethanol (wt%)	Glycerol (wt%)	Glucose (wt%)
1	1.048	0.021	0.034	34.893	1.003	0.019	0.005	34.953	1.000	0.057	0.017	34.855
2	1.092	0.054	0.006	34.881	1.026	0.194	0.049	34.520	1.000	0.114	0.033	34.709
4	1.004	0.233	0.075	34.397	1.052	0.393	0.099	34.028	1.000	0.230	0.067	34.415
8	1.105	0.817	0.217	32.978	1.106	0.806	0.203	33.007	1.000	0.466	0.134	33.814
12	1.254	1.210	0.322	32.002	1.221	1.695	0.427	30.806	1.000	0.710	0.202	33.197
24	1.321	2.159	0.496	29.805	1.343	2.676	0.673	28.383	1.000	1.493	0.410	31.238
48	1.330	3.463	0.759	26.739	1.744	6.206	1.549	19.673	1.001	3.333	0.848	26.737
72	1.390	4.604	0.922	24.189	2.254	14.403	3.307	0	1.003	5.681	1.312	21.180

Table I.9 Theoretical fermentation data using 15wt% starting glucose and 7g/L yeast

	Experimental				Substrate-limiting model				Substrate inhibition model			
time (h)	Cells (wt%)	Ethanol (wt%)	Glycerol (wt%)	Glucose (wt%)	Cells (wt%)	Ethanol (wt%)	Glycerol (wt%)	Glucose (wt%)	Cells (wt%)	Ethanol (wt%)	Glycerol (wt%)	Glucose (wt%)
1	0.692	0.035	0.011	14.910	0.701	0.008	0.002	14.982	0.701	0.090	0.014	14.796
2	0.798	0.102	0.030	14.742	0.709	0.076	0.016	14.818	0.701	0.180	0.027	14.591
4	0.904	0.288	0.084	14.273	0.718	0.154	0.031	14.634	0.703	0.362	0.054	14.177
8	1.103	0.584	0.145	13.573	0.737	0.311	0.064	14.259	0.706	0.736	0.108	13.331
12	1.188	1.009	0.251	12.535	0.775	0.639	0.130	13.480	0.711	1.122	0.161	12.465
24	1.337	2.406	0.525	9.265	0.813	0.983	0.200	12.663	0.730	2.345	0.316	9.741
48	1.192	5.520	0.993	2.258	0.927	2.111	0.425	9.989	0.824	4.939	0.575	4.103
72	1.071	6.352	1.023	0.570	1.114	4.753	0.917	3.796	0.951	6.586	0.693	0.614

Table I.10 Theoretical fermentation data using 15wt% starting glucose and 5g/L yeast

	Experimental				Substrate-limiting model				Substrate inhibition model			
time (h)	Cells (wt%)	Ethanol (wt%)	Glycerol (wt%)	Glucose (wt%)	Cells (wt%)	Ethanol (wt%)	Glycerol (wt%)	Glucose (wt%)	Cells (wt%)	Ethanol (wt%)	Glycerol (wt%)	Glucose (wt%)
1	0.531	0.034	0.005	14.924	0.501	0.005	0.001	14.989	0.500	0.058	0.010	14.866
2	0.579	0.062	0.016	14.848	0.505	0.048	0.009	14.888	0.501	0.116	0.019	14.732
4	0.651	0.147	0.045	14.623	0.510	0.096	0.018	14.775	0.502	0.234	0.039	14.462
8	0.780	0.291	0.076	14.281	0.520	0.194	0.036	14.545	0.504	0.472	0.077	13.914
12	0.850	0.570	0.160	13.572	0.541	0.396	0.073	14.073	0.507	0.716	0.116	13.355
24	1.032	1.286	0.266	11.964	0.562	0.605	0.112	13.582	0.517	1.481	0.230	11.618
48	0.991	3.124	0.541	7.830	0.627	1.282	0.236	11.999	0.556	3.157	0.448	7.876
72	0.891	5.141	0.878	3.222	0.756	2.854	0.518	8.336	0.639	4.931	0.631	4.008

Table I.11 Theoretical fermentation data using 15wt% starting glucose and 3g/L yeast

	Experimental				Substrate-limiting model				Substrate inhibition model			
time (h)	Cells (wt%)	Ethanol (wt%)	Glycerol (wt%)	Glucose (wt%)	Cells (wt%)	Ethanol (wt%)	Glycerol (wt%)	Glucose (wt%)	Cells (wt%)	Ethanol (wt%)	Glycerol (wt%)	Glucose (wt%)
1	0.334	0.020	0.002	14.957	0.300	0.003	0	14.994	0.300	0.030	0.006	14.929
2	0.360	0.035	0.008	14.915	0.302	0.028	0.005	14.935	0.301	0.061	0.012	14.857
4	0.415	0.054	0.023	14.851	0.304	0.056	0.010	14.870	0.301	0.122	0.023	14.714
8	0.480	0.139	0.036	14.658	0.308	0.112	0.020	14.738	0.302	0.245	0.047	14.424
12	0.511	0.227	0.057	14.443	0.315	0.227	0.041	14.470	0.304	0.370	0.070	14.131
24	0.592	0.646	0.140	13.462	0.323	0.345	0.062	14.196	0.308	0.755	0.140	13.231
48	0.649	1.423	0.276	11.676	0.348	0.717	0.128	13.331	0.322	1.579	0.280	11.327
72	0.693	2.508	0.464	9.185	0.398	1.541	0.273	11.415	0.343	2.481	0.418	9.270

Table I.12 Theoretical fermentation data using 15wt% starting glucose and 1g/L yeast

	Experimental				Substrate-limiting model				Substrate inhibition model			
time (h)	Cells (wt%)	Ethanol (wt%)	Glycerol (wt%)	Glucose (wt%)	Cells (wt%)	Ethanol (wt%)	Glycerol (wt%)	Glucose (wt%)	Cells (wt%)	Ethanol (wt%)	Glycerol (wt%)	Glucose (wt%)
1	0.075	0.015	0.000	14.971	0.100	0.001	0	14.998	0.100	0.008	0.002	14.981
2	0.127	0.014	0.003	14.966	0.100	0.009	0.002	14.979	0.100	0.016	0.004	14.961
4	0.138	0.030	0.009	14.925	0.100	0.018	0.003	14.957	0.100	0.031	0.008	14.922
8	0.178	0.031	0.013	14.914	0.100	0.037	0.007	14.914	0.101	0.063	0.016	14.844
12	0.159	0.051	0.022	14.857	0.101	0.074	0.013	14.828	0.101	0.095	0.023	14.766
24	0.175	0.155	0.038	14.623	0.101	0.111	0.020	14.741	0.102	0.192	0.047	14.528
48	0.198	0.394	0.104	14.025	0.103	0.224	0.040	14.478	0.105	0.392	0.095	14.038
72	0.211	0.608	0.137	13.541	0.106	0.455	0.081	13.940	0.108	0.601	0.144	13.528

I.1.3. Graphical representation

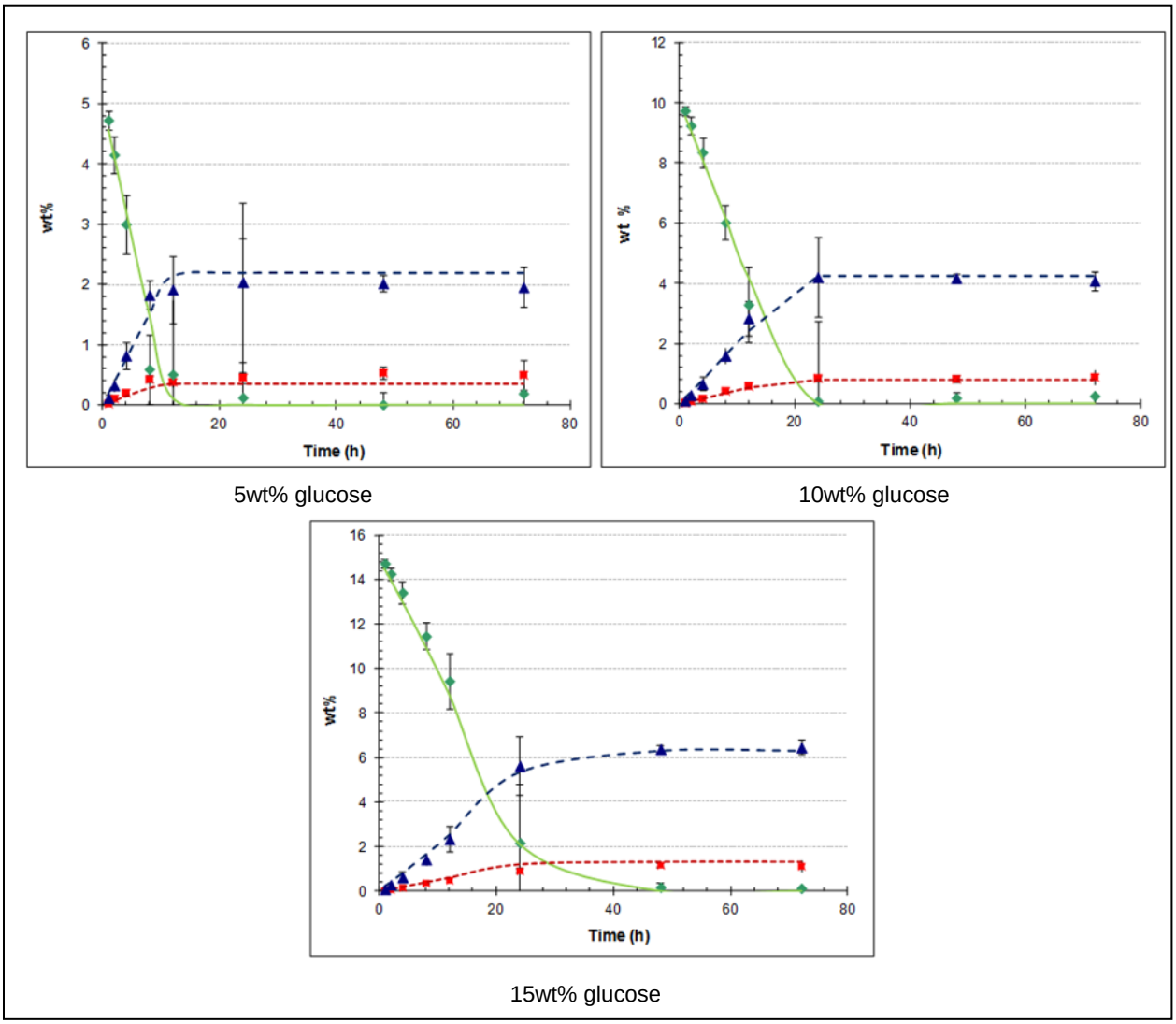

Figure I.1 Comparison of experimental fermentation data without substrate inhibition with substrate-limiting model using different starting sugar concentration and 10g/L yeast
(♦Experimental glucose, ▲ Experimental ethanol, ■ Experimental glycerol, — glucose model, --- ethanol model, ···· glycerol model)

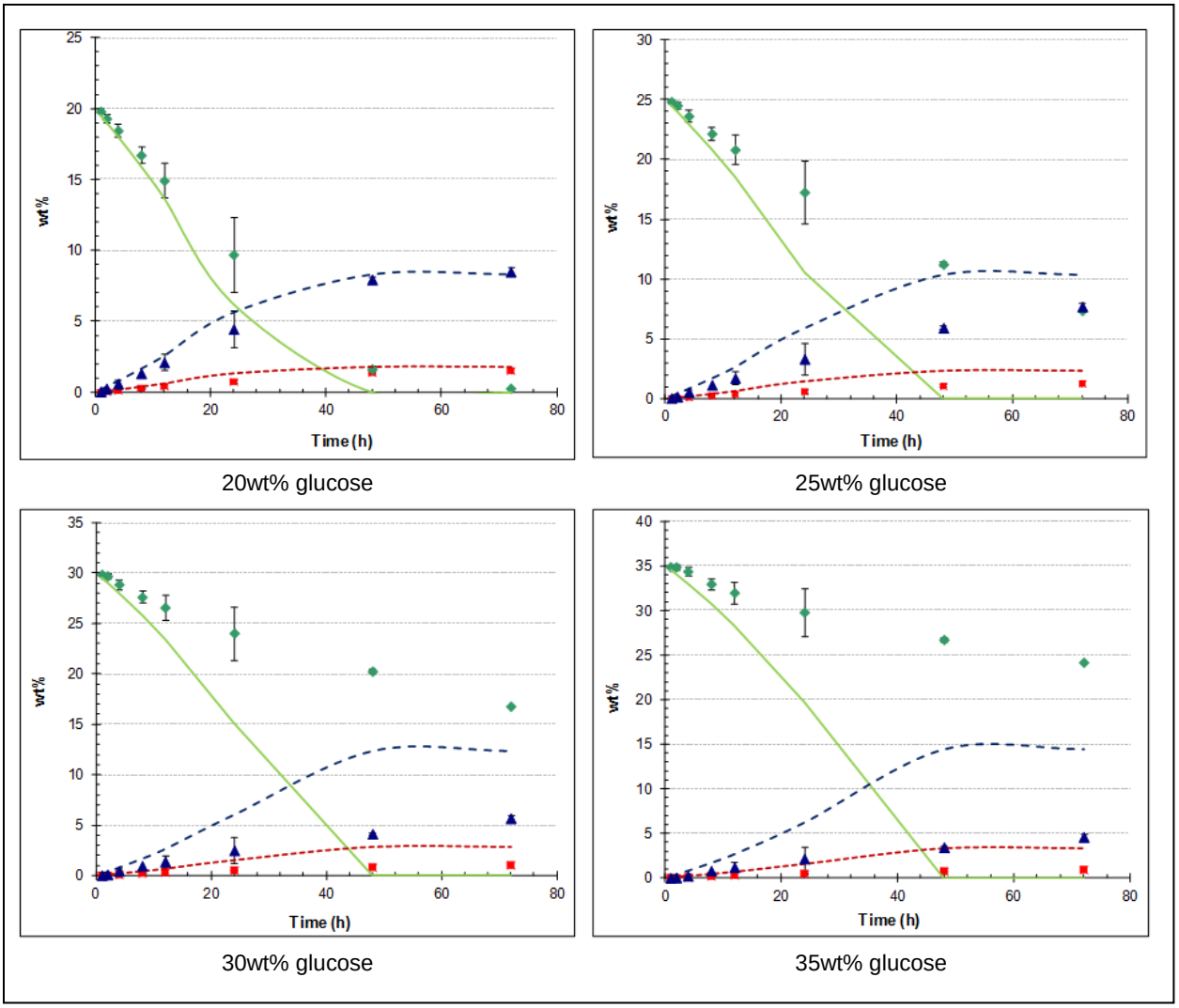

Figure I.2 Comparison of experimental fermentation data with substrate inhibition with substrate-limiting model using different starting sugar concentration and 10g/L yeast
(♦Experimental glucose, ▲ Experimental ethanol, ■ Experimental glycerol, — glucose model, --- ethanol model, ···· glycerol model)

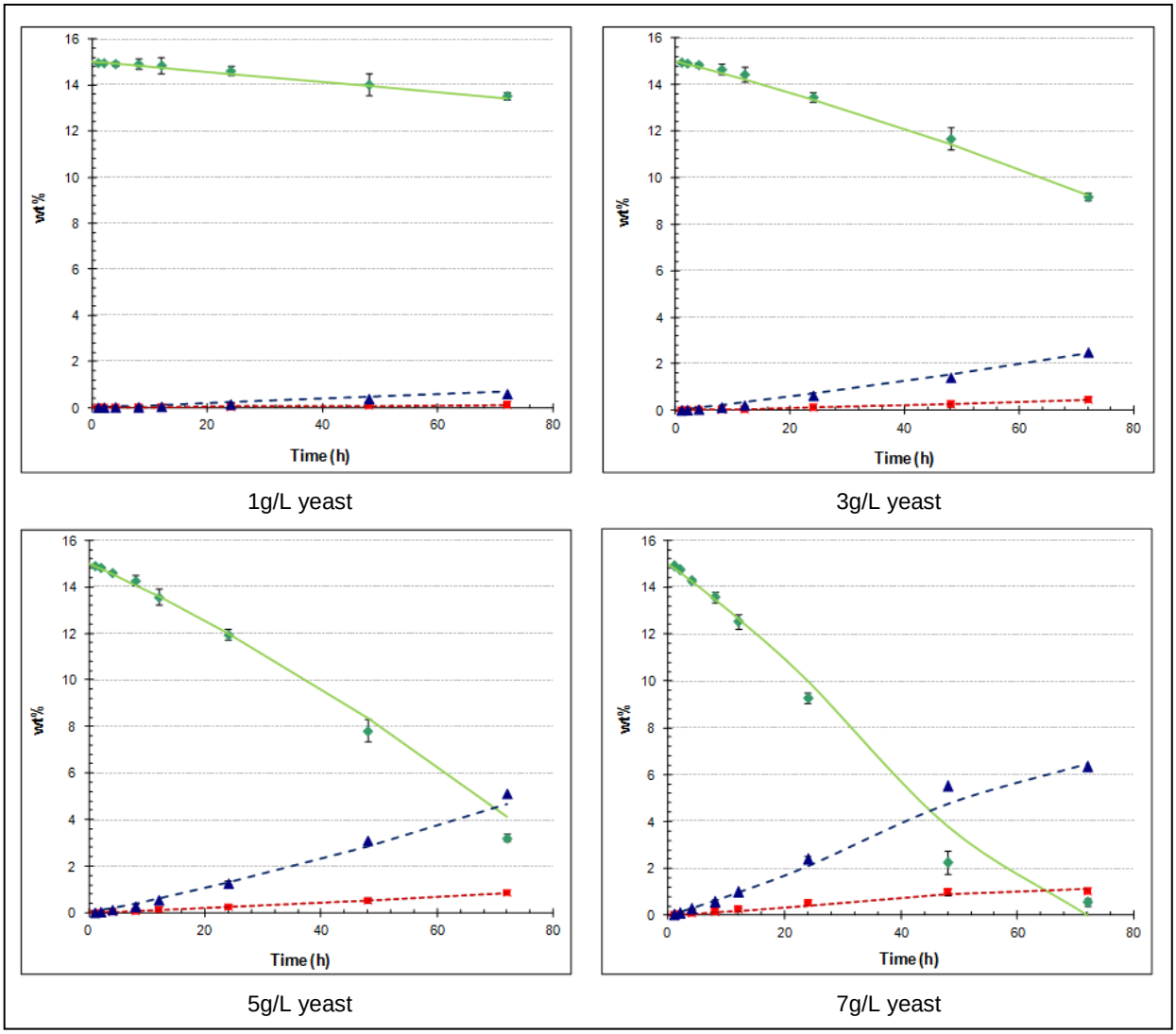

Figure I.3 Comparison of experimental fermentation data with substrate-limiting model using 15wt% glucose and different starting yeast concentrations

(♦Experimental glucose, ▲ Experimental ethanol, ■ Experimental glycerol, — glucose model, --- ethanol model, ···· glycerol model)

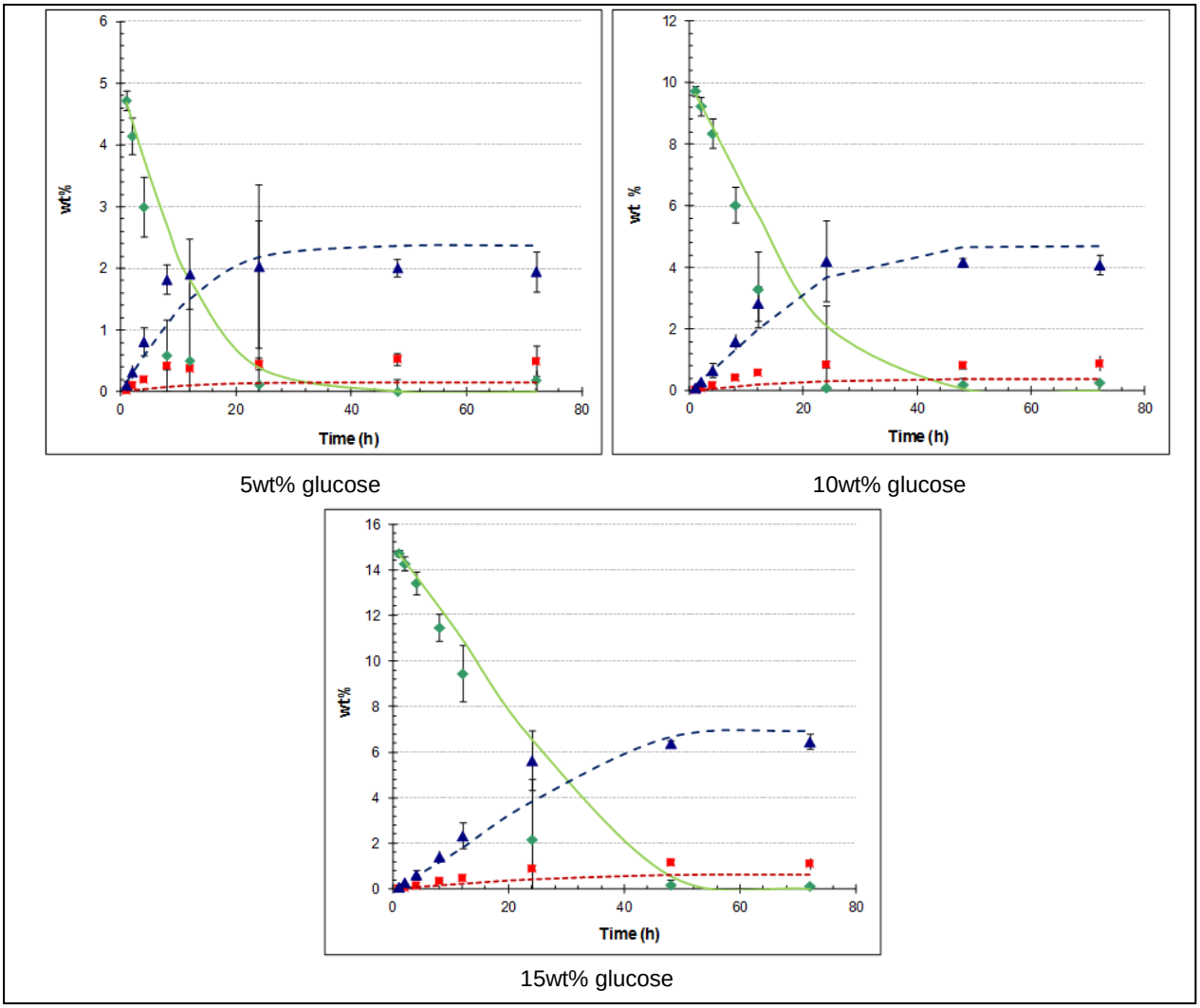

Figure I.4 Comparison of experimental fermentation data without substrate inhibition with substrate inhibition model using different starting sugar concentration and 10g/L yeast
(♦Experimental glucose, ▲ Experimental ethanol, ■ Experimental glycerol, — glucose model, --- ethanol model, ···· glycerol model)

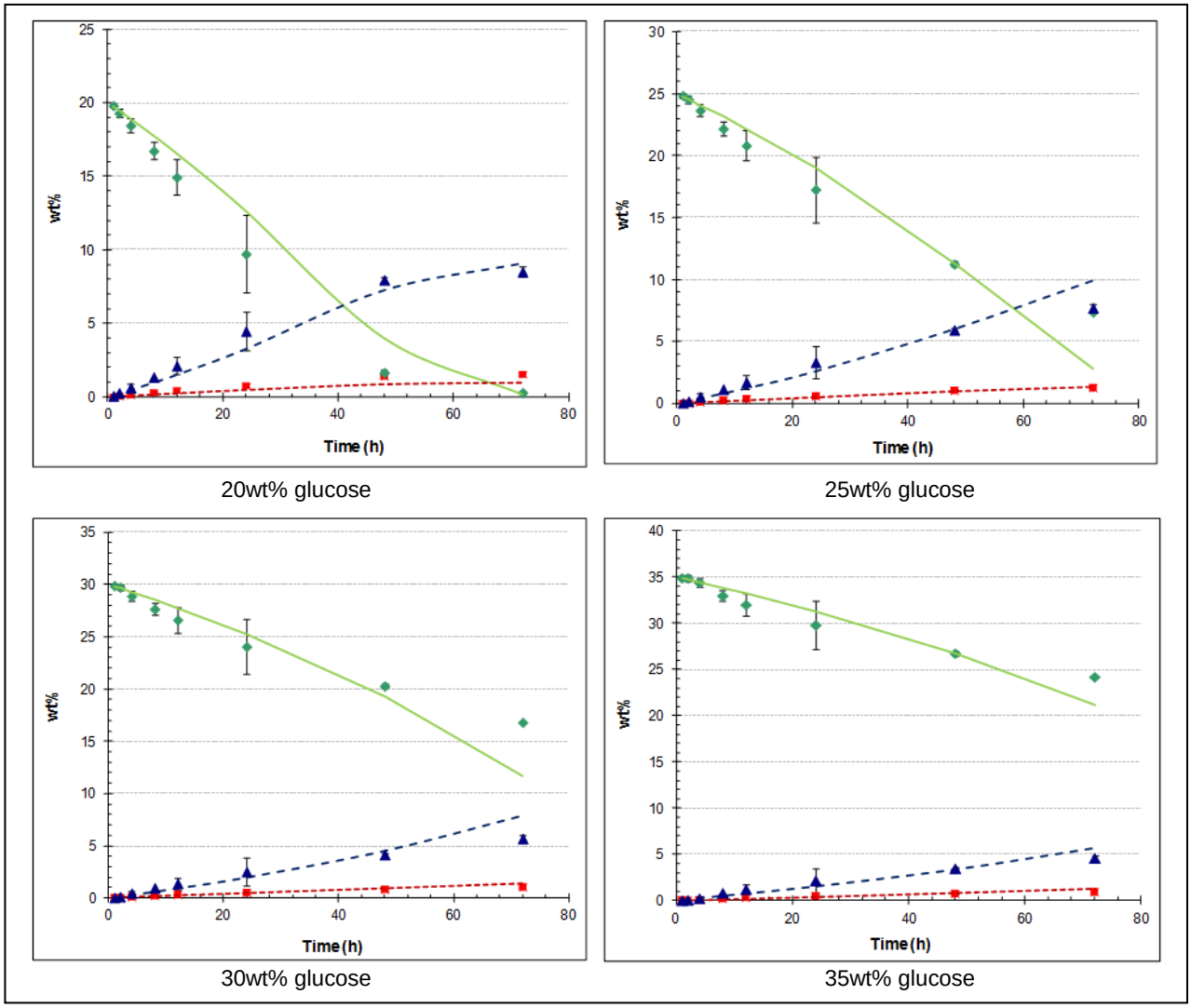

Figure I.5 Comparison of experimental fermentation data with substrate inhibition with substrate inhibition model using different starting sugar concentration and 10g/L yeast
(♦Experimental glucose, ▲ Experimental ethanol, ■ Experimental glycerol, — glucose model, --- ethanol model, ···· glycerol model)

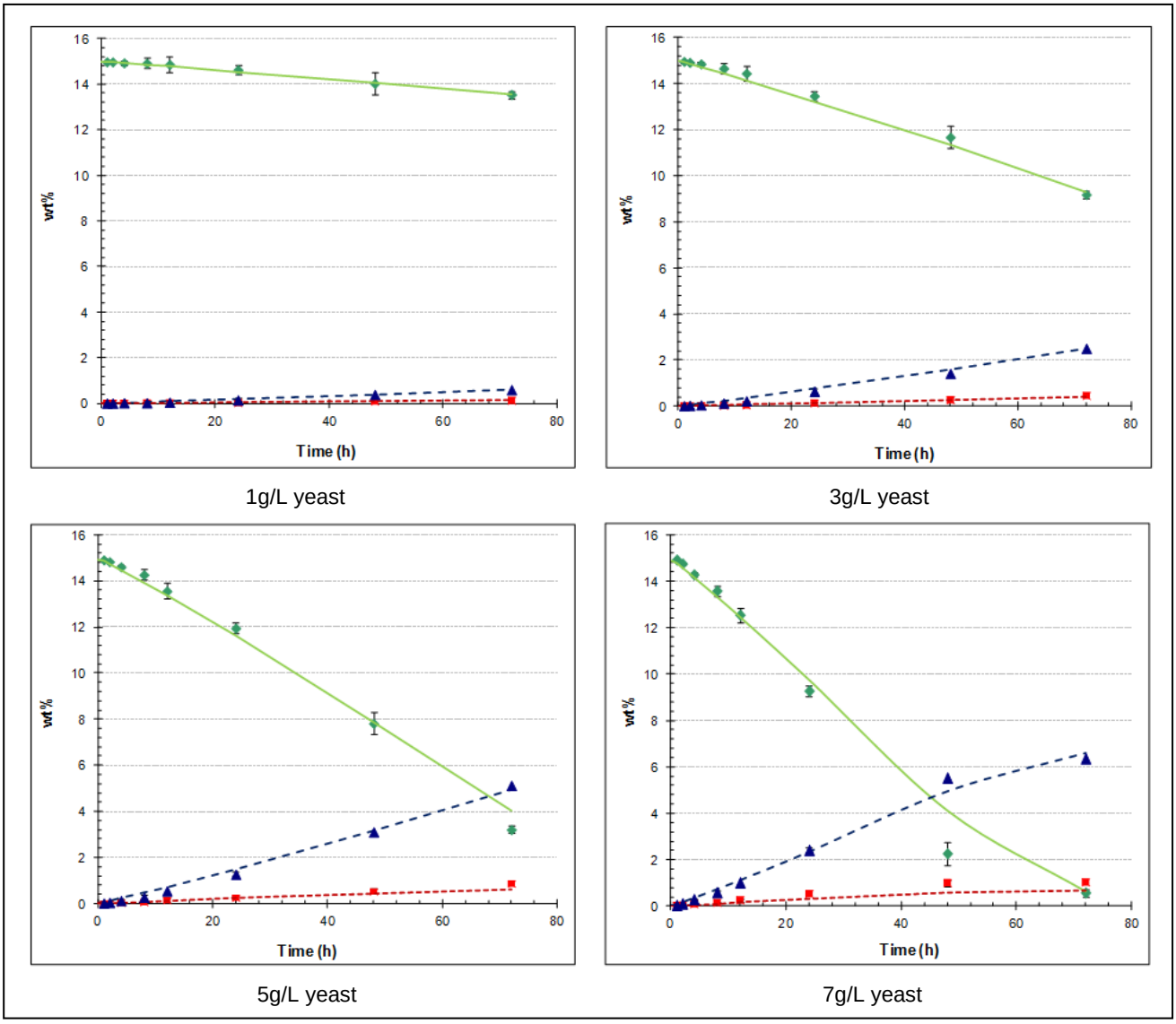

Figure I.6 Comparison of experimental fermentation data with substrate inhibition model using 15wt% glucose and different starting yeast concentrations
(♦Experimental glucose, ▲ Experimental ethanol, ■ Experimental glycerol, — glucose model, --- ethanol model, ···· glycerol model)

I.2 PERVAPORATION MODELLING

I.2.1. Method and calculations

The method used to model the partial water and ethanol flux will be presented in this section. The theoretical values of the partial fluxes of ethanol and water at a given mass fraction in the feed can be calculated by substituting the Greenlaw expression of the diffusion coefficient shown in Table I.13 into Fick's law, Equation 3.9, and solving for J_i.

$$J_i = -D_i \frac{dc_i}{dz}$$ Equation 3.9

Equation 3.9 was rewritten in terms of density (ρ) and mass fraction (y_i), as shown in Table I.13.

Table I.13 Partial flux model

Diffusion coefficient equation	Flux equation
$D_i = D_i^0 \rho_i \left(y_i + \beta_{ij} y_j\right)$	$J_i = \frac{D_i^0 \rho_i}{L}\left(\frac{(y_i)^2}{2} + \beta_{ij} y_i (1 - y_i)\right)$

The parameters D_i^0 and B_{ii} shown in Table I.13, was determined by using the Nelder-Mead simplex optimisation method discussed in Appendix H. The calculated results are given in Section I.2.2 and graphical representation of the results is given in Section I.2.3. The influence on the water flux due to the presence of glucose (see Section 3.3.2.2) was assumed constant as the effect was within the experimental error of the pervaporation experiments. Therefore, for the effect of glucose on the water flux, the experimental data at each different glucose concentration was averaged.

Table I.14 Parameters for partial flux models

Model	D_i^0 (m^2/s)	B_{ij}
Ethanol flux	$9.55\times10^{-9}\pm1.91\times10^{-10}$	$0.39\pm1.20\times10^{-5}$
Water flux	$6.52\times10^{-10}\pm7.77\times10^{-12}$	$0.75\pm9.69\times10^{-7}$
Water flux in the presence of glucose	$3.79\times10^{-10}\pm6.24\times10^{-11}$	0.5 ± 0.026

I.2.2. Calculated results

Table I.15 Ethanol flux

Mass fraction ethanol in feed	Experimental flux (kg/m^2h)	Greenlaw (kg/m^2h)
0.199	0.578	0.578
0.155	0.473	0.447
0.106	0.259	0.302
0.054	0.151	0.151

Table I.16 Water flux

Mass fraction ethanol in feed	Experimental flux (kg/m^2h)	Greenlaw (kg/m^2h)
0.199	0.275	0.271
0.155	0.298	0.280
0.106	0.284	0.289
0.054	0.300	0.299

Table I.17 Water flux in the presence of glucose

Mass fraction ethanol in feed	Experimental flux (kg/m^{2}h)	Greenlaw (kg/m^{2}h)
0.138	0.149	0.154
0.091	0.177	0.163
0.053	0.168	0.169

The relative percentage deviation modulus (RPDM) (Equation I.12) (Staniszewski *et al*., 2009:245) and R^2 (Equations I.11) was used to determine the accuracy of the models shown in Table I.18.

$$RPDM = \frac{100}{n}\sum_{i=1}^{n}\frac{|x_i - y_i|}{x_i} \qquad \text{Equation I.12}$$

with x the experimental value and y the theoretical model value

Table I.18 Accuracy of partial flux models

Partial flux	R^2	RPDM (%)
Ethanol flux	0.998	5.59
Water flux	0.999	2.51
Water flux in the presence of glucose	0.999	4.01

I.2.3. Graphical representation

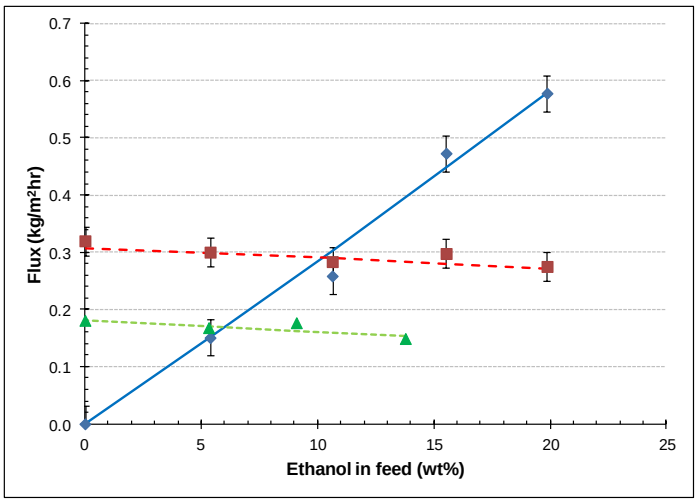

Figure I.7 Comparison of experimental partial flux with Greenlaw's model
(♦experimental ethanol flux, ■experimental water flux, ▲experimental water flux in the presence of glucose, — ethanol model, --- water model, ···· water model in the presence of glucose)

I.3 FERMENTATION COUPLED WITH PERVAPORATION MODELLING

I.3.1. Summary of equations in membrane-reactor system model

$$\frac{d\left(My_x\right)}{dt} = Mr_x$$ Equation I.1

$$\frac{d\left(My_{glycerol}\right)}{dt} = Mr_{glycerol}$$ Equation I.2

$$\frac{d\left(My_S\right)}{dt} = Mr_S$$ Equation I.3

$$\frac{d\left(MP_{ethanol}\right)}{dt} = Mr_{ethanol} - QP_{ethanol,permeate}$$ Equation I.4

$$\frac{d\left(M\right)}{dt} = -Q$$ Equation I.5

$$r_x = \mu X$$ Equation I.6

$$r_{P_i} = \nu_i X$$ Equation I.7

$$r_S = -\left(\frac{1}{Y_{P_i/S}}\frac{dP_i}{dt}\right)$$ Equation I.8

$$\mu = \mu_{\max}\frac{S}{K_{sx}+S}$$ Equation I.9

$$\nu_i = \nu_{\max,i}\frac{S}{K_{sp,i}+S}$$ Equation I.10

$$\mu_{\max} = 0.015 \times X_0^{\,0.551} - 0.012$$ Equation I.11

$$\nu_{\max,ethanol} = 9.17 \times 10^{-7} \times X_0^{\,5.034} + 0.093$$ Equation I.12

$$\nu_{\max,glycerol} = 8.29 \times 10^{-7} \times X_0^{\,4.590} + 0.018$$ Equation I.13

$$J_i = \frac{D_i^0 \rho_i}{L}\left(\frac{\left(y_i\right)^2}{2} + \beta_{ij} y_i (1-y_i)\right)$$ Equation 3.12

Equation I.1 to I.13 was solved simultaneously using the Runge-Kutta programme discussed in Appendix H.1. By calculating the water and ethanol content at each time interval using the results from the Runge-Kutta, the ethanol and water flux was calculated using Equation 3.12. The calculated water and ethanol flux was then used to determine the amount of water and ethanol that is removed from the system and the amount that is still left. This procedure was repeated at each time interval used in the Runge-Kutta programme (time intervals of 0.1h).

Table I.19 Parameters for membrane-reactor system model

Parameter	Value
Fermentation	
u_{max}	$0.015 \times X_0^{0.551} - 0.012$
$v_{max,ethanol}$	$9.17 \times 10^{-7} \times X_0^{5.034} + 0.093$
$v_{max,glycerol}$	$8.29 \times 10^{-7} \times X_0^{4.590} + 0.018$
K_{sx}	21.461±0.005
$K_{sp,\ ethanol}$	0.145±0.016
$K_{sp,\ glycerol}$	1.413±0.007
Ethanol flux	
D_i^0	$9.55 \times 10^{-9} \pm 1.91 \times 10^{-10}$
B_{ij}	$0.39 \pm 1.20 \times 10^{-5}$
Water flux	
D_i^0	$6.52 \times 10^{-10} \pm 7.77 \times 10^{-12}$
B_{ij}	$0.75 \pm 9.69 \times 10^{-7}$
Water flux in the presence of glucose	
D_i^0	$3.79 \times 10^{-10} \pm 6.24 \times 10^{-11}$
B_{ij}	0.5±0.026

I.3.2. Calculated results

Table I.20 Experimental and theoretical data in feed vessel of membrane-reactor system

	Experimental				Membrane reactor system model			
time (h)	Cells (wt%)	Ethanol (wt%)	Glycerol (wt%)	Glucose (wt%)	Cells (wt%)	Ethanol (wt%)	Glycerol (wt%)	Glucose (wt%)
1	1.242	0.031	0.004	14.932	1.017	0.192	0.046	14.529
2	1.314	0.052	0.008	14.882	1.034	0.387	0.093	14.051
8	1.493	1.822	0.327	10.796	1.132	1.622	0.387	11.030
12	1.694	3.690	0.681	6.447	1.193	2.504	0.591	8.884
24	1.848	5.886	1.235	1.067	1.317	5.323	1.182	2.126
26	1.704	5.935	1.272	0.527	1.324	5.591	1.250	1.076
28	1.902	5.625	1.632	0.078	1.327	5.779	1.287	0.231
30	1.833	5.682	1.413	0.078	1.327	5.659	1.291	0.055
32	1.767	5.272	1.634	0.124	1.327	5.461	1.291	0.055
34	1.842	5.038	1.747	0.044	1.327	5.269	1.291	0.055
36	1.905	5.023	1.621	0.056	1.327	5.084	1.291	0.055
38	1.930	4.951	1.473	0.199	1.327	4.906	1.291	0.055
40	1.905	4.484	1.876	0.030	1.327	4.733	1.291	0.055
42	1.895	4.583	1.597	0.103	1.327	4.567	1.291	0.055
44	1.911	4.392	1.668	0.073	1.327	4.407	1.291	0.055
46	1.836	4.291	1.644	0.062	1.327	4.252	1.291	0.055
48	1.807	4.050	1.778	0.024	1.327	4.529	1.291	0.055

Table I.21 Experimental and theoretical yields of membrane-reactor system

	Experimental		Membrane reactor system model	
time (h)	Total ethanol yield ($g.g^{-1}$)	Glycerol yield ($g.g^{-1}$)	Total ethanol yield ($g.g^{-1}$)	Glycerol yield ($g.g^{-1}$)
1	0.002	0.000	0.013	0.003
2	0.003	0.001	0.026	0.006
8	0.005	0.001	0.108	0.026
12	0.121	0.022	0.167	0.039
24	0.246	0.045	0.356	0.079
26	0.392	0.082	0.386	0.083
28	0.409	0.084	0.412	0.086
30	0.401	0.107	0.418	0.086
32	0.416	0.093	0.418	0.086
34	0.401	0.106	0.418	0.086
36	0.397	0.113	0.418	0.086
38	0.405	0.104	0.418	0.086
40	0.410	0.094	0.418	0.086
42	0.391	0.120	0.418	0.086
44	0.407	0.101	0.418	0.086
46	0.404	0.105	0.418	0.086
48	0.406	0.103	0.418	0.086

Table I.22 Experimental and theoretical data of pervaporation of membrane-reactor system

	Experimental		Membrane reactor system model	
time (h)	Ethanol flux (kg/m^2h)	Water flux (kg/m^2h)	Ethanol flux (kg/m^2h)	Water flux (kg/m^2h)
26	0.192	0.384	0.156	0.150
28	0.172	0.271	0.162	0.149
30	0.155	0.259	0.159	0.278
32	0.157	0.264	0.153	0.277
34	0.153	0.264	0.148	0.276
36	0.141	0.256	0.143	0.276
38	0.137	0.261	0.137	0.275
40	0.140	0.274	0.133	0.274
42	0.131	0.257	0.128	0.273
44	0.125	0.260	0.123	0.273
46	0.121	0.279	0.119	0.272
48	0.116	0.275	0.115	0.271

I.3.3. Graphical representation

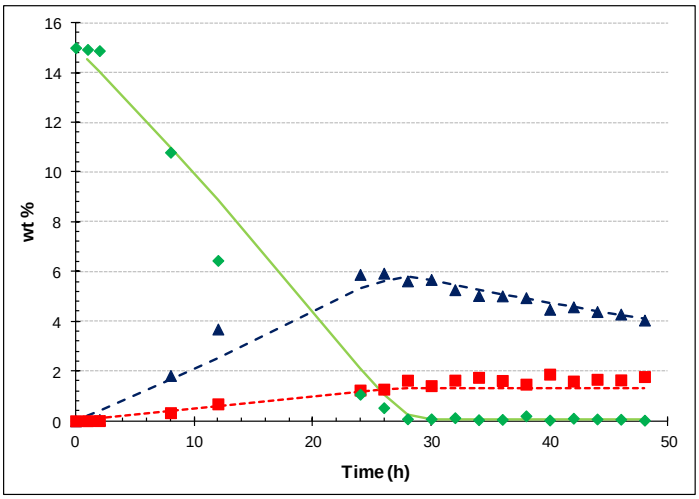

Figure I.8 Comparison of the membrane-reactor system model with experimental data
(♦ Experimental glucose, ▲ Experimental ethanol, ■ Experimental glycerol, — glucose model, --- ethanol model, ···· glycerol model)

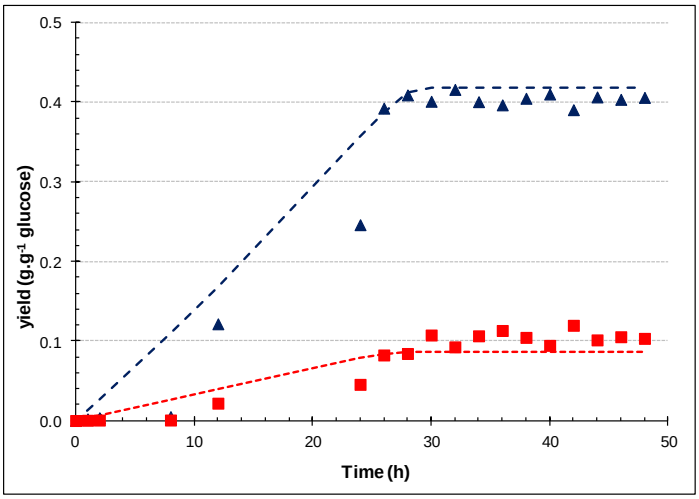

Figure I.9 Comparison of the membrane-reactor system model yields with experimental yields
(▲ Experimental ethanol yield, ■ Experimental glycerol yield, --- ethanol yield model, ···· glycerol yield model)

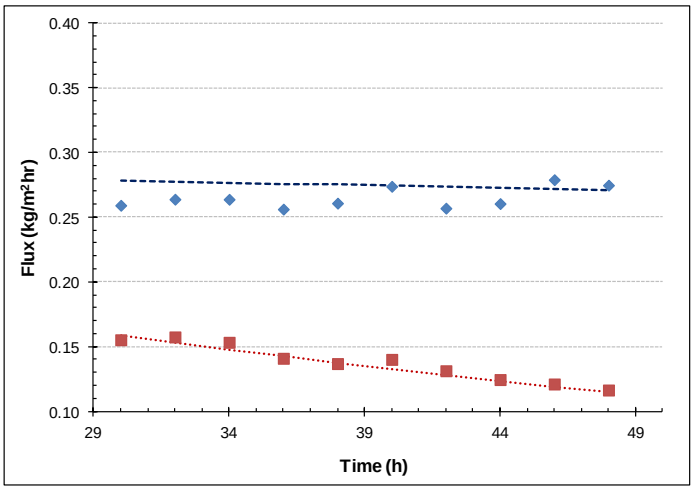

Figure I.10 Comparison of experimental ethanol and water flux with membrane-reactor system model

(♦experimental water flux, ■experimental ethanol flux, ···· ethanol model, --- water model)

I.4 REFERENCES

STANISZEWSKI, M., KUJAWSKI, W. & LEWANDOWSKA, W. 2009. Semi-continuous ethanol production in bioreactor from whey with co-immobilized enzyme and yeast cells followed by pervaporative recovery of product-Kinetic model predictions considering glucose repression. *Journal of Food Engineering*, 91: 240–249.

VAN DER GRYP, P. 2003. Separation by Pervaporation of Methanol from Tertiary Amyl Methyl Ether using a Polymeric Membrane. Potchefstroom: NWU. Potchefstroom campus. (Dissertation – M.Ing)